UNIVERSIDADE FEDERAL DO RIO GRANDE DO SUL
INSTITUTO DE CIÊNCIAS BÁSICAS DA SAÚDE
DEPARTAMENTO DE BIOQUÍMICA PROF. TUISKON DICK
PROGRAMA DE PÓS-GRADUAÇÃO EM CIÊNCIAS BIOLÓGICAS: BIOQUÍMICA

TESE DE DOUTORADO

BUSCA POR POTENCIAIS BIOMARCADORES E ALVOS TERAPÊUTICOS EM TUMORES CEREBRAIS: PAPEL DOS RECEPTORES METABOTRÓPICOS DE GLUTAMATO

Autora: Mery Stéfani Leivas Pereira
Orientador: Prof. Diogo Losch de Oliveira

Porto Alegre, Março de 2017.

CIP - Catalogação na Publicação

Leivas Pereira, Mery Stéfani
BUSCA POR POTENCIAIS BIOMARCADORES E ALVOS TERAPÊUTICOS EM TUMORES CEREBRAIS: PAPEL DOS RECEPTORES METABOTRÓPICOS DE GLUTAMATO / Mery Stéfani Leivas Pereira. -- 2017.
159 f.

Orientador: Diogo Lösch de Oliveira.

Tese (Doutorado) -- Universidade Federal do Rio Grande do Sul, Instituto de Ciências Básicas da Saúde, Programa de Pós-Graduação em Ciências Biológicas: Bioquímica, Porto Alegre, BR-RS, 2017.

1. glioblastoma. 2. mGluR. 3. antagonistas de mGluR. 4. agonistas de mGluR. I. Lösch de Oliveira, Diogo, orient. II. Título.

Elaborada pelo Sistema de Geração Automática de Ficha Catalográfica da UFRGS com os dados fornecidos pelo(a) autor(a).

"Tendemos a pensar no câncer como doença moderna porque suas metáforas são modernas. É uma doença de superprodução, de crescimento fulminante – crescimento impossível de parar, inclinado sobre o abismo do descontrole. A biologia moderna nos encoraja a imaginar a célula como uma máquina molecular. O câncer é essa máquina incapaz de saciar o comando inicial (crescer), que se transforma num autômato indestrutível, autoimpulsionado."

Siddhartha Mukherjee
em *"O Imperador de Todos os Males – Uma biografia do Câncer"*

Este trabalho foi realizado em Porto Alegre/RS sob a orientação do Prof. Dr. Diogo Losch de Oliveira no Laboratório de Neuroquímica Celular e colaboração da equipe do Prof. Dr. Fábio Klamt, Laboratório de Bioquímica Celular, ambos do Departamento de Bioquímica: Prof. Tuiskon Dick do Instituto de Ciências Básicas da Saúde, Universidade Federal do Rio Grande do Sul com financiamento da Coordenação de Aperfeiçoamento de Pessoal de Nível Superior (CAPES), do Conselho Nacional de Desenvolvimento Científico e Tecnológico (CNPq) e da Pró-Reitoria de Pesquisa desta Universidade (PROPESQ/UFRGS).

Parte deste trabalho foi desenvolvida no Centro de Pesquisa Pré-Clínica e Centro de Producão de Radio-fármacos, Instituto do Cérebro do Rio Grande do Sul – INSCER/PUCRS.

AGRADECIMENTOS

Primeiramente, agradeço aos meus pais por todo amor, paciência, dedicação, etc durante todos esses anos. O esforço que fizeram para garantir tudo o que foi necessário para meus estudos foi fundamental para que eu chegasse até essa fase. Muito obrigada! Amo incondicionalmente vocês!

Aos meus avós maternos, agradeço por toda criação e cuidado que tiveram comigo. Infelizmente, não deu tempo de vocês me verem doutora, mas sei que vocês acreditavam que eu conseguiria tudo que eu queria. Obrigada por tudo, vocês foram fundamentais para esse momento da minha vida! Amo vocês e sinto saudades imensas, todos os dias!

À minha vozinha Zirene, que também, infelizmente, não pôde me ver doutora, agradeço por todo amor. Também sei que ela acreditava muito em mim! Amo você, vó, e o vô Enídio também! Obrigada por tudo!

À minha família, por todo amor! Se eu listar todos, ocupa meia página! Então agradeço especialmente ao tio Cuca por ajudar na minha criação! Amo-te, tio!

Ao Geovani, agradeço por todo amor, cumplicidade, amizade e paciência, principalmente nesses últimos meses. Por ser a pessoa que mais me irrita e que mais me deixa feliz, apesar de isso ser meio contraditório! Por toda vida que já vivemos e que planejamos viver juntos. Pelos nossos sonhos! Amo-te incondicionalmente! Obrigada por tudo!

Agradeço à família do Geovani pelo acolhimento durante todos esses anos. Por eu fazer parte dessa família alegre e unida. Pela Alice, minha sobrinha, que torna meus finais de semana sempre mais felizes e esperados. A chegada dela foi fundamental nesses últimos anos de doutorado. Tornou tudo mais leve!

Aos meus cachorrinhos Nupe, Doby e Dick, sim, eu agradeço também aos cachorros, por todos os dias me receberem com a maior felicidade do mundo. Essa alegria foi fundamental após alguns dias de "cão" que passei no laboratório.

Aos meus colegas Cássio e Sandro pelas músicas, rizadas e amizade desde o mestrado. Vou sentir muita falta de vocês, pelo menos até ver vocês de novo e pensar "Por que eu senti falta???".

Aos colegas de laboratório, Ben Hur, Suelen, Kamila, Rico, Marcos, Charles, Diego, Joel, e Profº Renato, é claro, agradeço pela amizade e coleguismo durante todos esses anos. A convivência com vocês tornou os dias muito mais agradáveis e felizes!

Aos ICs, Natã, Gabi, Luana e Luca, apesar de não serem meus ICs, obrigada pela amizade, convivência e por terem ajudados meus colegas de laboratório! Emer, meu sobrinho, não me esqueci de ti, obrigada pela amizade e por ajudar meu cunhado!

À Lucimara e aos colegas de laboratório 24 F, agradeço pela amizade indescritivelmente divertida. Pelo companheirismo nos piores e nos melhores dias de doutorado. Pela luta diária contra as bactérias! Obrigada por tornarem os dias mais leves!

Ao Marco Antônio, agradeço por toda amizade, paciência e assistência durante o doutorado. Grande parte deste trabalho eu devo a ti! Obrigada mesmo por tudo! Sem palavras para descrever minha gratidão!

Agradeço ao Fábio pela amizade e por todo auxílio científico. Obrigada por todos os conselhos. Também devo esse doutorado a ti!

Ao Fabrício, agradeço pela amizade e por toda ajuda e dedicação ao nos demonstrar o processo cirúrgico de implantação de gliomas. Muito obrigada!

À Thainá, meu grude nesses últimos meses, obrigada por toda essa amizade e companheirismo! Sei que posso contar contigo pra qualquer coisa! Obrigada pelos ensinamentos, pela paciência, pela disponibilidade de horários (finais de semana e altas horas da noite), por tudo! És uma amiga que vou levar pra vida inteira! Foi um prazer trabalhar contigo diretamente mesmo que no finalzinho do doutorado.

À Chai, minha filha científica, agradeço por toda ajuda durante o doutorado. Obrigada pela amizade e companheirismo! Tenho muito orgulho de ti e sei que meu trabalho estará em excelentes mãos! Amo-te!

Ao meu orientador, Dioguinho, por todos esses anos de amizade e orientação. Obrigada pela confiança! Obrigada por guiar esse trabalho que a cada dia me apaixona mais! Espero que ele abra um infinito de possibilidades e tomara que consigamos lidar com todas elas! Obrigada por tudo!

Por último, mas não menos importante, a todos os meus amigos de longa data por tornar meus dias mais leves e alegres! Ainda bem que existem as redes sociais para manter o contato diário com as pessoas queridas que, infelizmente, não podemos ver com frequência devido à rotina maluca de cada um.

Aos amigos do CTBM, obrigada pela amizade que foi se desenvolvendo cada vez mais depois que saímos do colégio. É lindo de pensar como essa amizade se tornou infinita depois de tantos anos! Obrigada por deixarem meus dias mais alegres durante esse período a cada meme visualizado! Amo vocês do fundo do meu coração!

Ao meu jardim de flores mais lindas da Bio, Cris, Liv, Renata e Simone (a Julinha tb!), obrigada pela amizade florida regada a cada dia com o mais profundo amor! Obrigada por terem deixado meus dias mais belos durante essa fase! Amo muito vocês! Ah, e ao Gabi por ter fornecido a melhor trilha sonora possível para escrita desta tese!

À minha maninha do coração, Rhani, pela amizade crescente desde a nossa infância! Apesar de tu estares do outro lado do mundo, o amor permanece constante (e a saudade também). Amo-te!

À vida, por todas as oportunidades! À natureza, por todas as possibilidades!

SUMÁRIO

PARTE I

RESUMO

O glioblastoma (GBM) é o mais comum dos tumores primários malignos que afetam o Sistema Nervoso Central (SNC), sendo um dos cânceres mais letais. A ressecção cirúrgica desse tumor é o tratamento de intervenção inicial mais utilizado nos pacientes. Embora a radioterapia e a quimioterapia aumente a sobrevida, a maioria dos pacientes chega ao óbito em até um ano após o diagnóstico. Além disso, os GBM estão entre os tumores mais resistentes à radiação e à quimioterapia. Dessa forma, torna-se imprescindível a busca de novas estratégias terapêuticas que visem à melhora da qualidade de vida dos pacientes e ao aumento do tempo de sobrevida. O glutamato (L-Glu) é o aminoácido encontrado em maior concentração no SNC e ele exerce seus papéis fisiológicos e patológicos através da ativação de receptores de membrana metabotrópicos e ionotrópicos. Diversos estudos *in vitro* e *in vivo* têm demonstrado que células de GBM liberam altos níveis de L-Glu para o meio extracelular, o que promove a sua proliferação e migração, contribuindo para a malignidade deste tipo de tumor. De fato, é provável que a ligação desse aminoácido aos receptores metabotrópicos de glutamato (mGluR) relacione-se com a agressividade dos GBM, visto que eles são amplamente expressos nestas células. Dessa forma, o objetivo desta tese foi investigar o papel dos mGluR sobre a agressividade de GBM, buscando uma assinatura gênica que tenha valor como potencial biomarcador prognóstico e preditivo de tratamento complementar adjuvante.

Através da uma meta-análise de duas coortes de amostras de GBM humanos foi possível identificar uma assinatura gênica de mGluR com valor prognóstico, na qual biópsias com alta expressão gênica de mGluR3 e baixa de mGluR4 e mGluR6 predizem um desfecho antecipado para os pacientes. O potencial desses receptores sobre a malignidade desses tumores foi avaliado por experimentos *in vitro* utilizando o tratamento de linhagens de GBM com ligantes de mGluR. O bloqueio farmacológico de mGluR do grupo II pelo antagonista LY341495 e a ativação farmacológica de mGluR III por L-AP4 diminuíram a porcentagem de células de linhagem de GBM em 25-28 %. A combinação desses tratamentos não apresentou efeito sinérgico. O potencial da assinatura gênica também foi avaliado *in vivo* utilizando ratos implantados ortotopicamente com células da linhagem C6 e tratados intracisternalmente com os ligantes de mGluR e intraperitonealmente com quimioterápico padrão, a temozolamida. Os resultados obtidos nos experimentos *in vivo*, apesar de preliminares, em relação ao tratamento com os ligantes de mGluR, são muito promissores, permitindo várias perspectivas em relação a adaptações de protocolo e a realização de experimentos complementares.

Este estudo demonstrou que a avaliação da expressão gênica de mGluR3, 4 e 6 em biópsias de GBM humanos possui um grande potencial prognóstico. A diminuição do número de células da linhagem C6 após o tratamento *in vitro* com ligantes de mGluR (LY341495 e L-AP4) está de acordo com o comportamento de agressividade previsto nos estudos *in silico*. Embora mais experimentos *in vitro* e *in vivo* sejam necessários para melhor avaliação do potencial dessa assinatura gênica de mGluR, os resultados obtidos indicam que a avaliação da expressão dos oito subtipos de mGluR em biópsias de GBM pode ser considerada em âmbito clínico para guiar futuras intervenções quimioterápicas.

ABSTRACT

Glioblastoma (GBM) is the most common malignant primary tumor of Central Nervous System (CNS) and one of the most lethal cancers. Surgical resection of this tumor is the most commonly initial intervention treatment used in patients. Although radiotherapy and chemotherapy increase survival, it is expected that the majority of patients will die within a year after diagnosis. In addition, GBM are among the most radiation- and chemotherapy-resistant tumors. Thus, it is imperative to search for new therapeutic strategies that aim to improve patients' quality of life and to increase survival time. Glutamate (L-Glu) is the amino acid found in higher concentration in CNS and it exerts its physiological and pathological roles through the activation of metabotropic and ionotropic membrane receptors. Several studies have demonstrated *in vitro* and *in vivo* that GBM cells release high levels of L-Glu into extracellular medium. This event was shown to promote GBM proliferation and migration, contributing to the malignancy of this type of tumor. Indeed, it is likely that the binding of that amino acid to metabotropic glutamate receptors (mGluR) relates to GBM aggressiveness, since they are widely expressed in these cells. Thus, the objective of this work was to investigate the role of mGluR on GBM aggressiveness, searching for a gene signature that has potential value as biomarker to predict the prognosis and adjuvant complementary treatment.

Through the meta-analysis of two GBM human samples cohorts, it was possible to identify an mGluR gene signature with prognostic value, in which biopsies with high mGluR3 and low mGluR4 and mGluR6 gene expression predict an early outcome for patients. The potential of these receptors on the malignancy of these tumors was assessed by *in vitro* experiments through the treatment of GBM lineages with mGluR ligands. Pharmacological blockade of group II mGluR by LY341495 and pharmacological activation of group III mGluR by L-AP4 decreased the amount of C6 cells in 25-28 %. The combination of these treatments had no synergistic effect. The potential of the gene signature was also assessed *in vitro* using GBM-implanted rats treated intracisternally with mGluR ligands and intraperitoneally with standard chemotherapy, temozolomide. The results obtained in *in vivo* experiments, although very preliminary in relation to treatment with the mGluR ligands, are very promising, allowing several perspectives regarding protocol adaptations and the accomplishment of complementary experiments.

This study demonstrated that evaluation of mRNA levels of mGluR3, 4, and 6 in human GBM biopsies has a great prognostic potential. The decrease in number of C6 cells after *in vitro* treatment with mGluR ligands (LY341495 and L-AP4) is in accordance with the predicted aggressiveness behavior proposed *in silico.* Although further *in vitro* and *in vivo* experiments are required for better evaluation of mGluR gene signature potential, these results indicate that evaluation of the eight mGluR subtypes in GBM biopsies may be considered in clinical scope to guide future chemotherapeutic interventions.

APRESENTAÇÃO

No capítulo I, encontra-se uma revisão, já publicada em Janeiro de 2017 na Revista *Oncotarget*, avaliando os dados recentes da literatura sobre o potencial envolvimento da sinalização intracelular mediada por mGluR na progressão, agressividade e recorrência de tumores cerebrais malignos.

No capítulo II, encontra-se um estudo de metanálise utilizando duas coortes de pacientes, no qual foi observado uma promissora relação entre a expressão gênica de três subtipos de mGluR (*GRM3, GRM4 e GRM6*) e a sobrevida média de pacientes portadores de GBM. Esta associação foi observada através de uma análise de cluster hierárquico com base na expressão gênica de cada mGluR nas biópsias de GBM. A verificação do potencial dos receptores candidatos sobre a agressividade de GBM foi avaliada experimentalmente por estudos *in vitro* utilizando o tratamento de linhagens com ligantes de mGluR.

No capítulo III, encontra-se um artigo original descrevendo um protocolo alternativo de injeção intracisternal (cisterna cerebelomedular), o qual foi padronizado para a verificação *in vivo* do potencial dos receptores candidatos sobre a agressividade de GBM (Anexo).

LISTA DE ABREVIATURAS

Akt/PKB: Proteína cinase B
AMPAR: Receptor α-amino-3-hidroxi-5-metil-4-isoxazolepropionato
BCNU: *Carmustine*
BMP: B*one morphogenic proteins*
CNS: *Central Nervous System*
CSF: *Cerebrospinal fluid*
CTGBM: Células tronco de glioblastoma
GBM: Glioblastoma
DNA: *Deoxyribonucleic acid*
DMEM: *Dulbecco's Modified Eagle's medium*
EAAT2: Transportador de aminoácidos excitatórios do tipo 2
EGF: *Epidermal growth factor*
EGFR: *Epidermal growth factor receptor*
EUA: Estados Unidos da América
FBS: *Fetal Bovine Serum*
FDA: *US Food and Drug Administration*
[^{18}F]FDG: *Fludeoxyglucose* (^{18}F)
GluR: Receptores de Glutamato (*Glutamate receptors*)
HBSS: *Hank's balanced salt solution*
HR: *Hazard ratios*
iGluR: Receptores ionotrópicos de glutamato (*ionotropic glutamate receptors*)
INCA: Instituto Nacional do Câncer José de Alencar Gomes da Silva
IP3: inositol 1,4,5-trifosfato
KM: *Kaplan-Meier*
KPS: *Karnofsky Performance status*
L-Glu: L-glutamato (*L-Glutamate*)
MAPK: *Mitogen-activated protein kinase*
mGluR: Receptores metabotrópicos de glutamato (*metabotropic glutamate receptors*)
MGMT: O6-metilguanina-DNA-metiltransferase
MRI: *Magnetic resonance imaging*
mTOR: *Mechanistic target of rapamycin*
NF-κB: *Nuclear factor-kappaB*
NMDAR: Receptor N-metil-D-aspartato
OMS: Organização Mundial da Saúde
PI3K: *Phosphatidylinositol-4,5-bisphosphate 3-kinase*
PKC: Proteína cinase C
RT: *Room temperature*
SNC: Sistema nervoso central
SRB: *Sulforhodamine B*
SUV : *Standard uptake value*
TMZ: Temozolamida (*Temozolamide*)

INTRODUÇÃO

1. Tumores que afetam o Sistema Nervoso Central (SNC)

Dados epidemiológicos

Os tumores que afetam o Sistema Nervoso Central (SNC) representam menos de 2% de todas as neoplasias (**Tabela 1**) (Ferlay et al., 2015; GLOBOCAN, 2012). Apesar de este tipo de tumor ser relativamente raro, ele apresenta um amplo espectro de efeitos adversos, contribuindo de forma significativa para a mortalidade no mundo inteiro, e muitas vezes o prognóstico é deficiente (INCA, 2015; Ohgaki and Kleihues, 2005). A incidência tende a ser maior em países desenvolvidos e em desenvolvimento (**Fig. 1**), principalmente devido a um melhor acesso às tecnologias de diagnóstico e a uma melhor apuração de dados nessas regiões (Ohgaki and Kleihues, 2005). A melhora da tecnologia, principalmente no que tange aos exames menos invasivos (tomografia computadorizada, ressonância magnética e tomografia por emissão de pósitrons), também influencia nas taxas de incidência e mortalidade desta neoplasia, as quais têm aumentado durante os últimos anos (INCA, 2015).

Tabela 1 - Estimativas globais de incidência, mortalidade e prevalência dos tumores que afetam o SNC. Adaptado de GLOBOCAN (2012).

	Incidência[a]			Mortalidade[a]			Prevalência em 5 anos[a]		
	Número de casos	%[b]	Taxa idade-padronizada (TIP)[c]	Número de casos	%[b]	Taxa idade-padronizada (TIP)[c]	Número de casos	%[b]	Taxa idade-padronizada (TIP)[c]
Homens	139.608	1,9	3,9	106.376	2,3	3,0	190.011	1,2	7,3
Mulheres	116.605	1,8	3,0	83.006	2,3	2,1	152.903	0,9	5,9
Ambos os sexos	256.213	1,8	3,4	189.382	2,3	2,5	342.914	1,1	6,6

[a] Dados de incidência e mortalidade representativos de todas as idades. Prevalência em 5 anos representativo apenas para a população adulta.
[b] Porcentagem em relação a todas as neoplasias, exceto câncer de pele não melanoma.
[c] Taxa bruta (TB) é o número de novos casos ou óbitos por 100 mil pessoas por ano. Taxa idade-padronizada (TIP) é a taxa que a população teria se apresentasse uma estrutura etária padrão. Essa padronização é necessária quando se comparam várias populações que diferem em relação à idade, porque a idade tem uma forte influência sobre o risco de câncer.

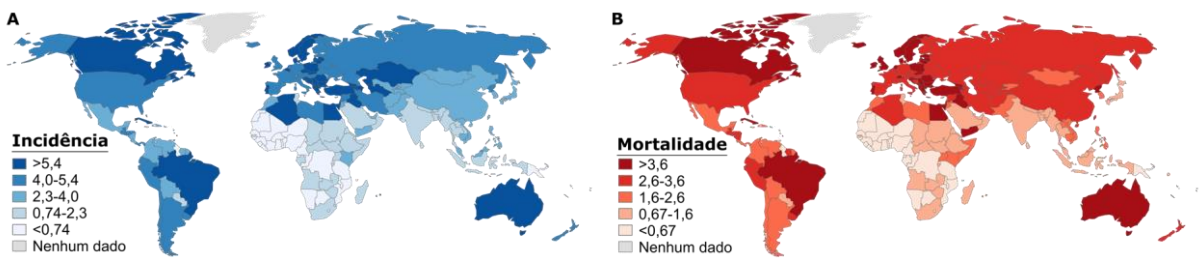

Fig. 1 – Representação espacial das taxas idade-padronizadas (TIP) de incidência (A) e de mortalidade (B) globais dos tumores que afetam o SNC ajustadas pela população mundial padrão (100 mil pessoas/ano). Adaptado de GLOBOCAN (2012).

As taxas globais de mortalidade (2,5/100 mil pessoas) são similares às de incidência (3,4/100 mil pessoas), o que indica que um pior prognóstico pode ser previsto para a maioria das

pessoas que desenvolvem esses tumores. Com base na estimativa mundial realizada pelo projeto GLOBOCAN (2012), a incidência dos tumores que afetam o SNC é ligeiramente mais alta no sexo masculino (3,9/100 mil homens) em comparação ao sexo feminino (3,0/100 mil mulheres) (**Tabela 1**), sendo o 14º tipo de câncer que mais afeta os homens e o 15º mais frequente em mulheres (**Fig. 2**). Em 2020 são estimados em torno de 300 mil novos casos de tumores que afetam o SNC e mais de 225 mil óbitos em decorrência destas neoplasias.

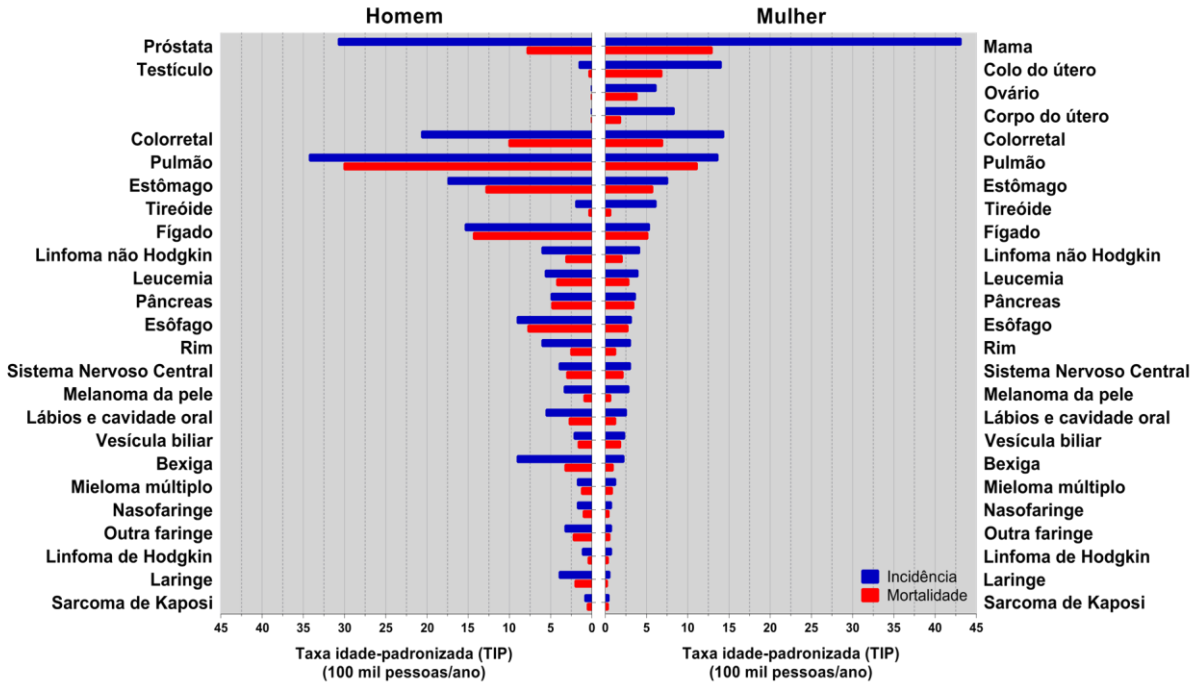

Fig. 2 – Gráfico comparativo das taxas de incidência e mortalidade globais entre homens e mulheres diagnosticados com câncer. Taxas padronizadas pela idade (TIP) e ajustadas pela população mundial padrão (100 mil pessoas/ano). Adaptado de GLOBOCAN (2012).

No Brasil, de acordo com a estimativa do Instituto Nacional do Câncer José de Alencar Gomes da Silva (INCA, 2015), o risco estimado para novos casos desses tumores em 2016 foi de 10,18/100 mil pessoas (5,50/100 mil homens e 4,68/100 mil mulheres) (**Tabela 2**), sendo a 10ª neoplasia mais comum neste país tanto no sexo feminino quanto masculino (**Tabela 3**). As taxas de incidência são mais altas nas regiões sul e sudeste (**Fig. 3**) e especificamente no Rio Grande do Sul são o 5º tipo de câncer mais frequente nas mulheres e o 8º nos homens, com uma taxa bruta para ambos os sexos de 20,74/100 mil pessoas (**Tabela 2**). De acordo com as informações obtidas pelo projeto GLOBOCAN (2012), em 2020 são estimados para o Brasil 14.045 novos casos de tumores que afetam o SNC, assim como 11.851 mortes de pacientes diagnosticados com este tipo de câncer.

Tabela 2 – Estimativas de incidência e número de novos casos de tumores que afetam o SNC no Brasil[a]. Adaptado de INCA (2016).

	Homens				Mulheres				Ambos os sexos			
	Estados		Capitais		Estados		Capitais		Estados		Capitais	
	Nº de casos	Taxa Bruta (TB)	Nº de casos	Taxa Bruta (TB)	Nº de casos	Taxa Bruta (TB)	Nº de casos	Taxa Bruta (TB)	Nº de casos	Taxa Bruta (TB)	Nº de casos	Taxa Bruta (TB)
Brasil	5.440	5,5	1.290	5,86	4.830	4,68	1.250	5,2	10.270	10,18	2.540	11,06
RS	630	11,45	70	9,97	540	9,29	80	9,98	1170	20,74	150	19,95

[a] Números arredondados para múltiplos de 10.
[b] Taxa bruta (TB) é o número de novos casos por 100 mil pessoas por ano (não padronizada pela idade).

Tabela 3 - Distribuição proporcional dos 10 tipos de neoplasias mais incidentes no Brasil em ambos os sexos, exceto câncer de pele não melanoma. Adaptado de INCA (2016).

Homens			Mulheres		
Localização primária	**Número de casos***	**%**	**Localização primária**	**Número de casos***	**%**
Próstata	61.200	28,6	Mama feminina	57.960	28,1
Traquéia, brônquio e pulmão	17.330	8,1	Cólon e reto	17.620	8,6
Cólon e reto	16.660	7,8	Colo do útero	16.340	7,9
Estômago	12.920	6,0	Traquéia, brônquio e pulmão	10.890	5,3
Cavidade oral	11.140	5,2	Estômago	7.600	3,7
Esôfago	7.950	3,7	Corpo do útero	6.950	3,4
Bexiga	7.200	3,4	Ovário	6.150	3,0
Laringe	6.360	3,0	Glândula tireóide	5.870	2,9
Leucemias	5.540	2,6	Linfoma não Hodgkin	5.030	2,4
Sistema nervoso central	5.440	2,5	Sistema nervoso central	4.830	2,3

* Números arredondados para múltiplos de 10.

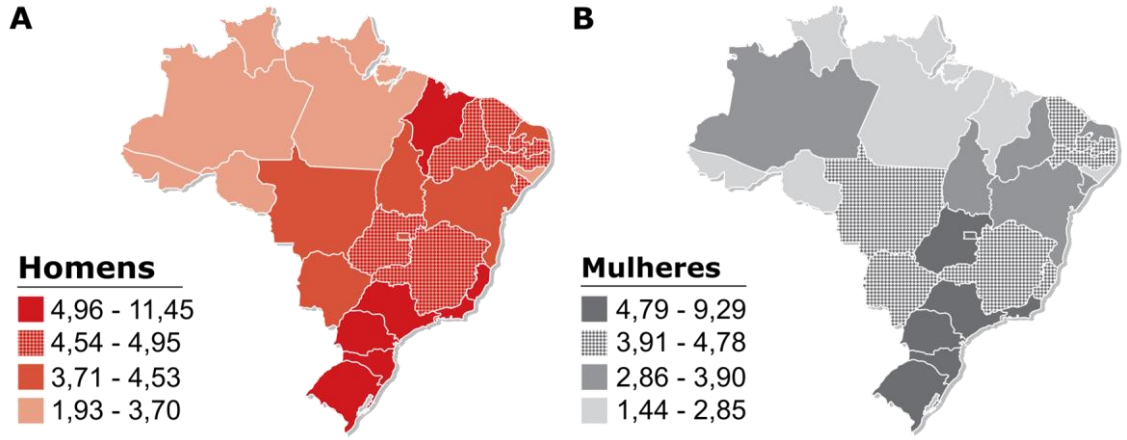

Fig. 3 – Representação espacial das taxas brutas de incidência dos tumores que afetam o SNC nas regiões do Brasil em homens (A) e mulheres (B) (100 mil pessoas/ano). Adaptado de INCA (2016).

Classificação dos tumores que afetam o SNC

Ao contrário de outros tipos de câncer, os tumores que afetam o SNC não apresentam estadiamento (Ostrom et al., 2015). De acordo com a Organização Mundial da Saúde (OMS), sua classificação é representada por uma escala de malignidade dessas neoplasias (Louis et al., 2007). Tumores de grau I representam lesões com potencial proliferativo baixo e com possibilidade de cura após ressecção cirúrgica. Neoplasias de grau II naturalmente se infiltram nos tecidos cerebrais adjacentes e, apesar de sua baixa atividade proliferativa, geralmente retornam após ressecção cirúrgica. Alguns desses tumores tendem a progredir a graus mais elevados de malignidade. A designação grau III é geralmente reservada a lesões com evidências histológicas de malignidade, incluindo atipia nuclear e uma rápida atividade proliferativa.

Tumores de grau IV são neoplasias citologicamente malignas com alta atividade mitótica e presença de necrose, as quais estão associadas a uma rápida evolução da doença pré- e pós-operatória levando, geralmente, ao óbito. Algumas neoplasias de grau IV também se caracterizam pela infiltração generalizada do tecido circundante, assim como por uma propensão à disseminação cranioespinhal (Louis et al., 2007).

Os tumores primários malignos que afetam o SNC estão entre os mais temidos tipos de câncer, não somente pelo prognóstico deficiente, mas também pelas repercussões diretas na qualidade de vida dos pacientes e na sua função cognitiva (Omuro and DeAngelis, 2013). Estudos demonstram que mais de 117.000 pacientes foram diagnosticados com estes tipos de tumores nos EUA entre 2008-2012, totalizando 32,8 % dos pacientes que apresentaram tumores primários que afetam o SNC neste período (**Fig. 4**) (Ostrom et al., 2015).

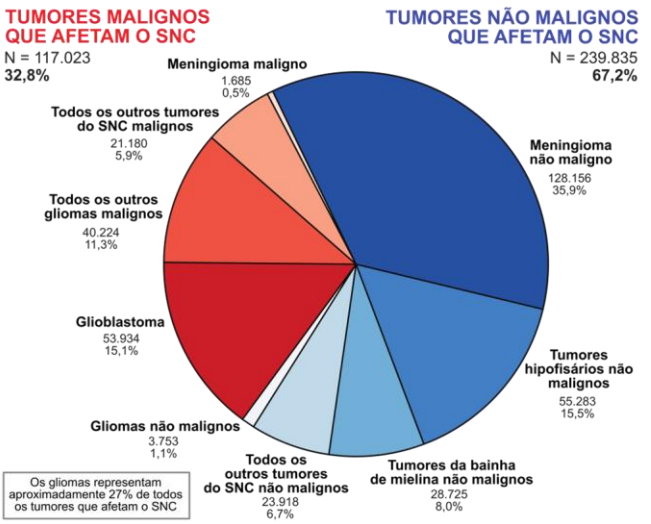

Fig. 4 – Distribuição dos tumores primários malignos e não malignos que afetam o SNC nos EUA entre 2008-2012 (N=356.858 pessoas). Adaptado de Ostrom et al., (2015).

2. Gliomas

Dados epidemiológicos

Os gliomas são o tipo histológico mais frequente dos tumores primários que afetam o SNC, (Dai and Holland, 2001), representando, entre 2008-2012 nos EUA, aproximadamente 27 % de todas estas neoplasias (**Fig. 4**) (Ostrom et al., 2015). Os gliomas malignos, os quais compreendem os gliomas de grau III e grau IV, representam 80 % dos pacientes diagnosticados com tumores malignos que afetam o SNC, com uma incidência de 17.000 novos casos ao ano nos EUA (Ostrom et al., 2015). Estes tumores são mais comuns em pessoas da terceira idade entre 60-80 anos e é esperado que o número de pacientes aumente de acordo com o envelhecimento da população (Ostrom et al., 2015).

Origem, fatores de risco e prevenção

Estas neoplasias originam-se de células gliais, como por exemplo, astrócitos e oligodendrócitos, ou de suas células progenitoras e células associadas à vascularização e às meninges (Dai and Holland, 2001). A maioria dos gliomas ocorre nos lobos frontal, temporal, parietal e occipital (60,8%), sendo que apenas uma pequena proporção ocorre fora do cérebro (Ostrom et al., 2015).

Somente a exposição à radiação e algumas síndromes genéticas são consideradas fatores de risco bem definidos para o desenvolvimento de gliomas. A radiação ionizante é um fator de risco ambiental e sua associação foi demonstrada, principalmente, em estudos com crianças que receberam irradiação no crânio para terapia de câncer e em indivíduos expostos a bombas atômicas e testes de armas nucleares (Bondy et al., 2008). As síndromes hereditárias que estão associadas ao desenvolvimento de gliomas incluem: *Cowden*, *Turcot*, *Li-Fraumeni*, neurofibromatose do tipo 1 e 2 e esclerose tuberosa (Gu et al., 2009; Hottinger and Khakoo, 2007). Uma história familiar de glioma é raramente observada, porém, quando presente, está associada ao aumento em dobro do risco de se desenvolver este tipo de tumor (Omuro and DeAngelis, 2013).

O risco de desenvolvimento de gliomas não é aumentado por: exposição a telefones celulares e outros tipos de campos eletromagnéticos, ferimentos na cabeça, ingestão de comidas contendo compostos N-nitrosos ou aspartame, uso de pesticidas, etc (Omuro and DeAngelis, 2013). Além disso, os gliomas estão inversamente relacionados à presença de doenças atópicas como, por exemplo, asma, eczema e rinite alérgica (Linos et al., 2007). Medidas preventivas, como, por exemplo, mudanças no estilo de vida, não são suficientes para a prevenção de gliomas. Diagnóstico e tratamento precoce não melhoram o desfecho, impedindo a utilização de *screening* para esta doença (Omuro and DeAngelis, 2013).

Classificação dos gliomas

Durante o último século, a nosologia dos tumores cerebrais foi amplamente baseada em conceitos de histogênese, na qual essas neoplasias eram classificadas de acordo com suas

semelhanças microscópicas com prováveis células de origem e seus respectivos níveis de diferenciação (Louis et al., 2007). Dessa forma, a classificação dos tumores do SNC realizada pela OMS em 2007 agrupou todos os gliomas com um fenótipo astrocitário separadamente daqueles que apresentavam um fenótipo oligodendroglial, independente do fato de vários astrocitomas serem clinicamente similares ou discrepantes entre si (Louis et al., 2016).

Em 2016 a OMS fez uma atualização da classificação dos tumores cerebrais de 2007, na qual pela primeira vez foram utilizados parâmetros moleculares para complementar os dados histológicos (**Tabela 4**) (Louis et al., 2016). Logo, a partir de 2016 todos os gliomas difusamente infiltrantes, sejam fenotipicamente astrocíticos ou oligodendrogliais, estão agrupados juntos. A classificação dos gliomas difusos é baseada no padrão de comportamento e crescimento desses tumores e também em mutações genéticas compartilhadas, principalmente nos genes *IDH1* e *IDH2* (Isocitrato desidrogenase I e II, respectivamente). Resumidamente, os astrocitomas difusos são agora nosologicamente mais semelhantes aos oligodendrogliomas que aos astrocitomas pilocíticos: as árvores genealógicas foram redesenhadas (Louis et al., 2016).

Tabela 4 - Classificação e graduação da maioria dos gliomas segundo a Organização Mundial da Saúde (OMS) em 2016. Modificado de Louis et al., (2016).

		Grau			
		I	**II**	**III**	**IV**
Astrocitomas e oligodendrogliomas difusos	Astrocitoma difuso, *IDH*-mutante		x		
	Astrocitoma anaplásico, *IDH*-mutante			x	
	Glioblastoma, *IDH*-selvagem				x
	Glioblastoma, *IDH* mutante				x
	Glioma difuso de linha média, H3 K27M-mutante				x
	Oligodendroglioma, *IDH*-mutante e 1p/19q-codeletado		x		
	Oligodendroglioma, *IDH*-mutante e 1p/19q-codeletado			x	
Outros astrocitomas	Astrocitoma pilocítico	x			
	Astrocitoma subependimal de células gigantes	x			
	Xantoastrocitoma pleomórfico		x		
	Xantoastrocitoma pleomórfico anaplásico			x	
Ependimomas	Subependimoma	x			
	Ependimoma Mixopapilar	x			
	Ependimoma		x		
	Ependimoma, *RELA* fusão-positiva		x	x	
	Ependimoma anaplásico			x	
Outros gliomas	Glioma angiocêntrico	x			
	Glioma cordoide do terceiro ventrículo		x		

Devido à sua alta incidência e relevância clínica, neste trabalho será dada uma maior ênfase ao glioblastomas (GBM), um astrocitoma difuso de grau IV.

2.1. Glioblastoma (GBM)

Dados epidemiológicos dos GBM

O GBM é o mais comum dos tumores primários malignos que afetam o SNC, sendo um dos cânceres humanos mais letais (Cloughesy et al., 2014; Omuro and DeAngelis, 2013). A incidência anual global desta neoplasia é estimada em 3/100 mil pessoas (Gramatzki et al., 2016). Para muitos países europeus, os GBM representaram mais de 30 % dos tumores que afetam o SNC entre 1995-2002 (**Tabela 5**) (Sant et al., 2012).

Tabela 5 – Número de casos e porcentagem de distribuição em alguns países europeus de tumores que afetam o SNC diagnosticados entre 1995-2002. Adaptado de Sant et al., (2012).

País	Nº de casos	E + TPC	ANOS + OT	AA	AP	GBM	OD	ODA	OG	TNG	PNET + MDB	M	N	TVS	NE
Alemanha	987	1,6	3,7	1,0	1,1	35,8	1,8	1,1	6,3	1,5	0,8	36,3	5,7	1,6	1,7
Áustria	3.328	2,6	15,7	2,4	1,3	52,8	1,3	0,6	5,8	0,4	3,3	9,2	2,6	0,2	1,8
Bélgica	2.461	2,8	17,1	5,7	1,7	32,8	4,5	1,5	3,5	0,5	1,0	24,6	0,9	2,9	0,5
Escócia	2.478	2,3	10,4	5,2	1,5	43,3	3,5	2,2	7,1	0,9	1,1	12,4	5,6	2,6	1,9
Eslováquia	1.887	2,8	17,5	14,6	2,1	20,8	3,3	1,6	1,8	0,3	0,6	28,9	4,9	0,3	0,5
Eslovênia	689	2,6	5,8	10,2	3,6	57,9	5,5	3,8	3,9	1,0	2,3	2,2	0,3	0,0	0,9
Espanha	1.338	4,0	23,8	8,1	2,1	34,3	3,2	0,7	8,6	1,0	2,1	9,7	0,4	0,3	1,7
França	808	1,5	13,8	3,8	1,4	43,6	13,6	1,7	7,4	0,4	1,6	7,9	2,1	0,5	0,7
Holanda	2.850	3,1	31,7	6,5	1,6	29,3	5,3	1,9	5,5	0,5	1,5	10,4	2,0	0,5	0,2
Inglaterra	16.523	2,2	11,6	4,2	0,9	33,2	2,9	1,2	7,1	0,6	0,7	21,4	11,2	1,5	1,3
Irlanda	2.190	1,8	12,0	9,2	1,6	31,2	2,6	1,2	4,2	0,4	0,9	19,6	12,5	2,2	0,6
Irlanda do Norte	637	5,2	22,8	5,8	0,9	24,3	2,2	3,6	7,4	0,9	1,0	14,3	6,3	1,4	3,9
Islândia	209	1,9	10,0	4,8	2,9	30,6	2,4	0,0	1,0	1,0	0,5	39,7	3,8	1,4	0,0
Itália	6.355	2,7	9,0	6,7	0,6	39,2	3,9	1,0	6,7	0,6	1,2	23,5	2,7	1,1	1,1
Malta	202	1,5	7,9	7,4	1,0	26,2	1,5	0,5	5,9	1,0	0,5	39,1	4,5	0,5	2,5
Noruega	3.723	2,2	5,8	3,9	1,3	29,3	3,0	1,4	7,0	0,8	1,2	30,9	8,2	2,2	2,8
País de Gales	796	1,6	16,2	6,0	0,5	36,7	5,0	0,9	21,6	0,3	2,3	4,2	0,6	0,5	3,6
Polônia	1.313	3,0	19,6	5,8	0,6	31,8	3,6	1,8	13,2	0,5	3,1	12,5	0,8	1,3	2,4
Portugal	481	4,2	20,0	4,6	2,3	43,4	6,9	5,2	5,6	0,8	1,2	3,1	0,2	0,6	1,9
República Checa	329	0,9	16,1	10,3	1,5	45,3	1,8	1,8	9,8	0,9	0,9	6,7	0,9	2,2	0,9
Suécia	8.289	2,5	5,1	10,6	1,2	18,1	2,2	1,0	5,6	0,7	0,9	35,1	13,1	2,7	1,2
Suíça	771	2,2	15,3	8,4	2,0	52,1	5,2	2,6	3,9	0,4	1,3	4,9	0,9	0,5	0,3
Total	58.644	2,5	12,2	6,3	1,2	33,1	3,3	1,3	6,5	0,6	1,2	21,6	7,2	1,6	1,4

E + TPC = Ependimomas e tumores do plexo coroide; ANOS + OT= Astrocitoma não especificado e outros subtipos; AA = Astrocitoma anaplásico; AP = Astrocitoma pilocítico; GBM = Glioblastoma; OD = Oligodendroglioma; ODA = Oligodendroglioma anaplásico; OG = Outros gliomas; TNG = Tumores não gliomas; PNET + MDB = Tumor primitivo neuroectodermal e meduloblastoma; M = Meningioma; N = Neurinoma; TVS = Tumores dos vasos sanguíneos e NE = Morfologia não especificada.

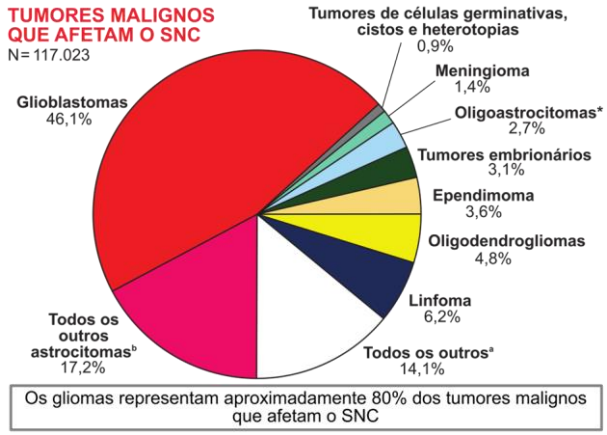

Fig. 5 – Distribuição dos tumores primários malignos que afetam o SNC por histologia (n=117.023). Dados avaliados nos EUA entre 2008-2012.Adaptado de Ostrom et al., (2015).

a. Inclui glioma maligno, não-identificados, tumores do plexo coróide, outros tumores neuroepiteliais, tumores mistos neurogliais, tumores da região pineal, tumores da bainha de mielina, outros tumores de nervos cranianos e da coluna vertebral, tumores mesenquimais, lesões melanocíticas primárias, outras neoplasias relacionados às meninges, outras neoplasias hematopoiéticas e hemangioma. b. Inclui astrocitoma pilocítico, astrocitoma difuso, astrocitoma anaplásico astrocitomas variantes.

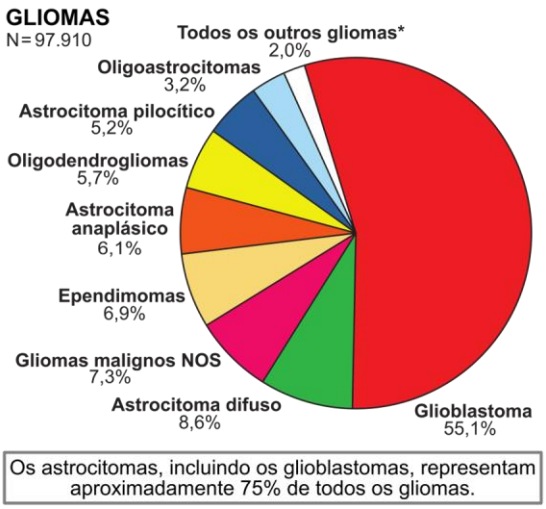

Fig. 6 – Distribuição dos gliomas primários por histologia (n=97.910). Dados avaliados nos EUA entre 2008-2012.Adaptado de Ostrom et al., (2015).

* Inclui astrocitomas variantes, outros tumores neuroepiteliais e tumores neuro-gliais mistos. NOS = Não identificados

Entre os anos de 2008-2012 nos EUA, os GBM foram responsáveis por 15,1 % de todos os tumores primários que afetam o SNC (**Fig. 4**), por 46,1 % de todos os tumores primários malignos que afetam o SNC (**Fig. 5**) e pela maioria dos gliomas primários (55,1 %) (**Fig. 6**). Quando combinados a outros astrocitomas, esses tumores representaram aproximadamente 75 % de todos os gliomas neste país (**Fig. 6**) (Ostrom et al., 2015).

Nos EUA, a taxa de incidência dos GBM entre 2008-2012 foi a maior em relação aos demais tumores cerebrais malignos analisados no estudo, 3,2/100 mil pessoas (**Tabela 6**), sendo o 4º mais frequente na faixa etária de 35-44 anos, o 3º aos 45-54 anos e o 2º mais predominante em pessoas acima de 55 anos (Ostrom et al., 2015). Em 2016, foram previstos 12.120 novos casos para este país.

Tabela 6 – Número total, média anual e taxas anuais padronizadas pela idade de casos de glioblastomas ocorridos nos EUA entre 2008-2012 de acordo com o gênero. Adaptado de Ostrom et al., (2015).

	Número total de casos (2008-2012)	Média anual[a]	Taxa idade- padronizada (TIP)[b]	95% Intervalo de confiança (IC)
Total	53.934	10.787	3,20	(3,17-3,22)
Homens	30.955	6.191	3,99	(3,94-4,03)
Mulheres	22.979	4.596	2,53	(2,50-2,56)

[a] Calculada divindindo-se o número total de casos em 5 anos (2008-2012) por 5.
[b] Taxa bruta (TB) é o número de novos casos por 100 mil pessoas por ano. Taxa idade-padronizada (TIP) é a taxa que a população teria se apresentasse uma estrutura etária padrão.

Tabela 7 – Número total, média anual e taxas anuais padronizadas pela idade de casos de glioblastomas ocorridos nos EUA entre 2008-2012 de acordo com a raça[a]. Adaptado de Ostrom et al., (2015).

	Número total de casos (2008-2012)	Média anual[b]	Taxa idade- padronizada (TIP)[c]	95% Intervalo de confiança (IC)
Brancos	48.942	9.788	3,45	(3,42-3,48)
Negros	3.165	633	1,76	(1,70-1,82)
Índios americanos/Nativos do Alasca	193	39	1,54	(1,31-1,79)
Asiáticos/Ilhéus do Pacífico	1.187	237	1,59	(1,50-1,69)

[a] Indivíduos com raça não identificada foram excluídos (n=2.176)
[b] Calculada divindindo-se o número total de casos em 5 anos (2008-2012) por 5.
[c] Taxa bruta (TB) é o número de novos casos ou por 100 mil pessoas por ano. Taxa idade-padronizada (TIP) é a taxa que a população teria se apresentasse uma estrutura etária padrão.

Tabela 8 – Taxa de incidência[a] especificadas por faixa etária de casos de glioblastomas ocorridos nos EUA entre 2008-2012. Adaptado de Ostrom et al., (2015).

0-19 anos	20-34 anos	35-44 anos	45-54 anos	55-64 anos	65-74 anos	75-84 anos	85+ anos
TIP (95%IC)	TIP (95%IC)	TIP (95%IC)	TIP (95%IC)	TIP (95%IC)	TIP (95%IC)	TIP (95%IC)	TIP (95%IC)
0,16 (0,15-0,17)	0,42 (0,40-0,45)	1,21 (1,16-1,25)	3,54 (3,47-3,62)	8,08 (7,95-8,21)	13,05 (12,84-13,27)	15,24 (14,94-15,54)	9,12 (8,77-9,48)

[a] Taxa bruta (TB) é o número de novos casos ou óbitos por 100 mil pessoas por ano. Taxa idade-padronizada (TIP) é a taxa que a população teria se apresentasse uma estrutura etária padrão.

No período entre 2008-2012, os GBM diagnosticados nos EUA foram 1,6 vezes mais comuns em homens (**Tabela 6**) e a taxa de incidência foi aproximadamente duas vezes maior entre pessoas brancas quando comparadas às negras (**Tabela 7**) (Ostrom et al., 2015). Neste mesmo país e período, a incidência destes tumores aumentou com a idade, com taxas maiores entre 75-84 anos (**Tabela 8**). Entretanto, a idade mediana para ocorrência deste tumor foi de 64

anos (Ostrom et al., 2015).

Apesar de a sobrevida ser prolongada pela radioterapia realizada após a cirurgia, a história clínica dos pacientes portadores de GBM é curta, visto que a maioria chega ao óbito em até um ano após o diagnóstico (DeAngelis, 2001). O óbito ocorre por recorrência do crescimento tumoral local e invasão cerebral (Kleihues and Cavenne, 2000). Nos países europeus, entre os anos 2000-2002, os pacientes com GBM apresentam um pior prognóstico em relação aos pacientes com outros tipos de tumores cerebrais (**Tabela 9**), sendo que a taxa estimada de sobrevivência após 5 anos do diagnóstico foi de 2,7 % (Sant et al., 2012).

Tabela 9 - Taxa de sobrevida* estimada dos pacientes após 5 anos do diagnóstico de alguns tumores que afetam o SNC nas regiões europeias entre 2000-2002. Adaptado de Sant et al., (2012).

Grupo Morfológico	Norte Europeu	Reino Unido e Irlanda	Europa Central	Europa Oriental	Sul Europeu	Todos os casos
Ependimoma e Tumores do plexo coroide	86,3 (77,5-92,3)	84,8 (77,0-90,5)	83,8 (69,5-92,7)	66,5 (47,6-80,5)	88,1 (74,7-95,6)	83,5 (79,0-87,3)
Astrocitoma não especificado e outros subtipos	49,4 (42,7-55,8)	39,0 (34,7-43,3)	35,4 (29,9-40,9)	28,0 (22,5-33,8)	42,6 (33,9-51,1)	38,5 (35,9-41,1)
Astrocitoma anaplásico	10,8 (7,8-14,4)	17,6 (13,5-22,2)	28,8 (19,3-39,0)	11,7 (7,1-17,4)	18,1 (11,8-25,4)	15,8 (13,6-18,2)
Astrocitoma pilocítico	81,9 (68,4-90,3)	80,6 (68,4-88,6)	79,7 (62,6-89,9)	57,3 (33,5-75,8)	97,3 (74,7-100,0)	80,5 (74,1-85,6)
Glioblastoma	1,9 (1,2-2,9)	2,2 (1,6-2,9)	4,4 (3,2-5,9)	2,2 (1,0-4,4)	2,8 (1,8-4,3)	2,7 (2,3-3,2)
Oligodendroglioma	74,1 (64,4-81,8)	65,8 (57,5-73,0)	75,5 (61,8-85,2)	47,8 (32,4-62,0)	63,8 (51,4-74,1)	67,2 (62,5-71,6)
Oligodendroglioma anaplásico	35,1 (21,2-49,5)	35,5 (24,4-46,9)	29,7 (13,4-48,3)	6,1 (1,3-16,6)	33,3 (14,7-53,6)	31,5 (25,0-38,3)
Outros gliomas	46,6 (40,5-52,6)	39,4 (34,2-44,7)	38,5 (30,4-46,7)	20,9 (12,6-30,9)	27,0 (18,3-36,6)	38,5 (35,4-41,7)
Tumores não gliomas	88,1 (66,8-97,7)	54,5 (36,2-70,2)	51,7 (24,9-74,7)	51,1 (10,4-83,8)	69,5 (35,6-91,1)	64,0 (53,0-73,5)
Tumor primitivo neuroectodermal e meduloblastoma	48,9 (33,7-62,7)	53,1 (37,8-66,4)	53,2 (37,6-67,1)	11,8 (2,7-28,2)	30,7 (13,9-49,4)	44,9 (37,6-52,0)
Meningioma	93,4 (91,3-95,2)	85,9 (82,8-88,7)	89,0 (83,6-93,5)	79,5 (73,1-85,0)	84,2 (79,7-88,2)	88,7 (87,2-90,0)
Neurinoma	98,3 (95,7-100,0)	97,6 (94,6-99,7)	90,0 (76,5-97,8)	80,2 (63,1-91,3)	89,1 (75,4-96,9)	96,5 (94,7-98,0)
Tumor dos vasos sanguíneos	95,8 (88,5-99,6)	93,5 (85,1-98,5)	75,7 (22,1-97,1)	52,2 (21,7-77,3)	100,0 (-)	93,1 (88,2-96,6)
Morfologia não especificada	70,7 (55,3-82,5)	22,3 (12,5-34,4)	35,0 (19,3-51,9)	12,4 (2,8-30,4)	40,4 (21,9-59,0)	38,7 (31,5-45,9)

*Taxa de sobrevida representada em % (95 % de intervalo de confiança).

Ostrom et al., (2015) demonstrou que nos EUA (1995-2012) a taxa de sobrevida para os pacientes com GBM é um pouco maior que a europeia: 5,1 % após 5 anos do diagnóstico. Em Cantão de Zurique, a mediana de sobrevida entre os anos 1980-1994 foi de apenas 4,9 meses. O estudo de outra coorte de pacientes deste mesmo local entre os anos 2005-2009 mostrou um aumento da mediana de sobrevida, a qual passou a ser de 11,5 meses. Este melhor prognóstico deve-se principalmente a melhoras no diagnóstico e na terapia durante esses anos, visto que a partir de 2005 o tratamento com o quimioterápico padrão, temozolamida, tornou-se disponível neste local para o tratamento destes tumores (Gramatzki et al., 2016).

Em pacientes com GBM, há uma correlação negativa entre idade de diagnóstico e o

desfecho dos pacientes, ou seja, quanto mais avançada é a idade, menor é o tempo de sobrevida (**Fig. 7B**). Não há uma correlação entre o gênero e o tempo de sobrevida dos pacientes (**Fig. 7A**) (Gramatzki et al., 2016; Ohgaki and Kleihues, 2005; Ostrom et al., 2015).

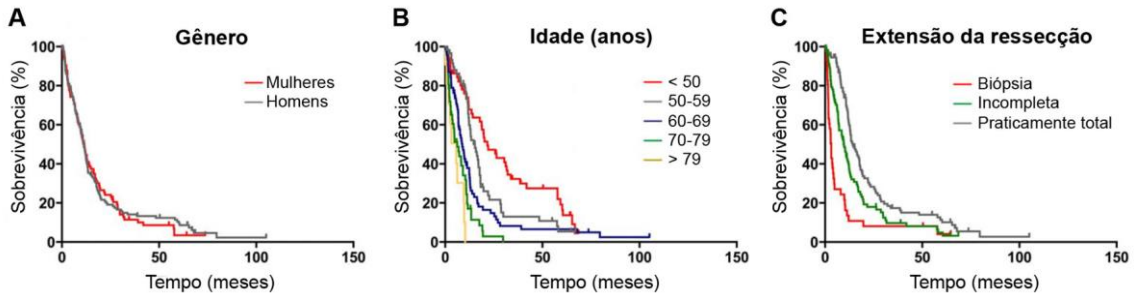

Fig. 7 – Desfecho da coorte de pacientes de Cantão de Zurique diagnosticados com glioblastoma entre 2005-2009. (A) Correlação do desfecho com o gênero; (B) correlação do desfecho com a idade e (C) correlação do desfecho com a extensão da ressecção do tumor. Adaptado de Gramatzki et al. (2016).

Classificação dos GBM

Segundo a classificação da OMS em 2016, o GBM é dividido principalmente em dois subtipos: *IDH*-selvagem e *IDH*-mutante (**Tabela 10**). Os GBM *IDH*-selvagens correspondem mais frequentemente à definição clínica *glioblastoma primário* ou *glioblastoma de novo*, sendo responsável por aproximadamente 90 % dos casos e predominando em pacientes acima dos 55 anos (Louis et al., 2016). Os GBM *IDH*-mutantes correspondem praticamente aos chamados *glioblastomas secundários*, os quais apresentam uma história clínica precedente de gliomas difusos de baixo grau. Esta neoplasia surge preferencialmente em pacientes mais jovens e ocorre em 10 % dos casos de GBM (Louis et al., 2016). Existe outra subclasse, os GBM NOS, um diagnóstico que é reservado para aqueles tumores nos quais uma avaliação completa de *IDH* não pode ser realizada (Louis et al., 2016).

Tabela 10 - Características dos dois tipos de glioblastomas (GBM), segundo a nova classificação dos tumores que afetam o SNC, organizada pela OMS em 2016. Adaptado de Louis et al., (2016).

	GBM *IDH*-selvagem	**GBM *IDH*-mutante**
Sinônimo	Glioblastoma primário; *IDH*-selvagem	Glioblastoma secundário; *IDH*-mutante
Neoplasia precursora	Não identificável; Desenvolvimento *de novo*	Astrocitoma difuso; Astrocitoma anaplásico
Proporção dos glioblastomas	~90%	~10%
Idade mediana no diagnóstico	~62 anos	~44 anos
Razão Homem/Mulher	1,42:1	1,05:1
Duração média da história clínica	4 meses	15 meses
Sobrevida global mediana		
Cirurgia + Radioterapia	9,9 meses	24 meses
Cirurgia + Radioterapia + Quimioterapia	15 meses	31 meses
Localização	Supratentorial	Preferencialmente frontal
Necrose	Extensiva	Limitada
Mutação no promotor *TERT*	72%	26%
Mutações em *TR53*	27%	81%
Mutações em *ATRX*	Excepcional	71%
Mutações em *EGFR*	35%	Excepcional
Mutações em *PTEN*	24%	Excepcional

Características dos GBM

Esses tumores são caracterizados histologicamente por células pleomórficas, alta atividade mitótica, proliferação vascular e necrose. Do ponto de vista molecular, os GBM são tumores altamente heterogêneos (Theeler et al., 2012). Verhaak et al., (2010) propôs uma subclassificação molecular dos GBM. A subclasse *proneural* é caracterizada por alterações em *PDGFRA*, *CDK6*, *CDK4* e *MET* e por mutações frequentes em *IDH1*. O subtipo *clássico* é caracterizado pela amplificação de *EGFR* e perda de *PTEN* e *CDKN2A*. O subtipo *mesenquimal* é caracterizado por mutação e/ou perda de *NF1*, *TP53* e *CDKN2A*. O subtipo *neural* não é caracterizado por uma assinatura gênica específica, mas apresenta expressão de marcadores neuronais (Cloughesy et al., 2014).

Devido ao fato das células nestes tumores variarem em tamanho e formato, estes gliomas já foram designados *glioblastomas multiformes*, um termo não mais utilizado. Os GBM, assim como outros gliomas malignos, são altamente invasivos, infiltrando-se em torno do parênquima cerebral. Entretanto, são tipicamente confinados ao SNC, não fazendo metástases (Omuro and DeAngelis, 2013). Os mecanismos de invasão e progressão dos GBM ainda não foram totalmente elucidados. Sabe-se que a invasibilidade da célula neoplásica está relacionada à mobilidade e à capacidade de adesão e de proteólise da matriz extracelular (Pilkington, 1994). Além disso, o crescimento tumoral requer a indução de angiogênese. Esse processo é regulado por fatores indutores e inibidores de proliferação e migração de células endoteliais (Hamel and Westphal, 2000; Pilkington, 1994; Vajkoczy et al., 1999). A proliferação microvascular acentuada é uma das principais características do GBM e é traduzida principalmente por proliferação de células endoteliais (Wesseling et al., 1997).

Pacientes portadores de GBM geralmente apresentam diversos sintomas neurológicos como dores de cabeça e mudanças na personalidade, além de um rápido e exacerbado aumento da pressão intracranial (Kleihues et al., 1995). Geralmente os tumores estão localizados nos hemisférios cerebrais, principalmente no lobo frontal e temporal (Kleihues et al., 1995). GBM intraventriculares, de cerebelo e medula espinhal são raros, assim como no tronco encefálico.

Estes últimos são mais comuns em crianças (Dohrmann et al., 1976).

A imagem por ressonância magnética (IRM) do cérebro com ou sem contraste é, geralmente, escolhida como modalidade de diagnóstico quando há suspeita de um tumor cerebral (Omuro and DeAngelis, 2013). Estes tumores se apresentam como uma lesão de formato irregular, com uma zona periférica em anel que capta contraste, ao redor de uma área central de necrose, a qual geralmente é hipodensa (Kleihues and Cavenne, 2000). Análises de cortes de cérebro com GBM não tratados mostram que essa estrutura em anel não representa a borda tumoral mais externa, e as células do glioma podem ser encontradas 2 cm além da margem (Burger et al., 1988). Estes tumores são caracteristicamente cercados pelo edema da substância branca, sendo geralmente unifocais, mas podendo ser multifocais (Omuro and DeAngelis, 2013).

Tratamento dos GBM

Após a neuroimagem, a ressecção cirúrgica do glioma maligno é o tratamento de intervenção inicial mais utilizado nos pacientes (DeAngelis, 2001) com o intuito de aliviar os sintomas de massa, alcançar uma redução celular e fornecer um tecido adequado para caracterização histológica e molecular do tumor (Omuro and DeAngelis, 2013). Uma excisão total está associada a uma sobrevida mais longa (**Fig. 7C**) e a uma melhora na função neurológica (DeAngelis, 2001; Gramatzki et al., 2016). Entretanto, uma ressecção cirúrgica completa é virtualmente impossível devido ao caráter infiltrativo destes tumores (Cloughesy et al., 2014). Os sobreviventes geralmente são jovens, com boa saúde e habilitados para fazer uma ressecção praticamente total do tumor e do peritumor, seguidos de radioterapia e quimioterapia (DeAngelis, 2001).

O regime convencional de radioterapia fracionada é de uma dose entre 4500-6000 cGy dada em frações diárias de 180-200 cGy durante 5-6 semanas (Khan et al., 2016). O uso da radioterapia de intensidade modulada tem sido amplamente preferido devido a uma melhor capacidade de alvo, porém, até o momento, não há evidências de superioridade em relação a

outras técnicas focais de radioterapia. Devido ao fato de ser uma doença infiltrativa difusa, não há atualmente alguma função definida para o uso da cirurgia estereotáxica ou braquiterapia como parte de tratamento de primeira linha (Tsao et al., 2005).

A temozolamida (TMZ) é a quimioterapia padrão usada para o tratamento dos GBM. Esta droga é um agente alquilante de DNA administrado oralmente e concomitantemente com a radioterapia. Sua adição ao tratamento aumenta a mediana de sobrevida dos pacientes para 15 meses, em relação aos 12 meses daqueles tratados somente com radioterapia. A taxa de sobrevida após 2 anos da cirurgia é de 27 % e 10 %, respectivamente (Hegi et al., 2005). Em adição à TMZ, o outro agente aprovado pela *US Food and Drug Administration* (FDA) é o agente alquilante carmustina (BCNU), o qual é implantada no leito do tumor após sua ressecção (Westphal et al., 2003). Como quimioterapia de segunda linha, o BCNU tem sido testado isoladamente ou em combinação com TMZ, irinotecano, cisplatina ou talidomida. Em um *trial* clínico de fase II, o tratamento de pacientes com recorrência de GBM somente com BCNU foi capaz de prologar a vida dos pacientes em 6 meses, apesar de causar toxicidade hepática e pulmonar (Jungk et al., 2016).

Embora a radioterapia e a quimioterapia aumentem a sobrevida do paciente, os GBM estão entre os tumores mais resistentes à radiação e à quimioterapia (Cloughesy et al., 2014; Masui et al., 2012). Dessa forma, novas abordagens de tratamento são necessárias visando principalmente moléculas de superfície ou vias de sinalização que regulam especificamente as células de GBM em proliferação.

3. Glutamato

O glutamato (L-Glu) é o aminoácido encontrado em maior concentração no SNC, desempenhando um papel metabólico muito importante (Krebs, 1935). Os propósitos metabólicos deste aminoácido incluem a síntese de proteínas, manutenção do metabolismo energético e fixação da amônia, ou sua utilização como neurotransmissor.

Este aminoácido é considerado o principal mediador de sinais excitatórios do SNC

(Collingridge and Lester, 1989; Danbolt, 2001; Fonnum, 1984; Headley and Grillner, 1990), onde participa de inúmeros eventos fisiológicos e plásticos, tais como: memória e aprendizado (Izquierdo et al., 2006), adaptação ao ambiente extracelular (Ozawa et al., 1998), proliferação e migração celular (McDonald and Johnston, 1990). O L-Glu também apresenta um papel no desenvolvimento e envelhecimento do SNC (Segovia et al., 2001), incluindo indução (Durand et al., 1996; Hanse et al., 1997; Kurihara et al., 1997) e eliminação de sinapses (Rabacchi et al., 1992), migração (Komuro and Rakic, 1993), diferenciação e morte celular (Danbolt, 2001; Komuro and Rakic, 1993; McDonald and Johnston, 1990).

Em sinapses, a sinalização glutamatérgica ocorre após a liberação do L-Glu na fenda sináptica (Danbolt, 2001; Fonnum, 1984). A ocorrência de um potencial de ação no terminal pré-sináptico acarretará uma despolarização da membrana plasmática, permitindo a liberação das vesículas que contém L-Glu de uma maneira Ca^{2+}-dependente (Danbolt, 2001; Fonnum, 1984). O L-Glu liberado na fenda sináptica liga-se a seus receptores presentes no botão pós-sináptico, exercendo sua função excitatória (Danbolt, 2001; Fonnum, 1984). O término da sinalização ocorre por um mecanismo denominado captação de glutamato (Balcar and Li, 1992; Danbolt, 2001; Logan and Snyder, 1972). Este é o principal mecanismo responsável pela manutenção dos níveis extracelulares de L-Glu abaixo dos níveis considerados tóxicos (Danbolt, 2001). Este processo é realizado por transportadores de L-Glu presentes na membrana plasmática de neurônios e células gliais, principalmente astrócitos (Rothstein et al., 1996).

3.1. Receptores glutamatérgicos (GluR)

O L-Glu exerce seus papéis fisiológicos e patológicos através da ativação de seus receptores de membrana (GluR), tanto neuronais quanto gliais (Ozawa et al., 1998). Os GluR são divididos em duas classes: metabotrópicos (mGluR) e ionotrópicos (iGluR) (Danbolt, 2001; Nakanishi et al., 1998; Ozawa et al., 1998). Os iGluR são acoplados a um canal iônico cátion-específico e são subdivididos em três subtipos: receptor α-amino-3-hidroxi-5-metil-4-isoxazolepropionato (AMPAR), receptor cainato e receptor N-metil-D-aspartato (NMDAR)

(Danbolt, 2001; Ozawa et al., 1998). Por outro lado, os mGluR são acoplados a proteínas G (Danbolt, 2001; Ozawa et al., 1998; Tanabe et al., 1992) e existem oito subtipos, os quais são subclassificados em três grupos com base na homologia genética, a via de sinalização celular a qual estão acoplados e a farmacologia. O grupo I inclui mGluR 1 e 5, o grupo II inclui mGluR 2 e 3 e o grupo III inclui mGluR 4, 6, 7 e 8 (Niswender and Conn, 2010). Já foi demonstrado que os GluR encontram-se expressos numa variedade de linhagens celulares e ressecções de tumores, tais como, câncer de estômago, câncer coloretal, câncer de próstata, carcinoma de células escamosas e melanoma (Stepulak et al., 2009).

3.1.1 Receptores metabotrópicos glutamatérgicos (mGluR)

Os mGluR são receptores acoplados à proteína G que pertencem à família C de receptores metabotrópicos e que participam da modulação da transmissão sináptica e da excitabilidade neuronal em todo SNC. O L-Glu se liga em um grande domínio extracelular e transmite sinais através do receptor até outras proteínas parceiras de sinalização intracelular (Niswender and Conn, 2010).

Em geral, os receptores do grupo I acoplam-se à G_q/G_{11} e ativam a fosfolipase C_β, resultando na hidrólise de fosfolipídeos de membrana e gerando inositol 1,4,5-trifosfato (IP3) e diacilglicerol. Esta via clássica leva à mobilização de cálcio e ativação da proteína cinase C (PKC). No entanto, agora é sabido que estes receptores podem modular vias de sinalização adicionais incluindo outras cascatas *downstream* da proteína G_q, assim como vias provenientes de $G_{i/o}$, G_s e outras moléculas independentes de proteínas G (Nicoletti et al., 2007; Niswender and Conn, 2010). Em contraste, os receptores dos grupos II e III são acoplados predominantemente a proteínas $G_{i/o}$. Receptores ligados a $G_{i/o}$ são classicamente acoplados à inibição da adenilato ciclase e regulam diretamente canais iônicos e outros parceiros de sinalizações *downstream* via liberação de subunidades $G_{\beta\gamma}$ (De Blasi et al., 2001; Niswender and Conn, 2010) (**Tabela 11**).

Um grande número de estudos pré-clínicos sugere que ligantes para os subtipos específicos de mGluR têm potencial para o tratamento de várias doenças do SNC, incluindo

depressão, distúrbios de ansiedade, esquizofrenia, síndromes de dor, epilepsia, doença de Alzheimer, doença de Parkinson, entre outros. Dados de estudos clínicos que usaram ligantes de mGluR estão começando a surgir e estão fornecendo forte prova de conceito para eficácia clínica de alguns destes compostos (Niswender and Conn, 2010).

Tabela 11 - Principais características dos mGluR. Modificado de Niswender and Conn (2010).

Grupo	Receptores	Expressão no SNC	Localização Sináptica	Via de sinalização do Grupo
I	mGluR1	• Difundida em neurônios • Papilas gustativas	Predominantemente pós-sináptica	• Estímulo da Fosfolipase C • Estímulo da adenilato ciclase (alguns sistemas) • Fosforilação da MAP cinase
	mGluR5	• Difundida em neurônios e astrócitos		
II	mGluR2	• Difundida em neurônios	Pré-sináptica e pós-sináptica	• Inibição da adenilato ciclase • Ativação dos canais de K^+ • Inibição dos canais de Ca^{++}
	mGluR3	• Difundida em neurônios e astrócitos		
III	mGluR4	• Difundida em neurônios • Abundante em cerebelo • Papilas gustativas	Predominantemente pré-sináptica	• Inibição da adenilato ciclase • Ativação dos canais K^+ • Inibição dos canais de Ca^{++} • Estímulo da fosfodiesterase de GMPc (somente mGluR6)
	mGluR6	• Retina	Pós-sinápticas em células bipolares de retina	
	mGluR7	• Difundida em neurônios	Zona ativa dos terminais pré-sinápticos	
	mGluR8	• Menor e mais restrita em relação a mGlur4/7	Predominantemente pré-sináptica	

Os mGluR estão expressos em vários tipos de células de câncer, incluindo gliomas, e são também encontrados em células tronco progenitoras (Nicoletti et al., 2007). Além disso, mGluR são considerados melhores alvos de fármacos em relação aos iGluR. Estes receptores, ao contrário dos receptores NMDA e AMPA, "modulam" ao invés de apenas "mediar" a transmissão sináptica excitatória (D'Onofrio et al., 2003). A possibilidade de que compostos que atuem nos mGluR possam ser bem toleradas por pacientes têm sido enfatizada na literatura (Bruno et al., 2001; Nicoletti et al., 1996).

3.1.2 Glutamato como fator de crescimento para glioblastomas

Um grande número de estudos *in vitro* e *in vivo* demonstrou que células de GBM liberam altos níveis de L-Glu para o meio extracelular, o que promove a sua proliferação e migração, contribuindo para a malignidade deste tipo de câncer (Behrens et al., 2000; Takano et al., 2001; Ye and Sontheimer, 1999). A secreção autócrina do L-Glu ocorre principalmente via trocador cistina-glutamato (xCT), o qual catalisa a troca de cistina extracelular por L-Glu intracelular numa razão estequiométrica de 1:1 (Noch and Khalili, 2009; Takano et al., 2001). Além disso, o excesso de L-Glu no microambiente ao redor do tumor também é mantido devido aos baixos níveis de captação desse aminoácido pelas células neoplásicas, o que é causado pela perda do

transportador de aminoácidos excitatórios do tipo 2 (EAAT2) na membrana destas células. (Takano et al., 2001; Ye and Sontheimer, 1999). Além disso, o L-Glu facilita a expansão do tumor, pois causa a morte dos neurônios circundantes através do mecanismo conhecido como excitotoxicidade, o qual é mediado pela ativação dos receptores NMDA permeáveis à Ca^{2+} (de Groot and Sontheimer, 2011; Nicoletti et al., 2007; Sontheimer, 2008; Takano et al., 2001)

A ativação do iGluR AMPA desempenha um papel crucial na malignidade de células de GBM, permitindo a sua proliferação e sobrevivência (Ishiuchi et al., 2002). Os receptores AMPA agregam-se como homo ou hetero tetrâmeros de subunidades GluR1-4 e, dependendo da composição das subunidades, podem formar canais permeáveis (contendo GluR 1, 3 e 4) ou impermeáveis (contendo GluR2) à Ca^{2+} (Yelskaya et al., 2013). A maioria dos receptors AMPA no SNC é impermeável à Ca^{2+} (Ishiuchi et al., 2002). Células de GBM que expressam receptores AMPA permeáveis à Ca^{2+} apresentam uma migração e proliferação elevada e o seu bloqueio com o antagonista NBQX leva à inibição do crescimento do glioma e a indução de apoptose (Ishiuchi et al., 2002; Rzeski et al., 2001). A superexpressão de receptores AMPA permeáveis à Ca^{2+} aumenta a proliferação de células de GBM através de um processo de sinalização dependente da via de sinalização da Akt/PKB (Ishiuchi et al., 2007; Yoshida et al., 2006). Essa sinalização promove a síntese de proteínas, permitindo a sobrevivência e crescimento das células tumorais, inibindo a apoptose e sendo crucial para a conversão de astrocitomas anaplásicos em GBM (glioblastoma secundário) (Sonoda et al., 2001).

Existem evidências crescentes de que mGluR estão relacionados à agressividade dos GBM (Nicoletti et al., 2007).

3.1.3 mGluR como alvos terapêuticos de glioblastomas

Estudos *in vitro*

Culturas de GBM têm sido amplamente utilizadas para elucidar o papel dos mGluR na agressividade desta neoplasia. Alguns destes estudos utilizaram linhagens de GBM como modelo, outros, culturas primárias de ressecções de GBM. Ensaios de proliferação,

invasibilidade e migração foram feitos concomitantemente com o tratamento com antagonistas e agonistas dos mGluR para esclarecer a função que estes receptores apresentam sobre a agressividade dessas células malignas. Dentre os mGluR, o grupo II (mGluR2 e mGluR3) é o mais estudado em gliomas, com os genes sendo expressos (mRNA) e as proteínas imunodetectadas (Western Blot) na maioria das amostras de ressecções humanas, culturas primárias e linhagens de GBM. Muitos estudos demonstraram que o bloqueio farmacológico deste grupo reduz a proliferação de células de GBM *in vitro* (Arcella et al., 2005; D'Onofrio et al., 2003) e pode promover uma diferenciação astroglial de células tronco de glioblastoma (CTGBM), células que suportam o crescimento tumoral e a recorrência e que são resistentes à radioterapia e à quimioterapia (Ciceroni et al., 2008; Zhou et al., 2014).

As vias de sinalização da MAPK e da PI3K, as quais são normalmente ativadas em resposta a agentes proliferativos (Schaeffer and Weber, 1999), suportam a proliferação dos GBM, induzida pelo estímulo de mGluR3 (Arcella et al., 2005; Ciceroni et al., 2008; D'Onofrio et al., 2003). A ativação desse receptor também está relacionada a outras vias envolvidas na agressividade de GBM: vias dos receptores de BMP e de EGF. BMP (*bone morphogenic proteins*) são proteínas presentes no soro utilizado nos meios de cultura conhecidas por promover a diferenciação astroglial de CTGBM (Piccirillo and Vescovi, 2006) através da sua ligação a receptores de membrana da família BMP/TGF-ß/activina levando à fosforilação de proteínas SMAD1/5/8 (Fukuda and Taga, 2006). A ativação da via mGluR3-MAPK por L-Glu endógeno pode limitar a diferenciação astroglial induzida por SMAD1/5/8, contribuindo, assim, para apoiar o estado indiferenciado das CTGBM e, eventualmente, o crescimento do GBM (Ciceroni et al., 2008). A ativação concomitante de EGFR (*epidermal growth factor receptor*) e mGluR3 pode agir sinergicamente sobre a agressividade de GBM, visto que a inibição simultânea desses receptores causou máxima apoptose em células de GBM, assim como reduziu sua migração (Yelskaya et al., 2013).

O bloqueio de mGluR3 das CTGBM permite a ação citotóxica da TMZ e a ativação desse receptor controla a expressão de proteínas envolvidas no mecanismo de quimioresistência

(Ciceroni et al., 2013). O eixo mGluR3-PI3K-Akt/PKB está envolvido neste processo com pelo menos duas vias *downstream* à Akt/PKB também implicadas: a via de NF-κB e a de mTOR (Ciceroni et al., 2013). A eficácia clínica da TMZ é limitada pela enzima de reparação de DNA, O6-metilguanina-DNA-metiltransferase (MGMT), a qual remove adutos de DNA gerados por agentes alquilantes (Gerson, 2004). O sinergismo entre TMZ e o bloqueio do mGluR3 é mediado pela inibição da expressão proteica de MGMT (Ciceroni et al., 2013).

Outro mGluR tem sido correlacionados à agressividade de células cancerígenas (Willard and Koochekpour, 2013). A expressão ectópica de mGluR1 em melanócitos normais induz a hiperproliferação dessas células e a sua transformação em tumores malignos (Marín and Chen, 2004). Entretanto, somente um estudo foi realizado para descrever o papel deste receptor sobre a proliferação e progressão de GBM (Zhang 2015). A inibição de mGluR1 diminuiu acentuadamente a viabilidade das células de GBM através de um processo que suprime a ativação da via PI3K-Akt/PKB-mTOR (Zhang et al., 2015).

A maioria desses estudos *in vitro* sugerem que a ativação endógena de mGluR3 sustenta a proliferação das células de GBM e que as vias de sinalização da MAPK e PI3K estão envolvidas neste processo. Todos estes resultados são particularmente interessantes de um ponto de vista terapêutico, pois ligantes dos receptores glutamatérgicos metabotrópicos do grupo II representam uma classe de drogas em expansão dotados de uma alta afinidade ao receptor, penetração cerebral e um perfil bom de segurança e tolerabilidade (Bruno et al., 2001; Schoepp et al., 1999). Devido a isso, alguns desses trabalhos avaliaram o efeito desses compostos em modelos *in vivo*.

Estudos *in vivo*

A infusão sistêmica contínua de antagonistas de mGluR3 foi capaz de reduzir o crescimento das células de GBM em dois modelos *in vivo*: implantação dessas células no tecido cerebral (Arcella et al., 2005; Ciceroni et al., 2008; Ciceroni et al., 2013) ou em tecidos periféricos (Arcella et al., 2005; Zhou et al., 2014). Estes dois modelos são complementares,

pois o crescimento tumoral em um tecido periférico macio (ex: implantação subcutânea) baseia-se exclusivamente na taxa de proliferação celular e em um fornecimento adequado de nutrientes, enquanto que o crescimento de um tumor implantado no cérebro, ou seja, confinado no crânio, necessita de uma série de processos, tais como a morte excitotóxica dos neurônios circundantes e a expressão de enzimas que degradam a matriz extracelular (Bowman et al., 1999).

O tratamento contínuo com um antagonista de mGluR3 foi capaz de sinergizar com a TMZ, reduzindo o tamanho dos tumores formados pela implantação intracranial xenográfica de CTGBM (Ciceroni et al., 2013). Replicando os dados *in vitro*, somente o bloqueio de mGluR3 ou somente o tratamento com a TMZ não foram eficientes para reduzir o tamanho dos tumores formados pela implantação de CTGBM (Ciceroni et al., 2013).

A atividade antitumoral do bloqueio de mGluR1 também foi demonstrada *in vivo* utilizando-se um modelo xenográfico de implantação intracranial das células de GBM. A redução do volume tumoral foi observada após a implantação de células mGluR1-silenciadas e após o tratamento crônico das células não silenciadas com antagonistas de mGluR1 (Zhang et al., 2015).

O tratamento contínuo com os antagonistas de mGluR1 e mGluR3 não causou toxicidade sistêmica ou comprometimento motor nos animais. Além disso, aqueles que receberam doses agudas do antagonista de mGluR3 sobreviveram (Ciceroni et al., 2013; Zhang et al., 2015). Todos estes fatos corroboram com a ideia de que as drogas que bloqueiam seletivamente mGluR1 ou mGluR3 são potenciais candidatas ao tratamento não citotóxico de pacientes com GBM.

Coorte de pacientes

Somente um estudo avaliou o perfil da expressão gênica (mRNA) dos mGluR em ressecções de GBM obtidas de uma coorte (87 pacientes). Este estudo visava avaliar o valor prognóstico da expressão gênica tumoral de mGluR3 (Ciceroni et al., 2013). Os pacientes foram estratificados de acordo com a expressão gênica de mGluR3 e o estado metilado do promotor

para MGMT. Em resumo, altos níveis de mGluR3-mRNA nos tumores são preditivos de uma sobrevida mais curta em pacientes que após a ressecção cirúrgica receberam radioterapia seguida do tratamento com TMZ. Além disso, o estado de metilação do promotor do gene para MGMT nos tumores influencia na sobrevida somente naqueles pacientes cujas ressecções apresentavam baixos níveis de mGluR3-mRNA (Ciceroni et al., 2013).

Estes dados encorajam a utilização de antagonistas de mGluR3 como terapia complementar adjuvante para o tratamento de pacientes com GBM e sugerem que a expressão gênica de mGluR3 possa ser avaliada em amostras desses tumores para melhor prever a sobrevida dos pacientes.

OBJETIVO

Objetivo geral

Investigar o papel dos receptores metabotrópicos de glutamato (mGluR) sobre a malignidade de glioblastomas (GBM) *in silico*, *in vitro* e *in vivo*, buscando uma assinatura gênica com potencial valor prognóstico e preditivo de tratamento complementar adjuvante.

Objetivos específicos

1. Realizar uma revisão bibliográfica dos estudos que avaliaram o envolvimento da sinalização intracelular mediada por mGluR na progressão, agressividade e recorrência de gliomas.

2. Realizar uma meta-análise de dados de microarranjo de amostras de GBM e avaliar o caráter preditivo de desfecho de cada um dos oito subtipos de mGluR isoladamente e/ou combinados , identificando aqueles que apresentam um maior potencial para ser biomarcador prognóstico.

3. Avaliar o potencial dos receptores candidatos sobre a proliferação das células de GBM através de experimentos *in vitro* utilizando o tratamento de linhagens dessas neoplasias com ligantes de mGluR.

4. Avaliar o potencial dos receptores candidatos sobre o crescimento tumoral de GBM através de experimentos *in vivo* utilizando como modelo ratos implantados ortotopicamente com células dessa neoplasia e tratados intracisternalmente com os ligantes de mGluR e intraperitonealmente com a quimioterapia padrão, temozolamida.

CAPÍTULO I

Artigo publicado

Metabotropic glutamate receptors as a new therapeutic target for malignant gliomas.

Revista: Oncotarget

Qualis-CAPES-CBII: A1

Fator de Impacto: 5.008

Justificativa: O estudo do papel do glutamato sobre a agressividade de gliomas já vem sendo estudado há algumas décadas. Entretanto, poucos estudos avaliaram o papel específico dos receptores metabotrópicos de glutamato (mGluR) no desenvolvimento de gliomas.

Objetivo geral: O objetivo desta revisão foi reunir os estudos que avaliaram o papel dos mGluR sobre a agressividade de gliomas.

Objetivo específico: Analisar quais mGluR são mais estudados *in vitro* e *in vivo* na literatura verificando quais vias de sinalização intracelular eles estão envolvidos.

Metabotropic glutamate receptors as a new therapeutic target for malignant gliomas

Mery Stefani Leivas Pereira[1], Fábio Klamt[2], Chairini Cássia Thomé[1], Paulo Valdeci Worm[3,4] and Diogo Losch de Oliveira[1]

[1] Department of Biochemistry, Laboratory of Cellular Neurochemistry, Instituto de Ciências Básicas da Saúde, Universidade Federal do Rio Grande do Sul, Porto Alegre, Brazil

[2] Department of Biochemistry, Laboratory of Cellular Biochemistry, Instituto de Ciências Básicas da Saúde, Universidade Federal do Rio Grande do Sul, Porto Alegre, Brazil

[3] Department of Neurosurgery, Cristo Redentor Hospital – GHC – Porto Alegre RS, Brazil

[4] Department of Neurosurgery, São José Hospital, Complexo Hospitalar Santa Casa, Porto Alegre RS, Brazil

Correspondence to: *Mery Stefani Leivas Pereira,* ***email***: *meryslpereira@gmail.com*

Keywords: mGluR, glioblastoma, brain cancer

Received: *June 29, 2016* ***Accepted***: *January 03, 2017* ***Published***: *Febraury 12, 2017*

ABSTRACT

Metabotropic glutamate receptors (mGluR) are predominantly involved in maintenance of cellular homeostasis of central nervous system. However, evidences have suggested other roles of mGluR in human tumors. Aberrant mGluR signaling has been shown to participate in transformation and maintenance of various cancer types, including malignant brain tumors. This review intends to summarize recent findings regarding the involvement of mGluR-mediated intracellular signaling pathways in progression, aggressiveness, and recurrence of malignant gliomas, mainly glioblastomas (GBM), highlighting the potential therapeutic applications of mGluR ligands. In addition to the growing number of studies reporting mGluR gene or protein expression in glioma samples (resections, lineages, and primary cultures), pharmacological blockade *in vitro* of mGluR1 and mGluR3 by selective ligands has been shown to be anti-proliferative and anti-migratory, decreasing activation of MAPK and PI3K pathways. In addition, mGluR3 antagonists promoted astroglial differentiation of GBM cells and also enabled cytotoxic action of temozolomide (TMZ). mGluR3-dependent TMZ toxicity was supported by increasing levels of MGMT transcripts through an intracellular signaling pathway that sequentially involves PI3K and NF-κB. Further, continuous pharmacological blockade of mGluR1 and mGluR3 have been shown to reduced growth of GBM tumor in two independent *in vivo* xenograft models. In parallel, low levels of mGluR3 mRNA in GBM resections may be a predictor for long survival rate of patients. Since several Phase I, II and III clinical trials are being performed using group I and II mGluR modulators, there is a strong scientifically-based rationale for testing mGluR antagonists as an adjuvant therapy for malignant brain tumors.

INTRODUCTION

Gliomas are the most common type of primary brain tumor and are often fast growing with a poor prognosis for patient [1]. The World Health Organization (WHO) classified gliomas in 2016 using molecular parameters in addition to their histological and immunohistochemical resemblance to presumed cells of origin and graded them by increasing degrees of undifferentiation, anaplasia, and aggressiveness (*i.e.*, mitotic figures, necrosis, and vascular endothelial hyperplasia) [2, 3]. High-grade gliomas represent 60-75% of all cases and include grade III anaplastic astrocytoma, anaplastic oligodendroglioma, mixed anaplastic oligoastrocytoma, and grade IV glioblastoma [4]. Glioblastoma (GBM) is the most common malignant primary brain tumor and is one of the most lethal human cancers [2, 5]. Recently, GBM was classified in three groups: (1) GBM, IDH-wildtype

(about 90% of cases, generally corresponds to the clinical definition of primary GBM and is prevalent in patients over 55 years); (2) GBM, IDH-mutant (about 10 % of cases, corresponds closely to so-called secondary GBM and preferentially arises in younger patients); and (3) GBM, NOS (a diagnosis that is reserved for those tumors for which full IDH evaluation cannot be performed) [3]. In United States, GBM accounts for 15.1% of all primary brain tumors, 46.1% of primary malignant brain tumors, and its annual incidence is 3.2 per 100,000 people (or 10,787 new cases diagnosed per year) [6]. Even though GBM may develop at any age, it is more common in elderly with a higher incidence rate in ages between 75 to 84 years (15.24 new cases per 100,000 people between these ages per year). In addition, GBM is 1.6 times more common in males and its incidence rate is 2 times higher among caucasians [6].

Regarding histology, GBM is characterized by considerable cellularity and mitotic activity, vascular proliferation, and necrosis [7]. Because GBM cells vary in size and shape, *i.e.*, they are pleomorphic, this glioma was frequently called *glioblastoma multiforme*, a term no longer in use. From a molecular point of view, GBM is a highly heterogeneous tumor [8]. Genome-wide expression studies have revealed 4 transcriptional subclasses of GBM, displaying features reminiscent of distinct cell types: classical, mesenchymal, proneural, and neural [9, 10]. Classical subclass typically displays chromosome 7 amplifications, chromosome 10 deletions, *EGFR* amplification, *EGFR* mutations, and *Ink4a/ARF* locus deletion. Mesenchymal subclass displays a high frequency of *NF1* mutation/deletion, high expression of *CHI3L1*, *MET*, and genes involved in tumor necrosis factor and nuclear factor-κB (NF-κB) pathways. Proneural GBM is characterized by alterations of *PDGFRA* and mutations in *IDH1* and *TP53*, sharing gene expression features with low-grade gliomas and secondary GBM (*i.e.,* low-grade gliomas later recurred as GBM). Neural subclass is characterized by expression of neuronal markers. Many molecular abnormalities and mutations overlap across transcriptional subclasses, for example *PTEN* loss, and a large number of very rare mutations have been described [11, 12].

Although GBM is typically confined to Central Nervous System (CNS) and rarely performing metastases in distant organs, this and other malignant gliomas are highly invasive, infiltrating surrounding brain parenchyma [5]. After initial diagnosis, standard treatment for GBM consists of maximal surgical resection [13, 14]. This practice aims to relieve mass effect, achieve cytoreduction, and provide adequate tissue for histologic and molecular tumor characterization. Although surgical resection can greatly reduce tumor bulk, complete tumor excision is frequently not reached due to infiltrative nature of GBM cells [15]. After surgical resection, adjuvant radiotherapy combined with chemotherapy should be considered for all patients. A radiotherapy dose of 60 Gy is frequently used [13]. In addition, the DNA alkylating agent named temozolomide (TMZ) is orally administered as first-line chemotherapy [5, 16]. This regimen is supported by a randomized phase III study [17], which demonstrated TMZ increased median survival to 15 months *versus* 12 months with radiotherapy alone (hazard ratio - HR = 0.63; $P < .001$). Two-year survival rate was also increased: 27% for chemotherapy plus radiotherapy *versus* 10% for radiotherapy alone [17]. Alternatively, biodegradable polymers containing the alkylating agent carmustine (BCNU) can be implanted into tumor bed after surgical resection. Nevertheless, a phase III trial has indicated a modest survival benefit of this regimen [18]. A humanized vascular endothelial growth factor (VEGF) monoclonal antibody named bevacizumab had been recently introduced as first-line monotherapy for progressive GBM [19]. Approval of bevacizumab by U.S. Food and Drug Administration was based on improvement of radiologic response rates observed in two single-arm or noncomparative phase II trials [20, 21]. However, two recent multicenter, phase III, randomized, double-blind, placebo-controlled trials [22, 23], have demonstrated bevacizumab increased median progression-free survival (10.6 *vs*. 6.2 months, HR: 0.64, $p < 0.0001$ [22]; 10.7 *vs*. 7.3 months, HR: 0.79, $p = 0.004$ [23]) but not overall survival of patients (16-17 months).

Although radiotherapy and chemotherapy improve patient's survival, GBM remains among the most lethal and resistant malignant tumor [2, 24], and recurrence is nearly universal after a median progression-free survival of 7 to 10 months [25]. Thus, development of new therapies targeting surface molecules or signaling pathways that specifically regulate GBM proliferation or differentiation seems necessary.

In this context, in the present review we summarized the recent evidences demonstrating the participation of mGluR-mediated signaling pathways in GBM proliferation and differentiation, highlighting the putative role of these receptors as new molecular target for management and treatment of this neoplasia.

GLUTAMATE AS A GROWTH FACTOR FOR GLIOBLASTOMA

Several *in vitro* and *in vivo* studies have demonstrated GBM cells can release high levels of glutamate (L-Glu) to extracellular fluid. Released L-Glu may act as a neurotrophic factor, promoting proliferation and migration of glioma cells as well as contributing to tumor malignancy [26-28]. L-Glu autocrine secretion occurs mainly by cystine-glutamate antiporter (xCT), which exchanges extracellular cystine (Cys) for intracellular L-Glu at a 1:1 stoichiometric ratio [27, 29] (Figure 1, step 1). Moreover, due to loss of excitatory amino acid transporter 2 (EAAT2), GBM cells possess

a low re-uptake rate of L-Glu from extracellular fluid, which keeps this aminoacid at a high concentration in extracellular fluid and increases tumor malignancy [27, 30] (Figure 1, step 2). Furthermore, higher levels of L-Glu can trigger a mechanism of neuronal cell death called excitotoxicity [31], which facilitates tumor bulk expansion [27, 32-34] (Figure 1, step 3).

Extracellular L-Glu activates two classes of membrane receptors: ionotropic glutamate receptors (iGluR: AMPA, NMDA and Kainate receptors), which are

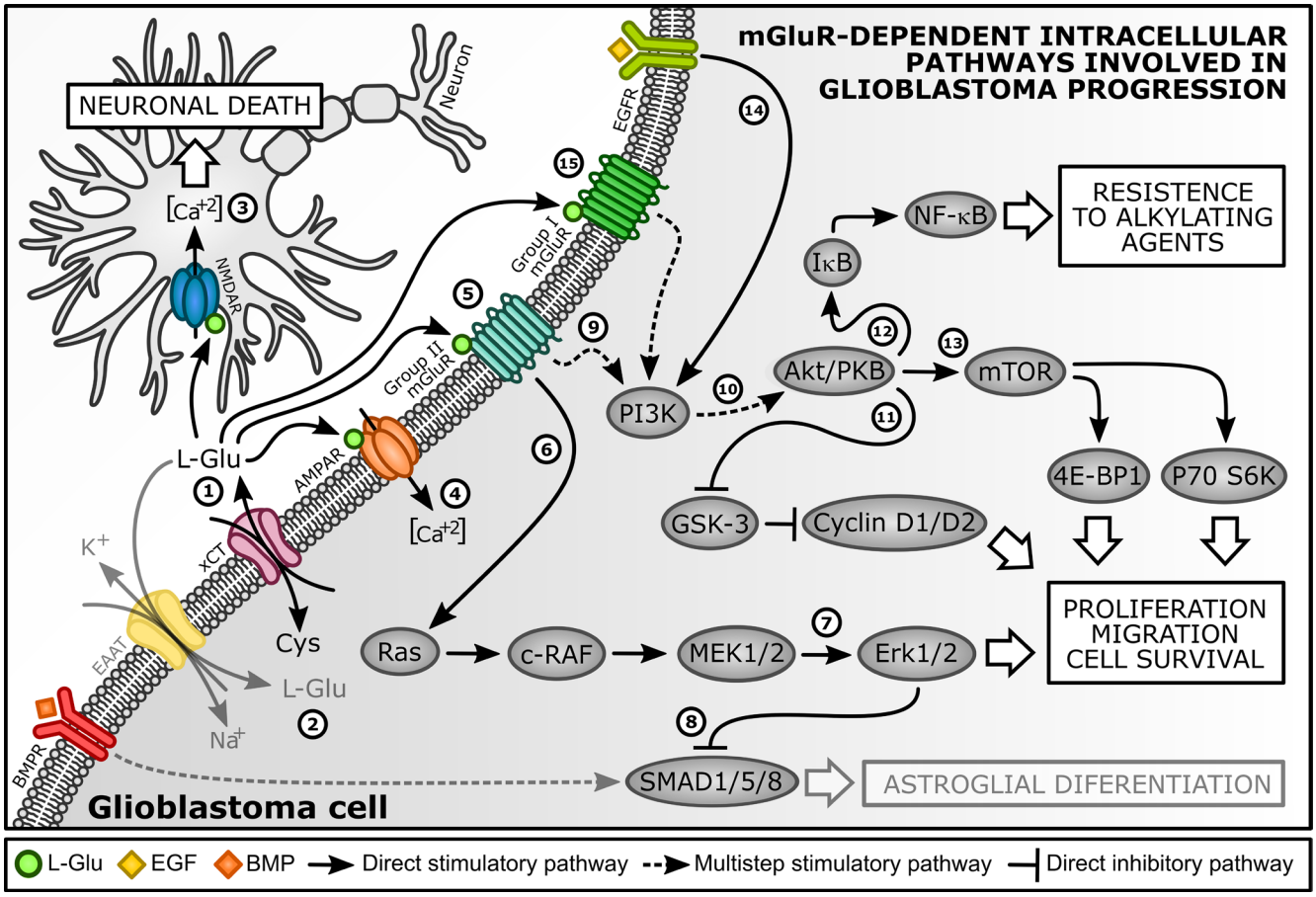

Figure 1 : Regulation of GBM proliferative pathways by metabotropic glutamate receptors (mGluR). (1) GBM cells can release low levels of L-Glu mainly by xCT antiporter [27, 28]. (2) Due to loss of EAAT2, GBM cells possessed a low re-uptake rate of L-Glu, maintaining high concentrations of this amino acid in tumor environment [30]. (3) High levels of L-Glu can activate specific NMDAR, which causes neuronal death by excitotoxicity and facilitates tumor bulk expansion [27]. (4) GBM cells expressing mutated Ca^{+2}-permeable AMPAR exhibited enhanced migration and proliferation and its blockade led to inhibition of growth and induction of apoptosis [42]. (5) mGluR3 activation by L-Glu induced GBM proliferation and kept these cells under undifferentiated state. In contrast, mGluR3 inhibition eliminated this constraint and promoted astroglial differentiation [68, 73, 76, 78]. (6) Accordingly to Arcella et al. (2005) [73] and Ciceroni et al. (2013) [77], MAPK axis supported mGluR3-induced GBM proliferation, (7) since mGluR3 stimulation increased Erk1/2 phosphorylation and its blockade reduced p-Erk1/2 levels. mGluR3 inhibition plus MEK1/2 blockade showed an additive antiproliferative effect on GBM cells [68]. (8) Moreover, mGluR3-dependet activation of MAPK pathway limited SMAD1/5/8-induced astroglial differentiation, which kept GBM cells under undifferentiated state. Exogenous SMAD1/5/8 stimulation or MEK inhibition prevented this effect [76]. (9) mGluR3 activation stimulated (10) phosphorylation of Akt/PKB *via* PI3K activation and this effect was reversed by receptor inhibition [73, 77]. (11) mGluR3-PI3K axis activation presented a permissive role on GBM cell cycle progression, since mGluR3 inhibition by LY341495 decreased cyclin D1/D2 immunocontent [68, 73], an early marker of G1/S phase transition [79]. (12) mGluR3-PI3K axis was also related to GBM chemoresistance. GSC become sensitive to TMZ, an alkylating agent, only if mGluR3 was inhibited or silenced [77], which was also mimicked by PI3K blockade. NF-κB activation by Akt/PKB limits pro-apoptotic activity of alkylating agents in GBM cells [100]. TMZ increased levels of p-IκB and this effect was reversed by mGluR3 or PI3K blockers. NF-κB bockade enabled TMZ toxicity, occluding permissive action of mGluR3 inhibition, indicating NF-κB lies downstream of Akt/PKB in pathway that restrains TMZ toxicity. (13) Akt/PKB also regulates mTOR, which promotes mRNA translation and protein synthesis through p70 S6K and 4E-BP1 phosphorylation [103]. This signaling pathway was showed to support GBM cells survival [106]. (14) Concomitant activation of EGFR and mGluR3 could act synergistically in GBM aggressiveness, since simultaneous inhibition of these receptors caused maximum apoptosis in GBM cells, as well as reduced their migration. (15) mGluR1 stimulation promoted GBM cells survival through PI3K-Akt/PKB-mTOR pathway activation [41]. mGluR1 inhibition markedly decreased cell viability and inhibited PI3K and Akt/PKB phosphorylation. mGluR1 inhibition also decreased levels of p-mTOR and P70 S6K

Table 1A: RNA expression of group I mGluR subtypes in cellular malignant glioma models.

Metabotropic glutamate receptors		mRNA			
		Sample		Expression	Reference
Group I	mGluR1	Human Glioma Lineage	U-87 MG	Yes	[72]
				No	[73]
			U-343	Yes	[72]
			MOGGCCM	Yes	[72]
		Resection	AZ21 (Low grade astrocytoma)	Yes	[48]
			AZ8 (Low grade astrocytoma)	Yes	[48]
			AZ7 (Low grade astrocytoma)	Yes	[48]
			AZ6 (Low grade astrocytoma)	Yes	[48]
			AZ5 (Low grade astrocytoma)	Yes	[48]
			AZ4 (Low grade astrocytoma)	Yes	[48]
			AZ3 (Low grade astrocytoma)	No	[48]
			AZ2 (Low grade astrocytoma)	Yes	[48]
			GB4 (Glioblastoma)	Yes	[48]
			GB3 (Glioblastoma)	Yes	[48]
			GB2 (Glioblastoma)	Yes	[48]
			GB1 (Glioblastoma)	No	[48]
	mGluR5	Human Glioma Lineage	U-87 MG	Yes	[72]
				No	[73, 74]
			U-343	Yes	[72]
			MOGGCCM	Yes	[72]
			U-178 MG	Yes	[74]
			U-251	No	[68]
		Primary culture from human glioma	FCN-9	No	[68]
			MZC-12	No	[68]
			CDR-97	No	[68]
		Resection	Anaplastic astrocytoma (52 years old)	No	[79]
			Astrocytoma grade II (12 years old)	Yes	[79]
			Glioblastoma (53 years old)	No	[79]
			Glioblastoma (68 years old)	No	[79]
			Glioblastoma (82 years old)	No	[79]
			Glioblastoma (58 years old)	No	[79]
			Glioblastoma (55 years old)	No	[79]
			Astrocytoma grade I (38 years old)	No	[79]
			AZ21 (Low grade astrocytoma)	Yes	[48]
			AZ8 (Low grade astrocytoma)	No	[48]
			AZ7 (Low grade astrocytoma)	Yes	[48]
			AZ6 (Low grade astrocytoma)	Yes	[48]
			AZ5 (Low grade astrocytoma)	Yes	[48]
			AZ4 (Low grade astrocytoma)	No	[48]
			AZ3 (Low grade astrocytoma)	Yes	[48]
			AZ2 (Low grade astrocytoma)	Yes	[48]
			GB4 (Glioblastoma)	Yes	[48]
			GB3 (Glioblastoma)	Yes	[48]
			GB2 (Glioblastoma)	Yes	[48]
			GB1 (Glioblastoma)	Yes	[48]

ligand-gated ion channels, and metabotropic glutamate receptors (mGluR), which are coupled to G proteins [35, 36]. mGluR family comprises eight subtypes subdivided in three groups according to their sequence homology, pharmacology, and associated-signaling pathway. Group I mGluR are coupled to G_q proteins and their activation stimulates phospholipase C (PLC) and phosphatidylinositol 4,5-biphosphate (PIP_2) hydrolysis. PIP_2 hydrolysis generates inositol (1,4,5)-trisphosphate (IP_3) and diacylglycerol (DAG), which stimulates intracellular Ca^{2+} release from endoplasmic reticulum and activates protein kinase C (PKC), respectively [33]. In contrast, mGluR of group II and III are coupled predominantly to $G_{i/o}$ proteins, inhibiting adenylyl cyclase (AC) and, thus, decreasing ion channel activity and other downstream signaling pathways [37, 38] (Figure 2).

Table 1B: RNA expression of group II mGluR subtypes in cellular malignant glioma models.

Metabotropic glutamate receptors		mRNA			
		Sample		Expression	Reference
Group II	mGluR2	Human Glioma Lineage	U-87 MG	Yes	[72, 73]
			U-343	Yes	[72]
			MOGGCCM	Yes	[72]
			U-251	Yes	[68]
		Primary culture from human glioma	FCN-9	No	[68]
			MZC-12 and MSS-5	Yes	[68]
			FLS-10	No	[68]
			LTN-12	No	[68]
			BRT-3	No	[68]
			CRL-8	No	[68]
			CDR-97	No	[68]
			Glioma Stem Cells	No	[76-78]
		Resection	Glioblastoma	Yes	[78]
			AZ21 (Low grade astrocytoma)	Yes	[48]
			AZ8 (Low grade astrocytoma)	Yes	[48]
			AZ7 (Low grade astrocytoma)	Yes	[48]
			AZ6 (Low grade astrocytoma)	Yes	[48]
			AZ5 (Low grade astrocytoma)	Yes	[48]
			AZ4 (Low grade astrocytoma)	Yes	[48]
			AZ3 (Low grade astrocytoma)	Yes	[48]
			AZ2 (Low grade astrocytoma)	Yes	[48]
			GB1, GB2, GB3 and GB4 (Glioblastomas)	Yes	[48]
	mGluR3	Human Glioma Lineage	U-87 MG	Yes	[72, 73]
			U-343	No	[72]
			MOGGCCM	Yes	[72]
			U-251	Yes	[68]
		Primary culture from human glioma	FCN-9	Yes	[68]
			MZC-12	Yes	[68]
			FLS-10, LTN-12 and CDR-97	No	[68]
			MSS-5	Yes	[68]
			BRT-3	Yes	[68]
			CRL-8	Yes	[68]
			Glioma Stem Cells	Yes	[76-78]
		Resection	Glioblastoma	Yes	[78]
			AZ21 (Low grade astrocytoma)	Yes	[48]
			AZ8 (Low grade astrocytoma)	Yes	[48]
			AZ7 (Low grade astrocytoma)	Yes	[48]
			AZ6 (Low grade astrocytoma)	Yes	[48]
			AZ5 (Low grade astrocytoma)	Yes	[48]
			AZ4 (Low grade astrocytoma)	Yes	[48]
			AZ3 (Low grade astrocytoma)	Yes	[48]
			AZ2 (Low grade astrocytoma)	Yes	[48]
			GB1, GB3 and GB4 (Glioblastomas)	Yes	[48]
			GB2 (Glioblastoma)	No	[48]
			U-343	Yes	[72]
			MOGGCCM	Yes	[72]
		Resection	AZ21 (Low grade astrocytoma)	Yes	[48]
			AZ8 (Low grade astrocytoma)	No	[48]
			AZ7 (Low grade astrocytoma)	Yes	[48]
			AZ6 (Low grade astrocytoma)	Yes	[48]
			AZ5 (Low grade astrocytoma)	Yes	[48]
			AZ4 (Low grade astrocytoma)	Yes	[48]
			AZ3 (Low grade astrocytoma)	Yes	[48]
			AZ2 (Low grade astrocytoma)	Yes	[48]
			GB1, GB3 and GB4 (Glioblastomas)	Yes	[48]
			GB2 (Glioblastoma)	No	[48]

Table 1C: RNA expression of group III mGluR subtypes in cellular malignant glioma models.

Metabotropic glutamate receptors		mRNA			
		Sample		Expression	Reference
Group III	mGluR4	Human Glioma Lineage	U-87 MG	No	[72, 73]
			U-343	Yes	[72]
			MOGGCCM	Yes	[72]
		Resection	AZ21 (Low grade astrocytoma)	Yes	[48]
			AZ8 (Low grade astrocytoma)	Yes	[48]
			AZ7 (Low grade astrocytoma)	Yes	[48]
			AZ6 (Low grade astrocytoma)	No	[48]
			AZ5 (Low grade astrocytoma)	Yes	[48]
			AZ4 (Low grade astrocytoma)	Yes	[48]
			AZ3 (Low grade astrocytoma)	No	[48]
			AZ2 (Low grade astrocytoma)	No	[48]
			GB1, GB2, GB3 and GB4 (Glioblastoma)	Yes	[48]
	mGluR6	Human Glioma Lineage	U-87 MG	Yes	[72]
			U-343	Yes	[72]
			MOGGCCM	Yes	[72]
		Resection	AZ21 (Low grade astrocytoma)	Yes	[48]
			AZ8 (Low grade astrocytoma)	No	[48]
			AZ7 (Low grade astrocytoma)	No	[48]
			AZ6 (Low grade astrocytoma)	No	[48]
			AZ5 (Low grade astrocytoma)	No	[48]
			AZ4 (Low grade astrocytoma)	No	[48]
			AZ3 (Low grade astrocytoma)	No	[48]
			AZ2 (Low grade astrocytoma)	No	[48]
			GB4 (Glioblastoma)	Yes	[48]
			GB3 (Glioblastoma)	Yes	[48]
			GB2 (Glioblastoma)	Yes	[48]
			GB1 (Glioblastoma)	No	[48]
	mGluR7	Human Glioma Lineage	U-87 MG	Yes	[72]
				No	[73]
			U-343	Yes	[72]
			MOGGCCM	Yes	[72]
		Resection	AZ21 (Low grade astrocytoma)	Yes	[48]
			AZ8 (Low grade astrocytoma)	Yes	[48]
			AZ7 (Low grade astrocytoma)	Yes	[48]
			AZ6 (Low grade astrocytoma)	Yes	[48]
			AZ5 (Low grade astrocytoma)	Yes	[48]
			AZ4 (Low grade astrocytoma)	No	[48]
			AZ3 (Low grade astrocytoma)	Yes	[48]
			AZ2 (Low grade astrocytoma)	Yes	[48]
			GB1, GB2, GB3 and GB4 (Glioblastoma)	Yes	[48]
	mGluR8	Human Glioma Lineage	U-87 MG	Yes	[72]
			U-343	Yes	[72]
			MOGGCCM	Yes	[72]
		Resection	AZ21 (Low grade astrocytoma)	Yes	[48]
			AZ8 (Low grade astrocytoma)	No	[48]
			AZ7 (Low grade astrocytoma)	Yes	[48]
			AZ6 (Low grade astrocytoma)	Yes	[48]
			AZ5 (Low grade astrocytoma)	Yes	[48]
			AZ4 (Low grade astrocytoma)	Yes	[48]
			AZ3 (Low grade astrocytoma)	Yes	[48]
			AZ2 (Low grade astrocytoma)	Yes	[48]
			GB1, GB3 and GB4 (Glioblastoma)	Yes	[48]
			GB2 (Glioblastoma)	No	[48]

Beyond the well-established role of glutamate receptors in glutamatergic neurotransmission, several evidences are emerging regarding the role of these receptors in cancer biology, especially in malignant brain tumors [39-41].

Activation of a mutated Ca^{+2}-permeable form of AMPA receptors (AMPAR) enhanced migration and proliferation of high-grade gliomas (Figure 1, step 4). Blockage of AMPAR by NBQX led to inhibition of glioma growth and induced apoptosis of remaining cells [42, 43]. AMPAR-mediated tumor proliferation seemed to involve a Ca^{2+}-dependent activation of Akt/PKB signaling pathway [44], since both NBQX (AMPAR antagonist) and Wortmannin (specific inhibitor of PI3K) reduced the Akt/PKB phosphorylation and decreased the number of tumoral viable cells in culture [45].

Parallel to iGluR, several evidences have demonstrated that mGluR are also functionally important for proliferation and differentiation of distinct types of cancer, including GBM [46]. Group III mGluR is involved in malignancy of a lot of cancers [47]. The implication of mGluR7 in tumor formation has yet to be characterized [46]. mGluR6 gene expression was shown to correlate with higher-grade pediatric CNS tumors [48]. Increased expression of mGluR4 and mGluR8 was reported in human lung adenocarcinoma samples and lung carcinoma cell line and treatment with mGluR8 agonist reduced cell growth and increased apoptosis in this lineage [49]. mGluR4 is overexpressed in more than 40% of malignant melanomas, laryngeal squamous cell carcinomas, and breast carcinomas and its overexpression was correlated with increased mortality in colorectal carcinoma [50]. mGluR4 inhibition suppressed proliferation of mGluR4-expressing colon cancer cell lines [50] whereas mGluR4 activation reduced cell proliferation in medulloblastoma cell lines and inhibits medulloblastoma cell xenografts progression in nude mice [51]. In addition, approximately 77% of human medulloblastoma samples expressed mGluR4, which was inversely correlated with tumor severity, spread, and recurrence [51].

Among Group I mGluR, increased mGluR5 immunoreactivity in human oral squamous cell carcinomas is associated with improved overall survival [52]. mGluR5 antagonist reduced tumor cell migration, invasion, and adhesion in human tongue cancer cells [52] and inhibits cell proliferation of laryngeal cancer [53]. Additionally, mGluR5 overexpression has been shown to induce melanoma development in transgenic mice [54]. Ectopic expression of mGluR1 in normal melanocytes induced melanocyte hyperproliferation *in vitro* and promote melanoma tumor development *in vivo* [55-59]. mGluR1 expression has been widely explored in breast cancer, supporting angiogenesis in these tumors, and silencing of this receptor (GRM1 shRNA) resulted in inhibition of cell proliferation [60]. In addition, mutations and single nucleotide polymorphisms (SNPs) of GRM1 were described in prostate cancer [61] and eight somatic variations of GRM1 were identified in cancers, including lung adenocarcinoma [62]. Group II mGluR is also implicated in a variety of cancer types [47], including melanoma [63]. Both group I and II mGluR are involved in glioma progression and the action *in vitro* and *in vivo* of agonists and antagonists of these receptors will be reported in detail in this review.

The above-mentioned evidences indicate that group I and III mGluR may be considered a potential therapeutic target for both gliomas and other forms of cancer. Moreover, from physiological and pharmacological point of view, there is a growing number of evidences suggesting mGluR are better drug targets than iGluR [64-67]. Compared to iGluR, mGluR play a 'modulatory' rather than 'mediatory' role in glutamatergic excitatory synaptic transmission [68-71]. Consequently, mGluR ligands (such as agonists or antagonists) might lead to more subtle effects on fast excitatory transmission than iGluR antagonists, which indicates their therapeutic use may be more tolerable for patients [64, 65].

IN VITRO STUDIES EVALUATING THE ROLE OF mGluR ON GLIOMA PROLIFERATION

Glioma cell cultures have been widely used to elucidate the role of mGluR in cancer malignancy. Some studies have used GBM lineages as cellular model [68, 72-75] while others have used primary cultures from human GBM resections [68, 76-79]. Table 1 (A, B and C) and Table 2 summarizes current literature evaluating mRNA expression and protein immunocontent of mGluR, respectively, in glioma cultures and human glioma resections. Group II mGluR (mGluR2/3) was the most investigated (expressed - mRNA - and immunodetected - protein) in the majority of human glioma biopsy samples, primary cultures, and glioma lineages. In order to clarify the role of mGluR on proliferation, invasiveness, and migration, several assays were performed treating GBM cells with antagonists and/or agonists of these receptors.

Arcella et al. (2005) showed pharmacological blockade of mGluR2/3 induced antiproliferative effects in U-87 MG glioma cell line. Daily addition (four days) of mGluR2/3 antagonists (LY 341495 - 1 μM; MTPG - 100 μM; or EGLU - 100 μM) to U-87 MG cultures reduced cell proliferation in a time-dependent manner, while did not induce apoptosis [73] (Figure 1, step 5). However, this treatment altered cell cycle, since FACS analysis showed antagonist reduced percentage of cells in S and G2M phases after two but not after four days of exposure. Furthermore, in cultures deprived of serum by 72 h, LY 341495 treatment reduced EGF-induced cyclin D1/D2 protein expression (early marker of the G1/S phase transition [79]).

In another study, using primary cultures from human GBM biopsies, D'Onofrio et al. (2003) showed

pharmacological blockade of mGluR3 reduced cell proliferation [68]. This effect was observed in all selected cultures mGluR3$^+$. Application of antagonist LY 341495 (1 μM) to growing medium once a day (for four days) reduced linear phase of growth in mGluR3+ cultures, with cell number being substantially reduced at 4th day of treatment. Cell growth was restored two days after washing out LY 341495, indicating that antiproliferative effect was reversible (*i.e.*, antagonist was cytostatic, not cytotoxic). For excluding involvement of other mGluR, authors performed an additional experiment using lower concentrations of LY 341495 and this antagonist was able to reduce linearly cell growth at concentrations of 1 and 10 nM, indicating that inhibition of mGluR3 was responsible for antiproliferative effect of LY 341495. This result was further corroborated by evidence that EGLU (100 μM), another antagonist of mGluR3, mimicked LY 341495 action on cell growth.

Glioma stem cells (GSC) are brain tumor-initiating undifferentiated cells [80], which have multipotential differentiation capacity, high tumorigenic potential and low proliferation rate [81, 82]. Normally, GSC are obtained from adult human GBM biopsy samples and form in culture classical floating aggregates, named tumor spheres. These cells are very chemoresistant and radioresistant and therefore probably responsible for tumor progression and recurrence after conventional GBM resection [82]. Ciceroni et al. (2008) and Zhou et al. (2014) observed GSC express mGluR3 protein (but not mGluR2) and its pharmacological blockade promoted an astroglial differentiation of GSC [76, 78]. Zhou et al. (2014) showed mGluR3 blockade by LY 341495 (100 nM) for 48 h resulted in a decreased proliferation combined with an increase in GSC GFAP$^+$ cells (classical marker for mature astrocytes) and a decrease of GSC nestin$^+$ cells (classical marker for neural stem cells) [78]. In addition, stimulation of mGluR3 for 48 h by specific agonist LY 379268 (100 nM) has no effect on GSC proliferation and differentiation, which suggests mGluR3 activity is necessary to maintain proliferation but is incapable of stimulating it *per se* (Figure 1, step 5).

Ciceroni et al. (2008) showed treatment of GSC with antagonist LY 341495 (100 nM) promoted astrocytic-like differentiation of cells (increasing GFAP$^+$ cells) and nestin$^+$ cells were virtually absent after 14 days of treatment [76]. Treatment with agonist LY 379268 (100 nM) did not affect differentiation of cells. In another set of experiments, these authors cultured GSC under differentiating conditions (medium deprived of mitogens and containing 10% of fetal calf serum) for 8 days and received treatments with mGluR3 ligants. After, cells were enzymatically dissociated, transferred to uncoated 96-well plates, and regrown under proliferating conditions without any mGluR3 ligants (medium containing epidermal growth factor - EGF - plus basic fibroblast growth factor - bFGF - and lacking serum) for plus 12 days. Treatment of cells with agonist LY 379268 during differentiation phase led to formation of tumor spheres in proliferative phase. In contrast, cells treated with antagonist LY 341495 originated cultures containing exclusively adherent astrocyte-like cells. This indicated that treatment with mGluR3 antagonist was sufficient to maintain GSC towards astroglial differentiation even under conditions in which they normally proliferate and maintain their undifferentiated state (Figure 1, step 5).

For both above-mentioned studies [76, 78], GSC did not respond to agonist LY 379268 probably because mGluR3 were constantly stimulated by L-Glu already present in culture medium. Concentrations of extracellular L-Glu in GSC cultured for 8 and 14 days under differentiating conditions (medium deprived of mitogens and containing serum) were about 60 μM and 70 μM, respectively [76]. These concentrations exceed the reported EC_{50} value for L-Glu and recombinant mGluR3 by 5-10 fold [83], which is sufficient to saturate all mGluR3.These results point to the notion that activation of mGluR3 by endogenous L-Glu allows proliferation of GSC by limiting astroglial differentiation and that receptor blockage eliminates this constraint, thereby promoting cell differentiation. This hypothesis is supported by work performed by Yelskaya et al. (2013), in which U-87 MG cultures where treated with Riluzole (1-100 μM), a drug that blocks the secretion of L-Glu and enhances its uptake from extracellular space [47]. Riluzole inhibited proliferation of cells in a dose-dependent manner, suggesting that absence of L-Glu in extracellular medium prevents glutamate-dependent proliferation and putative activation of mGluR3 in U-87 MG cells [84].

Group II mGluR are known to be able to activate the MAPK and PI3K pathways [37, 85-89], which are usually activated in response to proliferating agents [90, 91]. Arcella et al. (2005) [73] showed treatment of U-87 MG cultures with antagonist LY 341495 (1 μM) reduced activation of MAPK (assessed by WB analysis of p-Erk1/2) and PI3K (assessed by WB analysis of p-Akt/PKB) pathways. All of these effects were reversed by addition of agonist LY 379268 (1 μM), which was inactive *per se*. WB analysis also showed exposure to LY 341495 did not alter mGluR2/3 immunocontent (at least up to four days of treatment). Another study indicated that activation of mGluR3 could have a permissive role on stimulation of MAPK and PI3K pathways in GSCs dissociated cultures [77]. GSCs dissociated from tumor spheres were starved from mitogens and then treated with agonist LY 379268 (100 nM), which inhibited forskolin-stimulated cyclic adenosine monophosphate (cAMP) formation and increased p-Erk1/2 and p-Akt/PKB levels. All these effects were reversed by antagonist LY341495 (100 nM). In addition, treatment with LY 341495 also reversed EGF- and bFGF-induced increase in p-Erk1/2 and p-Akt/PKB levels. LY 341495 alone did not affect EGF receptor (EGFR) autophosphorylation in response to

EGF, which suggests that this drug had no direct effects on EGFR (Figure 1, step 6, 7, 9 and 10).

D'Onofrio et al (2003) examined the immunocontent of cyclin D1 and D2 and the activation of MAPK pathway in primary GBM cell cultures in serum-deprived conditions and in proliferative conditions (cells incubated with EGF for 8 h, for assessment of cyclin D1/D2, or for 10 min, for assessment of MAPK pathway) [68]. Addition of 1 μM of mGluR3 antagonist LY 341495 (in combination with EGF) reduced EGF-induced increase in immunocontent of both cyclin D1/D2 and p-Erk1/2. Effect on cyclin D1/D2 protein expression was partially reversed by agonist LY 379268 (1 μM) (Figure 1, step 11). To assess whether inhibition of MAPK pathway was the only mechanism responsible for antiproliferative effect of LY 341495, authors studied association of this drug with MAPK kinase (MEK) inhibitor, PD 98059. Both LY 341495 (1 μM) and PD 98059 (30 μM) reduced cell number in about 45%. Ability of LY 341495 and PD 98059 to reduce Erk1/2 phosphorylation suggests mGluR2/3-MAPK axis supports proliferation rate of human GBM cells. Since anti-proliferative effect of LY 341495 was not totally obliterated by PD 98059, other proliferation pathways may be also being controlled by mGluR2/3 in GBM cells (Figure 1, step 6 and 7).

Ciceroni et al. (2008) focused on interaction between mGluR3 and bone morphogenetic proteins (BMP), which are known to promote astroglial differentiation of GSC [92]. BMP bind to membrane receptors of BMP/TGF-ß/activin family, which leads to phosphorylation and translocation of Smad1/5/8 proteins to nucleus [93]. Addition of exogenous BMP4 (100 ng/mL) plus mGluR3 agonist LY 379268 (100 nM) prevented BMP4-induced nuclear translocation and phosphorylation of Smad. Inhibitory action of LY 379268 was unaffected by non-metabolizable cAMP analogue, 8-Bromo-cAMP (1 mM), but was prevented by MAPK kinase (MEK) inhibitor, UO126 (30 μM), which was inactive *per se*. Moreover, cultures exposed to mGluR3 antagonist LY 341495 (100 nM) enhanced Smad1/5/8 phosphorylation to an extent similar to BMP4. These results suggested that activation of mGluR3 could inhibit BMP4 receptor signaling by activation of MAPK pathway. In addition, activation of mGluR3-MAPK pathway by endogenous L-Glu presented in medium may limit BMP4-induced differentiating activity, thus contributing to support undifferentiated state of GSCs, and eventually GBM growth and relapse [76] (Figure 1, step 8).

Yelskaya et al. (2013) reported that a combination of mGluR2/3 antagonist LY 341495 and Gefitinib, an EGFR inhibitor, works most efficiently to inhibit proliferation and migration of U-87 MG cells and induced apoptosis in this cell lineage [84]. They also investigated the efficacy of different classes of drugs (AMPAR antagonist - NBQX; mGluR2/3 antagonist - LY341495; EGFR inhibitor - Gefitinib; and PI3K inhibitors - Wortmannin and PI 828) in inhibiting proliferation of U-87 MG cells (24 h). A combination of Gefitinib (25 μM) with LY 341495 (1 μM) or PI 828 (2 μM) was more effective to inhibit proliferation of U-87 MG cells when compared to individual drugs alone. Using TUNEL assay, authors showed treatment with Gefitinib resulted in increased apoptosis compared to control group. Gefitinib in combination with PI 828 or Wortmannin (5 μM) did not increase apoptosis in cell cultures. However, treatment with Gefitinib plus NBQX (5 μM) or Gefitinib plus LY 341495 increased apoptosis compared to Gefitinib, NBQX or LY 341495 alone. Maximum percentage of apoptosis was observed in treatment with Gefitinib plus LY341495. Distance migrated by cells (wound healing assay) was significantly reduced with Gefitinib plus LY 341495 treatment when compared to treatments with Gefitinib or LY 341495 alone or control group (Figure 1, step 14).

An interesting question that arises from above-mentioned works is whether mGluR3 antagonists could interact with classical chemotherapies and whether activation of this receptor in malignant gliomas could control expression of proteins implicated in chemoresistance. In this context, Ciceroni et al. (2013) showed mGluR3 inhibition enables cytotoxic action of TMZ in GSC cultures [77]. TMZ (250 μM) did not affect cell viability when applied alone, but became toxic when combined with LY 341495 (100 nM) and LY 2389575 (100 nM), two mGluR3 antagonists. mGluR3 agonist LY 379268 (100 nM) was inactive *per se*, but reversed the permissive action of LY 341495 on TMZ toxicity. siRNA-induced knockdown of mGluR3 also enabled TMZ toxicity and antagonist LY 341495 did not further amplify TMZ toxicity in mGluR3 silenced cells [77]. This data suggests that a possible activation of mGluR3 by GSC-autocrine release of L-Glu could restrain toxic action of TMZ, increasing chemoresistance of these tumor cells (Figure 1, step 12). GSC were treated with other anticancer drugs (etoposide, irinotecan, irinotecan metabolite - SN 38, cisplatin or paclitaxel) alone or combined with mGluR3 antagonist LY341495 and these treatments had no significant effect on GSC viability, suggesting mGluR3 receptors selectively control responses of cells to TMZ and could not be extended to other chemotherapeutic agents.

In order to evaluate mechanisms underlying mGluR3-induced chemoresistance, Ciceroni et al. (2013) treated GSC with molecules that interfere in three major signaling pathways activated by mGluR3 [77]: inhibition of adenylyl cyclase (AC) activity, activation of MAPK pathway and activation of PI3K pathway [85, 88, 94, 95]. Cell permeable cAMP analog, 8-Bromo-cAMP (1 mM), did not affect synergism between mGluR3 blockade and TMZ. MAPK kinase (MEK) inhibitor, UO126 (30 μM), had mild effect on TMZ toxicity. In contrast, PI3K inhibitor LY 294002 (10 μM) had a permissive action on TMZ toxicity, mimicking the effect of mGluR3 blockade. Actions of LY 294002 and LY 341495 were less than

addictive, suggesting mGluR3 inhibition facilitates cytotoxicity by limiting activation of PI3K pathway. This hypothesis was supported by the use of GSCs expressing a constitutively active form of t PI3K substrate, Akt/PKB [96]. In these cells, in which PI3K pathway was active in spite of mGluR3 blockade, synergism between LY 341495 and TMZ was largely attenuated (Figure 1, step 12).

The sensitivity of cancer cell lineages to various inhibitors and chemotherapeutic drugs is often associated with genetic mutations of key elements in the Ras-Raf-MEK-ERK and PI3K-PTEN-Akt/PKB-mTOR pathways [97, 98]. Akt/PKB is known to activate nuclear factor-κB (NF-κB) by phosphorylating IκB kinase [99], which limits the pro-apoptotic activity of DNA-alkylating agents in glioma cells [100]. In Ciceroni et al. (2013) study, treatment with TMZ activated NF-κB, showed by increased levels of IκB phosphorylation. This effect was reversed by mGluR3 antagonist, LY 341495, or by PI3K inhibitor, LY 294002. The specific NF-κB inhibitor JSH-23 (10 μM) [101] enabled TMZ toxicity and occluded permissive action of LY 341495 in GSCs. Similar effects were obtained with salicylic acid, which also inhibits NF-κB [102]. As opposed to LY 341495, JSH-23 could still enhance TMZ toxicity in GSCs expressing the constitutively active form of Akt/PKB, indicating NF-κB lies downstream to Akt/PKB in pathway that restrains TMZ toxicity (Figure 1, step 12). Akt/PKB also regulates mammalian target of rapamycin (mTOR), which promotes mRNA translation and protein synthesis by phosphorylating p70 S6K and 4E-BP1 [103].

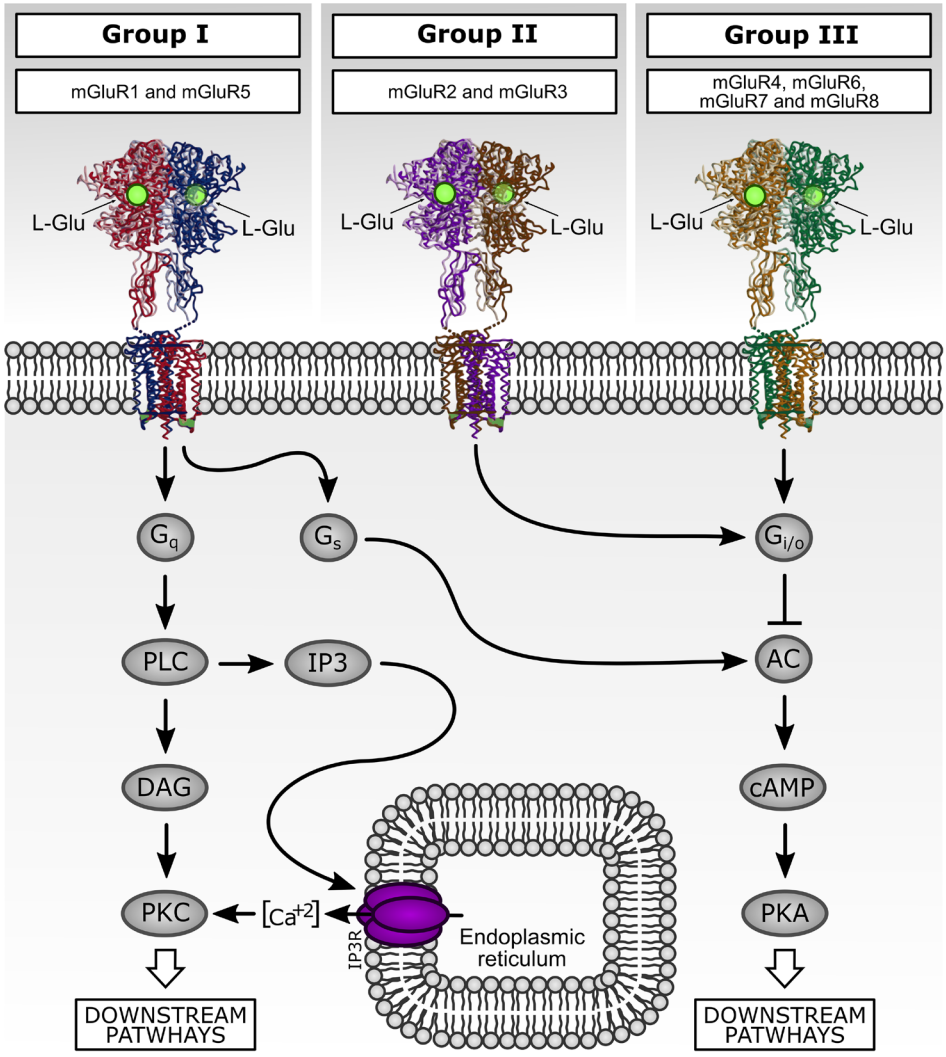

Figure 2 : . Downstream signaling pathways activated by metabotropic glutamate receptors (mGluR). mGluR family comprises eight subtypes subdivided in three groups according their sequence homology, pharmacology, and second messenger signaling pathway association. Group I mGluR are coupled to G_q proteins and their activation stimulates phospholipase C (PLC) and phosphatidylinositol 4,5-biphosphate (PIP_2) hydrolysis. PIP_2 hydrolysis generates inositol (1,4,5)-trisphosphate (IP_3) and diacylglycerol (DAG), which stimulates intracellular Ca^{2+} release from endoplasmic reticulum and activates protein kinase C (PKC), respectively. In contrast, mGluR of group II and III are coupled predominantly to $G_{i/o}$ proteins and classically related to inhibition of adenylyl cyclase (AC) and directly regulate ion channel activity and other downstream signaling partners *via* liberation of $G_{\beta\gamma}$ subunits.

mGluR stimulation activates mTOR pathway [104, 105] and inhibitors of Akt/PKB-mTOR pathway are under development for treatment of cancer, including malignant gliomas [106, 107]. In Ciceroni et al. (2013) work, it was shown selective mTOR inhibitor rapamycin (10 nM) did not mimic, but rather abolished permissive action of mGluR3 blockade on TMZ toxicity (Figure 1, step 13).

Clinical efficacy of TMZ is limited by DNA-repairing enzyme, O6-methylguanine-DNA methyltransferase (MGMT), which removes DNA adducts generated by alkylating agents [108]. In Ciceroni et al. (2013) [77] study, GSC clones constitutively expressed MGMT and treatment with TMZ alone increased MGMT mRNA levels 3 h after its application and slightly reduced MGMT protein levels at 24 and 48 h. When TMZ was combined with LY 341495, MGMT mRNA did not increase and MGMT protein levels were markedly reduced. Moreover, action of LY341495 was mimicked by siRNA-induced knockdown of mGluR3, or PI3K inhibitor (LY 294002), or by NF-κB inhibitor (JSH-23). Finally, the permissive action of LY 341495, LY 294002, or JSH-23 was no longer seen in GSC overexpressing MGMT, demonstrating that synergistic action of mGluR3 blockade and TMZ treatment was mediated by inhibition of MGMT expression. This hypothesis was supported by evidence that treatment with MGMT inhibitor, O6-benzylguanine (10 μM), enabled TMZ toxicity. These results suggest that mGluR3-dependent TMZ toxicity restrains is supported by induction of MGMT transcription *via* an intracellular signaling pathway that sequentially involves PI3K and NF-κB.

A recent study described, for the first time, an anti-cancer role of mGluR1 in gliomas [41]. Zhang et al. (2015) showed treatment with selective mGluR1 antagonist Bay 36-7620 (50μM) or Riluzole (50μM), a glutamate release inhibitor approved for amyotrophic lateral sclerosis [47, 109], markedly decreased cell viability and increased LDH release in U-87 MG lineage. These treatments and mGluR1 knockdown (using siRNA technology) significantly increased apoptotic rate in these glioma cells. In addition,

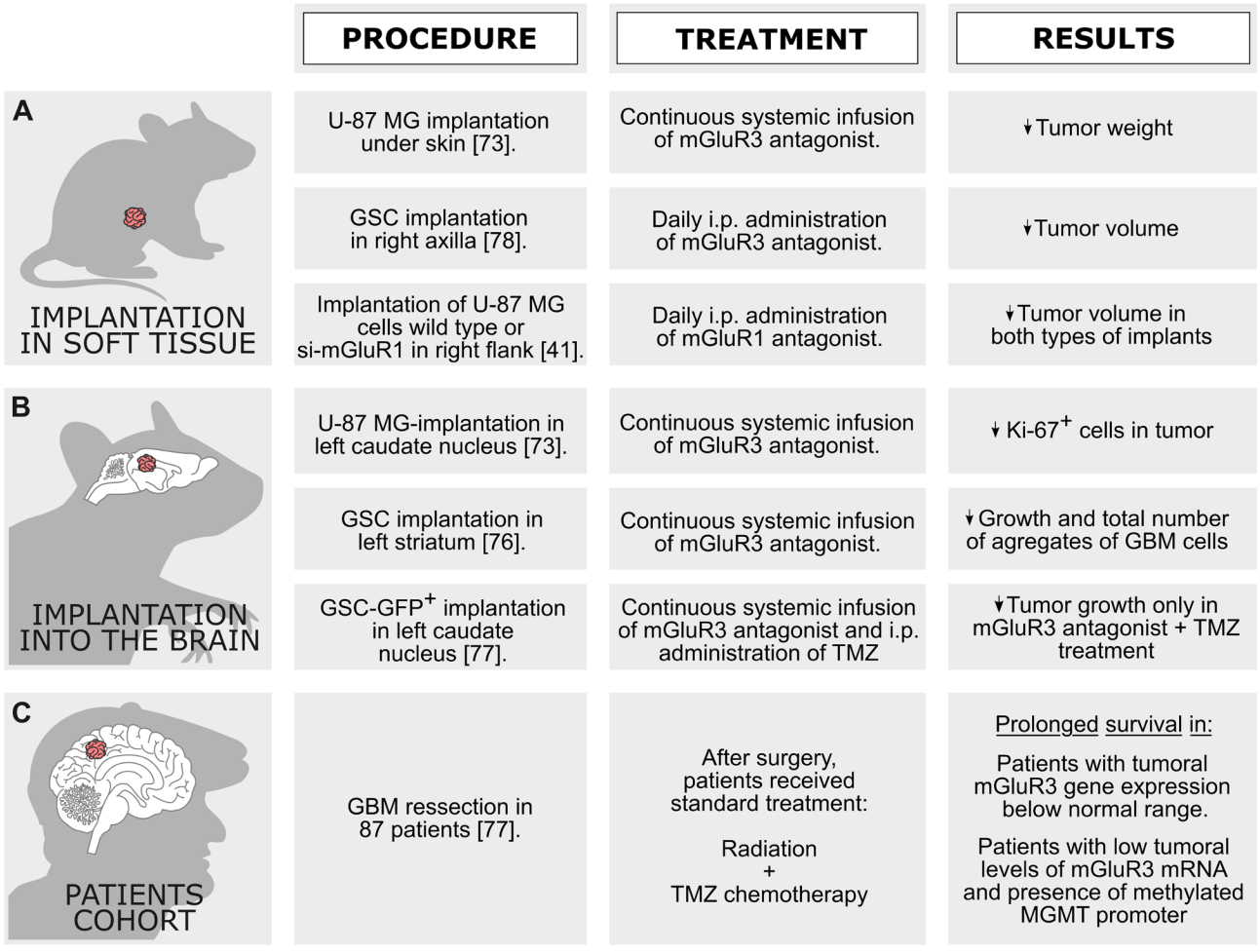

Figure 3 : *In vivo* models employed to study the role of mGluR on brain tumor growth and aggressiveness. A. and **B.** Effects of mGluR ligands in two mice xenograft models. **C.** Relation between tumoral mGluR3 mRNA expression and GBM patients' survival.

Riluzole or Bay 36-7620 increased immunocontent of cleaved PARP and caspase-3, whereas immunocontent of pro-PARP and pro-caspase-3 was not altered. Similar results were observed after mGluR1 knockdown. Authors also tested whether treatment with Riluzole or Bay 36-7620 and transfection with mGluR1 targeted siRNA could induce inhibition of PI3K activity in U87 cells. U-87 MG cells showed a significantly decreased phosphorylation of PI3K after mGluR1 blockade as well as after mGluR1 targeted siRNA. mGluR1-dependent inhibition of PI3K resulted in inhibition of Akt/PKB phosphorylation at both Ser473 and Thr308 residues. Moreover, mGluR1 inhibition decreased expression levels of p-mTOR and P70 S6K, one of the best-characterized targets of mTOR complex. In contrast, expression of PTEN was not changed by antagonists or siRNA transfection. All these data provided strong evidence that activation of PI3K-Akt/PKB-mTOR pathway was suppressed after mGluR1 inhibition (Figure 1, step 15).

The majority of above-mentioned *in vitro* works indicates that endogenous activation of mGluR1 and mGluR3 increase the proliferation of GBM cells and that MAPK and PI3K pathways may be involved in this process. All of these studies are particularly interesting from a therapeutic standpoint since ligands of these types of mGluR represent an expanding class of drugs endowed with high receptor affinity, elevated brain penetration, and good profile of safety and tolerability [65, 83]. These features make these drugs potential candidates for *in vivo* studies evaluating progression and aggressiveness of malignant brain tumors.

IN VIVO STUDIES EVALUATING THE ROLE OF mGluR ON GLIOMA TUMOR PROGRESSION

Arcella et al. (2005) [73] have shown that a continuous systemic infusion of mGluR2/3 antagonist LY 341495 reduced growth of GBM cells in two independent *in vivo* models. U-87 MG cells were implanted under skin (2 x 10^6 cells/mL) of mice, which were subcutaneously implanted with osmotic minipumps releasing saline, LY 341495 (1 mg/kg per day), EGLU (1 mg/kg per day), LY 379268 (1 mg/kg per day), or LY 341495 plus LY 379268 during 28 days. Analysis of tumor weight showed chronic infusion of antagonists LY 341495 or EGLU reduced GBM growth. On the other hand, infusion of mGluR2/3 agonist LY 379268 did not affect tumor growth and failed to fully reverse LY341495 effect. These results corroborate with Zhou et al. (2014) *in vitro* study [78], in which activation of mGluR2/3-dependent signaling pathway is necessary to maintain tumor growth but is incapable of stimulating it *per se*.

In another set of experiments, Arcella et al. (2005) implanted U-87 MG cells into brain left caudate nucleus of nude mice and immunohistochemical analysis revealed that these cells showed a higher expression of mGluR2/3 and Ki-67 (a cellular marker for proliferation) [73]. After magnetic resonance imaging (MRI) analysis (7^{th} day after cell implantation), selected mice with similar tumor sizes were subcutaneously implanted with osmotic minipumps releasing either saline or antagonist LY 341495 (10 mg/kg per day). Treatment during 7 days with LY 341495 reduced tumor size and drug effect was particularly evident during exponential phase of tumor growth (between the 21^{st} and 28^{th} days after cell implantation). Withdrawal of LY 341495 on 21^{st} day allowed growing of tumor to the same extent as control group, suggesting effect of LY 341495 was reversible and cytostatic. Treatment with LY 341495 also reduced the number of Ki-67^+ cells in tumor specimens.

These two xenograft models above-described may be complementary (Figure 3A and 3B). Growth of implanted cells in a soft tissue (*i.e.*, subcutaneously) evaluates mainly proliferation rate of tumor on an adequate energy supply. On the other hand, growth of glioma cells in brain requires multiple processes, such as excitotoxic-mediated neuronal death, expression of enzymes that degrade extracellular matrix, and expression of ion channels that drive movement of water out of cell [110]. Unfortunately, work performed by Arcella et al. (2005) have no information regarding outcome of mice treated with LY 341495, since animals were not allowed to survive beyond the 4^{th} week of tumor growth. Nevertheless, authors said none of the five mice died during the four weeks of observation in group treated with this antagonist [73].

Ciceroni et al. (2008) showed continuous pharmacological blockade of mGluR3 reduced growth of infiltrating brain tumors originating from GSC xenografts [76]. GSC spheres were suspended in their growing medium and then infused into left striatum of nude mice (3 x 10^5 cells/3 µL). Immediately after cell transplantation, mice were subcutaneously implanted with osmotic minipumps releasing mGluR3 agonist LY 379268 or antagonist LY 341495 (both at a rate of 1 mg/kg per day during 3 months), or filled with saline solution. MRI analysis carried out at 3 months showed signal alterations in brain parenchyma of control and LY 379268 treated mice, however, no changes were observed in mice treated with antagonist LY 341495. Histological analysis revealed presence of small and large aggregates of GBM cells in brain parenchyma, which were characterized by nuclear atypia and high mitotic activity. These features are consistent with primitive advanced-stage GBM, where tumors migrate and disseminate asymmetrically along blood vessels and fiber tracts and not grow uniformly [111]. Cell aggregates were consistently found in ipsilateral neostriatum, as well as along the intra- and inter-hemispheric white matter in both control and LY 379268 treated mice. On the other hand, aggregates were absent or present to a very low extent in animals treated

Table 2: Protein immunocontent of mGluR subtypes in cellular malignant glioma models.

Metabotropic glutamate receptors		Protein (Western Blot)			
		Sample		Expression	Reference
Group I	mGluR1	Human Glioma Lineage	U-87 MG	Yes	[41]
			U-373	No	[75]
		Resection	Astrocytoma II	No	[75]
			Astrocytoma Anaplastic	No	[75]
			Glioblastoma	No	[75]
	mGluR5	Human Glioma Lineage	U-87 MG	Yes	[41, 75]
			U-373	Yes	[75]
			U-118	Yes	[75]
		Resection	Astrocytoma II	Yes	[75]
			Astrocytoma Anaplastic	Yes	[75]
			Glioblastoma	Yes	[75]
Group II	mGluR2/3	Human Glioma Lineage	U-87 MG	Yes	[68]
			U-373	No	[68]
			A172	Yes	[68]
		Primary culture from human glioma	FCN-9	Yes	[68]
			MZC-12	Yes	[68]
			MSS-5	Yes	[68]
			BRT-3	Yes	[68]
			CRL-8	Yes	[68]
			GSS 98	Yes	[68]
			DMD 126	Yes	[68]
			MTR4	Yes	[68]
			Glioma Stem Cells	Yes	[76, 77]
		Resection	Astrocytoma II	Yes	[75]
			Astrocytoma Anaplastic	Yes	[75]
			Glioblastoma	Yes	[75]
	mGluR2	Primary culture from human glioma	Glioma Stem Cells	No	[78]
		Resection	Glioblastoma	Yes	[78]
	mGluR3	Primary culture from human glioma	Glioma Stem Cells	Yes	[78]
		Resection	Glioblastoma	Yes	[78]

with antagonist LY 341495, which indicates that mGluR3 blockage inhibited GSC-dependent generation of tumor cell progeny and/or reduced the growth of GBM malignant cells.

Zhou et al. (2014) used a model of subcutaneous implantation of GSC ($1x10^3$ cells) in right axilla of mice [78]. After 3 weeks of GSC implantation, tumors were large, ulcerative and had complete capsule. HE stained reveled cells with dark nuclei without evidences of necrosis. Intercellular heteromorphism was obvious and vascular structure was clear. Mice treated with LY 341495 intraperitoneally (1 mg/kg per day) presented a reduced tumor volume when compared to animals treated with agonist LY 379268 (1 mg/kg per day) and vehicle. This result was sustained during 10^{th}, 15^{th} and 20^{th} days after cells implantation.

Ciceroni et al. (2013) have evaluated the effect of mGluR3 inhibition plus TMZ treatment on tumor growth in nude mice implanted with human GSCs in brain parenchyma [77]. All mice were subcutaneously implanted with osmotic minipumps releasing LY 341495 antagonist (3mg/kg per day for 28 days) or saline. At the same time, mice received three injections of TMZ (70mg/kg, intraperitoneally) or vehicle (every day) during the 1^{st} week following minipump implantation. In one experiment, mice received drug treatments during 15 days after GSC implantation and were killed 30 days later (i.e. 45 days after cell implantation). In the other experiment, mice were treated with drugs during 45 days after GSC implantation and killed 30 days later (i.e. 75 days after cell implantation). Control mice (i.e., minipump releasing saline and vehicle injected intraperitoneally) showed presence of GSCs in brain with typical morphology of GBM. For mice killed 45 days after cell implantation, tumor cells were confined to medial portion of caudate nucleus close to wall of lateral ventricle. Mice killed at 75^{th} day showed infiltrating mass tumors in ipsilateral caudate nucleus. Moreover, tumor cells spread to ipsi- and contralateral portion of corpus callosum. Treatment of animals with LY 341495 or TMZ alone did not alter tumor

growth in all analyzed brain areas. However, a combined treatment with TMZ plus LY341495 significantly reduced tumor growth in analyzed brain areas. The authors did not observe any signs of systemic toxicity or motor impairment in mice treated with LY 341495 (3 mg/kg per day). In addition, in this work mice survived to acute experiments using doses higher than 300 mg/kg of LY 341495.

Zhang et al. (2015) also demonstrated an anti-tumor activity of mGluR1 inhibition *in vivo* using a U-87 MG xenograft GBM model in nude mice [41]. After implantation of U-87 MG, tumor-bearing mice were treated every day with Bay 36-7620 (mGluR1 antagonist - 10 mg/kg) intraperitoneally during 24 days. Treatment reduced significantly tumor volume from 22nd to 30th days when compared to control group. In other experiment, nude mice were injected with si-mGluR1 transfected U-87 MG cells or si-control transfected U-87 MG cells. As expected, tumor in si-mGluR1 group had a smaller volume when compared to si-control group.

Association between antitumoral features and apparently non-toxic effects of mGluR antagonists *in vivo* indicates these drugs are potential candidates for an adjuvant treatment for GBM in humans.

PATIENTS COHORT TO EVALUATE THE ROLE OF mGluR ON GLIOMA AGGRESSIVENESS

Only one study has evaluated the profile of mGluR mRNA expression in a cohort of patients with GBM (Figure 3C) [77]. It was analyzed a possible relationship between expression levels of mGluR3 and survival rate of patients with GBM undergoing surgery followed by radiotherapy and TMZ chemotherapy. The transcript of mGluR3 was measured by quantitative PCR in selected regions of tumor in a cohort of 87 patients. 'Normal' mGluR3 mRNA levels were defined as those measured in autoptic brain samples with no histological abnormalities. Levels of mGluR3 mRNA below normal range were detected in 42 GBM biopsies (48.3%), whereas 45 tumor samples (51.7%) presented higher mRNA levels. Kaplan-Meier (KM) survival analysis showed a prolonged survival rate for patients with tumoral mGluR3 RNA expression below normal range. Interestingly, five patients who survived longer than 36 months showed tumoral mGluR3 mRNA expression below normal range. On multivariate analysis, Karnofsky performance score and mGluR3 mRNA emerged as independent predictors for survival. Authors also stratified patients for mGluR3 expression and methylation of MGMT promoter. Group with low tumoral mGluR3 mRNA levels and methylated MGMT promoter showed a significantly higher survival rate as compared to low tumoral mGluR3 mRNA and unmethylated MGMT promoter group.

In summary, low levels of mGluR3 mRNA in tumor specimens may be a predictor for long survival rate in patients with GBM. In addition, methylation state of MGMT gene promoter influenced survival only in those patients whose GBM biopsies presented low expression of mGluR3 RNA. These data may encourage the use of mGluR3 antagonists as adjuvant drugs for treatment of GBM and suggest transcript levels of mGluR3 should be a potential predictor of GBM patients' survival.

CONCLUSIONS

A large number of preclinical studies have suggested that metabotropic glutamate receptors could be considered a prospective molecular target for treatment of several brain disorders, including depression [112], anxiety disorders [113], Alzheimer's disease [114], Parkinson's disease [115], and more recently malignant brain tumors. Several *in vitro* and *in vivo* studies have supported the putative involvement of mGluR-mediated signaling on progression, aggressiveness, and recurrence of malignant gliomas, which points to the notion that specific subtype-selective mGluR ligands may be considered as potential adjuvant chemotherapy for glioma treatment. Several academic groups [116-118], Pfizer [119], Roche [120, 121], Novartis [122] and Merck [123] have employed receptor structure-based design of mGluR selective negative allosteric modulators (NAMs) in their studies and ligand-receptor binding models were refined using mutagenesis and structure-activity data. Even though pharmaceutical and toxicological properties of all mGluR ligands are not yet entirely determined for humans (such as effective and maximum tolerable doses), several clinical studies on Phase I, II and III are being performed using mGluR modulators for treatment of distinct brain disorders and cancer. Addex Pharmaceuticals (Geneva, Switzerland) are recently performing a Phase I clinical trials on its mGluR5 ligand ADX48621 for the treatment of depression and anxiety (ClinicalTrials.gov Identifier: NCT02447640). Similarly, a compound LY 2140023, a prodrug of the group II metabotropic glutamate receptor agonist LY 404039, has been tested in a Phase III for the treatment of patients with schizophrenia (ClinicalTrials.gov Identifier: NCT01328093). Regarding cancer treatment, Barbara Ann Karmanos Cancer Institute in collaboration with National Cancer Institute (NCI) are performing a Phase I clinical trial to evaluated the efficacy of riluzole, a mGluR 1 blocker, into reduce the breast cancer growth (NCT00903214). If any of these compounds eventually obtain approval by the Food and Drug Administration (FDA), there will be a strong scientifically-based rationale for testing distinct group I and II mGluR antagonists in the treatment of malignant brain tumors through prospective, large-scale and randomized clinical trials.

Abbreviations

8-Bromo-cAMP: Non-metabolisable cAMP analogue
AC: Adenylyl cyclase
AMPAR: Ionotropic glutamate receptor AMPA
Bay 36-7620: mGluR1 antagonist
BCNU: Carmustine
bFGF: Basic fibroblast growth factor
BMP: Bone morphogenetic proteins
cAMP: Cyclic adenosine monophosphate
CD133: Stem cell marker
CNS: Central nervous system
Cys: Cystine
DAG: Diacylglycerol
DCG-IV: Group II mGluR agonist
DHPG: Group I mGluR agonist
EAAT2: Excitatory amino acid transporter 2
EAAT3: Excitatory amino acid transporter 3
EGF: Epidermal growth factor
EGFR: EGF receptor
EGLU: Selective group II antagonist
FACS: Fluorescence-activated cell sorting
FCS: Fetal calf serum
GBM: Glioblastoma
GFAP: Glial fibrillary acidic protein
GluR: Glutamate receptors
GSC: Glioma stem cells
HR: Hazard ratio
iGluR: Ionotropic glutamate receptors
IP_3: Inositol (1,4,5)-trisphosphate
i.p.: intraperitoneal injection
JSH-23: NF-κB inhibitor
L-Glu: L-glutamate
LY 2389575: Group II mGluR antagonist
LY 294002: PI3K inhibitor
LY 341495: Group II mGluR antagonist
LY 379268: Group II mGluR agonist
MAPK: Mitogen-activated protein kinase
MEK: MAPK kinase
mGluR: Metabotropic glutamate receptors
MGMT: O6-methylguanine-DNA methyltransferase
MPEP: Selective group I antagonist
MRI: Magnetic resonance imaging
mTOR: Mammalian target of rapamycin
NBQX: AMPAR antagonist
NF-κB: Nuclear factor-κB
NMDAR: Ionotropic glutamate receptor NMDA
P70 S6K: p70 ribosomal protein S6 kinase
PCR: Polymerase chain reaction
PD 98059: MEK inhibitor
PI 828: PI3K inhibitor
PI3K: Phosphatidylinositol-4,5-bisphosphate 3-kinase
PiP_2: Phosphatidylinositol-4,5-bisphosphate
PKC: Protein kinase C
PLC: Phospholipase C
siRNA: Small interfering RNA
SN 38: Irinotecan metabolite
TMZ: Temozolomide
UO126: MEK inhibitor
VEGF: Vascular endothelial growth factor
WHO: World Health Organization
Wortmannin: PI3K inhibitor
xCT: Cystine-glutamate antiporter.

CONFLICTS OF INTEREST

There is no conflict of interest.

REFERENCES

1. Westphal M and Lamszus K. The neurobiology of gliomas: from cell biology to the development of therapeutic approaches. Nature reviews Neuroscience. 2011; 12(9):495-508.
2. Cloughesy TF, Cavenee WK and Mischel PS. Glioblastoma: from molecular pathology to targeted treatment. Annu Rev Pathol. 2014; 9:1-25.
3. Louis DN, Perry A, Reifenberger G, von Deimling A, Figarella-Branger D, Cavenee WK, Ohgaki H, Wiestler OD, Kleihues P and Ellison DW. The 2016 World Health Organization Classification of Tumors of the Central Nervous System: a summary. Acta Neuropathol. 2016; 131(6):803-820.
4. Louis DN, Ohgaki H, Wiestler OD, Cavenee WK, Burger PC, Jouvet A, Scheithauer BW and Kleihues P. The 2007 WHO classification of tumours of the central nervous system. Acta Neuropathol. 2007; 114(2):97-109.
5. Omuro A and DeAngelis LM. Glioblastoma and other malignant gliomas: a clinical review. JAMA. 2013; 310(17):1842-1850.
6. Ostrom QT, Gittleman H, Fulop J, Liu M, Blanda R, Kromer C, Wolinsky Y, Kruchko C and Barnholtz-Sloan JS. CBTRUS Statistical Report: Primary Brain and Central Nervous System Tumors Diagnosed in the United States in 2008-2012. Neuro Oncol. 2015; 17 Suppl 4:iv1-iv62.
7. Kleihues P, Soylemezoglu F, Schäuble B, Scheithauer BW and Burger PC. Histopathology, classification, and grading of gliomas. Glia. 1995; 15(3):211-221.
8. Theeler BJ, Yung WK, Fuller GN and De Groot JF. Moving toward molecular classification of diffuse gliomas in adults. Neurology. 2012; 79(18):1917-1926.
9. Verhaak RG, Hoadley KA, Purdom E, Wang V, Qi Y, Wilkerson MD, Miller CR, Ding L, Golub T, Mesirov JP, Alexe G, Lawrence M, O'Kelly M, Tamayo P, Weir BA, Gabriel S, et al. Integrated genomic analysis identifies clinically relevant subtypes of glioblastoma characterized by abnormalities in PDGFRA, IDH1, EGFR, and NF1. Cancer Cell. 2010; 17(1):98-110.

10. Phillips HS, Kharbanda S, Chen R, Forrest WF, Soriano RH, Wu TD, Misra A, Nigro JM, Colman H, Soroceanu L, Williams PM, Modrusan Z, Feuerstein BG and Aldape K. Molecular subclasses of high-grade glioma predict prognosis, delineate a pattern of disease progression, and resemble stages in neurogenesis. Cancer Cell. 2006; 9(3):157-173.

11. Bredel M, Scholtens DM, Harsh GR, Bredel C, Chandler JP, Renfrow JJ, Yadav AK, Vogel H, Scheck AC, Tibshirani R and Sikic BI. A network model of a cooperative genetic landscape in brain tumors. JAMA. 2009; 302(3):261-275.

12. Yadav AK, Renfrow JJ, Scholtens DM, Xie H, Duran GE, Bredel C, Vogel H, Chandler JP, Chakravarti A, Robe PA, Das S, Scheck AC, Kessler JA, Soares MB, Sikic BI, Harsh GR, et al. Monosomy of chromosome 10 associated with dysregulation of epidermal growth factor signaling in glioblastomas. JAMA. 2009; 302(3):276-289.

13. Tsao MN, Mehta MP, Whelan TJ, Morris DE, Hayman JA, Flickinger JC, Mills M, Rogers CL and Souhami L. The American Society for Therapeutic Radiology and Oncology (ASTRO) evidence-based review of the role of radiosurgery for malignant glioma. Int J Radiat Oncol Biol Phys. 2005; 63(1):47-55.

14. DeAngelis LM. Brain tumors. N Engl J Med. 2001; 344(2):114-123.

15. Wang Y and Jiang T. Understanding high grade glioma: molecular mechanism, therapy and comprehensive management. Cancer Lett. 2013; 331(2):139-146.

16. Malmström A, Grønberg BH, Marosi C, Stupp R, Frappaz D, Schultz H, Abacioglu U, Tavelin B, Lhermitte B, Hegi ME, Rosell J, Henriksson R and NCBTSG. Temozolomide *versus* standard 6-week radiotherapy *versus* hypofractionated radiotherapy in patients older than 60 years with glioblastoma: the Nordic randomised, phase 3 trial. Lancet Oncol. 2012; 13(9):916-926.

17. Stupp R, Mason WP, van den Bent MJ, Weller M, Fisher B, Taphoorn MJ, Belanger K, Brandes AA, Marosi C, Bogdahn U, Curschmann J, Janzer RC, Ludwin SK, Gorlia T, Allgeier A, Lacombe D, et al. Radiotherapy plus concomitant and adjuvant temozolomide for glioblastoma. N Engl J Med. 2005; 352(10):987-996.

18. Westphal M, Hilt DC, Bortey E, Delavault P, Olivares R, Warnke PC, Whittle IR, Jääskeläinen J and Ram Z. A phase 3 trial of local chemotherapy with biodegradable carmustine (BCNU) wafers (Gliadel wafers) in patients with primary malignant glioma. Neuro Oncol. 2003; 5(2):79-88.

19. Niyazi M, Harter PN, Hattingen E, Rottler M, von Baumgarten L, Proescholdt M, Belka C, Lauber K and Mittelbronn M. Bevacizumab and radiotherapy for the treatment of glioblastoma: brothers in arms or unholy alliance? Oncotarget. 2016; 7(3):2313-2328.

20. Friedman HS, Prados MD, Wen PY, Mikkelsen T, Schiff D, Abrey LE, Yung WK, Paleologos N, Nicholas MK, Jensen R, Vredenburgh J, Huang J, Zheng M and Cloughesy T. Bevacizumab alone and in combination with irinotecan in recurrent glioblastoma. J Clin Oncol. 2009; 27(28):4733-4740.

21. Kreisl TN, Kim L, Moore K, Duic P, Royce C, Stroud I, Garren N, Mackey M, Butman JA, Camphausen K, Park J, Albert PS and Fine HA. Phase II trial of single-agent bevacizumab followed by bevacizumab plus irinotecan at tumor progression in recurrent glioblastoma. J Clin Oncol. 2009; 27(5):740-745.

22. Gilbert MR, Dignam J, Won M, Blumenthal DT, Vogelbaum MA, Aldape KD, Colman H, Chakravarti A, Jeraj R, Armstrong TS, Wefel JS, Brown PD, Jaeckle KA, Schiff D, Atkins JN, Brachman D, et al. RTOG 0825: Phase III double-blind placebo-controlled trial evaluating bevacizumab (Bev) in patients (Pts) with newly diagnosed glioblastoma (GBM). J Clin Oncol 31, 2013 (suppl; abstr 1). 2013.

23. Chinot O, Wick W, Mason W, Henriksson R, Saran F, Nishikawa R, Hilton M, Abrey LE and Cloughesy T. OT-03. Phase III trial of bevacizumab added to standard radiotherapy and temozolomide for newly-diagnosed glioblastoma: Mmature progression-free survival and preliminary overall survival results in AVAGLIO. Neuro-Oncology. 2012; 14(suppl 6):vi101-vi105.

24. Masui K, Cloughesy TF and Mischel PS. Review: molecular pathology in adult high-grade gliomas: from molecular diagnostics to target therapies. Neuropathol Appl Neurobiol. 2012; 38(3):271-291.

25. Omuro AM, Faivre S and Raymond E. Lessons learned in the development of targeted therapy for malignant gliomas. Mol Cancer Ther. 2007; 6(7):1909-1919.

26. Behrens PF, Langemann H, Strohschein R, Draeger J and Hennig J. Extracellular glutamate and other metabolites in and around RG2 rat glioma: an intracerebral microdialysis study. J Neurooncol. 2000; 47(1):11-22.

27. Takano T, Lin JH, Arcuino G, Gao Q, Yang J and Nedergaard M. Glutamate release promotes growth of malignant gliomas. Nat Med. 2001; 7(9):1010-1015.

28. Ye ZC and Sontheimer H. Glioma cells release excitotoxic concentrations of glutamate. Cancer Res. 1999; 59(17):4383-4391.

29. Noch E and Khalili K. Molecular mechanisms of necrosis in glioblastoma: the role of glutamate excitotoxicity. Cancer Biol Ther. 2009; 8(19):1791-1797.

30. Ye ZC, Rothstein JD and Sontheimer H. Compromised glutamate transport in human glioma cells: reduction-mislocalization of sodium-dependent glutamate transporters and enhanced activity of cystine-glutamate exchange. J Neurosci. 1999; 19(24):10767-10777.

31. Olney JW. Excitotoxicity, apoptosis and neuropsychiatric disorders. Curr Opin Pharmacol. 2003; 3(1):101-109.

32. de Groot J and Sontheimer H. Glutamate and the biology of gliomas. Glia. 2011; 59(8):1181-1189.

33. Nicoletti F, Arcella A, Iacovelli L, Battaglia G, Giangaspero F and Melchiorri D. Metabotropic glutamate receptors: new

targets for the control of tumor growth? Trends Pharmacol Sci. 2007; 28(5):206-213.

34. Sontheimer H. A role for glutamate in growth and invasion of primary brain tumors. J Neurochem. 2008; 105(2):287-295.

35. Simeone TA, Sanchez RM and Rho JM. Molecular biology and ontogeny of glutamate receptors in the mammalian central nervous system. J Child Neurol. 2004; 19(5):343-360; discussion 361.

36. Ozawa S, Kamiya H and Tsuzuki K. Glutamate receptors in the mammalian central nervous system. Prog Neurobiol. 1998; 54(5):581-618.

37. Niswender CM and Conn PJ. Metabotropic glutamate receptors: physiology, pharmacology, and disease. Annu Rev Pharmacol Toxicol. 2010; 50:295-322.

38. De Blasi A, Conn PJ, Pin J and Nicoletti F. Molecular determinants of metabotropic glutamate receptor signaling. Trends Pharmacol Sci. 2001; 22(3):114-120.

39. Cavalheiro EA and Olney JW. Glutamate antagonists: deadly liaisons with cancer. Proc Natl Acad Sci U S A. 2001; 98(11):5947-5948.

40. Kalariti N, Pissimissis N and Koutsilieris M. The glutamatergic system outside the CNS and in cancer biology. Expert Opin Investig Drugs. 2005; 14(12):1487-1496.

41. Zhang C, Yuan XR, Li HY, Zhao ZJ, Liao YW, Wang XY, Su J, Sang SS and Liu Q. Anti-cancer effect of metabotropic glutamate receptor 1 inhibition in human glioma U87 cells: involvement of PI3K/Akt/mTOR pathway. Cell Physiol Biochem. 2015; 35(2):419-432.

42. Ishiuchi S, Tsuzuki K, Yoshida Y, Yamada N, Hagimura N, Okado H, Miwa A, Kurihara H, Nakazato Y, Tamura M, Sasaki T and Ozawa S. Blockage of Ca(2+)-permeable AMPA receptors suppresses migration and induces apoptosis in human glioblastoma cells. Nat Med. 2002; 8(9):971-978.

43. Rzeski W, Turski L and Ikonomidou C. Glutamate antagonists limit tumor growth. Proc Natl Acad Sci U S A. 2001; 98(11):6372-6377.

44. Ishiuchi S, Yoshida Y, Sugawara K, Aihara M, Ohtani T, Watanabe T, Saito N, Tsuzuki K, Okado H, Miwa A, Nakazato Y and Ozawa S. Ca2+-permeable AMPA receptors regulate growth of human glioblastoma *via* Akt activation. J Neurosci. 2007; 27(30):7987-8001.

45. Sonoda Y, Ozawa T, Aldape KD, Deen DF, Berger MS and Pieper RO. Akt pathway activation converts anaplastic astrocytoma to glioblastoma multiforme in a human astrocyte model of glioma. Cancer Res. 2001; 61(18):6674-6678.

46. Teh J and Chen S. mGlu Receptors and Cancerous Growth. Wiley Interdiscip Rev Membr Transp Signal. 2012; 1(2):211-220.

47. Yu LJ, Wall BA, Wangari-Talbot J and Chen S. Metabotropic glutamate receptors in cancer. Neuropharmacology. 2016.

48. Brocke KS, Staufner C, Luksch H, Geiger KD, Stepulak A, Marzahn J, Schackert G, Temme A and Ikonomidou C. Glutamate receptors in pediatric tumors of the central nervous system. Cancer Biol Ther. 2010; 9(6):455-468.

49. Li L, Homan KT, Vishnivetskiy SA, Manglik A, Tesmer JJ, Gurevich VV and Gurevich EV. G Protein-coupled Receptor Kinases of the GRK4 Protein Subfamily Phosphorylate Inactive G Protein-coupled Receptors (GPCRs). J Biol Chem. 2015; 290(17):10775-10790.

50. Chang HJ, Yoo BC, Lim SB, Jeong SY, Kim WH and Park JG. Metabotropic glutamate receptor 4 expression in colorectal carcinoma and its prognostic significance. Clin Cancer Res. 2005; 11(9):3288-3295.

51. Iacovelli L, Arcella A, Battaglia G, Pazzaglia S, Aronica E, Spinsanti P, Caruso A, De Smaele E, Saran A, Gulino A, D'Onofrio M, Giangaspero F and Nicoletti F. Pharmacological activation of mGlu4 metabotropic glutamate receptors inhibits the growth of medulloblastomas. J Neurosci. 2006; 26(32):8388-8397.

52. Park SY, Lee SA, Han IH, Yoo BC, Lee SH, Park JY, Cha IH, Kim J and Choi SW. Clinical significance of metabotropic glutamate receptor 5 expression in oral squamous cell carcinoma. Oncol Rep. 2007; 17(1):81-87.

53. Stepulak A, Luksch H, Uckermann O, Sifringer M, Rzeski W, Polberg K, Kupisz K, Klatka J, Kielbus M, Grabarska A, Marzahn J, Turski L and Ikonomidou C. Glutamate receptors in laryngeal cancer cells. Anticancer Res. 2011; 31(2):565-573.

54. Choi KY, Chang K, Pickel JM, Badger JD and Roche KW. Expression of the metabotropic glutamate receptor 5 (mGluR5) induces melanoma in transgenic mice. Proc Natl Acad Sci U S A. 2011; 108(37):15219-15224.

55. Marín YE and Chen S. Involvement of metabotropic glutamate receptor 1, a G protein coupled receptor, in melanoma development. J Mol Med (Berl). 2004; 82(11):735-749.

56. Pollock PM, Cohen-Solal K, Sood R, Namkoong J, Martino JJ, Koganti A, Zhu H, Robbins C, Makalowska I, Shin SS, Marin Y, Roberts KG, Yudt LM, Chen A, Cheng J, Incao A, et al. Melanoma mouse model implicates metabotropic glutamate signaling in melanocytic neoplasia. Nat Genet. 2003; 34(1):108-112.

57. Chen S, Zhu H, Wetzel WJ and Philbert MA. Spontaneous melanocytosis in transgenic mice. J Invest Dermatol. 1996; 106(5):1145-1151.

58. Zhu H, Reuhl K, Zhang X, Botha R, Ryan K, Wei J and Chen S. Development of heritable melanoma in transgenic mice. J Invest Dermatol. 1998; 110(3):247-252.

59. Ohtani Y, Harada T, Funasaka Y, Nakao K, Takahara C, Abdel-Daim M, Sakai N, Saito N, Nishigori C and Aiba A. Metabotropic glutamate receptor subtype-1 is essential for *in vivo* growth of melanoma. Oncogene. 2008; 27(57):7162-

7170.

60. Speyer CL, Hachem AH, Assi AA, Johnson JS, DeVries JA and Gorski DH. Metabotropic glutamate receptor-1 as a novel target for the antiangiogenic treatment of breast cancer. PLoS One. 2014; 9(3):e88830.
61. Ali S, Shourideh M and Koochekpour S. Identification of novel GRM1 mutations and single nucleotide polymorphisms in prostate cancer cell lines and tissues. PLoS One. 2014; 9(7):e103204.
62. Esseltine JL and Ferguson SS. Regulation of G protein-coupled receptor trafficking and signaling by Rab GTPases. Small GTPases. 2013; 4(2):132-135.
63. Prickett TD, Wei X, Cardenas-Navia I, Teer JK, Lin JC, Walia V, Gartner J, Jiang J, Cherukuri PF, Molinolo A, Davies MA, Gershenwald JE, Stemke-Hale K, Rosenberg SA, Margulies EH and Samuels Y. Exon capture analysis of G protein-coupled receptors identifies activating mutations in GRM3 in melanoma. Nat Genet. 2011; 43(11):1119-1126.
64. Nicoletti F, Bruno V, Copani A, Casabona G and Knöpfel T. Metabotropic glutamate receptors: a new target for the therapy of neurodegenerative disorders? Trends Neurosci. 1996; 19(7):267-271.
65. Bruno V, Battaglia G, Copani A, D'Onofrio M, Di Iorio P, De Blasi A, Melchiorri D, Flor PJ and Nicoletti F. Metabotropic glutamate receptor subtypes as targets for neuroprotective drugs. J Cereb Blood Flow Metab. 2001; 21(9):1013-1033.
66. Récasens M, Guiramand J, Aimar R, Abdulkarim A and Barbanel G. Metabotropic glutamate receptors as drug targets. Curr Drug Targets. 2007; 8(5):651-681.
67. Niswender CM, Jones CK and Conn PJ. New therapeutic frontiers for metabotropic glutamate receptors. Curr Top Med Chem. 2005; 5(9):847-857.
68. D'Onofrio M, Arcella A, Bruno V, Ngomba RT, Battaglia G, Lombari V, Ragona G, Calogero A and Nicoletti F. Pharmacological blockade of mGlu2/3 metabotropic glutamate receptors reduces cell proliferation in cultured human glioma cells. J Neurochem. 2003; 84(6):1288-1295.
69. Dietrich D, Kral T, Clusmann H, Friedl M and Schramm J. Presynaptic group II metabotropic glutamate receptors reduce stimulated and spontaneous transmitter release in human dentate gyrus. Neuropharmacology. 2002; 42(3):297-305.
70. Dubé GR and Marshall KC. Modulation of excitatory synaptic transmission in locus coeruleus by multiple presynaptic metabotropic glutamate receptors. Neuroscience. 1997; 80(2):511-521.
71. Knöpfel T and Uusisaari M. (2007). Modulation of Excitation by Metabotropic Glutamate Receptors. Inhibitory Regulation of Excitatory Neurotransmission.
72. Stepulak A, Luksch H, Gebhardt C, Uckermann O, Marzahn J, Sifringer M, Rzeski W, Staufner C, Brocke KS, Turski L and Ikonomidou C. Expression of glutamate receptor subunits in human cancers. Histochem Cell Biol. 2009; 132(4):435-445.
73. Arcella A, Carpinelli G, Battaglia G, D'Onofrio M, Santoro F, Ngomba RT, Bruno V, Casolini P, Giangaspero F and Nicoletti F. Pharmacological blockade of group II metabotropic glutamate receptors reduces the growth of glioma cells *in vivo*. Neuro Oncol. 2005; 7(3):236-245.
74. Corti C, Clarkson RW, Crepaldi L, Sala CF, Xuereb JH and Ferraguti F. Gene structure of the human metabotropic glutamate receptor 5 and functional analysis of its multiple promoters in neuroblastoma and astroglioma cells. J Biol Chem. 2003; 278(35):33105-33119.
75. Aronica E, Gorter JA, Ijlst-Keizers H, Rozemuller AJ, Yankaya B, Leenstra S and Troost D. Expression and functional role of mGluR3 and mGluR5 in human astrocytes and glioma cells: opposite regulation of glutamate transporter proteins. Eur J Neurosci. 2003; 17(10):2106-2118.
76. Ciceroni C, Arcella A, Mosillo P, Battaglia G, Mastrantoni E, Oliva MA, Carpinelli G, Santoro F, Sale P, Ricci-Vitiani L, De Maria R, Pallini R, Giangaspero F, Nicoletti F and Melchiorri D. Type-3 metabotropic glutamate receptors negatively modulate bone morphogenetic protein receptor signaling and support the tumourigenic potential of glioma-initiating cells. Neuropharmacology. 2008; 55(4):568-576.
77. Ciceroni C, Bonelli M, Mastrantoni E, Niccolini C, Laurenza M, Larocca LM, Pallini R, Traficante A, Spinsanti P, Ricci-Vitiani L, Arcella A, De Maria R, Nicoletti F, Battaglia G and Melchiorri D. Type-3 metabotropic glutamate receptors regulate chemoresistance in glioma stem cells, and their levels are inversely related to survival in patients with malignant gliomas. Cell Death Differ. 2013; 20(3):396-407.
78. Zhou K, Song Y, Zhou W, Zhang C, Shu H, Yang H and Wang B. mGlu3 receptor blockade inhibits proliferation and promotes astrocytic phenotype in glioma stem cells. Cell Biol Int. 2014; 38(4):426-434.
79. Hamel PA and Hanley-Hyde J. G1 cyclins and control of the cell division cycle in normal and transformed cells. Cancer Invest. 1997; 15(2):143-152.
80. Singh SK, Hawkins C, Clarke ID, Squire JA, Bayani J, Hide T, Henkelman RM, Cusimano MD and Dirks PB. Identification of human brain tumour initiating cells. Nature. 2004; 432(7015):396-401.
81. Stupp R and Hegi ME. Targeting brain-tumor stem cells. Nat Biotechnol. 2007; 25(2):193-194.
82. Codrici E, Enciu AM, Popescu ID, Mihai S and Tanase C. Glioma Stem Cells and Their Microenvironments: Providers of Challenging Therapeutic Targets. Stem Cells Int. 2016; 2016:5728438.
83. Schoepp DD, Jane DE and Monn JA. Pharmacological agents acting at subtypes of metabotropic glutamate receptors. Neuropharmacology. 1999; 38(10):1431-1476.
84. Yelskaya Z, Carrillo V, Dubisz E, Gulzar H, Morgan

D and Mahajan SS. Synergistic inhibition of survival, proliferation, and migration of U87 cells with a combination of LY341495 and Iressa. PLoS One. 2013; 8(5):e64588.

85. Ferraguti F, Baldani-Guerra B, Corsi M, Nakanishi S and Corti C. Activation of the extracellular signal-regulated kinase 2 by metabotropic glutamate receptors. Eur J Neurosci. 1999; 11(6):2073-2082.

86. Sanderson TM, Hogg EL, Collingridge GL and Corrêa SA. Hippocampal mGluR-LTD in health and disease: focus on the p38 MAPK and ERK1/2 pathways. J Neurochem. 2016.

87. Willard SS and Koochekpour S. Glutamate, glutamate receptors, and downstream signaling pathways. Int J Biol Sci. 2013; 9(9):948-959.

88. Chun-Jen Lin C, Summerville JB, Howlett E and Stern M. The metabotropic glutamate receptor activates the lipid kinase PI3K in Drosophila motor neurons through the calcium/calmodulin-dependent protein kinase II and the nonreceptor tyrosine protein kinase DFak. Genetics. 2011; 188(3):601-613.

89. Gerber U, Gee CE and Benquet P. Metabotropic glutamate receptors: intracellular signaling pathways. Curr Opin Pharmacol. 2007; 7(1):56-61.

90. Schaeffer HJ and Weber MJ. Mitogen-activated protein kinases: specific messages from ubiquitous messengers. Mol Cell Biol. 1999; 19(4):2435-2444.

91. Li X, Wu C, Chen N, Gu H, Yen A, Cao L, Wang E and Wang L. PI3K/Akt/mTOR signaling pathway and targeted therapy for glioblastoma. Oncotarget. 2016.

92. Piccirillo SG and Vescovi AL. Bone morphogenetic proteins regulate tumorigenicity in human glioblastoma stem cells. Ernst Schering Found Symp Proc. 2006; (5):59-81.

93. Fukuda S and Taga T. [Roles of BMP in the development of the central nervous system]. Clin Calcium. 2006; 16(5):781-785.

94. Nicoletti F, Bockaert J, Collingridge GL, Conn PJ, Ferraguti F, Schoepp DD, Wroblewski JT and Pin JP. Metabotropic glutamate receptors: from the workbench to the bedside. Neuropharmacology. 2011; 60(7-8):1017-1041.

95. Iacovelli L, Bruno V, Salvatore L, Melchiorri D, Gradini R, Caricasole A, Barletta E, De Blasi A and Nicoletti F. Native group-III metabotropic glutamate receptors are coupled to the mitogen-activated protein kinase/phosphatidylinositol-3-kinase pathways. J Neurochem. 2002; 82(2):216-223.

96. Fiory F, Oriente F, Miele C, Romano C, Trencia A, Alberobello AT, Esposito I, Valentino R, Beguinot F and Formisano P. Protein kinase C-zeta and protein kinase B regulate distinct steps of insulin endocytosis and intracellular sorting. J Biol Chem. 2004; 279(12):11137-11145.

97. McCubrey JA, Steelman LS, Chappell WH, Abrams SL, Franklin RA, Montalto G, Cervello M, Libra M, Candido S, Malaponte G, Mazzarino MC, Fagone P, Nicoletti F, Bäsecke J, Mijatovic S, Maksimovic-Ivanic D, et al. Ras/Raf/MEK/ERK and PI3K/PTEN/Akt/mTOR cascade inhibitors: how mutations can result in therapy resistance and how to overcome resistance. Oncotarget. 2012; 3(10):1068-1111.

98. McCubrey JA, Steelman LS, Chappell WH, Abrams SL, Montalto G, Cervello M, Nicoletti F, Fagone P, Malaponte G, Mazzarino MC, Candido S, Libra M, Bäsecke J, Mijatovic S, Maksimovic-Ivanic D, Milella M, et al. Mutations and deregulation of Ras/Raf/MEK/ERK and PI3K/PTEN/Akt/mTOR cascades which alter therapy response. Oncotarget. 2012; 3(9):954-987.

99. Vivanco I and Sawyers CL. The phosphatidylinositol 3-Kinase AKT pathway in human cancer. Nat Rev Cancer. 2002; 2(7):489-501.

100. Weaver KD, Yeyeodu S, Cusack JC, Baldwin AS and Ewend MG. Potentiation of chemotherapeutic agents following antagonism of nuclear factor kappa B in human gliomas. J Neurooncol. 2003; 61(3):187-196.

101. Shin HM, Kim MH, Kim BH, Jung SH, Kim YS, Park HJ, Hong JT, Min KR and Kim Y. Inhibitory action of novel aromatic diamine compound on lipopolysaccharide-induced nuclear translocation of NF-kappaB without affecting IkappaB degradation. FEBS Lett. 2004; 571(1-3):50-54.

102. Kopp E and Ghosh S. Inhibition of NF-kappa B by sodium salicylate and aspirin. Science. 1994; 265(5174):956-959.

103. Inoki K, Li Y, Zhu T, Wu J and Guan KL. TSC2 is phosphorylated and inhibited by Akt and suppresses mTOR signalling. Nat Cell Biol. 2002; 4(9):648-657.

104. Hou L and Klann E. Activation of the phosphoinositide 3-kinase-Akt-mammalian target of rapamycin signaling pathway is required for metabotropic glutamate receptor-dependent long-term depression. J Neurosci. 2004; 24(28):6352-6361.

105. Bernard PB, Castano AM, Bayer KU and Benke TA. Necessary, but not sufficient: insights into the mechanisms of mGluR mediated long-term depression from a rat model of early life seizures. Neuropharmacology. 2014; 84:1-12.

106. Argyriou AA and Kalofonos HP. Molecularly targeted therapies for malignant gliomas. Mol Med. 2009; 15(3-4):115-122.

107. Nicoletti F, Fagone P, Meroni P, McCubrey J and Bendtzen K. mTOR as a multifunctional therapeutic target in HIV infection. Drug Discov Today. 2011; 16(15-16):715-721.

108. Gerson SL. MGMT: its role in cancer aetiology and cancer therapeutics. Nat Rev Cancer. 2004; 4(4):296-307.

109. Willard SS and Koochekpour S. Glutamate signaling in benign and malignant disorders: current status, future perspectives, and therapeutic implications. Int J Biol Sci. 2013; 9(7):728-742.

110. Bowman CL, Yohe L and Lohr JW. Enzymatic modulation of cell volume in C6 glioma cells. Glia. 1999; 27(1):22-31.

111. Giese A. Glioma invasion—pattern of dissemination by mechanisms of invasion and surgical intervention, pattern of gene expression and its regulatory control by

tumorsuppressor p53 and proto-oncogene ETS-1. Acta Neurochir Suppl. 2003; 88:153-162.

112. Pilc A, Chaki S, Nowak G and Witkin JM. Mood disorders: regulation by metabotropic glutamate receptors. Biochem Pharmacol. 2008; 75(5):997-1006.

113. Swanson CJ, Bures M, Johnson MP, Linden AM, Monn JA and Schoepp DD. Metabotropic glutamate receptors as novel targets for anxiety and stress disorders. Nat Rev Drug Discov. 2005; 4(2):131-144.

114. Lee HG, Zhu X, O'Neill MJ, Webber K, Casadesus G, Marlatt M, Raina AK, Perry G and Smith MA. The role of metabotropic glutamate receptors in Alzheimer's disease. Acta Neurobiol Exp (Wars). 2004; 64(1):89-98.

115. Conn PJ, Battaglia G, Marino MJ and Nicoletti F. Metabotropic glutamate receptors in the basal ganglia motor circuit. Nature reviews Neuroscience. 2005; 6(10):787-798.

116. Mølck C, Harpsøe K, Gloriam DE, Clausen RP, Madsen U, Pedersen L, Jimenez HN, Nielsen SM, Mathiesen JM and Bräuner-Osborne H. Pharmacological characterization and modeling of the binding sites of novel 1,3-bis(pyridinylethynyl)benzenes as metabotropic glutamate receptor 5-selective negative allosteric modulators. Mol Pharmacol. 2012; 82(5):929-937.

117. Dalton JA, Gómez-Santacana X, Llebaria A and Giraldo J. Computational analysis of negative and positive allosteric modulator binding and function in metabotropic glutamate receptor 5 (in)activation. J Chem Inf Model. 2014; 54(5):1476-1487.

118. Gregory KJ, Nguyen ED, Reiff SD, Squire EF, Stauffer SR, Lindsley CW, Meiler J and Conn PJ. Probing the metabotropic glutamate receptor 5 (mGlus) positive allosteric modulator (PAM) binding pocket: discovery of point mutations that engender a "molecular switch" in PAM pharmacology. Mol Pharmacol. 2013; 83(5):991-1006.

119. Zhang L, Balan G, Barreiro G, Boscoe BP, Chenard LK, Cianfrogna J, Claffey MM, Chen L, Coffman KJ, Drozda SE, Dunetz JR, Fonseca KR, Galatsis P, Grimwood S, Lazzaro JT, Mancuso JY, et al. Discovery and preclinical characterization of 1-methyl-3-(4-methylpyridin-3-yl)-6-(pyridin-2-ylmethoxy)-1H-pyrazolo- [3,4-b]pyrazine (PF470): a highly potent, selective, and efficacious metabotropic glutamate receptor 5 (mGluR5) negative allosteric modulator. J Med Chem. 2014; 57(3):861-877.

120. Malherbe P, Kratochwil N, Mühlemann A, Zenner MT, Fischer C, Stahl M, Gerber PR, Jaeschke G and Porter RH. Comparison of the binding pockets of two chemically unrelated allosteric antagonists of the mGlu5 receptor and identification of crucial residues involved in the inverse agonism of MPEP. J Neurochem. 2006; 98(2):601-615.

121. Lundström L, Bissantz C, Beck J, Wettstein JG, Woltering TJ, Wichmann J and Gatti S. Structural determinants of allosteric antagonism at metabotropic glutamate receptor 2: mechanistic studies with new potent negative allosteric modulators. Br J Pharmacol. 2011; 164(2b):521-537.

122. Pagano A, Ruegg D, Litschig S, Stoehr N, Stierlin C, Heinrich M, Floersheim P, Prezèau L, Carroll F, Pin JP, Cambria A, Vranesic I, Flor PJ, Gasparini F and Kuhn R. The non-competitive antagonists 2-methyl-6-(phenylethynyl)pyridine and 7-hydroxyiminocyclopropan [b]chromen-1a-carboxylic acid ethyl ester interact with overlapping binding pockets in the transmembrane region of group I metabotropic glutamate receptors. J Biol Chem. 2000; 275(43):33750-33758.

123. Noeske T, Trifanova D, Kauss V, Renner S, Parsons CG, Schneider G and Weil T. Synergism of virtual screening and medicinal chemistry: identification and optimization of allosteric antagonists of metabotropic glutamate receptor 1. Bioorg Med Chem. 2009; 17(15):5708-5715.

124. Condorelli DF, Dell'Albani P, Corsaro M, Giuffrida R, Caruso A, Trovato Salinaro A, Spinella F, Nicoletti F, Albanese V and Giuffrida Stella AM. Metabotropic glutamate receptor expression in cultured rat astrocytes and human gliomas. Neurochem Res. 1997; 22(9):1127-1133.

CAPÍTULO II

Artigo em preparação para publicação

Metabotropic glutamate receptors as potential prognostic markers in glioblastomas.

Revista: Oncogene

Qualis-CAPES-CBII: A1

Fator de Impacto: 7.932

Justificativa: Até o momento, apenas um estudo avaliou o papel dos receptores metabotrópicos glutamatérgicos (mGluR) em coortes de pacientes com glioblastomas (GBM), verificando a expressão gênica de mGluR3 em biópsias de GBM.

Objetivo geral: Realizar uma meta-análise de dados de microarranjo de amostras de GBM obtidas de dois bancos de dados independentes depositados no *Gene Expression Omnibus database* (GSE16011 e GSE4412). Avaliar o nível de expressão gênicas dos oito subtipos de mGluR nas biópsias dessas coortes e correlacioná-los com os dados clínicos dos pacientes. Avaliar o potencial dos subtipos de mGluR como biomarcadores prognóticos e preditivos de tratamento.

Objetivo específico: Propor uma assinatura gênica dos mGluR capaz de predizer o desfecho dos pacientes.

METABOTROPIC GLUTAMATE RECEPTORS AS POTENTIAL PROGNOSTIC MARKERS IN GLIOBLASTOMAS

Mery Stefani Leivas Pereira[1*], Chairini Cássia Thomé[1], Marco Antônio Debastiani[2], Fábio Klamt[2], Diogo Losch de Oliveira[1*]

[1] *Laboratory of Cellular Neurochemistry, Department of Biochemistry, Instituto de Ciências Básicas da Saúde, Universidade Federal do Rio Grande do Sul, Porto Alegre, Brazil.*

[2] *Laboratory of Cellular Biochemistry, Department of Biochemistry, Instituto de Ciências Básicas da Saúde, Universidade Federal do Rio Grande do Sul, Porto Alegre, Brazil.*

*** Address for correspondence**:

Mery Stefani Leivas Pereira, MSc / Prof. Diogo Losch de Oliveira, PhD

Laboratory of Cellular Neurochemistry

Department of Biochemistry - Instituto de Ciências Básicas da Saúde

Universidade Federal do Rio Grande do Sul

Rua Ramiro Barcelos 2600 anexo

Porto Alegre, Brazil

Zip Code: 90035-003

Phone: +55 51 33085556

E-mail: meryslpereira@gmail.com or losch@ufrgs.br

ABSTRACT

BACKGROUND: Glioblastoma (GBM) is the most common primary malignant tumor in adults. Although surgical resection followed by radiotherapy and chemotherapy enhances patient's survival, GBM remains among the most lethal and resistant malignant tumor. Hence, there is a growing need to develop new therapies targeting surface molecules that specifically regulate GBM proliferation. Metabotropic glutamate receptors (mGluR) are G-protein-coupled receptors that participate in modulation of synaptic transmission and neuronal excitability. Several *in vitro* and *in vivo* studies demonstrated the involvement of mGluR in progression, aggressiveness, and recurrence of GBM. The purpose of the present research was to assess the potential prognostic and predictive value of the eight subtypes of mGluR, proposing a gene signature that has potential value as biomarker to predict the outcome of patients. **METHODS:** A meta-analysis of tissue microarray data was used to examine mGluR gene expression (*GRM*) association with survival in a cohort of 114 GBM patients (GSE16011) through Cox survival analysis and hierarchical clustering. The robustness of these findings was evaluated using another independent microarray dataset (GSE4412). Additionally, the potential role of the receptor signature proposed was verified *in vitro* by treating GBM cell lines with mGluR ligands. **RESULTS:** Meta-analysis of two cohorts of patients with glioblastomas led to the characterization of an mGluR gene signature, in which high *GRM3* levels together with low *GRM4* and *GRM6* levels in biopsies were associated with shorter overall patient survival. Contrarily, low *GRM3* levels with high *GRM4* and *GRM6* levels in GBM, predicted a longer overall survival. The potential of these receptors on the malignancy of these tumors was assessed by *in vitro* experiments through the treatment of GBM lineages with mGluR ligands for 72 h in absence of FBS. Pharmacological blockade of group II mGluR by LY341495 and pharmacological activation of group III mGluR by L-AP4 decreased the amount of C6 cells in 25-28 %. The combination of these treatments had no synergistic effect. **CONCLUSION:** This study indicates that mGluR gene expression levels can be used to indicate patient outcome. *In vitro* treatment of GBM cells with mGluR ligands (LY341495 e L-AP4) under non-proliferating conditions was in accordance with the predicted aggressiveness behavior proposed *in silico*. Although more *in vitro* studies in proliferating conditions are required, our meta-analysis indicates that evaluation of the eight mGluR subtypes in GBM biopsies may be considered to guide future chemotherapeutic interventions.

Key words: mGluR antagonists, mGluR agonists, SNC tumors, GBM patients' cohort.

INTRODUCTION

Gliomas are the most common brain tumor in adults and often represent a poor prognosis for patient [33]. These tumors are classified in increasing degrees of undifferentiation, anaplasia, and aggressiveness [5, 14]. High-grade gliomas represent 60–75% of cases and comprise grade III anaplastic astrocytoma, anaplastic oligodendroglioma, mixed anaplastic oligoastrocytoma, and grade IV glioblastoma (GBM) [13].

GBM accounts for the majority of primary malignant brain tumors in adults, being one of the most lethal human cancers [5, 18]. Its annual incidence rate in United Stated is 3.2 per 100,000 people and this neoplasia is more common in elderly, 75 to 84 ages, 1.6 times more prevalent in males and 2 times higher incident among caucasians [20]. In United States, GBM represents 15.1% of all primary brain tumors and 46.1% of primary malignant brain tumors [20]. This tumor is histologically characterized by considerable cellularity and mitotic activity, vascular proliferation, and necrosis [12]. Recently, this glioma was categorized in three groups: (1) GBM, IDH-wildtype (90% of cases, generally corresponds to so-called primary GBM and is prevalent in patients over 55 years); (2) GBM, IDH-mutant (10 % of cases, corresponds closely to clinical definition of secondary GBM and preferentially arises in younger patients); and (3) GBM, NOS (diagnosis reserved for tumors whose full IDH evaluation cannot be performed) [14].

Although this cancer is typically confined to Central Nervous System (CNS), with rare cases of metastasis in distant organs, GBM malignant cells are highly invasive, infiltrating surrounding brain parenchyma [18]. Standard treatment for GBM consists of maximal surgical resection in order to relieve mass effect, achieve cytoreduction, and provide adequate tissue for histologic and molecular tumor characterization [8, 29]. Although surgical procedure can greatly reduce tumor bulk, complete GBM excision is frequently not reached due to infiltrative nature of cells [31]. After surgical removal, adjuvant radiotherapy combined with chemotherapy should be considered for all patients [29]. The first-line chemotherapy is oral administration of the DNA

alkylating agent temozolomide (TMZ) [15, 18]. Treatment with radiotherapy followed TMZ administration increases median survival to 15 months versus 12 months with radiotherapy alone (hazard ratio - HR= 0.63; $P < .001$) [27]. Two-year survival rate is also increased to 27% for chemotherapy along with radiotherapy versus 10% for radiotherapy alone [27]. Additionally, a new alternative chemotherapy using biodegradable polymers containing the alkylating agent carmustine (BCNU) directly into the surgical cavity, followed by radiotherapy, causes only a modest survival benefit [32]. Thus, although radiotherapy and chemotherapy enhance patient survival, GBM remains among the most lethal and resistant malignant tumor [5, 16], with recurrence occurring usually after a median progression-free survival of 7 to 10 months [19]. For these reasons, there is a growing need to develop new therapies targeting surface molecules or signaling pathways that specifically regulate the proliferation, differentiation and invasion potential of GBM cells.

Several *in vitro* and *in vivo* studies demonstrated the involvement of metabotropic glutamate receptors (mGluR) in progression, aggressiveness, and recurrence of GBM [1, 3, 4, 7, 35, 36]. mGluR are protein-coupled receptors and there are eight subtypes, which are sub classified into three groups based on gene sequence homology, type of G protein coupling and selectivity of the ligand. Group I includes mGluR 1 and 5; group II includes mGluR 2 and 3; group III includes mGluR 4, 6, 7, and 8 [17]. Pharmacological blockade of mGluR1 and mGluR3 *in vitro* have shown anti-proliferative and anti-migratory effects, through a decrease in the activation of MAPK and PI3K pathways [1, 3, 7, 35]. Moreover, inhibition of mGluR3 by antagonists promoted astroglial differentiation of GBM tumor stem cells [3, 36] and enabled cytotoxic action of TMZ [4]. mGluR3-dependent TMZ toxicity was supported by an intracellular signaling pathway that sequentially involves PI3K and NF-κB, increasing levels of MGMT transcripts [4]. In addition, it was demonstrated that continuous pharmacological blockade of mGluR1 and mGluR3 reduced GBM tumor growth in two independent *in vivo* xenograft models [1, 3, 4, 35, 36]. Only one study evaluated the role of mGluR in a cohort of 87 GBM patients. Ciceroni et al. (2013) [4] showed an

association between mGluR3 mRNA expression in GBM resections and the survival of patients undergoing surgery followed by radiotherapy and chemotherapy with TMZ. In summary, their findings showed that low gene expression of mGluR3 in biopsies correlated with longer patient survival.

Due to the fact that all studies previously mentioned pointed to the notion that specific subtype-selective mGluR ligands may be considered as potential adjuvant chemotherapy for glioma treatment, an evaluation of the eight mGluR subtypes in GBM biopsies would be interesting to establish an adjuvant therapy. In this work, we assessed the prognostic value of the eight subtypes of mGluR, proposing a gene signature of these receptors capable of predicting the outcome of patients. To evaluate that, we used two different approaches: i) first we looked for a association of gene expression and patient survival using clinical and mRNA expression data from two large, homogeneous, well-defined microarray studies; ii) afterwards we sought to test the bioinformatics-obtained results *in vitro*, using GBM cell lines treated with mGluR ligands.

MATERIALS AND METHODS

Cohort Studies and Data Analysis

Microarray data acquisition

For glioma cohort analysis, we accessed a well-defined collection of glioma samples from the Erasmus University Medical Center tumor archive (Rotterdam, Netherlands), including gene expression data from biopsies and relevant clinical and pathologic information from 59 grade III patients and 114 grade IV patients (1989-2005) (testing cohort) [11]. The public microarray dataset was obtained from the Gene Expression Omnibus database (GSE16011). To test the validity of our results, we used an independent microarray dataset (GSE4412) (validation cohort). This cohort comprises microarray data from 26 grade III glioma biopsies and 59 grade IV glioma biopsies obtained from patients undergoing surgical treatment between 1996 and 2003 at the University of California (Los Angeles, USA) [9]. In both cohorts, grade IV biopsies were of the glioblastoma (GBM) type. Previous to all analyses, mGluR gene expression values were normalized.

Survival data analysis

Standard Kaplan-Meier mortality curves and their significance levels were generated for clusters of patients using GraphPad Prism 6 software (GraphPad Software, Inc. - San Diego, California, USA). The survival curves were compared using the log-rank test, and patients were clustered according to either biopsy mGluR gene expression level (*GRM*) or glioma grade (III or IV). Results were summarized by calculating hazard ratios (HR).

Cox proportional hazards regression models were used to test the contribution of several independent variables on mortality risk. Microarray gene expression and patient clinical information such as grade, age, sex, and KPS were the variables considered for the models, depending on the information available in each dataset. Results of the Cox analyses were

summarized by calculating hazard ratios (HR). Cox models were constructed using the survival package in R statistical environment [6].

Unsupervised hierarchical clustering analyses and visualization were performed with the R statistical environment using Euclidean distance and average linkage clustering options. The color intensity was set to the normalized log2 of the microarray signal.

***In vitro* Assays**

Materials

Dulbecco's Modified Eagle's medium (DMEM), Fetal Bovine Serum (FBS), penicillin/streptomycin and fungizone were obtained from Gibco®, Invitrogen™, USA. Cell culture chemicals and western blot assay reagents were purchased from Sigma-Aldrich Co., USA. mGluR ligands (EGLU, LY341495, LY379268, L-AP4, and MSOP) were purchased from Tocris Bioscience, USA. Tissue culture flasks and tissue culture testplates were obtained from Techno Plastic Products AG (TPP®), Switzerland. All other chemicals were purchased from local commercial suppliers.

Cell culture

C6 rat GBM lineage and the human GBM lines A-172, M059J, T98G, U-87 MG and U-138 MG were purchased from American Type Culture Collection (Rockville, Maryland, USA). GBM cells were grown in culture flasks containing 1 % DMEM, 23.8 mM $NaHCO_3$, 8.39 mM Hepes sodium salt (pH 7.4), 0.25 µg/mL fungizone, 50 U/mL penicillin, 50 µg/mL streptomycin and 5 % of fetal bovine serum (FBS), for C6 line, and 10% FBS for human lineages. All cultures were maintained at 37 ºC in a 95:5 air/CO_2 atmosphere.

Growth curve and Doubling time

The growth curve and doubling time of each GBM cell line were evaluated using

Sulforhodamine B (SRB) colorimetric assay, following NCI-60 protocol [30]. SRB assay is a consolidated protocol for cell density determination, based on the measurement of cellular protein content. Briefly, after time set for cultivation, cells were fixed with 10% (wt/vol) trichloroacetic acid during 1 h at 4 ºC and were washed with distilled water repeatedly. After drying at room temperature (RT), cells were stained with SRB during 15 min (RT). The excess of dye was removed by repeatedly washing with 1 % (vol/vol) acetic acid. The protein-bound dye was dissolved in 10 mM Tris base solution for optical density determination at 490 nm using a microplate reader. For cell number determination, increasing amounts of each GBM cells were pipetted into 96-multiwell plates (Falcon® Brand) ($1x10^3$-$50x10^3$ cells/well) and after cell adhesion on plate (about 2 h after seeding) SRB staining was performed. Cell density was calculated as a function of the number of seeded cells and the corresponding absorbance using GraphPad 6.0 software (Supplementary Figure 1).

For growth curves, cells were seeded in 96-multiwell plates (Falcon® Brand) in specific growing densities ($1x10^3$-$1x10^4$ cells/well) and cultured for 24, 48, 72, and 96 h. Analyses of growth curves of each GBM line allowed the choice of the number of cells that would be seeded to be in exponential growth in each experiment (Supplementary Figure 2). Doubling time for each GBM line was calculated as an exponential fuction at density of $8x10^3$ cells/well using GraphPad 6.0 software.

Cytotoxicity of chemotherapeutic agents

Resistance of chemotherapy was determined based on drug dose-response curves of TMZ and Carmustine (BCNU) (Sigma-Aldrich, Co.) using the SRB assay. The amount of GBM cells remaining in the well was calculated as a linear function of each GBM line cell density curve versus the absorbance of SRB. Cells were seeded ($8x10^3$ cells/well) in 96-multiwell plates (Falcon® Brand) and cultured for 72 h. Drug 25 % and 50 % growth inhibition (IC_{25} and IC_{50}) were calculated according to concentration-response curve of each lineage.

Wound healing assay

Cells were seeded in 24-multiwell plates (Falcon® Brand) in specific growing densities and cultured for 24h. A-172, M059J and U-138 MG lines were seeded at $1x10^5$ cells/well. T98G lineage was seeded at $1.5x10^5$ cells/well. C6 and U-87 MG lines were seeded at $4x10^5$ cells/well. After 24 h, DMEM with FBS was replaced with Hank's balanced salt solution (HBSS) containing 137 mM NaCl, 0.60 mM Na_2HPO_4, 3.00 mM $NaHCO_3$, 20 mM Hepes sodium salt, 5.00 mM KCl, 0.40 mM KH_2PO_4, 1.26 mM $CaCl_2$, 0.90 mM $MgSO_4$ and 5.55 mM glucose; pH 7.4. One scratch was made in the middle of each well and cultures were washed with HBSS afterwards, which was replaced with fresh DMEM containing 1 % of FBS. Phase contrast images were captured at 20X at 0, 6, 24 and 48 hours. Distance travelled by cells of each GBM line into the gap up to 48h was qualitatively evaluated by scales of area retake: + (0-30 %), ++ (31-70%) and +++ (71-100%).

Western blot immunoassay

Western Blot assay was performed according to Pereira et al., [21]. GBM cells of each lineage were homogenized in lysis buffer (5 mM Tris base, 1 mM EDTA, 0.1 % SDS and protease inhibitor cocktail; pH 7.0) and protein content was normalized to 2 µg protein/µL. Aliquots were diluted 1:1 in sample buffer (0.01 g % Bromophenol Blue, 60 mM Tris base, 20 % glycerol, SDS 2 % and 2-β-mercaptoethanol 5 %; pH 6.8) and proteins were separated by 8 % SDS-PAGE. Proteins were electro transferred to nitrocelulose membranes (GE Healthcare, USA) using a semi-dry transfer apparatus (Bio-Rad, Trans-Blot SD). After 1 h of incubation in blocking solution containing 3 % powdered albumin and 0.1 % Tween-20 in Tris–buffered saline (TBS; 10 mM Tris base, 30 mM NaCl, pH 7.4), membranes were incubated overnight with anti-mGluR3 IgG (0.2 µg/mL) (Abcam plc.), or anti-mGluR4 IgG (1 µg/mL) (Abcam plc.), or anti-mGluR6 IgG (1 µg/mL) (Santa Cruz Biotechnology, Inc.) or anti-β-actin IgG (0.033 µg/mL) (Santa Cruz Biotechnology, Inc.) at 4 ºC overnight. Afterwards, they were exposed to

horseradish peroxidase-conjugated anti-rabbit IgG (Dako, Agilent Pathology Solutions) or anti-mouse IgG (Dako, Agilent Pathology Solutions) diluted 1:1000 for 2 h at 4 ºC. Membranes were incubated in Super Signal West Pico Chemiluminescence Substrate (Thermo Fisher Scientific Inc., Massachusettd, USA) for production of chemiluminescence, which was detected by a chemoluminescent image analyzer (ImageQuant LAS 4000, GE Healthcare Life Sciences, Chicago, Illinois, USA). Band intensity was analysed using Image-J 1.36b Software (National Institutes of Health). β-actin was used as protein loading control.

Pharmacological assays

The pharmacological effect of group II and group III mGluR ligands was evaluated in medium with or without FBS. In the experiments performed in the presence of FBS, each C6 and U-87 MG lineages was seeded at the density of $8x10^3$ cells/well. In experiments performed without the addition of FBS, $1x10^4$ cells/well were seeded. After 24 h in culture, GBM cell lines were treated with mGluR ligands according to four different protocols, which will be better described in the results session. mGluR ligands concentrations used in this work were chosen according literature [1, 3, 4, 7, 34, 36]: 100 µM EGLU (highly selective group II mGluR antagonist); 100 nM or 1 µM LY341495 (highly potent and selective group II mGluR antagonist); 100 nM LY379268 (highly selective group II mGluR agonist); 100 µM MSOP (specific group III mGluR antagonist) and 100 µM L-AP4 (selective group III mGluR agonist). Control group received only vehicle (deionized H_2O). To verify if there was a synergistic interaction of mGluR ligands with chemotherapeutic agents, C6 and U-87 MG cells also underwent co-treatment with TMZ IC_{25} or BCNU IC_{25} (or vehicle, DMSO 0.05 %) during 72h. LY379268, group II agonist, and LY341495, group II antagonist, were administered in 100 nM concentration EGLU, group II antagonist, L-AP4, group III agonist, and MSOP, group III antagonist, were administered at a concentration of 100 µM. The mean of 6 independent experiments was collected and results were presented in percent (%) of remaining cells

(mean±SE) compared to control group.

Statistical analysis

Data from *in vitro* assays analysis were expressed as mean±SE of at least three independent experiments carried out in triplicate, and one way ANOVA test was used ($P<0.05$), followed by *Tukey* multiple comparison test (GraphPad Prisma 6 Software). Data from Western Blot technique were expressed as median (25 % percentile ;75% percentile) of six independent experiments, and Kruskal-Wallis test was used ($P<0.05$), followed by *Dunn's* multiple comparison test (GraphPad Prisma 6 Software).

RESULTS AND DISCUSSION

High-grade gliomas show typical characteristics in test cohort

To assess the association between grade and survival, Kaplan-Meier survival curve of patients from test cohort partitioned by histologic grade was plotted (**Figure 1**). Patients with grade III tumors (anaplastic astrocytoma, anaplastic oligoastrocytoma, and anaplastic oligodendroglioma) had a median survival of 1188 days, whereas patients with grade IV tumors (glioblastomas) had a median survival of 324 days (**Table 1**). Cox multivariable regression analysis was performed to verify the contribution of each clinical data on patients' outcome (**Table 2**). In this cohort, GBM patients were approximately 2.5 times more likely to have a worse prognosis than those with grade III gliomas (HR=2.570; SE=0.451; P<0.001) (**Figure 1**). These results are consistent with literature and confirm that histologic grade is a good predictor of survival [20, 23]. Confirming the literature [10], the increase in age was also associated to a short period of patient survival (HR=1.035; SE=0.008; P<0.001) (**Table 2**). The decrease in Karnofsky Performance status (KPS), a score used in medicine to categorize patient functional status [2], was also related to a prolonged life of patients, albeit the observed effect is mild (HR=-1.017; SE=0.0.007; P=0.019) (**Table 2**).

GRM expression correlates with patient survival in GBM biopsies of test cohort

Kaplan-Meier curves were used to evaluate the predictive value of gene expression of each mGluR presented in GBM biopsies (**Figure 2 A-H**). Test cohort (GSE16011) was stratified into two groups according to the level of individual gene expression of the eight mGluR subtypes (*GRM1-GRM8*). The red group represents patients whose tumor samples contained *GRM* values greater than median gene expression of each mGluR. The blue group represents patients whose GBM biopsies contained *GRM* value less than or equal to median gene expression of each mGluR. In test cohort, high levels of *GRM3* (**Figure 2C**) were predictive of

a poor prognosis for patients (HR=1.437; SE=0.294; P=0.045), as well as high levels of *GRM8* (**Figure 2H**) (HR=1.446; SE=0.294; P=0.044).

Cox proportional hazards regression models were used to test the contribution of the gene expression of each receptor on mortality, independently of the influence of other clinical variables, such as age, sex and KPS. (**Table 3**). Cox analysis revealed that increase in *GRM3* expression (HR=1.535; SE=0.146; P=0.003) and *GRM7* expression (HR=1.856; SE=0.298; P=0 .038) were significantly associated with poor prognosis for patients (**Table 3**). However, decrease in *GRM4* expression (HR=-1.805; SE=0.217; P=0.006) and *GRM5* expression (HR=-2.793; SE=0.489; P=0.036) were associated with shorter overall survival (**Table 3**).

To explore the gene expression profile of all mGluR subtypes in biopsies, a cluster analysis was carried out in test cohort (GSE16011). From this, it is possible to observe that patients were grouped according *GRM* expression in GBM biopsies into three groups (orange, yellow and black) (**Figure 3A**). The heatmap points that the main components for this clustering are *GRM3*, *GRM2*, *GRM4*, and *GRM6* genes. Orange cluster represents patients whose GBM biopsies expressed higher levels of *GRM3* and lower levels of *GRM2*, *4*, and *6*. Yellow cluster represents patients whose tumors were characterized by an inverse gene expression pattern – low *GRM3* expression and high *GRM2*, *4*, and *6* expressions. Black cluster is slightly different from yellow, since biopsies expressed lower levels of *GRM3* (**Figure 3A**).

Kaplan-Meier curves based on this new stratification showed that gene expression of the eight mGluR subtypes can be used to discriminate patients' outcomes (**Figure 3 B and C**). In **Figure 3B**, survival curves of patients of the three new clusters are represented. There was no statistical difference among these curves. As black group is very similar to yellow (characterized mainly by low expression of *GRM3* and high expression of *GRM2*, *4*, and *6*), patients of these two groups were merged in a new group (dark yellow) (**Figure 3C**). Patients from orange group had an overall survival rate shorter than those from yellow dark group (HR=1.432; SE=0.293; P=0.047). These results hint that the gene expression levels of mGluR3, 2, 4, and 6 in GBM

biopsies are able to predict GBM patients' outcome (**Figure 3C**).

GRM expression correlates with patient survival in GBM biopsies of validation cohort

To evaluate the robustness of our finding, we analyzed a second, independent dataset of biopsies from patients with high-grade gliomas (validation cohort – GSE4412). Validation cohort consists of 26 biopsies of patients with grade III gliomas (anaplastic astrocytoma, anaplastic oligoastrocytoma, and anaplastic oligodendroglioma), who had a median survival of 860 days, and 59 biopsies of patients with grade IV gliomas (GBM), who had a median survival of 237 Days (**Table 5**). Similarly to test cohort, histological glioma grade was associated to patients' survival (HR=3.2.47; SE=0.859 ; P<0.001) (**Figure 4**), but age and gender were not (**Table 5**).

The predictive value of gene expression of each mGluR was also evaluated in this cohort using the KM method (**Figure 5**), after median expression stratification. The results show that low levels of *GRM4* appeared to be predictive of worse prognosis for patients (HR=-1.873; SE=0.620; P=0.029) (**Figure 5D**), as well as low levels of *GRM6* (HR=-1.851; SE=0.591; P=0.035) (**Figure 5F**). Using cox analysis, it was observed that increase in *GRM3* expression was associated with higher risk of death (HR=1.422; SE=0.141; P=0.013) (**Table 6**), while increase in *GRM4* expression predicted a good prognosis for patients (HR=-1.446; SE=0.177; P=0.037) (**Table 6**).

The gene expression profile of all mGluR in validation cohort biopsies was also evaluated by cluster analysis (**Figure 6**). Again, patients from this cohort were also grouped into three clusters, according to *GRM* expression in biopsies (orange, yellow and black groups). In validation cohort, the major components for this clustering appear to be *GRM3*, *GRM6*, and *GRM4* genes. Differently from test cohort, in this cohort, *GRM2* did not seem to be an influent component in the clustering of patients (**Figure 6A**). Orange group contained patients whose GBM samples had high levels of *GRM3* and low of *GRM4* and *6*. Yellow group contained

patients whose biopsies expressed low levels of *GRM3* and high levels of *GRM4* and *6*. As observed in test cohort, black group was also very similar to yellow. Survival curves of the three clusters are shown in KM of **Figure 6B**. There was statistical difference among curves (P=0.023), supporting the idea that simultaneous analysis of all mRNA mGluR subtypes in GBM samples can be used to evaluate patients' outcome. As was done in test cohort, patients from black cluster were added to yellow cluster, since biopsies of both groups presented similar characteristics (low level of *GRM3* and high levels of *GRM4* and *6*). **Figure 6C** KM shows that patients from orange group had 2.13 times more chance of dying compared to patients in dark yellow group (HR=2.128; SE=0.751; P=0.008). In conclusion, gene expression levels of mGluR3, 4, and 6 in GBM biopsies were able to predict outcome of patients in validation cohort (**Figure 3C**).

Finally, Cox multivariate regression analysis was also used to evaluate the contribution of *GRM3*, *GRM4* and *GRM6*, as well as the interaction among them, on patient mortality (**Table 7**). Through this analysis it was verified that decrease in *GRM6* expression in biopsies from test cohort was related to a worse prognosis for patient (HR=-125.826; 2.430; P=0.047) and that interaction among the three genes was not predictive of outcome (**Table 7**). The same regression analysis was made in validation cohort (**Table 8**). In this cohort, increase in *GRM3* expression in tumors was related to a worse prognosis for patient (HR=2.169; SE=0.333; P=0.020). Besides, it was observed that there was an interaction between *GRM3* and *GRM6* expression in biopsies from this cohort (HR=0.508; SE=0.434; P=0.209).

Glutamate receptors gene expression signature may correlate with survival of GBM patients

In test cohort, KM curves of each mGluR revealed that high expression of *GRM3* and *GRM8* in GBM biopsies resulted in a worse prognosis for patients (**Figure 2 C and H**). On the other hand, in the same cohort, Cox proportional hazards regression analysis showed that

increase in *GRM3* and *GRM7* expression levels were associated with poor outcome of patients (**Table 3**). Thus, *GRM8* survival association observed in the KM curve may have been influenced by clinical variables (**Figure 2H**). Regression analysis also demonstrated that decrease in *GRM4* or *GRM5* levels in GBM biopsies predicted, respectively, a death risk of about 1.8 or 2.8 times higher in patients from test cohort (**Table 3**). Although Cox analysis of *GRM5* and *GRM7* showed a predictive association with patient's outcome, the analysis of **Figure 3A** clearly shows that these genes did not seem to contribute much to the clustering of this cohort.

In validation cohort, KM method revealed that increase in *GRM4* and *GRM6* expression levels predicted a longer survival (**Figure 5 D and F**). Although in the KM method *GRM3* did not present a predictive value of outcome (P=0.071), the cox analysis used to evaluate the contribution of each *GRM* showed that increase in GBM *GRM3* expression was correlated with a poor prognosis (**Table 6**). On the other hand, also using regression analysis, increase in *GRM4* levels in tumors was able to predict a better prognosis (**Table 6**). Additionally, differences in *GRM6* levels in GBM had no significant predictive value using cox analysis (**Table 6**). Nevertheless, these three genes appear to represent the major components that influenced the hierarchical clustering of the two cohorts, since the individual expression of one of the main components of the hierarchical cluster of test cohort, *GRM2*, had no predictive value alone in either cohorts and it did not seem to influence the grouping of validation cohort (**Figure 6A**).

The evaluation of interactions between *GRM3*, *GRM4*, and *GRM6* on patients' outcome in both cohorts was also tested by cox analysis (**Table 7** and **Table 8**). In test cohort, interactions between these gene expressions were not predictive of outcome. In validation cohort, the variable corresponding to interaction between *GRM3* and *GRM6* levels had statistical significance, which means the effect of either *GRM* expression is dependent on the levels of expression of the other receptor (**Table 8**). This result reinforces the results obtained with the other analyzes hinting for the hypothesis that low expression of *GRM3* and high expression of

GRM6 was related to a longer survival.

Overall, the meta-analysis of the gene expression of two cohorts of GBM patients led to the characterization of an mGluR signature, in which high *GRM3* expression together with low *GRM4* and/or *GRM6* expression are predictive of a poor outcome.

Protein expression profile of mGluR3, 4 and 6 in GBM lines

For *in vitro* assessment of mGluR gene signature potential, protein expression of mGluR3, 4 and 6 was first evaluated by western blot technique in six GBM lines: one derived from rat (C6) and the others from humans (A-172, M059J, T98G, U-87 and U-138). None of the lineages showed immunocontent for mGluR4 (**Figure 7C**). However, all of them expressed similar immunocontent for mGluR6 (**Figure 7B**). U-87 human lineage presented the highest immunocontent for mGluR3, in relation to other lines, which presented similar protein levels of this receptor (Median, 0.50 U.A.; 25 % percentile, 0.36 U.A.; 75 % percentile, 0.63 U.A.; P=0.0004) (**Figure 7A**).

Aggressive profile assessment of each GBM line

It was not possible to find two GBM lineages that *per se* could adequately assess the potential of mGluR gene signature, since none of them presented at the same time a profile with high expression of mGluR3 and low expression of mGluR4 or mGluR6. Due to this, we decided to evaluate the aggressiveness profile of each lineage in order to choose at least two lines with distinct aggression patterns for further pharmacological tests. Aggressiveness profile of each lineage was evaluated through the analysis of doubling time (**Supplementary Figure 2**), migratory capacity (**Supplementary Figure 3**) and resistance to TMZ, the standard chemotherapy for GBM (**Supplementary Figure 4**), and to BCNU (**Supplementary Figure 5**). **Table 9** summarizes all *in vitro* aggressiveness profile results of the GBM lines.

The lineage that presented the shortest doubling time was C6 rat line (24.84 h), followed

by the human lines A-172 (31.87 h) and U-87 (32.03 h). The most resistant GBM lineage to TMZ was U-138 (IC_{50}=925 µM), followed by T98G (IC_{50}=740 µM) and U-87 (IC_{50}=660 µM) lines (**Supplementary Figure 4**).T98G line was the most resistant to BCNU (IC_{50}>1 mM), followed by U-87 (IC_{50}=435 µM) and U-138 (IC_{50}=380 µM) (**Supplementary Figure 5**). C6 line was the least resistant GBM line to both chemotherapeutic agents (TMZ IC_{50}=245 µM; BCNU IC_{50}=65 µM). However, this rat lineage is one of the most migratory, along with U-138 and M059J human lines (**Table 9**). After analyzing mGluR3 and mGluR6 protein expression and aggressiveness results, C6 rat lineage and U-87 human lineage were chosen to continue the *in vitro* pharmacological studies in an attempt to test the association of mGluR gene signature with cellular markers of malignancy. Besides, among our panel of GBM lines, they are the most used lineages in studies that evaluate the role of glutamate receptors on aggressiveness of gliomas [1, 28, 35].

mGluR ligands cause antiproliferative effects on C6 and U-87 lineages only under non-proliferative conditions

Two types of group II antagonists were used in this work (EGLU and LY341495) to mimic a condition of mGluR3 receptor inactivation and group III agonist (L-AP4) was used to mimic a condition of mGluR6 receptor activation in GBM cultures. Co-treatment of GBM cells with agonist and antagonist of the same group was performed to verify if it caused the reversion of results obtained with isolated treatments.

Pharmacological treatment of GBM lineages in proliferative conditions

Three experimental protocols were performed to evaluate the action of ligands on C6 and U-87 lines under proliferating conditions. In the first protocol performed, culture medium (DMEM supplemented with FBS) containing treatments (100 µM EGLU, 100 nM LY341495, 1 µM LY341495 or 100 µM L-AP4) was renewed every day (**Supplementary Figure 6**). Daily

exchange (d.e.) of culture medium affected the proliferative rate of both C6 (DT = 35 h) and U-87 (DT = 50 h) lineages, when compared to DMEM group not changed daily (C6 DT = 22 h; U-87 DT = 29 h) (**Supplementary Figure 6A and C**, respectively). In addition, the use of this protocol did not significantly alter the percentage of GBM cells in well after 72h of treatment with ligands, when compared to control group (DMEM d.e.) (**Supplementary Figure 6B and D**).

As FBS contains L-Glu in its composition, this amino acid may be interfering with the effect of mGluR ligands on glutamate receptors. Thus, two treatment strategies have been performed. In the first one, C6 and U-87 cells were treated for 30 min with ligands at double concentration in 100 µL of DMEM not containing FBS. After this time, 100 µL of DMEM was added containing twice concentration of FBS required for culture of each GBM line. Neither combined treatment of EGLU with L-APA nor treatment with these ligands separately resulted in a significant change in percentage of cells in culture (**Supplementary Figure 7 A and D**). The interaction of mGluR ligands with chemotherapy was also evaluated using this protocol. Addition of TMZ or BCNU (IC_{25} double) in C6 line 30 min prior to addition of DMEM containing FBS decreased amount of cells after 72 h of culturing in 33.96 % (77.41$\pm$1.94) (**Supplementary Figure 7B**) and 74.78 % (36.60$\pm$1.50) (**Supplementary Figure 7C**), respectively, when compared to control group (111.40$\pm$10.08). In U-87 line, using the same protocol, TMZ treatment decreased amount of cells in 33.70 % (72.12$\pm$6.72) (**Supplementary Figure 7E**) and BCNU treatment decreased in 64.67 % (41.16$\pm$3.62) (**Supplementary Figure 7F**) when compared to control group (105.80$\pm$13.55). Treatment of ligands together with chemotherapeutics also had no additive effect on percentage of cells that remained in culture (**Supplementary Figure 7 B, C, E and F**).

As in the prior strategy C6 and U-87 cells were treated with higher concentrations of ligands and chemotherapeutics for 30 min, this short time of exposure to high concentrations of those ligands may have altered their effect on GBM lineages. For this reason, another approach

was used to test the effect of mGluR ligands on GBM lineages under proliferating conditions. C6 and U-87 cells were treated for 30 min with mGluR ligands (100 µM EGLU, 100 nM LY341495, 1 µM LY341495, 100 nM LY379268, 100 µM L-AP4 or 100 µM MSOP) in DMEM not containing FBS. After this time, the aliquot needed to maintain the appropriate final concentration of FBS for each lineage was added (5 % FBS for C6; 10 % FBS for U-87). Neither treatment alone with mGluR ligands, nor combined treatment among them caused a significant change in percentage of GBM cells after 72h (**Supplementary Figure 8**). In this protocol, the interaction between chemotherapeutics and ligands was also evaluated. C6 cultivation in presence of TMZ (IC_{25}) and BCNU (IC_{25}) resulted in a decrease of 30.84 % (65.57±3.19) and 37 % (58.47±6.05) of cells, respectively, after 72 h of exposure, when compared to control group (96.41±7.56). Using the same protocol, TMZ (IC_{25}) and BCNU (IC_{25}) treatment reduced U-87 cells in 39.42 % (62.83±1.41) and 22.25 % (80.00±3.35), respectively, in relation to control group (102.3±5.19). Addition of mGluR ligands to these conditions in both cultures did not cause additive effect (**Supplementary Figure 9** and **Supplementary Figure 10**).

Thus, treatment of C6 and U-87 lineages with mGluR ligands under proliferating conditions does not cause an antiproliferative effect on these GBM cells. This effect remains even in presence of chemotherapeutic agents, TMZ and BCNU.

Pharmacological treatment of GBM lineages in non-proliferating conditions

To definitively exclude the influence of components present in FBS, C6 and U-87 lineages ($1x10^4$ cells/well) were treated with mGluR ligands and chemotherapeutic agents for 72h in absence of FBS. In this culture condition, the proliferative rate of both GBM cell cultures was very low, or almost null (**Supplementary Figure 11**). In U-87 line, treatments with mGluR ligands had no effect on U-87 line (**Figure 8**). On the other hand, in C6 line, treatment with group II antagonists EGLU (100 µM) and LY341495 (100 nM) decreased the amount of cells in

about 25 % (77.28±4.88; 75.07±5.87, respectively) compared to control group (102.50±4.52) (**Figure 9 A and B**). Additionally, the concentration of 1 µM of LY341495 antagonist was able to decrease the amount of C6 cells in 42.78 % (59.73±5.71) (**Figure 9B**). The 30 min pre-treatment with agonist of group II (100 nM LY379268), reversed this effect (**Figure 9 A and B**). Treatment alone with this agonist did not alter the percentage of C6 cells after 72h of culture (**Figure 9 A and B**).

C6 treatment with group III agonist (100 µM L-AP4) also caused approximately 25 % (76.87±5.71) of decrease in amount of cells when compared to control group (102.50±4.52). Pre-treatment with group III antagonist (100 µM MSOP) for 30 min reversed this decrease (**Figure 9C**). Treatment of C6 lineage only with 100 µM MSOP did not change the percentage of cells after 72 h of culture (**Figure 9C**).

C6 lineage co-treatment with group II antagonists (100 µM EGLU) and with group III agonist (100 µM L-AP4) caused also about 25 % (76.43±2.91) of decrease in cells after 72h of culture in relation to control group (102.50±4.52) (**Figure 9E**). The same effect was seen in C6 co-treatment with 100 nM LY341495 and 100 µM L-AP4 (77.10±2.85) (**Figure 9E**). Co-treatment with 1 µM LY341495 and 100 µM L-AP4 was able to decrease the number of cells by 45.35 % (57.17±3.54) (**Figure 9E**). Pre-treatment (30 min) with group II agonist (LY379268 100 nM) together with group III antagonist (100 µM MSOP) reversed the effect caused by addition of co-treatment with group II antagonist (100 µM EGLU) in conjunction with group II agonist (100 µM L-AP4) (**Figure 9E**). Co-treatment only with 100 nM LY379268 plus 100 µM MSOP had no effect on percentage of C6 cells after 72 h of culture (**Figure 9E**).

mGluR ligands concentrations used in this work were chosen according to concentrations used in literature [22]. The concentration of 100 nM LY341495 affects mGluR2 (IC_{50} = 21 nM) and mGluR3 (IC_{50} = 14 nM) [24]. The concentration of 1 µM of LY341495, in addition to reaching receptors of group II mGluR, also affects two receptors of group III mGluR, mGluR7 (IC50 = 0.99 µM) and mGluR8 (IC50 = 0.17 µM)[24]. Thus, the marked decrease in

percentage of cells after treatment with 1 μM of LY341495 alone or in conjunction with L-AP4 may have occurred due to an inhibition of part of mGluR7 and mGluR8 that could be present in those cells.

Treatment of C6 and U-87 lines with TMZ and BCNU under non-proliferating conditions of culture did not follow the expected pattern for these GBM cells under proliferating conditions. TMZ and BCNU are alkylating agents whose cytotoxic effect is related to formation of interstrand crosslinks in DNA, which damages it and interfere in its translation and transcription, triggering tumoral cell death [25]. TMZ is classified in cell cycle–specific drugs, which are chemotherapeutic agents that are effective on cells that are actively growing and dividing [25]. Thus, the non-decrease in number of C6 and U-87 cells after 72 h of culture in DMEM without FBS and containing TMZ is explained by the fact that these cells were not in conditions that allowed proliferation (**Supplementary Figure 11 A and C** and **Supplementary Figure 12**). BCNU belongs to cell cycle–non-specific drugs, which are a group of chemotherapeutic agents that appears to be effective whether cancer cells are in cycle or are resting [25]. Even so, the presence of BCNU in culture medium without FBS was not able to decrease the amount of C6 cells after 72 h of culture (**Supplementary Figure 11 A** and **Supplementary Figure 13 A, B, and C**). Strangely, the use of the same protocol in U-87 lineage increased the percentage of cells (**Supplementary Figure 11 C** and **Supplementary Figure 13 D, E, and F**). These BCNU effects on GBM cultures under non-proliferating conditions may be related to the process of resistance to this chemotherapeutic agent. As showed in **Supplementary Figures 7 C and F**, a short exposure (30 min) of C6 and U-87 lines to BCNU in medium without FBS was sufficient to cause a cytotoxic effect on these cells. Thus, initial exposure of both lineages to IC_{25} of this chemotherapeutic under non-proliferating conditions may have caused considerable cell death. This cell death may have generated a signal for resting GBM cells to progress into active cell cycle, resulting in an increased number of proliferating cancer cells [26]. Thus, probably after 72 h of culture in medium without serum and

containing BCNU, the number of cells was reestablished, in the case of C6 lineage, or a greater growth occurred, in the case of U-87 line. It should be noted that U-87 lineage did not remain in a completely non-proliferating state in medium without FBS (**Supplementary Figure 11D**).

Treatment with chemotherapeutic agents in medium without FBS did not potentiate the effect of mGluR ligands on U-87 lineage (**Supplementary Figure 12 D, E, and F** and **Supplementary Figure 13 D, E, and F**). However, the effect of mGluR ligands treatment on C6 lineage was maintained in the presence of TMZ. Treatment with 100 μM EGLU, 100 nM LY341495, and 100 μM L-AP4 alone decreased the percentage of cells in the well by 26 % (63.27±3.69), 25.50 % (63.77±2.90), and 28.33 % (60.93±6.37), respectively, in relation to TMZ-only group (89.27±0.23). Combination of EGLU (100 μM) plus L-AP4 (100 μM) or LY341595 (100 nM) plus L-AP4 (100 μM) decreased the percentage of cells in 21.40 % (68.87±2.75) and 28.37 % (60.09±0.35), respectively, in relation to TMZ group (89.27±0.23). Treatment with 1 μM of LY341495 had the ability to decrease in 36.60 % (52.67±3.33) the number C6 cells when compared to TMZ treated group (89.27±0.23) and its co-treatment with L-AP4 100 μM reduced cell percentage in 34.63 % (54.63±3.02) (**Supplementary Figure 12 A, B, and C**). Co-treatment of the cells with the group II agonist (100 nM LY379268) and the group III antagonist (100 μM MSOP) did not alter the percentage of cells after 72 h of culture together with TMZ. In the presence of BCNU, occurred about 30 % of significant decrease in cell number in treatments with 1 μM LY341495 alone (75.97±8.42) and about 35 % in treatment with the same concentration of this antagonist combined with 100 μM L-AP4 (71.10±2.48), when compared to group treated with BCNU only (106.2+6.82) (**Supplementary Figure 13C**). Although there was no statistically significant decrease in relation to BCNU group, treatment with EGLU (100 μM) and LY341495 (100 nM) decreased the percentage of C6 cells in about 30% and treatment with L-AP4 (100 μM) reduced the percentage by 22%. Treatment with L-AP4 (100 μM) in conjunction with EGLU (100 μM) or LY341495 (100 nM) reduced percentage of C6 cells in approximately 25% and 30%, respectively, although there was no significance in

the statistic (**Supplementary Figure 13 A and B**).

These results indicate that pharmacological blockade of group II mGluR and pharmacological activation of group III mGluR decreased the amount of GBM cells in 25-28% after 72 h of culture under non-proliferating conditions. The combination of treatments that inhibit group II mGluR with those that activate group III mGluR had no synergistic effect, since it also decreased the number of GBM cells in the same proportion, indicating that the signaling pathway that allows the decrease in number of GBM cells in culture is the same. The addition of alkylating chemotherapeutics did not potentiate the effect of these treatments. However, the effect of mGluR ligands treatment on GBM was maintained in the presence of these drugs.

CONCLUSION

Meta-analysis of two cohorts of patients with GBM led to the identification of an mGluR gene signature with prognostic value, in which high *GRM3* expression together with low *GRM4* and *GRM6* expression in GBM tumors were associated with shorter overall patients' survival. The inverse profile expression of these receptors in biopsies (low *GRM3* expression together with high *GRM4* and *GRM6* expression) predicted a longer overall survival for GBM patients.

The potential of the mGluR gene signature on the malignancy of these tumors was assessed by *in vitro* experiments through the treatment of GBM lineages with groups II and III mGluR ligands for 72 h in absence of FBS. Pharmacological blockade of group II mGluR and pharmacological activation of group III mGluR decreased the amount of GBM cells in 25-28 %. The combination of these treatments had no synergistic effect, indicating that the signaling pathway that allows the decrease in number of GBM cells is the same. The addition of alkylating chemotherapeutics did not potentiate the effect of these treatments. Thus, *in vitro* treatment of GBM cells with mGluR ligands under non-proliferating conditions was in accordance with our mGluR meta-signature proposal. However, this is a condition that does not adequately mimic the environment in which GBM is inserted *in vivo*. As treatment with ligands did not have an effect on GBM cells cultured in medium containing serum, probably because it contains L-Glu in its composition, different *in vitro* experiments under proliferating conditions without addition of serum should be performed to better evaluate these receptors` involvement in GBM development and aggressiveness.

This article demonstrated that evaluation of mGluR3, 4, and 6 gene expression levels can be used as prognostic biomarker to indicate patient outcome. Although further *in vitro* experiments are required for better evaluation of mGluR gene signature potential, evaluation of the eight mGluR subtypes in GBM biopsies may be considered to guide future chemotherapeutic intervations.

ACKNOWLEDGMENTS

We would like to thank Prof. Dr. Guido Lenz for supplying the glioblastomas lineages. This work was financed by *Coordenação de Aperfeiçoamento de Pessoal de Nível Superior (CAPES), Conselho Nacional de Desenvolvimento Científico e Tecnológico (CNPq) – Edital Doenças Neurodegenerativas*, *Fundação de Amparo à Pesquisa do Estado do Rio Grande do Sul (FAPERGS)*, and *Financiadora de Estados e Projetos (FINEP)*.

REFERENCES

1 Arcella A, Carpinelli G, Battaglia G, D'Onofrio M, Santoro F, Ngomba RT *et al* (2005). Pharmacological blockade of group II metabotropic glutamate receptors reduces the growth of glioma cells in vivo. *Neuro Oncol* **7:** 236-245.

2 Babu R, Komisarow JM, Agarwal VJ, Rahimpour S, Iyer A, Britt D *et al* (2016). Glioblastoma in the elderly: the effect of aggressive and modern therapies on survival. *J Neurosurg* **124:** 998-1007.

3 Ciceroni C, Arcella A, Mosillo P, Battaglia G, Mastrantoni E, Oliva MA *et al* (2008). Type-3 metabotropic glutamate receptors negatively modulate bone morphogenetic protein receptor signaling and support the tumourigenic potential of glioma-initiating cells. *Neuropharmacology* **55:** 568-576.

4 Ciceroni C, Bonelli M, Mastrantoni E, Niccolini C, Laurenza M, Larocca LM *et al* (2013). Type-3 metabotropic glutamate receptors regulate chemoresistance in glioma stem cells, and their levels are inversely related to survival in patients with malignant gliomas. *Cell Death Differ* **20:** 396-407.

5 Cloughesy TF, Cavenee WK, Mischel PS (2014). Glioblastoma: from molecular pathology to targeted treatment. *Annu Rev Pathol* **9:** 1-25.

6 Core TR (2013). *A language and environment for statistical computing.* .

7 D'Onofrio M, Arcella A, Bruno V, Ngomba RT, Battaglia G, Lombari V *et al* (2003). Pharmacological blockade of mGlu2/3 metabotropic glutamate receptors reduces cell proliferation in cultured human glioma cells. *J Neurochem* **84:** 1288-1295.

8 DeAngelis LM (2001). Brain tumors. *N Engl J Med* **344:** 114-123.

9 Freije WA, Castro-Vargas FE, Fang Z, Horvath S, Cloughesy T, Liau LM *et al* (2004). Gene expression profiling of gliomas strongly predicts survival. *Cancer Res* **64:** 6503-6510.

10 Gramatzki D, Dehler S, Rushing EJ, Zaugg K, Hofer S, Yonekawa Y *et al* (2016). Glioblastoma in the Canton of Zurich, Switzerland revisited: 2005 to 2009. *Cancer* **122:** 2206-2215.

11 Gravendeel LA, Kouwenhoven MC, Gevaert O, de Rooi JJ, Stubbs AP, Duijm JE *et al* (2009). Intrinsic gene expression profiles of gliomas are a better predictor of survival than histology. *Cancer Res* **69:** 9065-9072.

12 Kleihues P, Soylemezoglu F, Schäuble B, Scheithauer BW, Burger PC (1995). Histopathology, classification, and grading of gliomas. *Glia* **15:** 211-221.

13 Louis DN, Ohgaki H, Wiestler OD, Cavenee WK, Burger PC, Jouvet A *et al* (2007). The 2007 WHO classification of tumours of the central nervous system. *Acta Neuropathol* **114:** 97-109.

14 Louis DN, Perry A, Reifenberger G, von Deimling A, Figarella-Branger D, Cavenee WK *et al* (2016). The 2016 World Health Organization Classification of Tumors of the Central Nervous System: a summary. *Acta Neuropathol* **131:** 803-820.

15 Malmström A, Grønberg BH, Marosi C, Stupp R, Frappaz D, Schultz H *et al* (2012). Temozolomide versus standard 6-week radiotherapy versus hypofractionated radiotherapy in patients older than 60 years with glioblastoma: the Nordic randomised, phase 3 trial. *Lancet Oncol* **13:** 916-926.

16 Masui K, Cloughesy TF, Mischel PS (2012). Review: molecular pathology in adult high-grade gliomas: from molecular diagnostics to target therapies. *Neuropathol Appl Neurobiol* **38:** 271-291.

17 Niswender CM, Conn PJ (2010). Metabotropic glutamate receptors: physiology, pharmacology, and disease. *Annu Rev Pharmacol Toxicol* **50:** 295-322.

18 Omuro A, DeAngelis LM (2013). Glioblastoma and other malignant gliomas: a clinical review. *JAMA* **310:** 1842-1850.

19 Omuro AM, Faivre S, Raymond E (2007). Lessons learned in the development of targeted therapy for malignant gliomas. *Mol Cancer Ther* **6:** 1909-1919.

20 Ostrom QT, Gittleman H, Fulop J, Liu M, Blanda R, Kromer C *et al* (2015). CBTRUS Statistical Report: Primary Brain and Central Nervous System Tumors Diagnosed in the United States in 2008-2012. *Neuro Oncol* **17 Suppl 4:** iv1-iv62.

21 Pereira MS, Zenki K, Cavalheiro MM, Thomé CC, Filippi-Chiela EC, Lenz G *et al* (2014). Cellular senescence induced by prolonged subculture adversely affects glutamate uptake in C6 lineage. *Neurochem Res* **39:** 973-984.

22 Pereira MS, Klamt F, Thomé CC, Worm PV, de Oliveira DL (2017). Metabotropic glutamate receptors as a new therapeutic target for malignant gliomas. *Oncotarget*.

23 Sant M, Minicozzi P, Lagorio S, Børge Johannesen T, Marcos-Gragera R, Francisci S *et al* (2012). Survival of European patients with central nervous system tumors. *Int J Cancer* **131:** 173-185.

24 Schoepp DD, Jane DE, Monn JA (1999). Pharmacological agents acting at subtypes of metabotropic glutamate receptors. *Neuropharmacology* **38:** 1431-1476.

25 Skeel RT (2007). *Antineoplastic drugs and biologic response modifiers: classification, use, and toxicity of clinically useful agents*, vol. 7th Edition. Lippincott Williams & Wilkins.

26 Soffietti WGaR (2012). *Handbook of Clinical Neurology: Neuro-Oncology*, vol. Part I

27 Stupp R, Mason WP, van den Bent MJ, Weller M, Fisher B, Taphoorn MJ *et al* (2005). Radiotherapy plus concomitant and adjuvant temozolomide for glioblastoma. *N Engl J Med* **352:** 987-996.

28 Takano T, Lin JH, Arcuino G, Gao Q, Yang J, Nedergaard M (2001). Glutamate release promotes growth of malignant gliomas. *Nat Med* **7:** 1010-1015.

29 Tsao MN, Mehta MP, Whelan TJ, Morris DE, Hayman JA, Flickinger JC *et al* (2005). The American Society for Therapeutic Radiology and Oncology (ASTRO) evidence-based review of the role of radiosurgery for malignant glioma. *Int J Radiat Oncol Biol Phys* **63:** 47-55.

30 Vichai V, Kirtikara K (2006). Sulforhodamine B colorimetric assay for cytotoxicity screening. *Nat Protoc* **1:** 1112-1116.

31 Wang Y, Jiang T (2013). Understanding high grade glioma: molecular mechanism, therapy and comprehensive management. *Cancer Lett* **331:** 139-146.

32 Westphal M, Hilt DC, Bortey E, Delavault P, Olivares R, Warnke PC *et al* (2003). A phase 3 trial of local chemotherapy with biodegradable carmustine (BCNU) wafers (Gliadel wafers) in patients with primary malignant glioma. *Neuro Oncol* **5:** 79-88.

33 Westphal M, Lamszus K (2011). The neurobiology of gliomas: from cell biology to the development of therapeutic approaches. *Nature reviews Neuroscience* **12:** 495-508.

34 Yelskaya Z, Carrillo V, Dubisz E, Gulzar H, Morgan D, Mahajan SS (2013). Synergistic inhibition of survival, proliferation, and migration of U87 cells with a combination of LY341495 and Iressa. *PLoS One* **8:** e64588.

35 Zhang C, Yuan XR, Li HY, Zhao ZJ, Liao YW, Wang XY *et al* (2015). Anti-cancer effect of metabotropic glutamate receptor 1 inhibition in human glioma U87 cells: involvement of PI3K/Akt/mTOR pathway. *Cell Physiol Biochem* **35:** 419-432.

36 Zhou K, Song Y, Zhou W, Zhang C, Shu H, Yang H *et al* (2014). mGlu3 receptor blockade inhibits proliferation and promotes astrocytic phenotype in glioma stem cells. *Cell Biol Int* **38:** 426-434.

TABLES

Table 1 – Clinical characteristics of test cohort (GSE16011)

		Age				Survival (Days)				
Grade	**n (M/F)**	**Min.**	**Max.**	**Mean ±SD**	**Median**	**Min.**	**Max.**	**Mean±SD**	**Median**	**% alive in 3 years**
III	59 (40/19)	24	81	47±12	45	68	4201	1472±1155	1188	54
IV (GBM)	114 (79/35)	14	81	52±13	53	58	4522	514±590	324	10

Table 2 - Hazard Ratio[a] for patient´s survival – Clinical covariates (Test cohort - GSE16011)

	Overall Survival	
Variables	**HR ± SE[b]**	**P-value**
Age (years)	1.035±0.008	<0.001*
Gender (Male)	1.039±0.207	0.855
KPS	0.983±0.007 → *HR* = -1.017	0.019*

a. Cox multivariate regression analysis was used to estimate hazard ratios (HR) for cohort clinical covariates; SE = Standard Error; *P ≤ 0.05.

b. HR≥1 indicates increased risk of death**;** HR<0 indicates decreased risk of death.

Table 3 - Hazard Ratio[a] for Grade IV (GBM) patient´s survival - Predictive value of each mGluR subtype gene (Test cohort - GSE16011)**.**

		Overall Survival	
Receptors	**Variables**	**HR±SE[b]**	**P-value**
mGluR1	Age (years)	1.036±0.008	<0.001*
	Gender (Male)	1.069±0.208	0.747
	KPS	0.981±0.007	0.007*
	GRM1	0.474±0.399	0.061
mGluR2	Age (years)	1.036±0.008	<0.001*
	Gender (Male)	1.090±0.211	0.682
	KPS	0.983±0.007	0.017*
	GRM2	0.744±0.216	0.171
mGluR3	Age (years)	1.037±0.008	<0.001*
	Gender (Male)	1.172±0.211	0.450
	KPS	0.981±0.007	0.007
	GRM3	1.535±0.146	0.003*
mGluR4	Age (years)	1.036±0.008	<0.001*
	Gender (Male)	1.130±0.209	0.560
	KPS	0.980±0.007	0.006*
	GRM4	0.554±0.217 → *HR*= -1.805	0.006*
mGluR5	Age (years)	1.036±0.008	<0.001*
	Gender (Male)	1.034±0.207	0.873
	KPS	0.982±0.007	0.011*
	GRM5	0.358±0.489 → *HR*= -2.793	0.036*
mGluR6	Age (years)	1.034±0.008	<0.001*
	Gender (Male)	1.025±0.208	0.906
	KPS	0.982±0.007	0.015*
	GRM6	0.583±0.353	0.127
mGluR7	Age (years)	1.034±0.008	<0.001*
	Gender (Male)	1.035±0.208	0.869
	KPS	0.980±0.007	0.006*
	GRM7	1.856±0.298	0.038*
mGluR8	Age (years)	1.035±0.008	<0.001*
	Gender (Male)	1.020±0.208	0.923
	KPS	0.983±0.007	0.020*
	GRM8	1.655±0.324	0.120

a. Cox multivariate regression analysis was used to estimate hazard ratios (HR) for cohort clinical covariates and mGluR gene expression (*GRM*); SE = Standard Error; *P ≤ 0.05.

b. HR≥1 indicates increased risk of death; HR<0 indicates decreased risk of death.

Table 4 – Clinical characteristics of validation cohort (GSE4412)

		Age				Survival (Days)				
Grade	**n (M/F)**	**Min.**	**Max.**	**Mean± SD**	**Median**	**Min.**	**Max.**	**Mean±SD**	**Median**	**% alive in 3 years**
III	26 (6 /20)	20	51	35±8	34	173	2516	1105±701	860	27
IV	59 (26/33)	18	82	49±16	47	7	1247	366±326	237	19

Table 5 - Hazard Ratio[a] for patient´s survival – Clinical covariates (Validation cohort – GSE4412)

	Overall Survival	
Variables	**HR±SE[b]**	**P-value**
Age (years)	1.009±0.011	0.400
Gender (Male)	0.875±0.310	0.667

a. Cox multivariate regression analysis was used to estimate hazard ratios (HR) for cohort clinical covariates and mGluR gene expression (*GRM*); SE = Standard Error.
b. HR≥1 indicates increased risk of death; HR<0 indicates decreased risk of death.

Table 6 - Hazard Ratio[a] for Grade IV (GBM) patient´s survival - Predictive value of each mGluR subtype gene (Validation cohort – GSE4412).

		Overall Survival	
Receptors	**Variables**	**HR±SE[b]**	**P-value**
mGluR1	Age (years)	1.003±0.010	0.744
	Gender (Male)	1.022±0.285	0.939
	GRM1	1.073±0.249	0.776
mGluR2	Age (years)	1.002±0.010	0.836
	Gender (Male)	1.001±0.282	0.996
	GRM2	1.507±0.431	0.342
mGluR3	Age (years)	1.008±0.010	0.471
	Gender (Male)	0.864±0.292	0.618
	GRM3	1.422±0.141	0.013*
mGluR4	Age (years)	1.005±0.010	0.605
	Gender (Male)	0.898±0.290	0.709
	GRM4	0.691±0.177→ *HR*= -1.446	0.037*
mGluR5	Age (years)	1.004±0.010	0.732
	Gender (Male)	1.032±0.288	0.912
	GRM5	0.979±0.149	0.889
mGluR6	Age (years)	1.005±0.010	0.640
	Gender (Male)	0.866±0.303	0.636
	GRM6	0.744±0.182	0.105
mGluR7	Age (years)	1.002±0.010	0.882
	Gender (Male)	1.018±0.285	0.949
	GRM7	0.679±0.357	0.278
mGluR8	Age (years)	1.002±0.010	0.880
	Gender (Male)	0.996±0.290	0.989
	GRM8	1.827±0.398	0.130

a. Cox multivariate regression analysis was used to estimate hazard ratios (HR) for cohort clinical covariates and mGluR gene expression (*GRM*); SE = Standard Error; *P ≤ 0.05.

b. HR≥1 indicates increased risk of death; HR<0 indicates decreased risk of death.

Table 7 - Hazard Ratio[a] for Grade IV (GBM) patient´s survival – Predictive value of mGluR gene interaction (Test cohort - GSE16011)

	Overall Survival	
Variables	**HR±SE[b]**	**P-value**
Age (years)	1.041±0.009	<0.001*
Gender (Male)	1.132±0.218	0.569
KPS	0.980±0.007	0.005*
GRM3	0.631±0.491	0.348
GRM4	0.212±0.880	0.078
GRM6	0.008±2.430 → *HR*= -125.826	0.047*
GRM3*:*GRM4	2.382±0.479	0.070
GRM3*:*GRM6	5.930±1.219	0.144
GRM4*:*GRM6	40.516±2.129	0.082
GRM3*:*GRM4*:*GRM6	0.680±1.128	0.732

a. Cox multivariate regression analysis was used to estimate hazard ratios (HR) for cohort clinical covariates and mGluR gene expression (*GRM*); SE = Standard Error; *P ≤ 0.05.

b. HR≥1 indicates increased risk of death; HR<0 indicates decreased risk of death.

Table 8 - Hazard Ratio[a] for Grade IV (GBM) patient´s survival – Predictive value of mGluR gene interaction (Validation cohort – GSE4412)

	Overall Survival	
Variables	**HR±SE[b]**	**P-value**
Age (years)	1.005±0.011	0,667
Gender (Male)	0.884±0.306	0.688
GRM3	2.169±0.333	0.020*
GRM4	0.986±0.698	0.984
GRM6	1.986±0.440	0.119
GRM3*:*GRM4	1.699±0.460	0.249
GRM3*:*GRM6	0.508±0.296	0.022*
GRM4*:*GRM6	0.705±0.563	0.535
GRM3*:*GRM4*:*GRM6	0.580±0.434	0.209

a. Cox multivariate regression analysis was used to estimate hazard ratios (HR) for cohort clinical covariates and mGluR gene expression (*GRM*); SE = Standard Error; *P ≤ 0.05.
b. HR≥1 indicates increased risk of death; HR<0 indicates decreased risk of death.

Table 9 – Comparative table containing the results of *in vitro* aggressiveness assays performed in six GBM lineages[a].

		M059J	**C6**	**A-172**	**U-138**	**T98G**	**U-87**
Doubling Time (h)		66.24	24.84	31.87	55.47	42.96	32.03
TMZ (μM)	IC_{25}	210	45	95	450	530	240
	IC_{50}	470	245	645	925	740	660
BCNU (μM)	IC_{25}	75	33	75	115	595	145
	IC_{50}	205	65	375	380	>1000	435
Wound Healing[b]		+++	+++	+	+++	+	+[c]

a. C6 lineage originates from rat and the others have human origin.

b. Distance travelled by cells of each GBM line into the gap up to 48h was qualitatively evaluated by scales of area retake: + (0-30 %), ++ (31-70%) and +++ (71-100%).

c. The migratory capacity of this lineage was not possible to measure properly, because cells accumulated, forming spheroids.

FIGURES

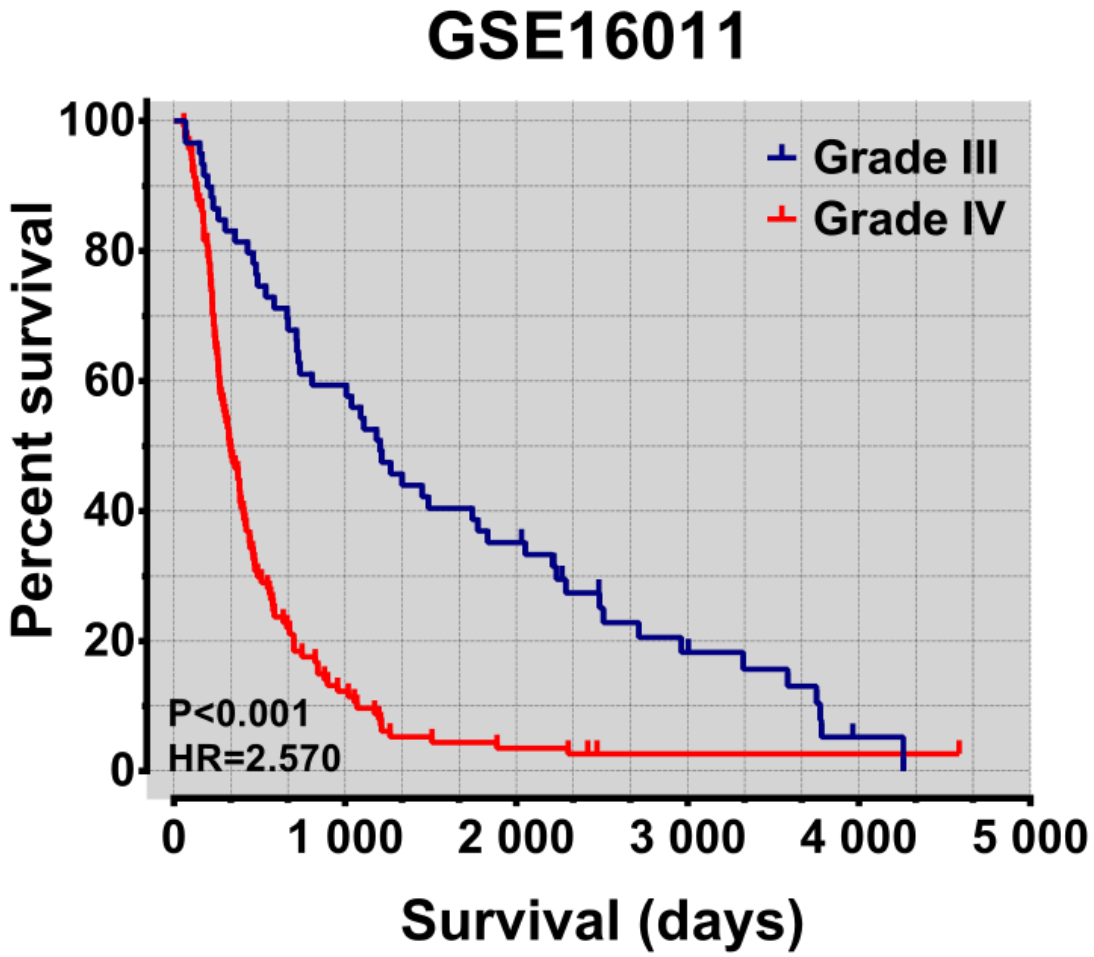

Figure 1 - Survival analysis of patients from test cohort (GSE16011). Kaplan-Meier survival plot of patients partitioned by grade III and IV. *Blue line*, survival probability of grade III (anaplastic astrocytoma, anaplastic oligoastrocytoma, and anaplastic oligodendroglioma) patients; *red line*, survival probability of grade IV (glioblastoma) patients. Patients diagnosed with grade IV gliomas had a poorer outcome compared to those diagnosed with grade III gliomas (HR=2.570; SE=0.451; P<0.001).

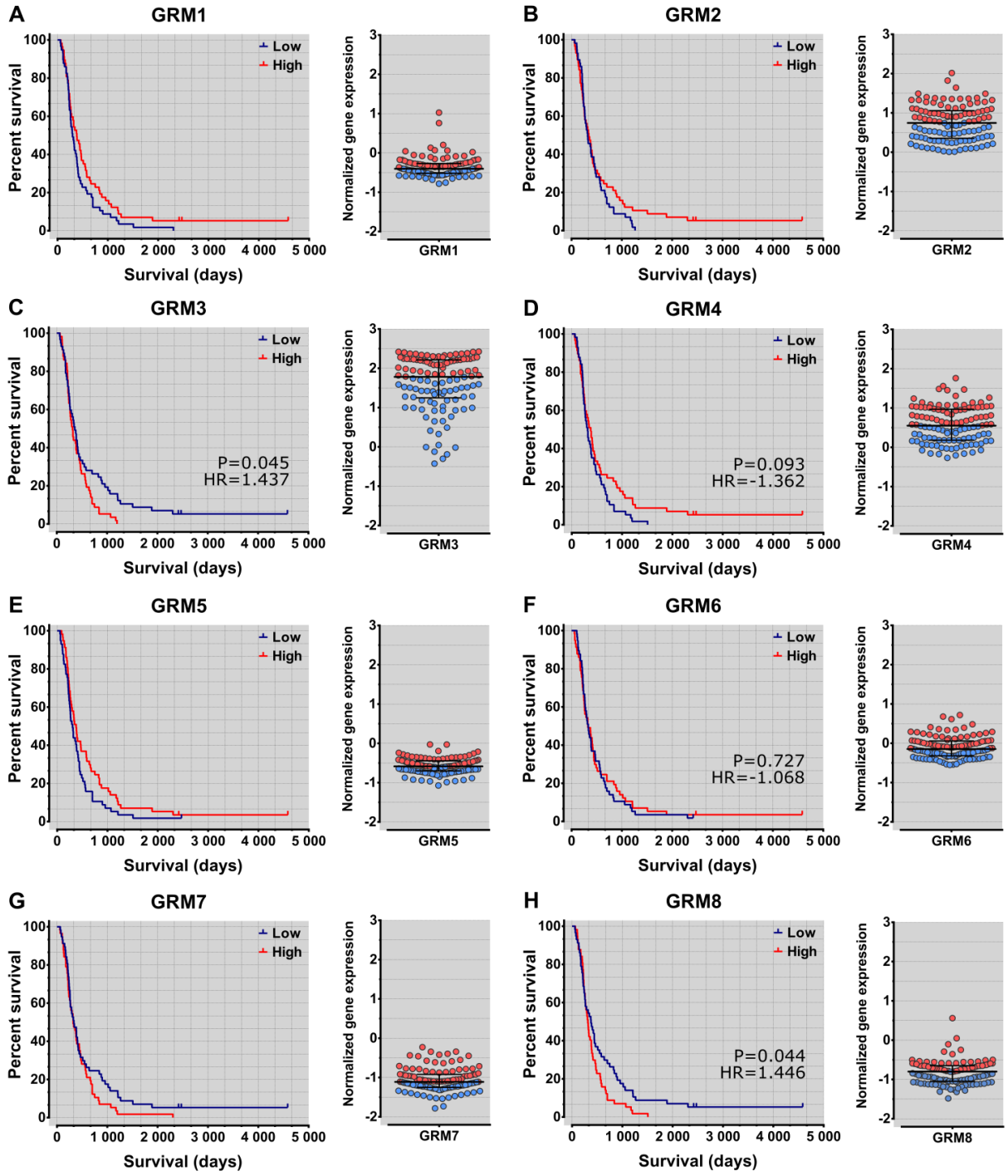

Figure 2 - Prognostic value of individual mGluR gene (*GRM*) expression in GBM biopsies obtained from patients of test cohort (GSE16011). (A-H) Kaplan-Meier (KM) survival curves of *GRM* expression levels. The dot plot beside each KM illustrates the subdivision of cohort (n= 114) in two groups, which was based on the median expression of each gene analyzed. *Group blue* represents patients with low *GRM* expression (≤ median), *group red* indicates patients with high *GRM* expression (> median). Differences in survival rates were assessed with the log-rank test. P-values <0.05 were considered significant.

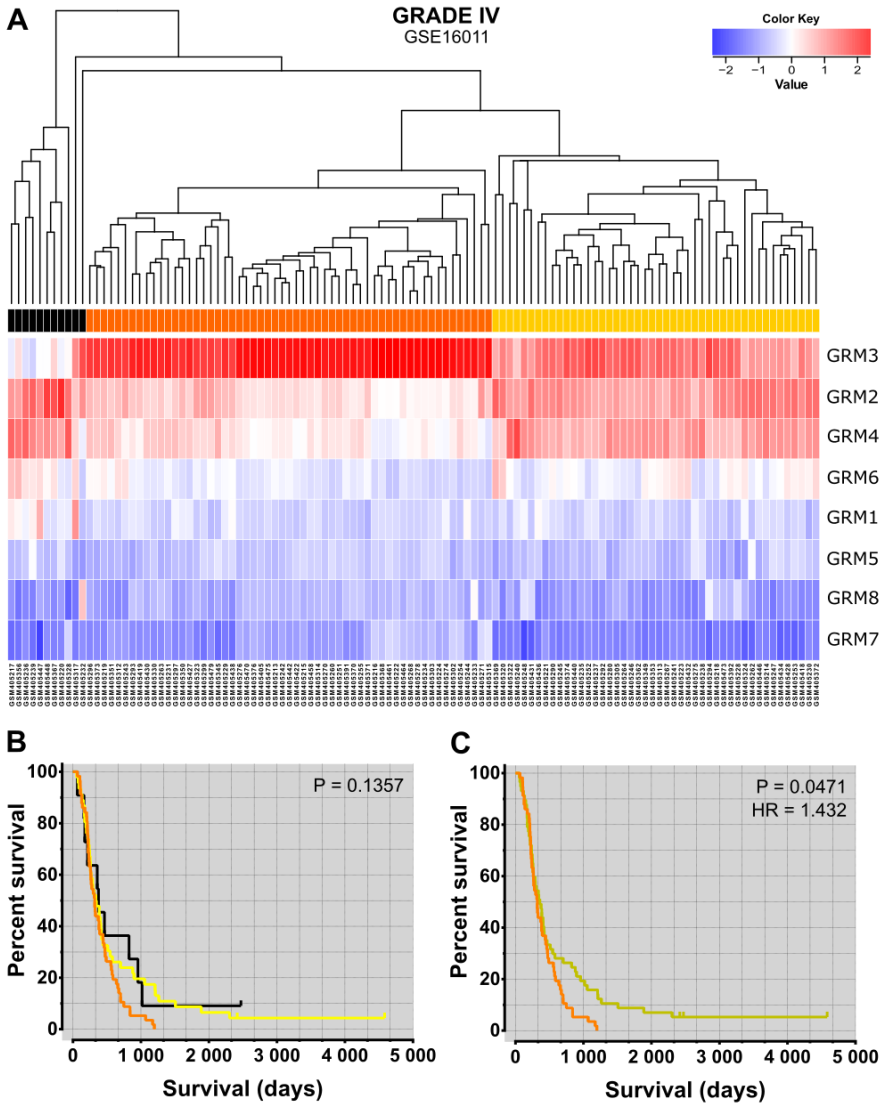

Figure 3 - Prognostic value of the gene expression meta-signature of mGluR subtypes in grade IV (GBM) biopsies obtained from patients of test cohort (GSE16011). (A) Unsupervised hierarchical clustering analysis of GBM samples is shown. This panel presents cohort data arranged according to gene expression profile of all eight mGluR subtypes (*GRM1-GRM8*). The color intensity is associated to the microarray gene expression signal (*red*, positive values; *blue*, negative values). (B) A Kaplan-Meier (KM) plot of the entire cohort data (n= 114) is shown, where patients were stratified according to hierarchical clustering analysis of the eight *GRM*. The orange color represents the patients whose GBM samples showed high expression of *GRM3* and low of *GRM2*, *GRM4* and *GRM6*. The yellow group is represented by patients whose biopsies presented low levels of *GRM3* and high levels of *GRM2*, *4* and *6*. In black group, are patients whose tumor samples show gene expression levels slightly different from those of the yellow group. (C) KM representation of cohort data, where patients of yellow and black groups were grouped into one, the dark yellow, due to the fact that GBM biopsies of both groups were characterized by a low expression of *GRM3* and high of *GRM2*, *4* and *6*. Risk of death was 1.4 times greater in patients from orange group than from dark yellow group (HR = 1.432; SE=0.293; P=0.0471). Differences in survival rates were assessed with log-rank test. P-values <0.05 were considered significant.

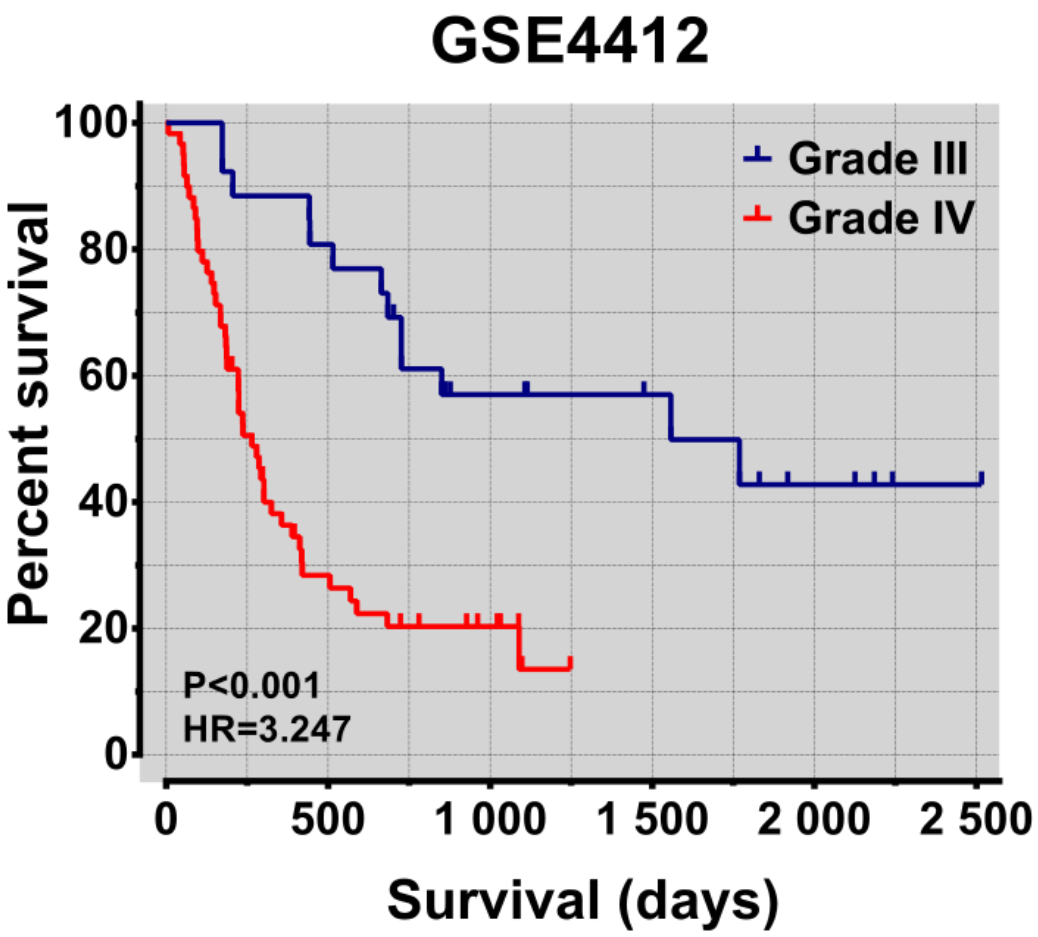

Figure 4 - Survival analysis of patients from validation cohort (GSE4412). Kaplan-Meier survival plot of patients partitioned by grade III and IV. *Blue line*, survival probability of grade III (anaplastic astrocytoma, anaplastic oligoastrocytoma, and anaplastic oligodendroglioma) patients; *red line*, survival probability of grade IV (glioblastoma) patients. Patients diagnosed with grade IV gliomas had a poorer outcome compared to those diagnosed with grade III gliomas (HR=3.247; SE=0.859; P<0.001).

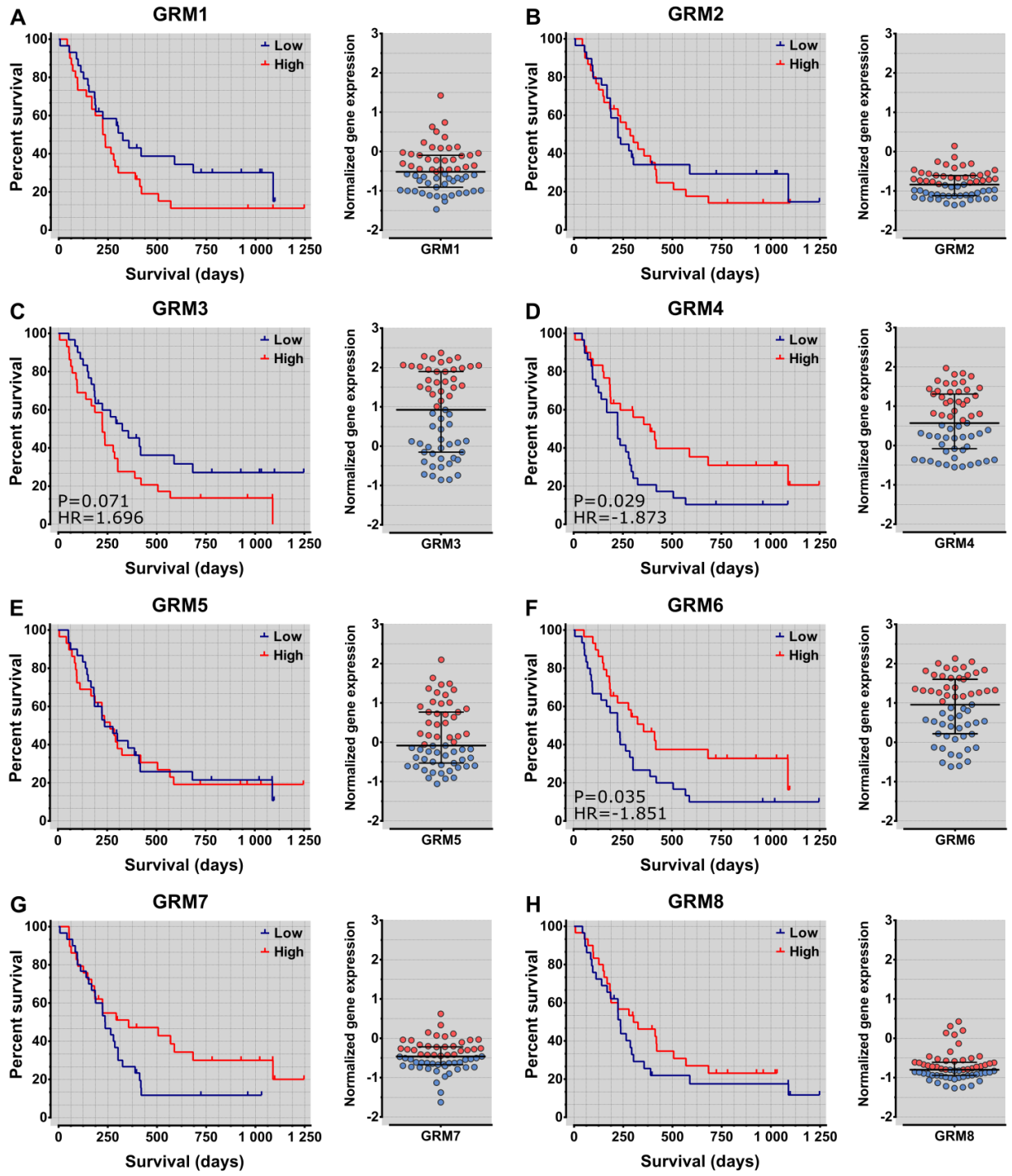

Figure 5 - Prognostic value of individual mGluR gene (*GRM*) expression in GBM biopsies obtained from patients of validation cohort (GSE4412). (A-H) Kaplan-Meier (KM) survival curves of *GRM* expression levels. The dot plot beside each KM illustrates the subdivision of cohort (n=59) in two groups, which was based on the median expression of each gene analyzed. *Group blue* represents patients with low *GRM* expression (≤ median), *group red* indicates patients with high *GRM* expression (> median). Differences in survival rates were assessed with the log-rank test. P-values <0.05 were considered significant.

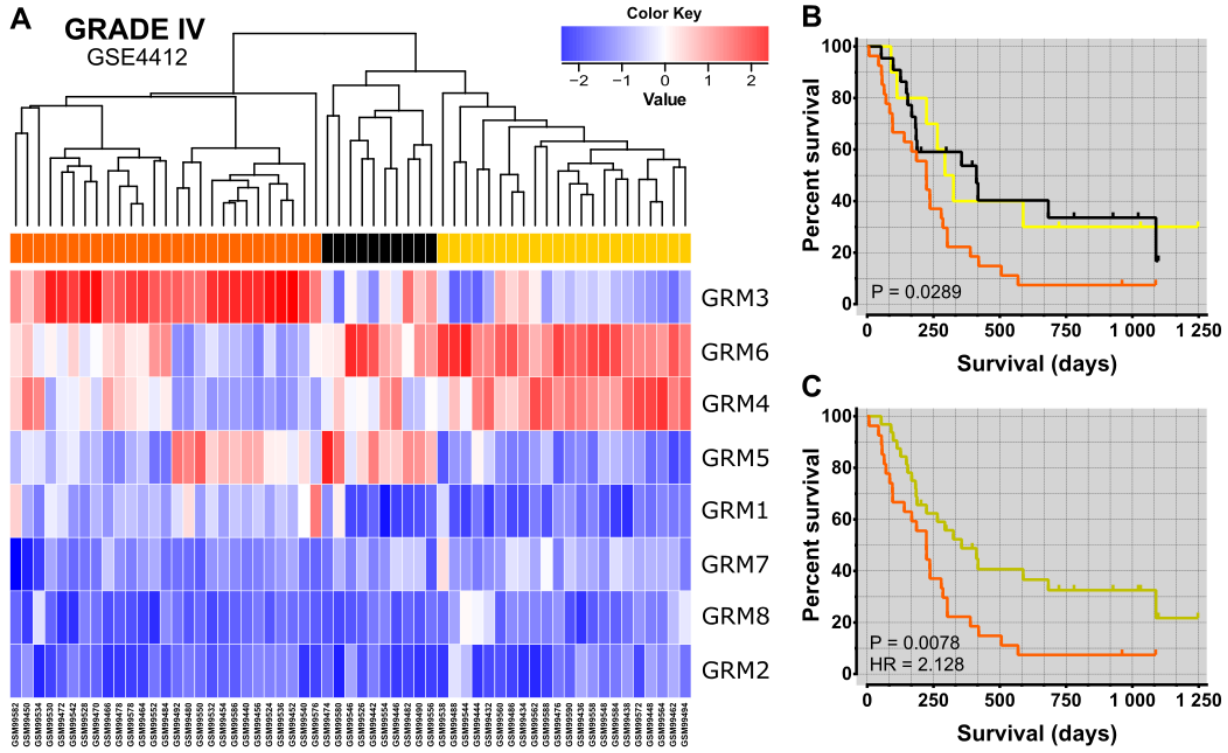

Figure 6 - Prognostic value of the concomitant gene expression of mGluR subtypes in grade IV (GBM) biopsies obtained from patients of validation cohort (GSE4412). (A) Unsupervised hierarchical clustering analysis of GBM samples is shown. This panel presents cohort data arranged according to gene expression profile of all eight mGluR subtypes (*GRM1-GRM8*). The color intensity is associated to the microarray gene expression signal (*red*, positive values; *blue*, negative values). (B) A Kaplan-Meier (KM) plot of the entire cohort data (n= 59) is shown, where patients were stratified according to hierarchical clustering analysis of the eight *GRM*. The orange color represents the patients whose GBM samples clearly show high expression of *GRM3* and low of *GRM4* and *GRM6*. The yellow group is represented by patients whose biopsies presented low levels of *GRM3* and high levels of *GRM4* and *6*. In black group, are patients whose tumor samples showed gene expression levels slightly different from those of the yellow group. (C) KM representation of cohort data, where patients of yellow and black groups were grouped into one, the dark yellow, due to the fact that GBM biopsies of both groups were characterized by a low expression of *GRM3* and high of *GRM 4* and *6*. Risk of death was 2.1 times greater in patients from orange group than from dark yellow group (HR = 2.128; SE=0.751; P = 0.0078). Differences in survival rates were assessed with log-rank test. P-values <0.05 were considered significant.

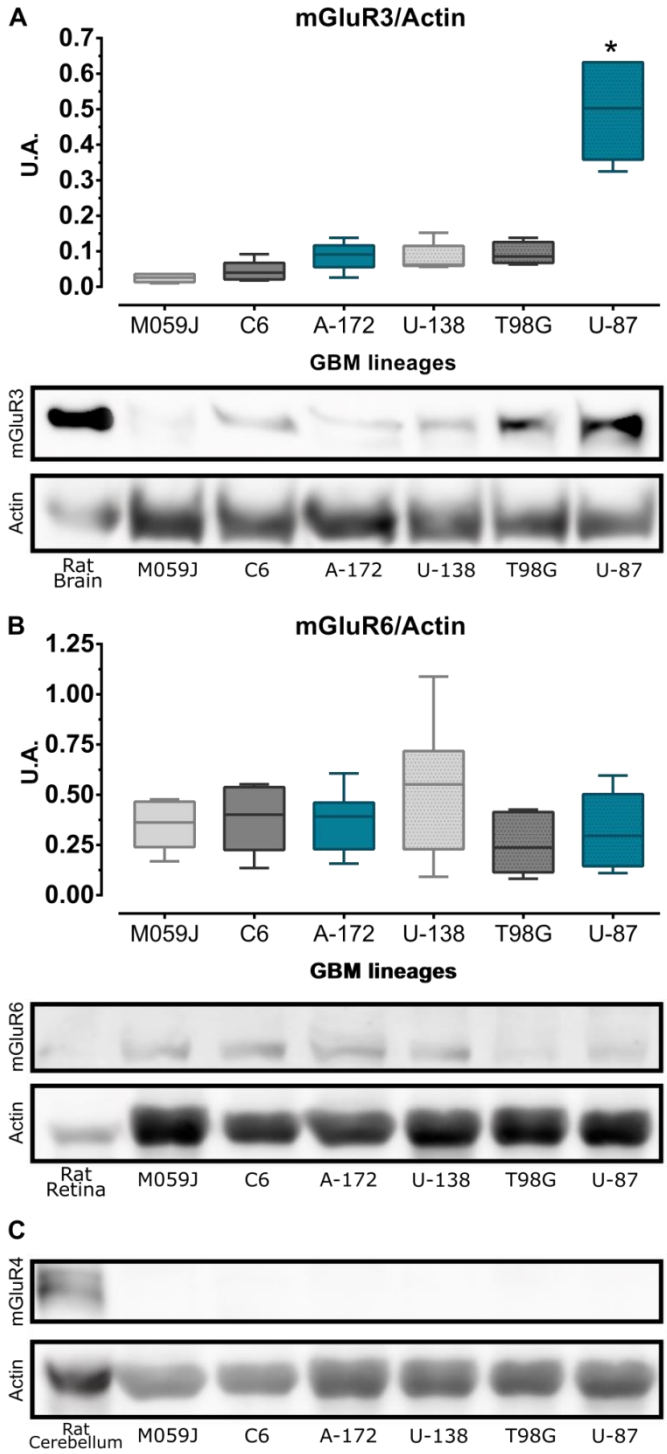

Figure 7 - mGluR 3, 4 and 6 immunocontent evaluated by western blot technique in six glioblastomas (GBM) cell lines. (A) U-87 lineage presented the highest level of mGluR3 protein expression. The other lines presented a similar immunocontent for this receptor. (B) All GBM lines analyzed presented a similar immunocontent for mGluR6. (C) None of GBM lineages showed protein expression for mGluR4. Samples of rat brain, rat retina and rat cerebellum were used as positive controls for mGluR3 (95 kDa), mGluR6 (190 kDa) and mGluR4 (102 kDa) proteins, respectively. β-actin (43 kDa) was used as constitutive protein. Data were plotted as median (25 % percentile; 75 % percentile) of six independent experiments. Kruskal-Wallis test was used, followed by *Dunn's* multiple comparison test. P-values <0.05 were considered significant.

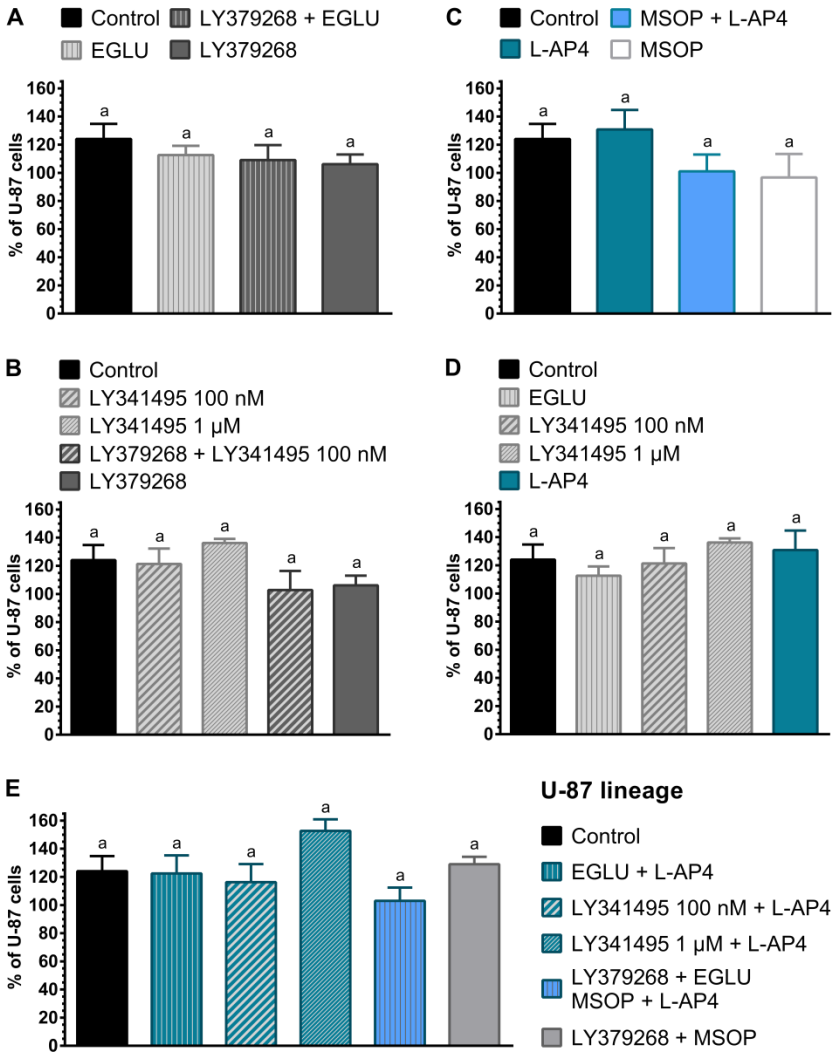

Figure 8 – Treatment of U-87 lineage with mGluR ligands for 72h in absence of FBS. Control group received only vehicle (deionized H_2O). mGluR ligands had no effect on percentage of U-87 cells. 100 µM EGLU (group II mGluR antagonist); 100 nM or 1 µM LY341495 (group II mGluR antagonist); 100 nM LY379268 (group II mGluR agonist); 100 µM MSOP (group III mGluR antagonist) and 100 µM L-AP4 (sgroup III mGluR agonist). The mean of 6 independent experiments carried out in triplicates was plotted and results were presented in percent (%) of remaining cells compared to control group (mean±SE). One way ANOVA test was used, followed by *Tukey* multiple comparison test. Distinct letters indicates statistical difference. P-values <0.05 were considered significant.

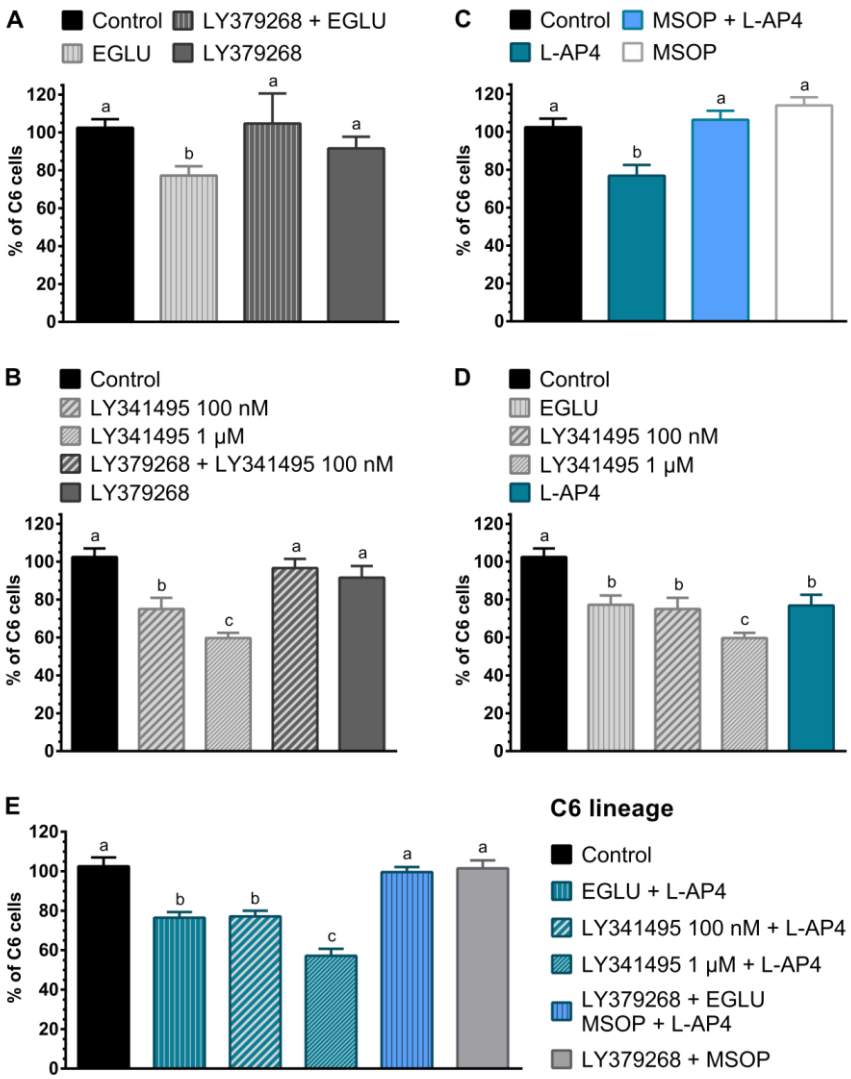

Figure 9 - Treatment of C6 lineage with mGluR ligands for 72h in absence of FBS. In relation to control group, (A) treatment with EGLU antagonist decreased percentage of C6 cells in 25.24%, (B) 100 nM LY341495 treatment decreased 27.45% of C6 cells, while higher concentration of this antagonist (1 µM) decreased in 42.78%. In (A) and (B), 30 min pre-treatment with LY379268 agonist, reversed this decrease and treatment alone with this agonist did not alter the percentage of C6 cells compared to control group. (C) Addition of L-AP4 agonist was able to decrease the amount of C6 cells in 25.65%, pre-treatment with MSOP for 30 min reversed this decrease and treatment only with MSOP did not change the percentage of C6 cells in relation to control group. (D) Comparison between treatments with EGLU and LY341495 antagonists and L-AP4 agonist. (E) Co-treatments of L-AP4 with EGLU, or 100 nM LY341495, or 1 µM LY341495 decreased percentage of cells by 26.08%, 25.42% and 45.35%, respectively. 30 min of pre-treatment with LY379268 together with MSOP reversed the decrease in percentage of C6 cells caused by treatment with L-AP4 plus EGLU. Co-treatment with LY379268 plus MSOP did not cause a decrease in number of C6 cells compared to control group. 100 µM EGLU (group II mGluR antagonist); 100 nM or 1 µM LY341495 (group II mGluR antagonist); 100 nM LY379268 (group II mGluR agonist); 100 µM MSOP (group III mGluR antagonist) and 100 µM L-AP4 (group III mGluR agonist). Control group received only vehicle (deionized H_2O). The mean of 6 independent experiments carried out in triplicates was plotted and results were presented in percent (%) of remaining cells compared to control group (mean±SE). One way ANOVA test was used, followed by *Tukey* multiple comparison test. Distinct letters indicates statistical difference. P-values <0.05 were considered significant.

SUPPLEMENTARY FIGURES

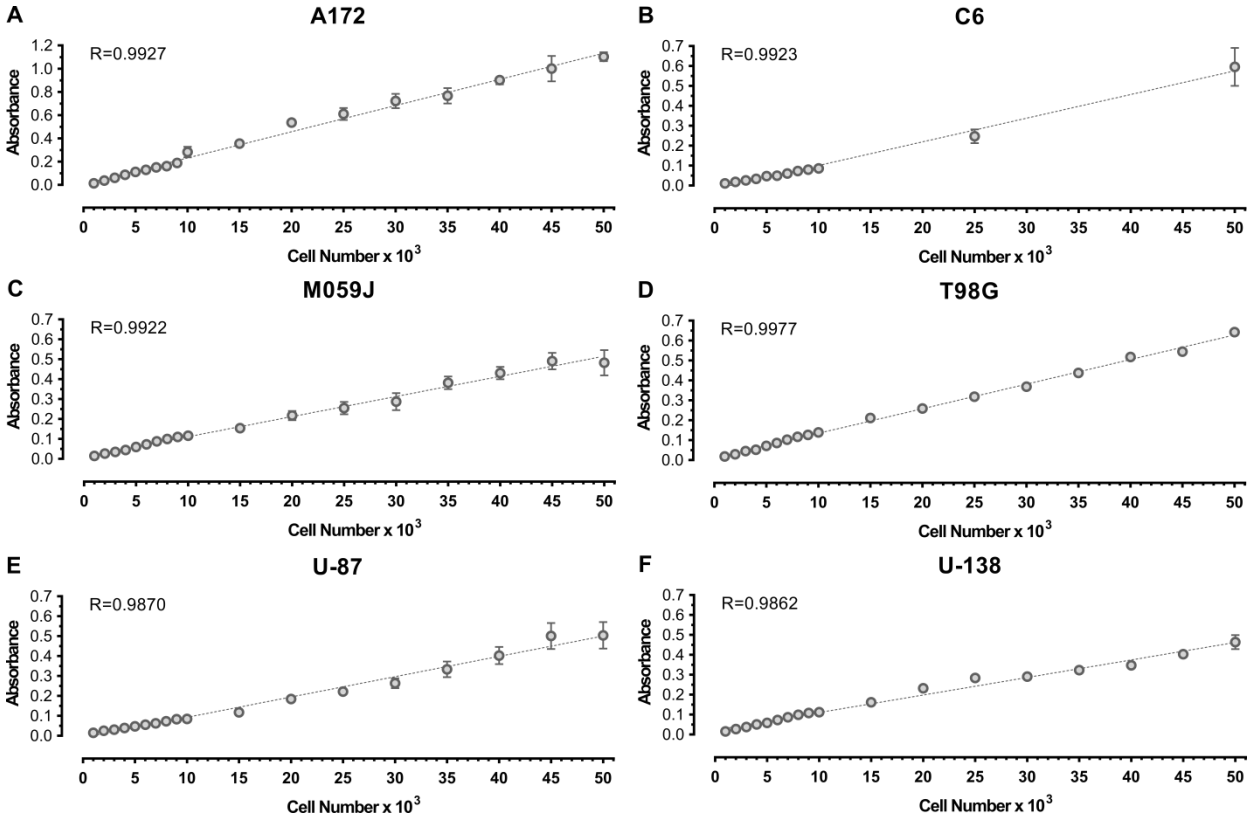

Supplementary Figure 1 – Graphical correlation between cell number and the corresponding SRB absorbance. To determine the number of cells per well, increasing amounts of each of glioblastoma lineages (C6 rat lineage and A-172, M059J, T98G, U-87 and U-138 human lineages) were seeded into 96-multiwell plates ($1x10^3$-$50x10^3$ cells/well) and after cell adhesion on plate (about 2 h after seeding) SRB staining was performed according to protocol described in material and methods. After, a graph showing on the x-axis the number of seeded cells and on y-axis the corresponding absorbance was plotted and the resulting equation of the line, calculated using GraphPad 6.0 software (Parameters: Linear regression), was used to determine cell density after *in vitro* assays used in this article. The mean of 3 independent experiments carried out in triplicates was plotted.

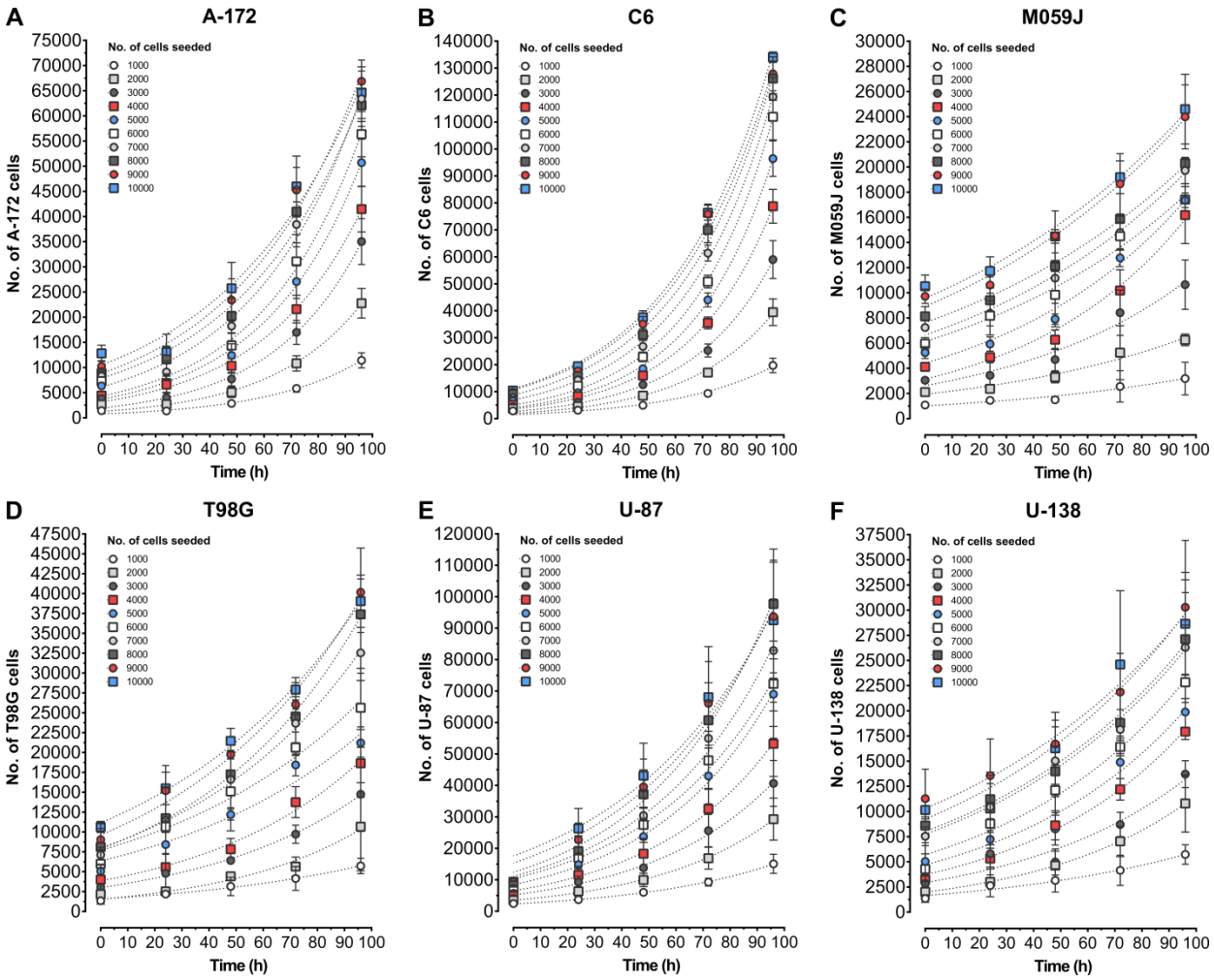

Supplementary Figure 2 – Growth curves of each of glioblastoma (GBM) lines. Cells were seeded in 96-multiwell plates in specific growing densities ($1x10^3$-$1x10^4$ cells/well) and cultured between 24-96 h. Analysis of growth curves of each GBM line (C6 rat lineage and A-172, M059J, T98G, U-87 and U-138 human lineages) using GraphPad 6.0 software (Curve fitting tool: Exponential growth curve) allowed the choice of the number of cells that would be seeded to be in exponential growth in each *in* vitro experiment performed in this article. The mean of 3 independent experiments performed in triplicates was plotted and results were expressed as number of GBM cells (mean±SE).

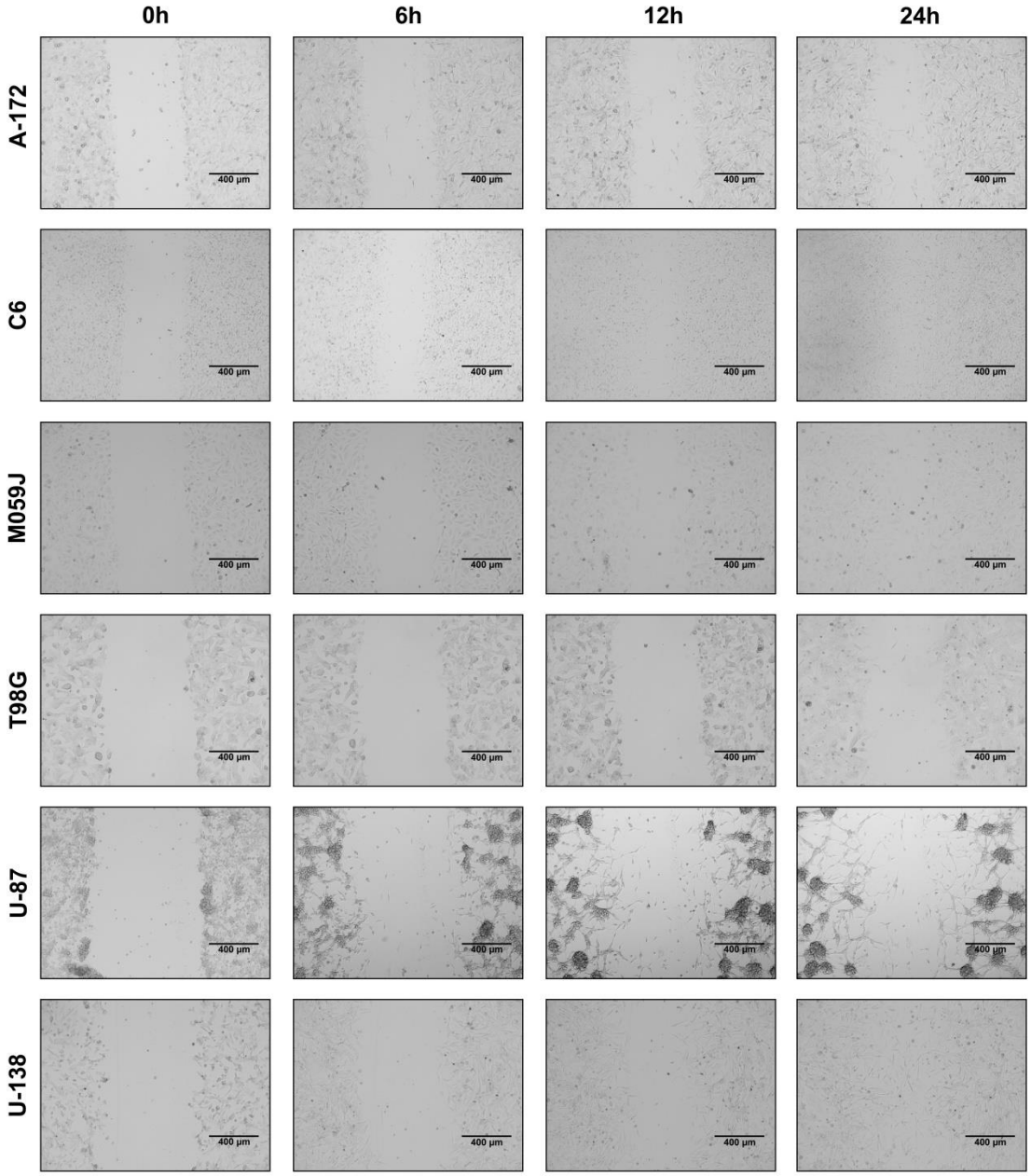

Supplementary Figure 3 - Migratory capacity of each glioblastoma. Cells were seeded in 24-multiwell plates (A-172, M059J and U-138 MG - $1x10^5$ cells/well; T98G - $1.5x10^5$ cells/well; C6 and U-87 MG - $4x10^5$ cells/well) and cultured for 24h. After, DMEM with FBS was replaced with Hank's balanced salt solution (HBSS – 137 mM NaCl, 0.6 mM Na_2HPO_4, 3 mM $NaHCO_3$, 20 mM Hepes sodium salt, 5 mM KCl, 0.4 mM KH_2PO_4, 1.26 mM $CaCl_2$, 0.9 mM $MgSO_4$ and 5.55 mM glucose - pH 7.4). After, one scratch was made in the middle of each well and cultures were washed with HBSS, which was replaced with fresh DMEM containing 1 % of FBS. Images were captured at 20X with a phase contrast inverted microscope at 0, 6, 24 and 48 h. C6, M059J and U-138 were the GBM lines with the highest migratory capacity, completing practically all gap after 48h. A-172 and T98G human lines were the ones with the lowest migratory capacity, occupying less than 30% of the gap. The migratory capacity of U-87 lineage was not possible to measure properly, because cells accumulated, forming spheroids. Each experiment was performed in triplicate and repeated three times. Distance travelled by cells of each GBM line into the gap up to 48h was qualitatively evaluated by scales of area retake and demonstrated in Table 9: + (0-30 %), ++ (31-70%) and +++ (71-100%).

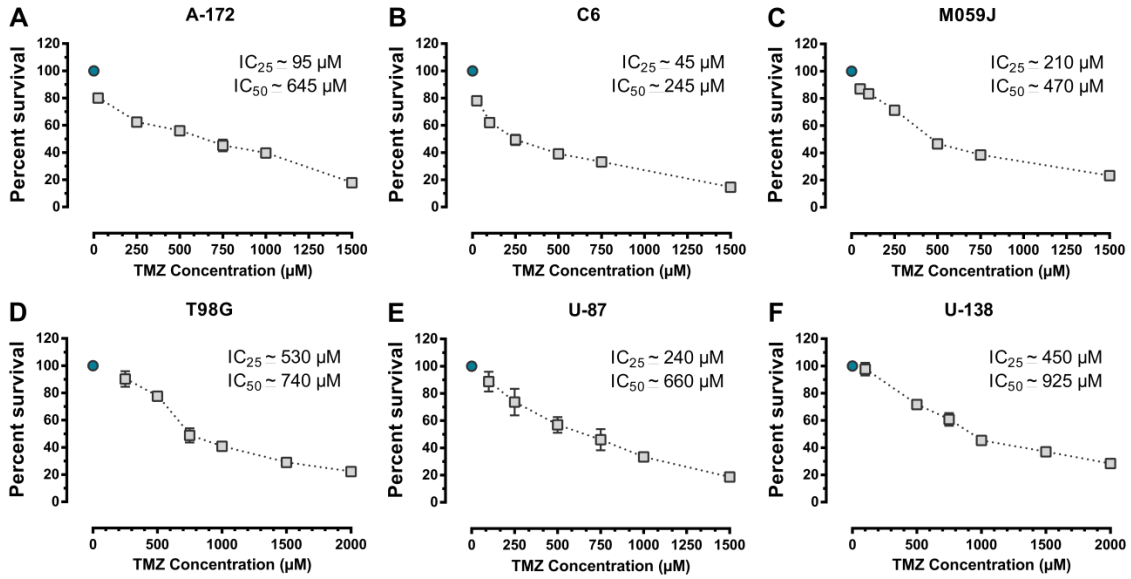

Supplementary Figure 4 – Evaluation of the cytotoxicity of chemotherapeutic agent temozolamide (TMZ) on each glioblastoma (GBM) lines. Cells were seeded ($8x10^3$ cells/well) in 96-multiwell plates and cultured for 72 h. Resistance of chemotherapy was determined based on drug dose-response curves of TMZ using SRB assay. The amount of GBM cells remaining in the well was calculated by the linear equation formed by cell density curve of each GBM line in relation to the absorbance of SRB (Supplementary Figure 1). IC_{25} and IC_{50} were calculated according to concentration-response curve of each lineage. The mean of 3 independent experiments performed in triplicates was plotted.

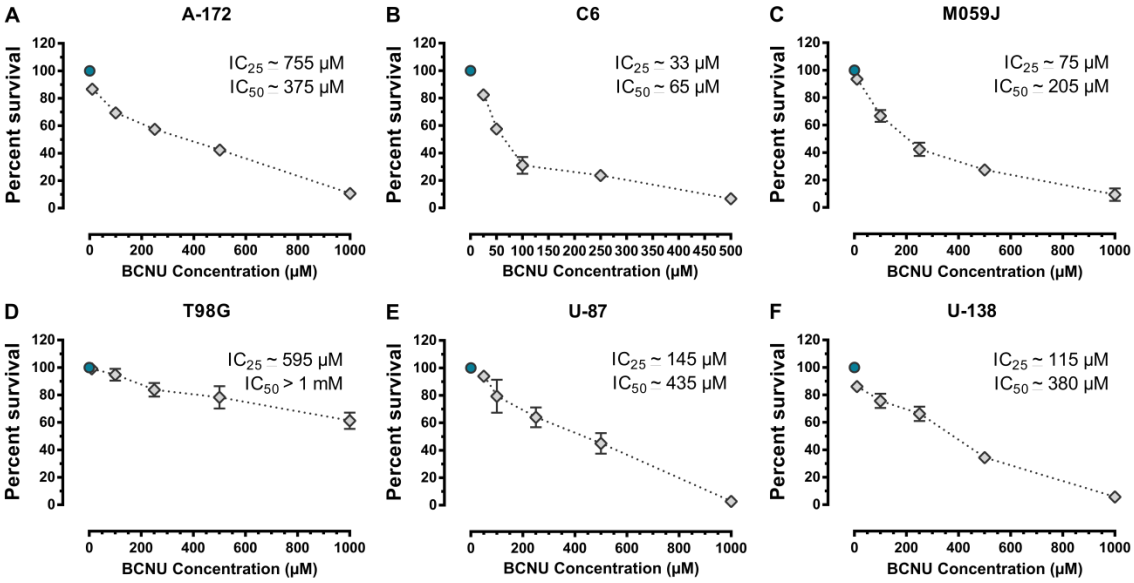

Supplementary Figure 5 – Evaluation of the cytotoxicity of chemotherapeutic agent carmustine (BCNU) on each glioblastoma (GBM) lines. Cells were seeded ($8x10^3$ cells/well) in 96-multiwell plates and cultured for 72 h. Resistance of chemotherapy was determined based on drug dose-response curves of BCNU using SRB assay. The amount of GBM cells remaining in the well was calculated by the linear equation formed by cell density curve of each GBM line in relation to the absorbance of SRB (Supplementary Figure 1). IC_{25} and IC_{50} were calculated according to concentration-response curve of each lineage. The mean of 3 independent experiments performed in triplicates was plotted.

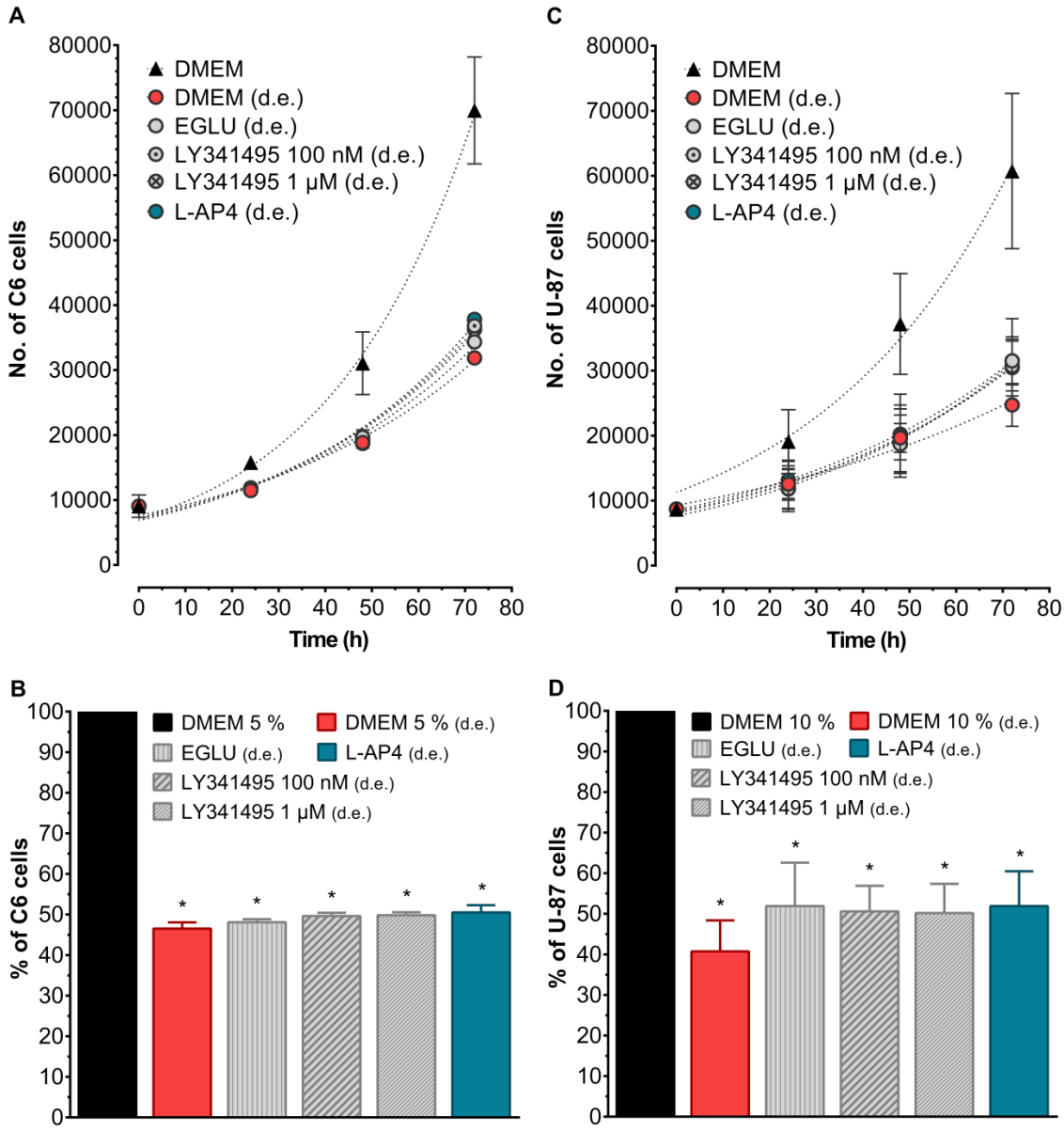

Supplementary Figure 6 – Daily addition of mGluR ligands in C6 and U-87 lineages for 72h in presence of FBS. Culture medium (DMEM supplemented with 5 % or 10 % FBS, for C6 and U-87 cultivation, respectively) containing treatments was renewed every day. In (A) and (C), daily exchange (d.e.) of culture medium (red bars) affected the proliferative rate of both C6 (DT=35 h) and U-87 (DT= 50 h) lineages, when compared to control group (DMEM not changed daily - black bars) (C6 DT=22 h; U-87 DT=29 h). Doubling time (DT) was calculated using GraphPad 6.0 software (Curve fitting tool: Exponential growth curve) and results were expressed as number of glioblastomas cells (mean±SE; n=3 performed in triplicate). (B) Daily treatment did not significantly alter the percentage of C6 cells in well after 72h, when compared to control group (DMEM d.e.). (D) In relation to control group (DMEM d.e.), daily treatment of U-87 cultures with mGluR ligands also did not significantly alter the percentage of cells in well after 72h. In (B) and (D), results were presented in percent (%) of remaining cells compared to control group (mean±SE; n=3 performed in triplicate). One way ANOVA test was used, followed by *Tukey* multiple comparison test. Distinct letters indicates statistical difference. P-values <0.05 were considered significant. 100 µM EGLU (group II mGluR antagonist); 100 nM or 1 µM LY341495 (group II mGluR antagonist); and 100 µM L-AP4 (group III mGluR agonist).

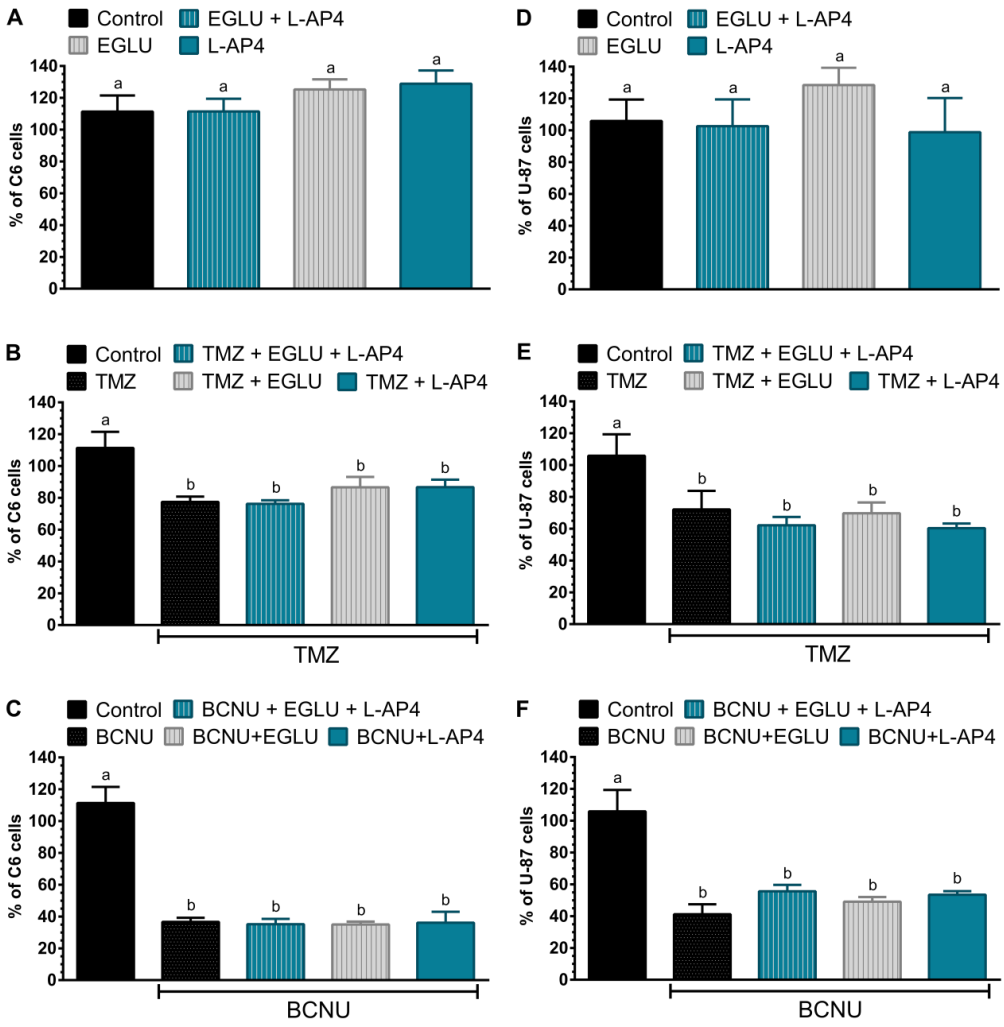

Supplementary Figure 7 – Treatment of C6 and U-87 lineages with mGluR ligands and chemotherapeutic agents for 72h in presence of FBS. Cells were treated (30 min) with ligands at double concentration of DMEM in absence of FBS (100 µL). After, 100 uL of DMEM containing twice concentration of FBS required for culture of each GBM line was added. Thus, up to 72 h in culture, without exchange, both lineages remained with the expected concentration of each ligand under suitable proliferating conditions (5 % FBS, for C6 line; 10 % FBS, for U-87 line). Neither combined treatment of EGLU with L-APA nor treatment with these ligands separately resulted in a significant change in percentage of C6 cells (A) and U-87 cells (D). In C6 lineage (B and C), addition of TMZ or BCNU (IC_{25} double), 30 min before addition of DMEM containing FBS, decreased amount of cells after 72 h of culturing in 33.96 % (77.41±1.94) and in 74.78 % (36.60±1.50), respectively, when compared to control group (111,40±10.08). In U-87 line, using the same protocol, (E) TMZ treatment decreased amount of cells in 33.70 % (72.12±6.72) and (F) BCNU treatment decreased in 64.67 % (41.16±3.62) when compared to control group (105.80±13.55). Treatment of ligands together with chemotherapeutics had no additive effect on percentage of C6 and U-87 cells that remained in culture (B, C, E and F). mGluR ligands final concentrations: 100 µM EGLU (group II mGluR antagonist) and 100 µM L-AP4 (group III mGluR agonist). Control group received only vehicle (deionized H_2O in A and D; DMSO 0.05 % in B, C, E, and F). The mean of 3 independent experiments performed in triplicates was plotted and results were presented in percent (%) of remaining cells compared to control group (mean±SE). One way ANOVA test was used, followed by *Tukey* multiple comparison test. Distinct letters indicates statistical difference. P-values <0.05 were considered significant.

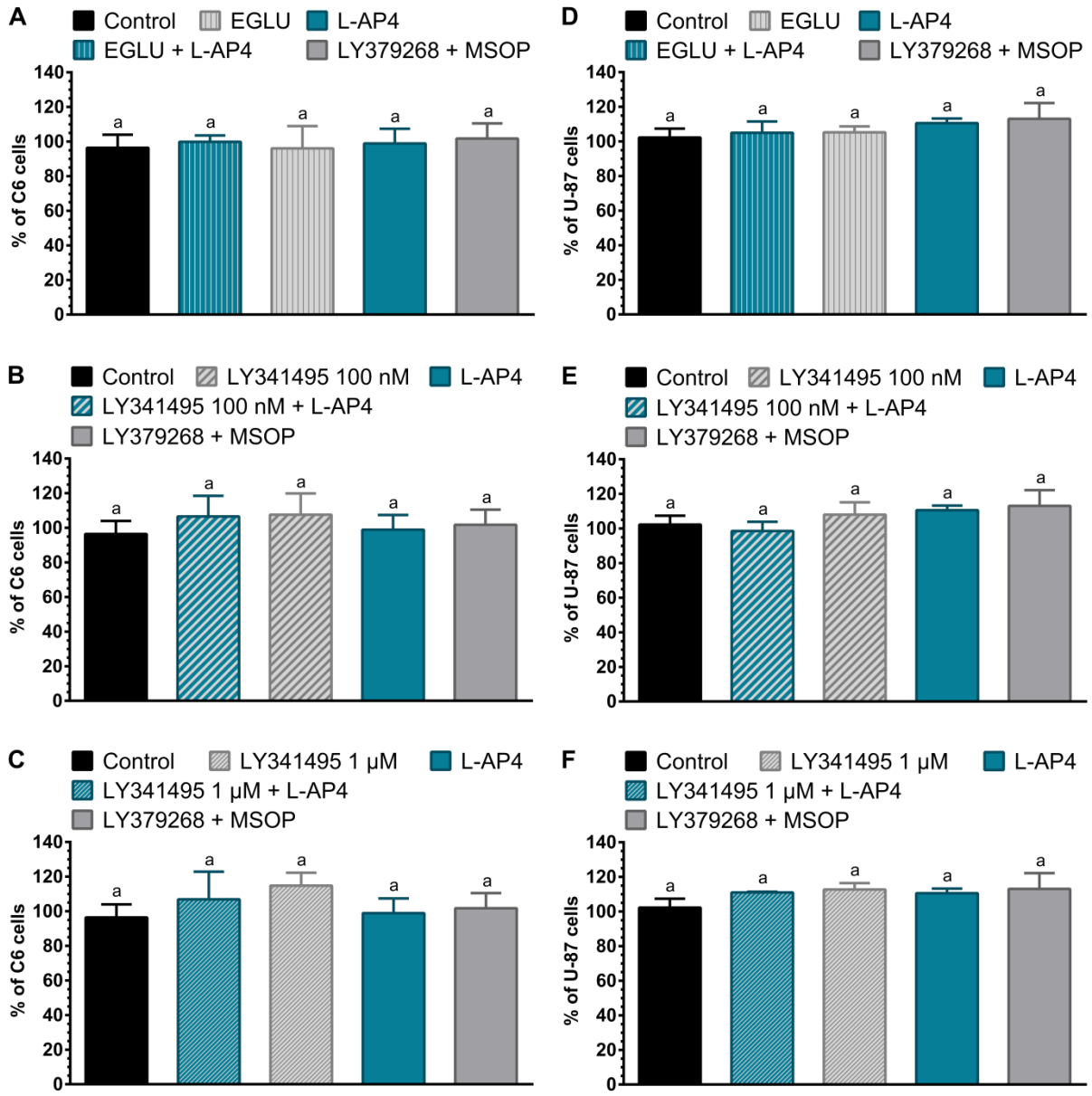

Supplementary Figure 8 – Treatment of C6 and U-87 lineages with mGluR ligands for 72h in presence of FBS. Cells were treated for 30 min with mGluR ligands in DMEM not containing FBS. After, the aliquot needed to maintain the appropriate final concentration of FBS for each lineage was added (5 % FBS, for C6 line; 10 % FBS, for U-87 line). After 72h of culture, neither treatment alone with each mGluR ligand, nor combined treatment among them caused a significant change in percentage of C6 cells (A-C) and U-87 cells (D-F). mGluR ligands final concentrations: 100 µM EGLU (group II mGluR antagonist); 100 nM or 1 µM LY341495 (group II mGluR antagonist); 100 nM LY379268 (group II mGluR agonist); 100 µM MSOP (group III mGluR antagonist) and 100 µM L-AP4 (group III mGluR agonist). Control group received only vehicle (deionized H_2O). The mean of 3 independent experiments performed in triplicates was plotted and results were presented in percent (%) of remaining cells compared to control group (mean±SE). One way ANOVA test was used, followed by *Tukey* multiple comparison test. Distinct letters indicates statistical difference. P-values <0.05 were considered significant.

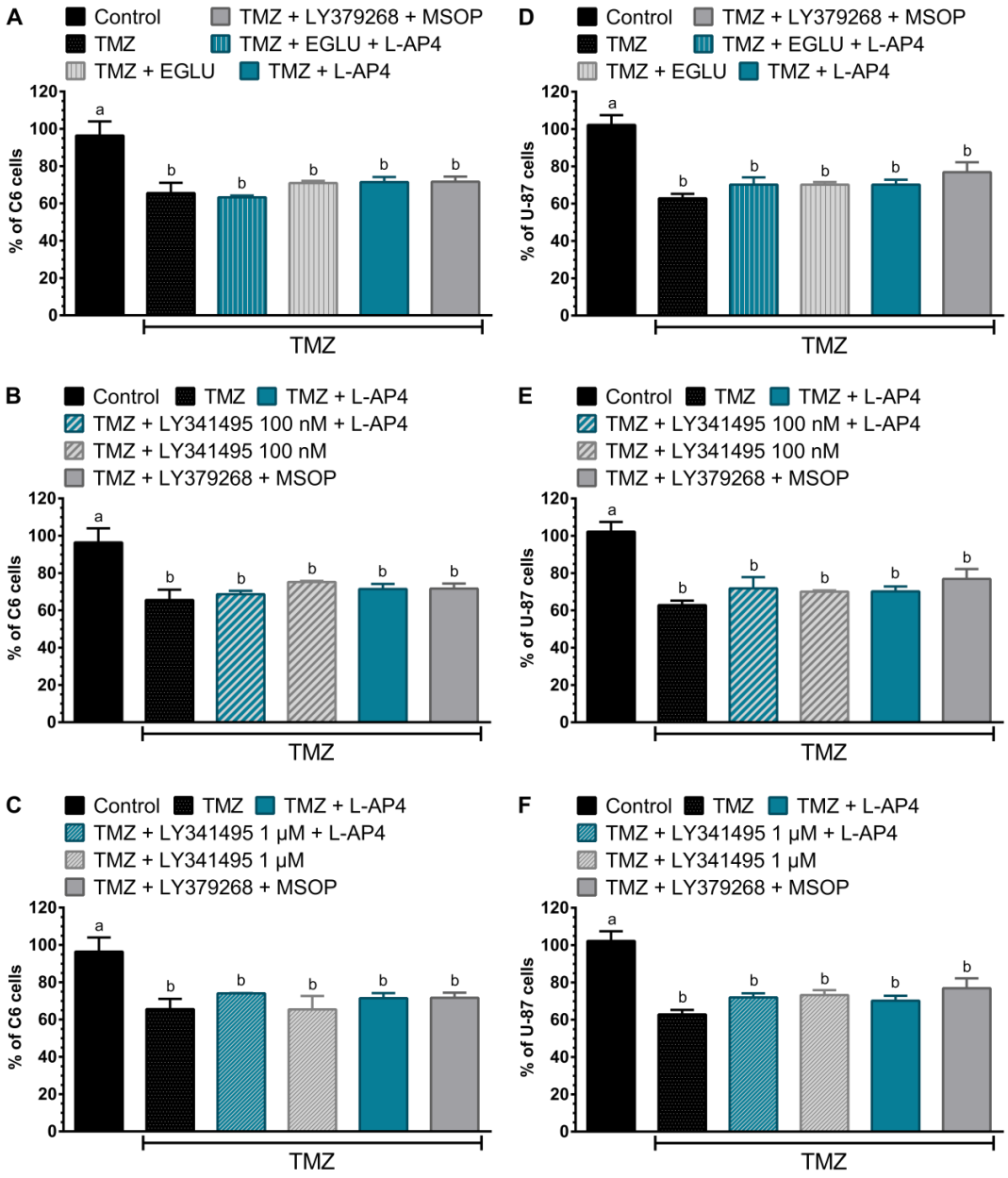

Supplementary Figure 9 – Treatment of C6 and U-87 lineages with mGluR ligands and TMZ for 72h in presence of FBS. Cells were treated for 30 min with mGluR ligands in DMEM not containing FBS. After, the aliquot needed to maintain the appropriate final concentration of FBS for each lineage was added (5 % FBS, for C6 line; 10 % FBS, for U-87 line). (A-C) C6 cultivation in presence of TMZ (IC_{25}) resulted in a decrease of 30.84 % (65.57±3.19) after 72 h of culture when compared to control group (96.41±7.56). (D-F) In U-87 lineage, TMZ (IC_{25}) treatment reduced cells in 39.42 % (62.83±1.41) in relation to control group (102.3±5.19). Addition of mGluR ligands to these conditions in both GBM cultures did not cause additive effect. mGluR ligands final concentrations: 100 µM EGLU (group II mGluR antagonist); 100 nM or 1 µM LY341495 (group II mGluR antagonist); 100 nM LY379268 (group II mGluR agonist); 100 µM MSOP (group III mGluR antagonist) and 100 µM L-AP4 (group III mGluR agonist). Control group received only vehicle (DMSO 0.05 %). The mean of 3 independent experiments performed in triplicates was plotted and results were presented in percent (%) of remaining cells compared to control group (mean±SE). One way ANOVA test was used, followed by *Tukey* multiple comparison test. Distinct letters indicates statistical difference. P-values <0.05 were considered significant.

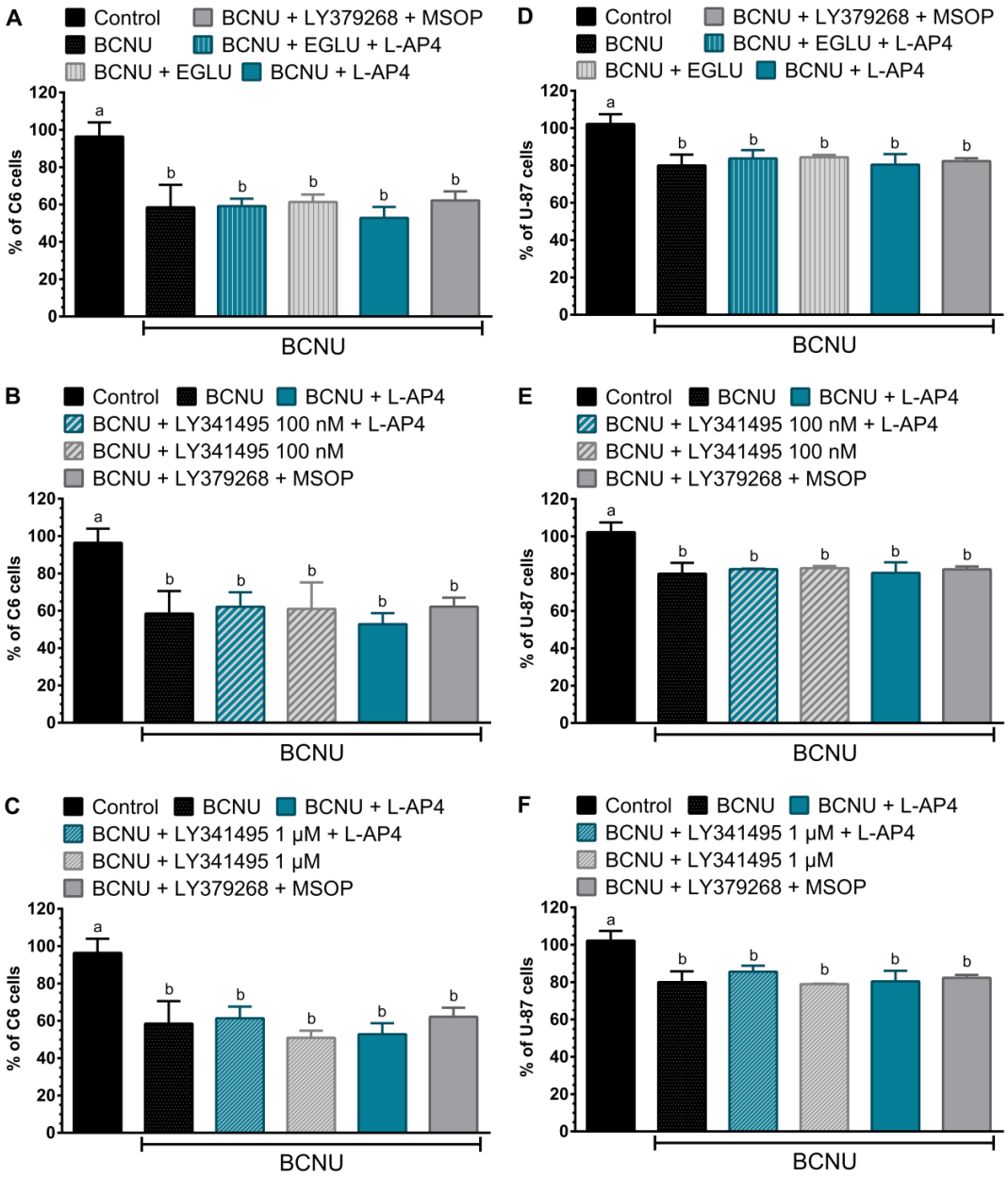

Supplementary Figure 10– Treatment of C6 and U-87 lineages with mGluR ligands and BCNU for 72h in presence of FBS. Cells were treated for 30 min with mGluR ligands in DMEM not containing FBS. After, the aliquot needed to maintain the appropriate final concentration of FBS for each lineage was added (5 % FBS, for C6 line; 10 % FBS, for U-87 line). (A-C) In relation to control group (96.41±7.56), BCNU (IC_{25}) treatment decreased percentage of C6 cells in 37 % (58.47±6.05) after 72 h of culture. In U-87 lineage (E and F), BCNU (IC_{25}) treatment reduced cells in 22.25 % (80.00±3.35), respectively, in relation to control group (102.3±5.19).). Addition of mGluR ligands to these conditions in both GBM cultures did not cause additive effect. mGluR ligands final concentrations: 100 µM EGLU (group II mGluR antagonist); 100 nM or 1 µM LY341495 (group II mGluR antagonist); 100 nM LY379268 (group II mGluR agonist); 100 µM MSOP (group III mGluR antagonist) and 100 µM L-AP4 (group III mGluR agonist). Control group received only vehicle (DMSO 0.05 %). The mean of 3 independent experiments performed in triplicates was plotted and results were presented in percent (%) of remaining cells compared to control group (mean±SE). One way ANOVA test was used, followed by *Tukey* multiple comparison test. Distinct letters indicates statistical difference. P-values <0.05 were considered significant.

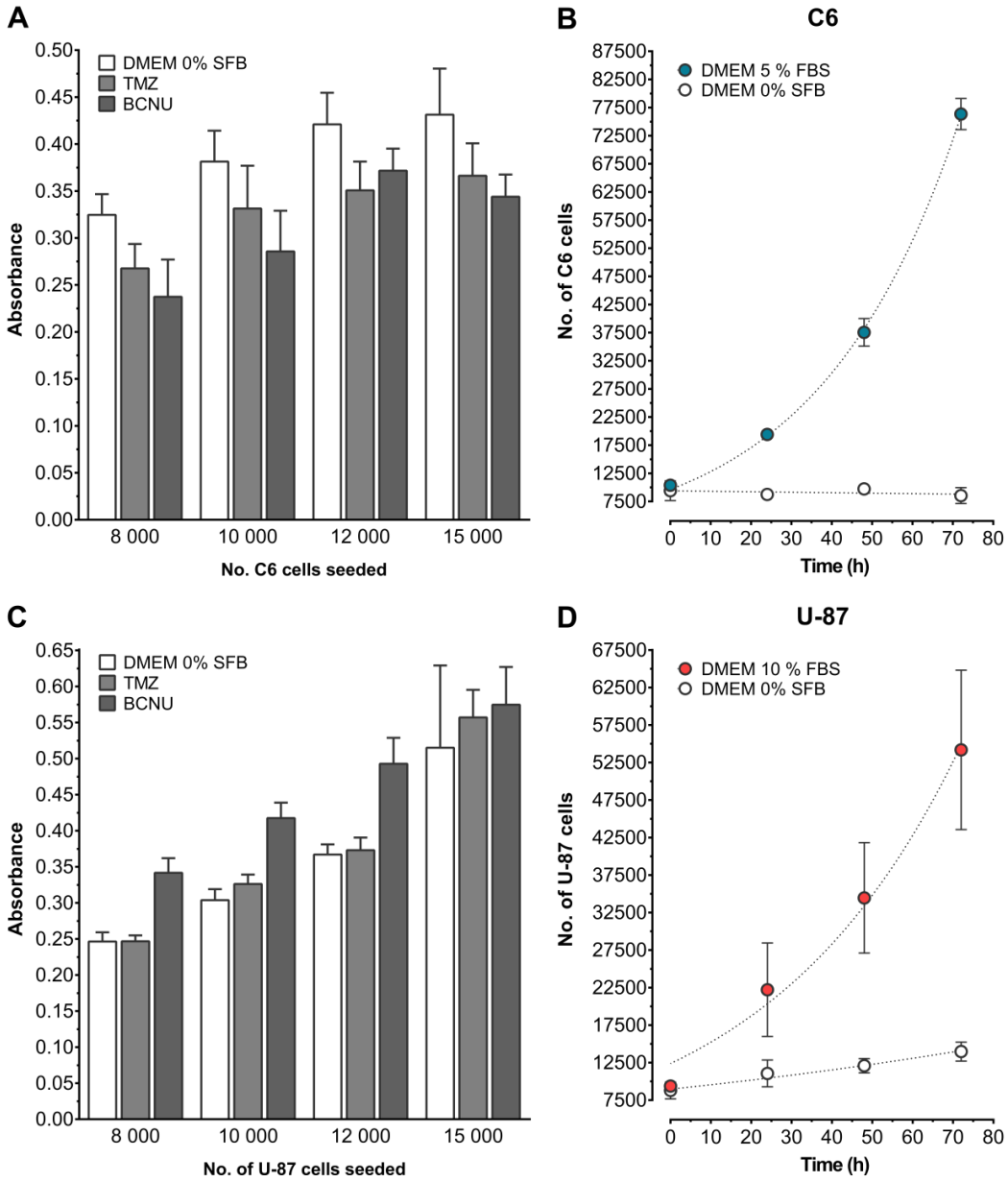

Supplementary Figure 11– C6 and U-87 glioma lines cultured for up to 72 h in culture medium without FBS. C6 (A) and U-87 (C) lineages were seeded in 96-multiwell plates in specific growing densities ($8x10^3$-$15x10^3$ cells/well) and cultured for 72h in absence of FBS with or without chemotherapeutic agents (IC_{25} of TMZ or BCNU). Analysis of absorbance (mean±SE; n=3 performed in triplicate) of each lineage after 72h allowed the choice of the number of cells that would be seeded for *in vitro* assays performed in non-proliferating conditions. Treatment of C6 and U-87 lines with TMZ and BCNU under non-proliferating conditions of culture did not follow the expected pattern for these GBM cells under proliferating conditions. (B) In this culture condition, the proliferative rate of C6 cells($1x10^4$ cells/well) was null compared to C6 cells cultured in DMEM containing 5 % of FBS (proliferating condition) (DT=24.13 h). (D) The proliferative rate of U-87 cells ($1x10^4$ cells/well) cultured without FBS was very low (DT=110.2 h) when compared to U-87 cells cultured in DMEM containing 10 % of FBS (proliferating condition) (DT=33.54 h). Doubling time (DT) was calculated using GraphPad 6.0 software (Curve fitting tool: Exponential growth curve). The mean of 3 independent experiments performed in triplicates was plotted and results were expressed as number of GBM cells (mean±SE).

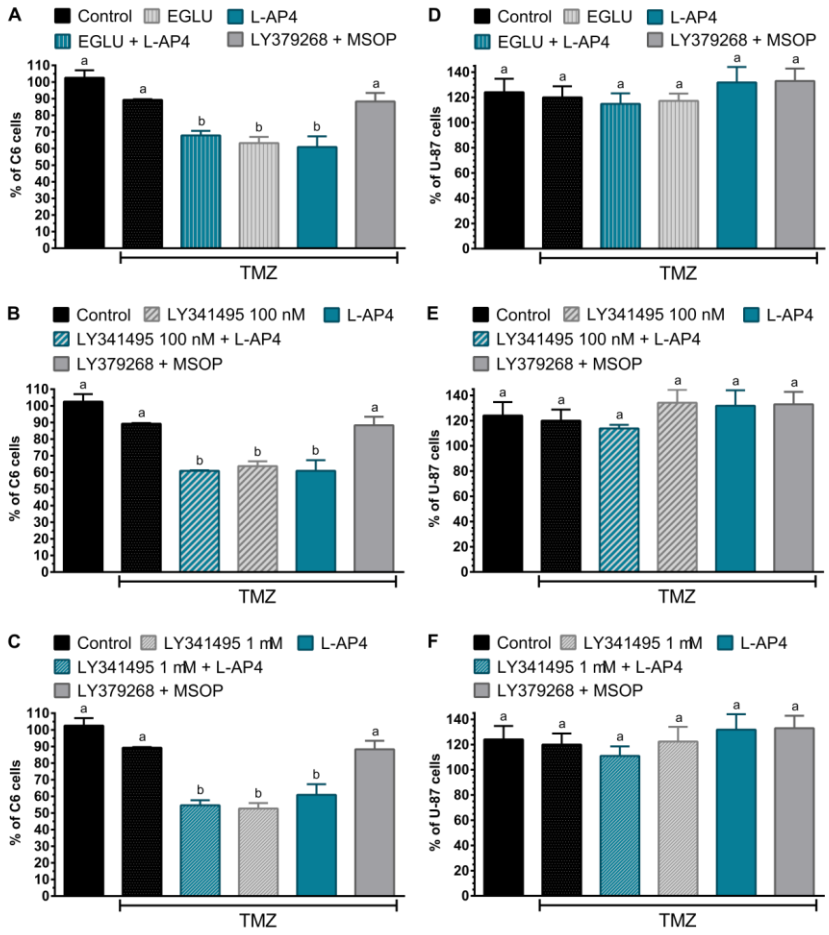

Supplementary Figure 12 – Treatment of C6 and U-87 lineages with mGluR ligands and TMZ for 72h in absence of FBS. (A-C) C6 under non-proliferating conditions of culture in presence of TMZ (IC_{25}) did not follow the expected pattern for these GBM cells under proliferating conditions, because did not present a statistical decrease in number of cells in relation to control group. However, the effect of mGluR ligands treatment on C6 lineage was maintained in presence of TMZ. Treatment with EGLU, LY341495 (100 nM), and L-AP4 alone decreased percentage of cells after 72 h in 26 % (63.27±3.69), 25.50 % (63.77±2.90), and 28.33 % (60.93±6.37), respectively, in relation to TMZ-only group (89.27±0.23). Combination of EGLU with L-AP4 or LY341595 (100 nM) with L-AP4 decreased percentage of cells in 21.40 % (68.87±2.75) and 28.37 % (60.09±0.35), respectively, in relation to TMZ group. Treatment with 1 µM of LY341495 had the ability to decrease the number C6 cells in 36.60 % (52.67±3.33) when compared to TMZ treated group. And its co-treatment with L-AP4 reduced cell percentage in 34.63 % (54.63±3.02). Co-treatment of C6 cells with LY379268 and MSOP did not alter the percentage of cells. (D-F) In U-87 lineage, TMZ (IC_{25}) treatment under non-proliferating conditions of culture also did not follow the expected pattern for these GBM cells under proliferating conditions, because did not present a decrease in number of cells in relation to control group. Treatment with TMZ in absence of FBS did not potentiate the effect of mGluR ligands on U-87 lineage. mGluR ligands final concentrations: 100 µM EGLU (group II mGluR antagonist); 100 nM or 1 µM LY341495 (group II mGluR antagonist); 100 nM LY379268 (group II mGluR agonist); 100 µM MSOP (group III mGluR antagonist) and 100 µM L-AP4 (group III mGluR agonist). Control group received only vehicle (DMSO 0.05 %). The mean of 3 independent experiments performed in triplicates was plotted and results were presented in percent (%) of remaining cells compared to control group (mean±SE). One way ANOVA test was used, followed by *Tukey* multiple comparison test. Distinct letters indicates statistical difference. P-values <0.05 were considered significant.

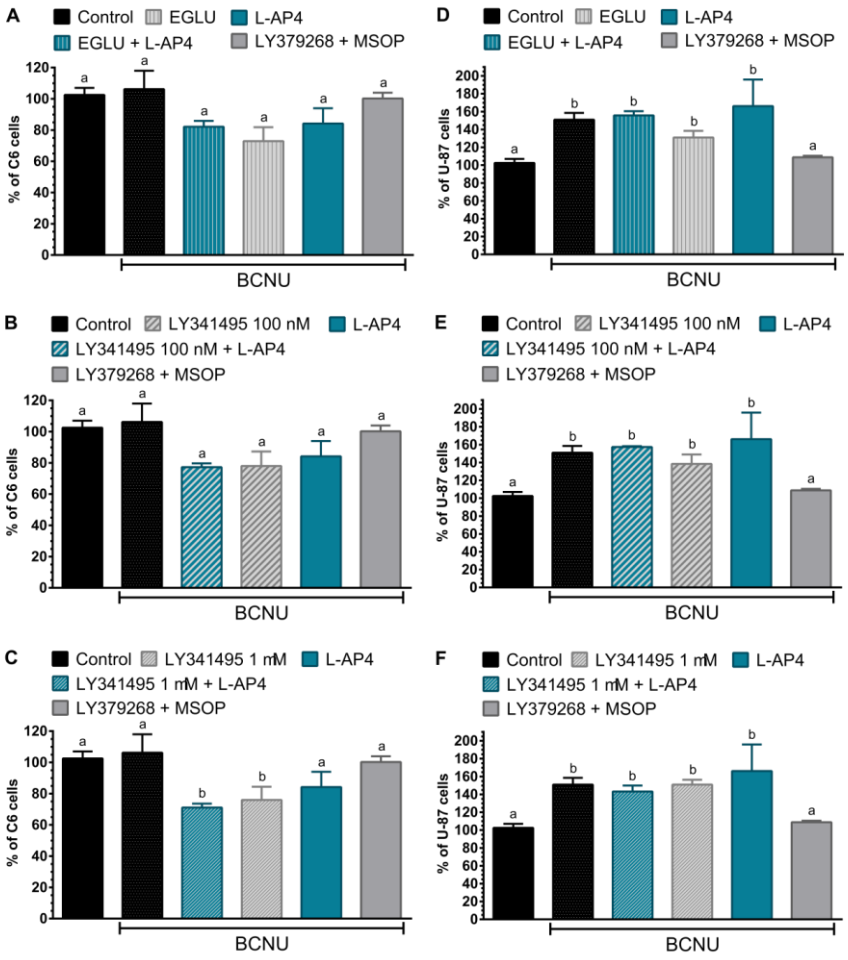

Supplementary Figure 13 – Treatment of C6 and U-87 lineages with mGluR ligands and BCNU for 72h in absence of FBS. (A-C) C6 under non-proliferating conditions of culture in presence of BCNU (IC_{25}) did not follow the expected pattern for these GBM cells under proliferating conditions, because did not present a decrease in number of cells in relation to control group. However, the effect of mGluR ligands treatment on C6 lineage was apparently maintained in presence of BCNU. Although there was no statistically significant decrease in relation to BCNU group, treatment with EGLU and LY341495 (100 nM) decreased percentage of C6 cells in about 30% and treatment with L-AP4 reduced the percentage by 22%. Co-treatment with L-AP4 in combination with EGLU or LY341495 (100 nM) reduced percentage of C6 cells in about 25% and 30%, respectively. In presence of BCNU, occurred 30.23 % of significant decrease in cell number in treatments with 1 µM LY341495 alone (75.97±8.42) and 35.10 % in combination with L-AP4 (71.10±2.48), when compared to group treated only with BCNU (106.2+6.82). (D-F) In U-87 lineage, BCNU (IC_{25}) treatment under non-proliferating conditions of culture also did not follow the expected pattern for these GBM cells under proliferating conditions, because increased the number of cells in relation to control group. Treatment with BCNU in absence of FBS did not potentiate the effect of mGluR ligands on U-87 lineage. mGluR ligands final concentrations: 100 µM EGLU (group II mGluR antagonist); 100 nM or 1 µM LY341495 (group II mGluR antagonist); 100 nM LY379268 (group II mGluR agonist); 100 µM MSOP (group III mGluR antagonist) and 100 µM L-AP4 (group III mGluR agonist). Control group received only vehicle (DMSO 0.05 %). The mean of 3 independent experiments performed in triplicates was plotted and results were presented in percent (%) of remaining cells compared to control group (mean±SE). One way ANOVA test was used, followed by *Tukey* multiple comparison test. Distinct letters indicates statistical difference. P-values <0.05 were considered significant.

CAPÍTULO III

Artigo em preparação para publicação

Rat cerebrospinal fluid treatment method through cisterna cerebellomedullaris injection.

Revista: JoVE (Journal of visualized experiments)

Qualis-CAPES-CBII: B4

Fator de Impacto: 1.1

Justificativa: Na neurobiologia, devido ao fato de muitos fármacos não ultrapassarem a barreira hemato-encefálica, uma das alternativa para testá-los em modelos *in vivo* é através da sua liberação direta no sistema nervoso central (SNC). Em geral, os protocolos de injeção crônica de fármacos diretamente no SNC envolvem procedimentos cirúrgicos para implantação de cânulas de tratamento. Dependendo do modelo *in vivo* usado, mais um procedimento cirúrgico para o tratamento poderia causar um sofrimento adicional ao animal.

Objetivo geral: Neste trabalho está descrito um protocolo de injeção intracisternal (na cisterna cerebelo-medular, também conhecida como cisterna magna) que não necessita de procedimento cirúrgico para sua execução, sendo um protocolo bem menos invasivo em relação aos demais tipos de injeções diretas no SNC. O protocolo descrito neste trabalho foi uma adaptação da técnica de punção de líquor nessa cisterna.

Objetivo específico: Demonstrar o passo-a-passo da técnica adaptada em nosso laboratório em vídeo.

TITLE:

Rat cerebrospinal fluid treatment method through cisterna cerebellomedullaris injection.

AUTHORS & AFFILIATIONS:

Mery S L Pereira [1*], Thainá G dos Santos[1], Diogo L de Oliveira [1*]

1 *Laboratory of Cellular Neurochemistry, Department of Biochemistry, Instituto de Ciências Básicas da Saúde, Universidade Federal do Rio Grande do Sul, Porto Alegre, Brazil.*

*Corresponding Author: Mery Stefani Leivas Pereira or Diogo Losch de Oliveira

Email Addresses: meryslpereira@gmail.com or losch@ufrgs.br

Tel: +55 51 33085556

KEYWORDS:

neurobiology, neuroscience, drug administration, intracisternal injection, cisterna magna, CSF treatment, central nervous system, surgical techniques, rodents

SHORT ABSTRACT:

In this work, we described a less invasive method of drug administration directly in rats' central nervous system through cisterna cerebellomedullaris injection. This methodology was specifically focused on delivery of glutamatergic receptor ligands directly into rat cerebrospinal fluid. This technique is suitable of adaptation for others drug classes and animal species.

LONG ABSTRACT:

Certain drugs lack the ability to cross blood-brain barrier and thus need to be placed directly into central nervous system (CNS). For this reason, for treatment of tumors that affect CNS, some chemotherapeutic or adjuvant therapies are applied directly into the brain after craniotomy to remove these tumors. Our laboratory studies the involvement of glutamatergic metabotropic receptors (mGluR) on glioma aggressiveness. For *in vivo* experiments, treatment of glioma-implanted rats was performed by a technique that delivers mGluR ligands directly into the cerebrospinal fluid (CSF) of rats by reverse puncture in cisterna cerebellomedullaris (also known as cisterna magna in humans). Animals were individually anesthetized fixed in a stereotatic rodent structure for head attachment. The heads were gently tilted downwards at an angle that allows better exposure of the cavity in which the magna cistern is located. A freehand injection was done in this cistern using a gingival needle coupled to a Hamilton syringe delivering 3 µL of the mGluR ligands directly into CSF. Immediately before infusion of treatments, a CSF puncture test was performed to verify if the needle reached the right spot. This type of injection can be adaptable for direct treatment of CNS of any rodent animal model using small volumes of a variety of other drugs.

INTRODUCTION:

The brain protects itself from pathogens and toxins derived from blood by severely restricting the transport of cells, particles and most hydrophilic molecules across the vascular endothelium of blood vessels in the brain. This protective mechanism is known as blood-brain barrier (BBB) [1]. Some drugs are unable to cross BBB, requiring direct Central Nervous System (CNS) delivery. To circumvent the BBB, these drugs can be delivered directly into the cerebrospinal fluid (CSF). CSF is initially derived from blood serum that has been filtered across the BBB and improved by choroid plexus, whose formations are found in each ventricle. Therefore CSF is generated in ventricles and flows unidirectionally from lateral ventricles through the 3rd ventricle into the 4th ventricle which empties into cisterna cerebellomedullaris (also known as cisterna magna in humans) where it is distributed over the outer surface of brain (subarachnoid space). From there, CSF is reintegrated into venous blood through the arachnoid villi or arachnoid granulations [2].

Metabotropic glutamate receptors (mGluR) are G-protein-coupled receptors that participate in modulation of synaptic transmission and neuronal excitability. mGluRs are classified in three groups based on sequence homology, G-protein coupling, and ligand selectivity: group I (mGluRs 1 and 5), group II (mGluRs 2 and 3), and group III (mGluRs, 4, 6, 7, and 8) [3]. Several *in vitro* and *in vivo* studies using mGluR ligands demonstrated the involvement of these receptors in progression, aggressiveness, and recurrence of a highly malignant type of CNS tumor, glioblastoma (GBM) [4-6]. Our laboratory, through an *in silico* meta-analysis study using cohorts of patients, observed a strong correlation among gene expression of mGluR3, 4 and 6 and the mean survival of patients with GBM. Patients whose GBM resections presented high mGluR3 gene expression concomitantly with low gene expression for mGluR4 and 6 had approximately 1.5 times higher chance of death compared to patients whose biopsies had low mGluR3 and high mGluR4 and 6 gene expression.

Pharmacological action of group II and III ligands was evaluated in C6 glioblastoma lineage, which showed immunocontent only for mGluR3 and 6 proteins. Treatment of these cells with group II antagonist (LY341495) or group III agonist (L-AP4) alone was able to decrease the number of cells in about 25%. Treatment with these ligands together had no synergistic effect. These results demonstrated a possible involvement of mGluR3 and mGluR6 in *in vitro* aggressiveness of GBM. To further evaluate the role of mGluR as biomarkers and therapeutic targets in this neoplasia, *in vivo* experiments on rats implanted with C6 lineage and treated with the same mGluR ligands used *in vitro* are required.

Initially, all mGluR ligands were analogues of L-glutamate. Those compounds were valuable to demonstrate protection *in vitro*, but showed limited applicability in animal models, particularly in chronic tests, due to low BBB penetration. Although in recent decades the synthesis of many more potent and selective mGluR ligands has been reported, which are already known to be effective in *in vivo* studies [7,8], some group III selective agonists, e.g., L-AP4, LSOP or (R,S)PPG, do not present oral bioavailability or BBB penetration. Therefore, *in vivo* experiments with central administration of these drugs are necessary [9].

The most cited routes for direct CNS delivery in rodents are intracerebroventricular (i.c.v.) and intracisternal (i.c.), although other studies describe direct injection into cerebral tissue. Intracerebroventricular injection methods are often described stereotactically and histological verification of the accuracy of the injection is also required to generate reliable data [10]. Most studies perform these treatments in lateral ventricles or in the 4th ventricle [11-14]. The most common intracisternal route is the injection into cisterna cerebellomedullaris, at the base of the skull. Likewise, intracisternal injection is often described steriotaxically and histological verification of accuracy is necessary [15,16]. Intracerebral injection (e.g., intrahippocampal, intraestriatal) is also accomplished using stereotactic vectors for locating the cerebral structure within the rodent brain [17].

Frequently, these procedures involve stereotactic placing of an injection cannula in a specific brain region. For chronic treatments, the cannula is connected to an injection device making it possible to infuse microliter quantities of drugs.

The glioma itself, as it expands, eventually pushes the brain structures, changing their stereotactic coordinates. Thus, the implantation of an injection cannula could be impractical, since it would not be possible to know for sure if treatment would be reaching or not the expected location. In addition, if the animals had already undergone an invasive surgery, another surgical procedure could cause more suffering. Hence, the methodology chosen for the chronic treatment with mGluR ligands cocktail was the intracisternal injection, through an adaptation of CSF puncture protocol realized in rodents. Once a week, rats were treated with LY341495 plus L-AP4, or vehicle, directly into CSF by reverse puncture in cisterna cerebellomedullaris, totaling 3 treatments. The advantage of this strategy of intracisternal treatment is the non-performance of stereotactic surgery, being a less invasive treatment compared to others and allowing a faster recovery of the animals. The animal is only positioned in stereotactic apparatus for head immobilization and injection is done manually. Like all types of direct treatment into CNS, small volumes of drugs should be administered to avoid an exacerbated increase of intracranial pressure. We recommend two researches for maximal efficient implementation of this procedure, one to puncture the cisterna with the needle and another to carry out the administration of treatments.

PROTOCOL FOR INTRACISTERNAL INJECTION (INTO CISTERNA CEREBELLOMEDULAR)

The protocol below has been approved by Ethical Committee on the use of animals of Universidade Federal do Rio Grande do Sul (CEUA-UFRGS) (Protocol: 31573) and is in compliance with the National Institutes of Health guidelines for the use of experimental animals. This injection protocol is an adaptation of the magna cistern puncture protocol for obtaining CSF, whose protocol was also published in JoVe article format [18]. To better perform this protocol it will be necessary the presence of two researchers, who will work together performing different and concomitant procedures.

Preparation of treatments

1. Prepare the treatments to be administered intracisternally in a sterile environment, preferably using autoclaved deionized water. Sterile preparation prevents contamination of the treatment with possible impurities and pathogens that may generate unwanted inflammatory response in the animals.

2. Do not forget to prepare the control treatment (vehicle) under the same conditions as the treatments of interest.

3. To facilitate administration of treatments, store them in well-identified 1.5 mL microcentrifuge tubes. Preparations and storage until the time of injection will depend on the type of drug injected into the animals.

Materials

1. Inhalational anesthetic delivery system;

2. Cylinder containing medical oxygen;

3. Inhalational anesthetic;

4. Confinement chamber adapted to receive inhalational anesthetic;

5. Inhalation mask adapted for rodents that will remain in stereotactic with the head lowered (an adaptation with plastic pasteur pipette is possible, see **Figure 1C**);

6. Stereotatic equipment;

7. Protection between stereotatic and animal to prevent loss of body heat;

8. Microsyringe for precision measurement (10 μL);

9. Support base for microsyringe (approximately 3 cm high);

10. Adhesive tape;

11. Insulin syringe (0.45 mm x 13 mm; 26 G);

12. Gingival needle (0.33 mm x 22 mm; 30 G);

13. Ultrafine and malleable hose used in HPLC devices (30 G);

14. Dental floss;

15. Stopwatch;

16. Light fixture;

17. Heating pad;

18. Sterile gauze;

19. Sterile saline solution as injection fluid;

20. Cylinder containing 70% ethanol;

21. Saline solution for eye lubrication;

22. Treatments and shelf for centrifuge microtubes;

23. Personal protective equipment.

Pre-Injection Procedure:

1. Before preparing all materials necessary for intracisternal injection, thoroughly clean the work area with 70% ethanol to sterilize it avoiding possible contamination. It is important to be mindful of the sterile area throughout the entire procedure.

2. Arrange the work area with all necessary equipment and materials in a way that allows the best optimization of the procedure.

3. Place the isoflurane solution inside anesthesia system. Turn on the following: light fixture, heating pad, and oxygen/isoflurane system.

Preparation of the treatment structure

The following procedures can be carried out by one of the researchers while the other manages the animal.

1. Fill a sterile insulin syringe with saline solution (about 200 μL).

2. Gently attach the syringe needle to the ultra-thin hose. Be **CAREFUL** to not pierce the hose or cut your finger.

3. Open the back protection of one of the sterile gingival needles and attach the needle to the other free end of the hose. Be **CAREFUL** to not pierce the hose or cut your finger.

4. If gauge of the hose is larger than that of the needle, use dental floss to firmly tie the hose to the base of the needle barrel in order to prevent any fluid from overflowing.

5. Remove the gingival needle protection and inject the saline contained in insulin syringe to fill the entire hose and gingival needle with this fluid. Remove the drop of solution that will form on the bevel by touching the needle on sterile gauze and reattach the needle protection.

6. Remove the insulin syringe from the hose, reattach the needle protection and let this syringe in an

accessible place for use before further treatment.

7. Connect the free end of the hose to the microsyringe. Secure the syringe with adhesive tape on the support base, making the marking of volumes visible.

8. Pull the plunger out of the microsyringe until the 1 μL labeling to form a bubble inside the gingival needle.

9. Remove the protection from the gingival needle and place the needle into centrifuge microtube containing the treatment to be injected.

10. Gently pull the syringe plunger to pick up 3-5 μL of the desired treatment. Observe while the hose is filled by the treatment. Be very careful to not form bubbles inside the treatment.

11. Check the formation of the 1 μL bubble between the fluid filling the hose and the treatment. Replace the protection of the gingival needle and leave the treatment structure in a place close to stereotactic.

Anesthesia of animals and positioning in stereotactic

While one of the researchers prepares the structure for treatment, the other one can carry out the anesthesia procedure and rat positioning in stereotactic apparatus.

1. Turn isoflurane to 5% and O_2 to 0.4 L/min and direct the gas flow to chamber. Place the rat in chamber and wait until breathing is significantly slowed.

2. Remove the animal from anesthesia chamber when it is completely unconscious.

3. Position the gas flow towards the stereotacic apparatus to keep the animal anesthetized. Place the animal on the inhalation mask positioned in stereotactic equipment for a few more time and perform a toe pinch to ensure the rat is completely unconscious.

4. Place the anesthetized rat on the stereotactic. Secure the head with the ear bars, leaving the

animal's head well leveled and well centered.

5. Gently tilt the animal's head downwards, leaving the snout at an angle of approximately 90 ° with the vertical axis, which allows better exposure of the cavity in which the cistern is located. Check with your forefinger this cavity.

6. To let the animal's head remain firmly in this position, pull the nasal cone over the region just above the eyes. Be **CAREFUL** to not injure the animal.

7. Shave the hair from the region in which the cistern is located and lubricate the animal's eyes with saline.

8. Turn the isoflurane level down to 2-3% for maintenance. It is important to occasionally check to make sure that rat is completely unconscious with a toe pinch throughout the injection procedure.

9. After setting up the isoflurane level, you are now ready to begin the injection.

Injection of treatments directly into CSF

1. Check again with your forefinger the depression in which the cisterna cerebellomedullaris is located.

2. Remove the needle protection from the injection structure. Hold the needle guard with the thumb and forefinger of one hand and using the forefinger of the other hand gently lift the hose over the animal's head and hold the part of the hose where the needle is connected with this hand.

3. Position the needle at an angle of approximately 60^{o} with the horizontal axis with the needle bevel facing the researcher.

4. Push the needle exactly in the middle of the cavity in which the cistern is located.

5. Puncture the cistern delicately by lowering the needle at the same inclination (60^{o}). First you will feel the needle piercing the animal's skin. By gently lowering the needle you will feel a small puncture resistance, at this point you will be practically piercing the dura mater and the arachnoid

mater. When you feel the needle pierce, advise your fellow researcher to gently pull the microsyringe plunger.

6. If the needle bevel has exactly hit the cisterna cerebellomedullaris, the cerebrospinal fluid will rise after the pull of the plunger. This process is observed as a backflow of treatment inside the syringe along with the 1 µl bubble formed between the fluid and the treatment solution.

7. If the needle bevel has not reached the cisterna, the cerebrospinal fluid will not rise. In this way, treatment does not rise, but the fluid filling the hose backflow inside the syringe and the bubble formed between the treatment and the fluid "increases in size" (vacuum formation).

8. If you have not reached the right spot, lower the needle a little more and ask your colleague to gently move the plunger back and forth until you find the point where the cisterna is located.

9. When you find the spot, ask your colleague to start the timer and inject the treatment at a very slow rate (approximately 0.5min/uL) always observing the timer.

10. After injection of the entire treatment (be **CAREFUL** to not inject the 1 uL bubble air!), remain holding the gingival needle for approximately 2 min to prevent the backflow of treatment. This period varies according to volume applied: the larger the volume of treatment, the longer the waiting time.

11. The gingival needle will have penetrated approximately 5-6 mm under the animal's skin. Remove the needle very gently to prevent the backflow of treatment.

12. Remove the animal from the stereotactic and place it on the heating pad until complete recovery of consciousness.

13. Monitor the animal daily after the injection for at least 3 days.

REPRESENTATIVE RESULTS:

In our work, we used intracisternal injection (into cisterna cerebellomedullaris) of only 3 uL.

We prepared treatment cocktail in sterile saline containing 10 nmol LY341495 and 100 nmol L-AP4 every 3 uL. **Figure 1** shows photos of the materials used to assemble the injection structure, as well as the assembled structure.

Unfortunately, in this article we will not be able to show the results of our treatments, because data are very preliminary. The results bellow show the efficiency of this intracisternal injection strategy through the application of methylene blue. 3 µl of methylene blue (10 mg/mL) were applied to rat cisterna cerebellomedullaris according to protocol described in previous section and according **Figure 2 A and B**. After 5 min of complete injection, the rat was euthanized. In **Figure 2C** is shown a cross section of spinal cord dyed by methylene blue injected in cisterna. **Figure 2D** shows in detail the cerebellum and part of the medulla oblongata. Between these two regions is the methylene blue dyeing exactly where the cisterna cerebellomedullaris was located.

As animal death by decapitation was performed within a few minutes (5 min) after application of methylene blue, it dyed only the exact place of the injection. Thus, if we had let methylene blue longer, it could have dyed more brain structures around the cisterna cerebellomedullaris. It should be noted that at the time of animal decapitation, methylene blue could be seen flowing along with the animal's cerebrospinal fluid.

DISCUSSION:

The wide diversity and heterogeneous distribution of mGluR subtypes in CNS makes these receptors particularly attractive drug targets [3]. A lot of studies validated the therapeutic utility of mGluR ligands in neurological and psychiatric disorders including depression [19], anxiety disorders [20], schizophrenia [21,22], pain syndromes [23], epilepsy [24], Alzheimer's disease [25], and Parkinson's disease [26], among others [3]. Several studies demonstrated the involvement of metabotropic glutamate receptors (mGluR) in progression, aggressiveness, and recurrence of glioblastomas (GBM) [4,6,27]. A

lot of in vitro studies were performed to evaluated the mGluR-mediated signaling in GBM, but only few studies have been able to assess the role of these receptors under GBM malignancy using in vivo models [7,8,28-30]. Probably this deficiency in in vivo studies may have occurred because not all mGluR ligands present oral bioavailability or blood brain barrier (BBB) penetration. Thus, one of the ways to use these BBB-impenetrable ligands in in vivo models would be through direct CNS treatment. As our laboratory intended to evaluate the effect of the in vivo administration of mGluR ligands cocktail (LY341495 and L-AP4) on GBM-implanted rats and one of these mGluR does not cross the BBB, we decided to adapt a less aggressive intracisternal injection protocol.

This intracisternal injection procedure was an adaptation of the CSF puncture protocol of the rat cisterna cerebellomedullaris [18]. A similar protocol was used in Liu, D et al. [31] study. The choice of this type of treatment was performed because it is a less invasive procedure than other types of direct injections into CNS realized in literature, which required stereotactic surgical procedures. The injection rate was very slow to not induce a sudden increase in intracranial pressure due to increase of CSF volume. The gingival needle used for injection was left at the injection site for a few minutes post-delivery and then retracted very slowly in order to prevent the CSF and treatment backflow through the injection canal. The animals were closely observed at least 3 days after injection in order to identify and/or differentiate any reactions caused by possible brain disruption or damage from the injection.

Analyzing our preliminary data, it was possible to notice that the weekly treatment of rats (one administration per week, totaling three treatments) with this type of injection did not cause external damage to animals. There was no inflammatory process at the external site of the injections and they did not show the appearance of suffering. Through the experiments with methylene blue, it was possible to conclude that this type of intracisternal injection was effective reaching exactly the site of spinal cord bathed by CSF concentrated in cisterna cerebellomedullaris. Although it is a

treatment procedure that requires two people to be executed, the noninvasive character of this type of injection of treatments directly in the CSF stands out in relation to the others, being able to be adaptable for any type of drug or rodent animal model.

ACKNOWLEDGMENTS:

This work was financed by *Coordenação de Aperfeiçoamento de Pessoal de Nível Superior (CAPES), Conselho Nacional de Desenvolvimento Científico e Tecnológico (CNPq) – Edital Doenças Neurodegenerativas, Fundação de Amparo à Pesquisa do Estado do Rio Grande do Sul (FAPERGS),* and *Financiadora de Estados e Projetos (FINEP)*.

DISCLOSURES:

The authors of this paper have no conflict of interest.

REFERENCES:

1 Ballabh, P., Braun, A. & Nedergaard, M. The blood-brain barrier: an overview: structure, regulation, and clinical implications. *Neurobiol Dis.* **16** (1), 1-13, doi:10.1016/j.nbd.2003.12.016, (2004).

2 Pardridge, W. M. Drug transport in brain via the cerebrospinal fluid. *Fluids Barriers CNS.* **8** (1), 7, doi:10.1186/2045-8118-8-7, (2011).

3 Niswender, C. M. & Conn, P. J. Metabotropic glutamate receptors: physiology, pharmacology, and disease. *Annu Rev Pharmacol Toxicol.* **50** 295-322, doi:10.1146/annurev.pharmtox.011008.145533, (2010).

4 Teh, J. & Chen, S. mGlu Receptors and Cancerous Growth. *Wiley Interdiscip Rev Membr Transp Signal.* **1** (2), 211-220, doi:10.1002/wmts.21, (2012).

5 Willard, S. S. & Koochekpour, S. Glutamate signaling in benign and malignant disorders: current status, future perspectives, and therapeutic implications. *Int J Biol Sci.* **9** (7), 728-742, doi:10.7150/ijbs.6475, (2013).

6 Yu, L. J., Wall, B. A., Wangari-Talbot, J. & Chen, S. Metabotropic glutamate receptors in cancer. *Neuropharmacology.* doi:10.1016/j.neuropharm.2016.02.011, (2016).

7 Ciceroni, C. *et al.* Type-3 metabotropic glutamate receptors regulate chemoresistance in glioma stem cells, and their levels are inversely related to survival in patients with malignant gliomas. *Cell Death Differ.* **20** (3), 396-407, doi:10.1038/cdd.2012.150, (2013).

8 Ciceroni, C. *et al.* Type-3 metabotropic glutamate receptors negatively modulate bone morphogenetic protein receptor signaling and support the tumourigenic potential of glioma-initiating cells. *Neuropharmacology.* **55** (4), 568-576, doi:10.1016/j.neuropharm.2008.06.064, (2008).

9 Flor, P. J., Battaglia, G., Nicoletti, F., Gasparini, F. & Bruno, V. Neuroprotective activity of metabotropic glutamate receptor ligands. *Adv Exp Med Biol.* **513** 197-223 (2002).

10 DeVos, S. L. & Miller, T. M. Direct intraventricular delivery of drugs to the rodent central nervous system. *J Vis Exp.* (75), e50326, doi:10.3791/50326, (2013).

11 Newman, T. A., Galea, I., van Rooijen, N. & Perry, V. H. Blood-derived dendritic cells in an acute brain injury. *J Neuroimmunol.* **166** (1-2), 167-172, doi:10.1016/j.jneuroim.2005.04.026, (2005).

12 Galea, I. *et al.* Immune-to-brain signalling: the role of cerebral CD163-positive macrophages. *Neurosci Lett.* **448** (1), 41-46, doi:10.1016/j.neulet.2008.09.081, (2008).

13 Serrats, J. *et al.* Dual roles for perivascular macrophages in immune-to-brain signaling. *Neuron.* **65** (1), 94-106, doi:10.1016/j.neuron.2009.11.032, (2010).

14 García-Bueno, B., Serrats, J. & Sawchenko, P. E. Cerebrovascular cyclooxygenase-1 expression, regulation, and role in hypothalamic-pituitary-adrenal axis activation by inflammatory stimuli. *J Neurosci.* **29** (41), 12970-12981, doi:10.1523/jneurosci.2373-09.2009, (2009).

15 Chen, Y., Imai, H., Ito, A. & Saito, N. Novel modified method for injection into the cerebrospinal fluid via the cerebellomedullary cistern in mice. *Acta Neurobiol Exp (Wars).* **73** (2), 304-311 (2013).

16 Chiavolini, D. *et al.* Method for inducing experimental pneumococcal meningitis in outbred mice. *BMC Microbiol.* **4** 36, doi:10.1186/1471-2180-4-36, (2004).

17 Drabek, T. *et al.* Microglial depletion using intrahippocampal injection of liposome-encapsulated clodronate in prolonged hypothermic cardiac arrest in rats. *Resuscitation.* **83** (4), 517-526, doi:10.1016/j.resuscitation.2011.09.016, (2012).

18 Liu, L. & Duff, K. A technique for serial collection of cerebrospinal fluid from the cisterna

magna in mouse. *J Vis Exp.* (21), doi:10.3791/960, (2008).

19 Pilc, A., Chaki, S., Nowak, G. & Witkin, J. M. Mood disorders: regulation by metabotropic glutamate receptors. *Biochem Pharmacol.* **75** (5), 997-1006, doi:10.1016/j.bcp.2007.09.021, (2008).

20 Swanson, C. J. *et al.* Metabotropic glutamate receptors as novel targets for anxiety and stress disorders. *Nat Rev Drug Discov.* **4** (2), 131-144, doi:10.1038/nrd1630, (2005).

21 Conn, P. J. & Jones, C. K. Promise of mGluR2/3 activators in psychiatry. *Neuropsychopharmacology.* **34** (1), 248-249, doi:10.1038/npp.2008.156, (2009).

22 Moghaddam, B. Targeting metabotropic glutamate receptors for treatment of the cognitive symptoms of schizophrenia. *Psychopharmacology (Berl).* **174** (1), 39-44, doi:10.1007/s00213-004-1792-z, (2004).

23 Bleakman, D., Alt, A. & Nisenbaum, E. S. Glutamate receptors and pain. *Semin Cell Dev Biol.* **17** (5), 592-604, doi:10.1016/j.semcdb.2006.10.008, (2006).

24 Alexander, G. M. & Godwin, D. W. Metabotropic glutamate receptors as a strategic target for the treatment of epilepsy. *Epilepsy Res.* **71** (1), 1-22, doi:10.1016/j.eplepsyres.2006.05.012, (2006).

25 Lee, H. G. *et al.* The role of metabotropic glutamate receptors in Alzheimer's disease. *Acta Neurobiol Exp (Wars).* **64** (1), 89-98 (2004).

26 Conn, P. J., Battaglia, G., Marino, M. J. & Nicoletti, F. Metabotropic glutamate receptors in the basal ganglia motor circuit. *Nat Rev Neurosci.* **6** (10), 787-798, doi:10.1038/nrn1763, (2005).

27 Willard, S. S. & Koochekpour, S. Glutamate, glutamate receptors, and downstream signaling pathways. *Int J Biol Sci.* **9** (9), 948-959, doi:10.7150/ijbs.6426, (2013).

28 Zhang, C. *et al.* Anti-cancer effect of metabotropic glutamate receptor 1 inhibition in human glioma U87 cells: involvement of PI3K/Akt/mTOR pathway. *Cell Physiol Biochem.* **35** (2), 419-432, doi:10.1159/000369707, (2015).

29 Arcella, A. *et al.* Pharmacological blockade of group II metabotropic glutamate receptors reduces the growth of glioma cells in vivo. *Neuro Oncol.* **7** (3), 236-245, doi:10.1215/s1152851704000961, (2005).

30 Zhou, K. *et al.* mGlu3 receptor blockade inhibits proliferation and promotes astrocytic phenotype in glioma stem cells. *Cell Biol Int.* **38** (4), 426-434, doi:10.1002/cbin.10207, (2014).

31 Liu, C. H., D'Arceuil, H. E. & de Crespigny, A. J. Direct CSF injection of MnCl(2) for dynamic manganese-enhanced MRI. *Magn Reson Med.* **51** (5), 978-987, doi:10.1002/mrm.20047, (2004).

FIGURES:

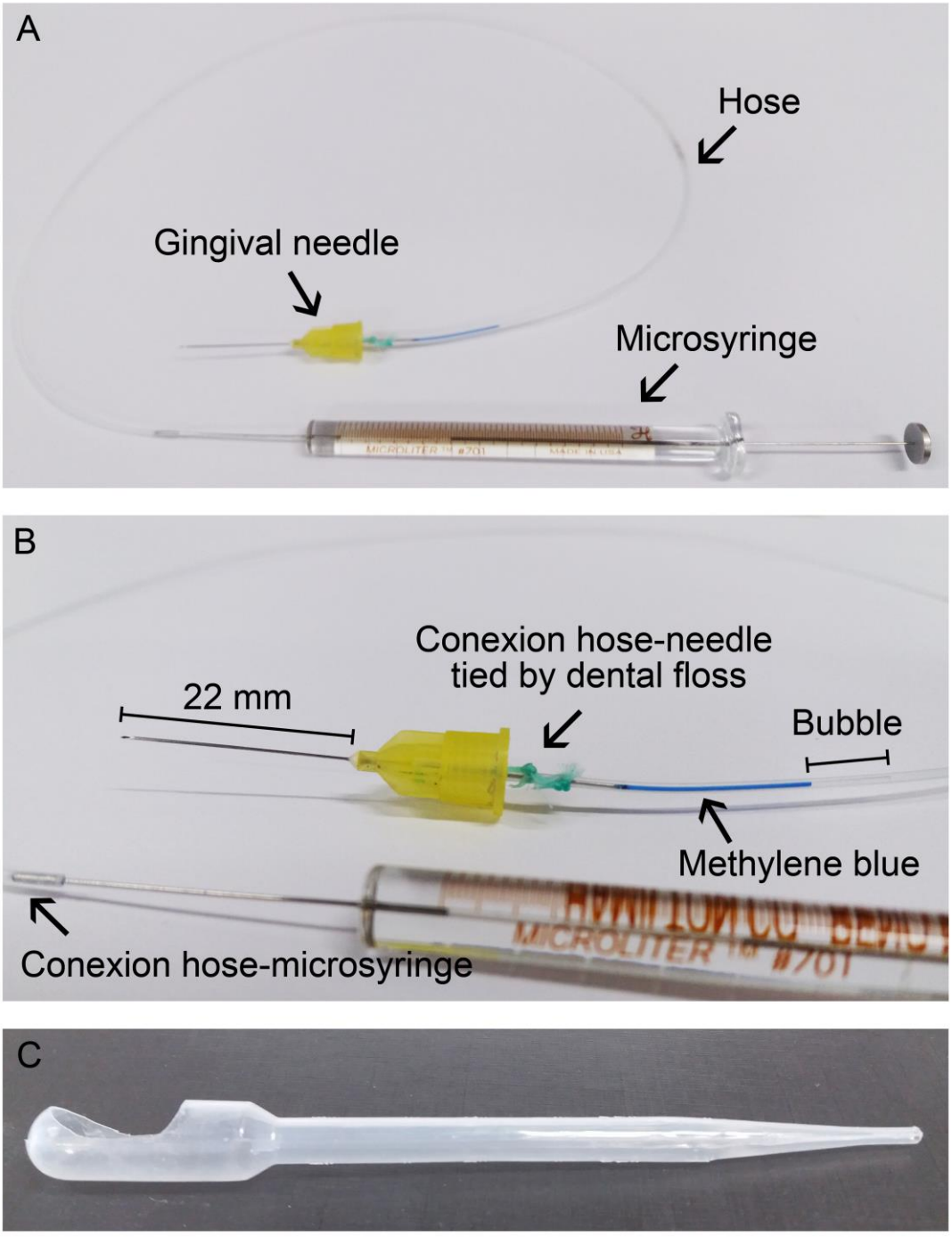

Figure 1 - Picture illustrating the materials used to assemble the injection structure, as well as the assembled structure. (A) and (B) Treatment structure for intracisternal injection: gingival needle (0.33mm x 22 mm; 30G), ultrafine and malleable hose used in HPLC devices (30G) and microsyringe for precision measurement (10 µL) (C) Mask adapted for anesthesia inhalation (plastic pasteur pipette).

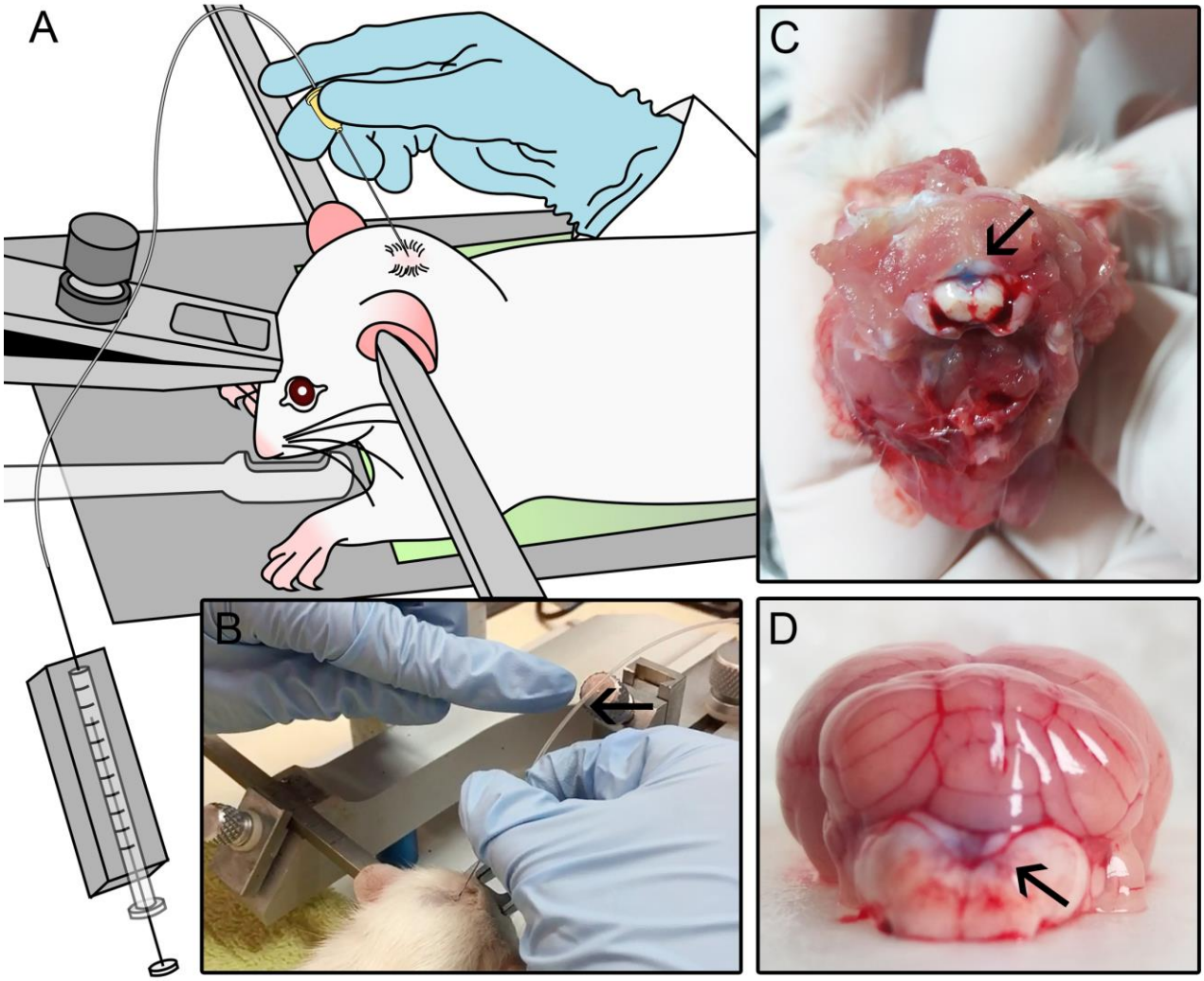

Figure 2 - Intracisternal injection procedure (cisterna cerebellomedullaris). (A) Schematic figure of intracisternal injection showing how rat's head is attached to stereotactic. The animal is placed in head-first prone position with the head remaining lowered due to approximation of the nasal cone of the stereotactic over the head, just above the eyes. The hair around the cavity in which the cisterna is located is shaved and a gingival needle connected to microsyringe by a very fine and malleable hose is punctured by one of the researchers exactly in the middle of this cavity. The other researcher assists in manipulating the microsyringe plunger. (B) Picture illustrating the procedure of intracisternal injection. The arrow indicates the bubble formed between treatment and the fluid filling the hose. (C) Cross section of rat spinal cord. The arrow shows the dyeing of spinal cord with methylene blue injected into cisterna cerebellomedullaris. (D) Picture illustrating the area between cerebellum and medulla oblongata dyed by methylene blue. The marked location is the exact point where the CSF remains deposited in this cisterna.

ANEXO

Estudo *in vivo* em processo de realização

Intracisternal treatment with mGluR ligands in glioblastoma-implanted rats.

Justificativa: Avaliar *in vivo* o potencial da assinatura gênica de mGluR proposta pelos experimentos *in silico*.

Objetivo geral: Realizar experimentos *in vivo* utilizando ratos ortotopicamente implantados com GBM e tratá-los intracisternalmente com ligantes e mGluR e intraperitonealmente com a quimioterapia padrão, temozolamida.

Objetivo específico: Avaliar o tamanho tumoral através de imagens de [^{18}F]FDG obtidas por microPET.

INTRACISTERNAL TREATMENT WITH mGluR LIGANDS IN GLIOBLASTOMA-IMPLANTED RATS

Mery Stefani Leivas Pereira [1*], Thainá Garbino dos Santos[1], Eduardo Rigon Zimmer[3,4], Samuel Greggio[4], Gianina Teribele Venturin[4], Diogo Losch de Oliveira [1*]

[1] Laboratory of Cellular Neurochemistry, Department of Biochemistry, Instituto de Ciências Básicas da Saúde, Universidade Federal do Rio Grande do Sul, Porto Alegre, Brazil.

[2] Laboratory of Cellular Biochemistry, Department of Biochemistry, Instituto de Ciências Básicas da Saúde, Universidade Federal do Rio Grande do Sul, Porto Alegre, Brazil.

[3] Department of Biochemistry, Instituto de Ciências Básicas da Saúde, Universidade Federal do Rio Grande do Sul, Porto Alegre, Brazil.

[4] Pre-Clinical Research Center and Radiopharmaceutical Production Center, Brain Institute of Rio Grande do Sul (BraIns), Pontifical Catholic University of Rio Grande do Sul (PUCRS), Porto Alegre, Brazil.

METHODS

Animals

In this study, 10 male Wistar rats, 60-70 days-old were housed in a rat vivarium at the Department of Biochemistry (ICBS/UFRGS), 3-4 per cage, at a light/dark cycle controlled room (12:12h), suitable temperature (22 ± 2 ° C), ventilation system, water and food *ad libitum*. Throughout this period, animals exhibiting signs of excessive suffering/pain were euthanized. The animals handling followed the "Policy on Humane Care and Use of Laboratory Animals" of the National Institutes of Health (NIH) and institutional policy, and were approved by Ethical Committee on the use of animals of Universidade Federal do Rio Grande do Sul (CEUA-UFRGS) (Protocol: 31573).

Orthopic implantation of C6 GBM cells

C6 cell brain implants were performed according to Figueiró et al., (2013). Briefly, C6 cells ($1,5\times10^6$/3 µL) were injected with a Hamilton microsyringe coupled to an infusion pump into the right striatum (coordinates with regard to bregma: 0.5 mm posterior, 3.0 mm lateral and depth of 6.0 mm) of 60-70 days-old male Wistar rats previously anesthetized intraperitoneally (i.p.) by ketamine/xylazine (90 mg/kg ketamine and 12 mg/kg xylazine). After 26 days of tumor growth, rats were anesthetized again with ketamine/xylazine i.p., the blood was collected by cardiac puncture for biochemical analysis, and death was performed by decapitation.

Treatment of animals

Animals received three types of treatment: Co-injection of mGluR ligands with C6 cells implantation, treatment with mGluR ligands directly into the cerebrospinal fluid through inverse puncture in cisterna cerebellomedullaris (intracisternal injection, i.c.) and intraperitoneal (i.p.) treatment with the standard clinical chemotherapy, temozolamide (TMZ). Timeline depicting

the experimental procedure is represented in **Figure 1**. Hence, animals were divided into 5 groups: 1) Control: mGluR ligands vehicle (Phosphate buffer solution - PBS) and TMZ vehicle (DMSO 10 %); 2) Cocktail 1: LY341495 (group II mGluR antagonist) + L-AP4 (group III mGluR agonist) and DMSO 10%; 3) Cocktail 2: LY341495 + L-AP4 + LY379268 (group II mGluR agonist) + MSOP (group III mGluR antagonist) and DMSO 10%; 4) TMZ: PBS and TMZ; 5) Cocktail 1 + TMZ: LY341495 + L-AP4 and TMZ.

Co-injection of mGluR ligands with C6 cells

24 h before the implantation of glioma cells into right striatum, C6 cultures were pre-treated *in vitro* with a mGluR ligands cocktail (100 nM LY341495; 100 nM LY379268; 100 µM L-AP4; 100 µM MSOP), or vehicle, according to the group in which they were to be injected. Concentration of *in vitro* treatments were chosen according to literature (Arcella et al., 2005; Ciceroni et al., 2008; Ciceroni et al., 2013; D'Onofrio et al., 2003; Zhou et al., 2014). Just before the injection, a cocktail of mGluR ligands (1 nmol LY341495; 1 nmol LY379268; 10 nmol L-AP4; 10 nmol MSOP) was prepared in 3 µL of DMEM 5 % FBS. $1{,}5\times10^{6}$ of C6 cells were resuspended in 3 µL of mGluR cocktail, or vehicle, according to the group in which they were to be injected. Ligands concentrations were chosen according to intraestriatal treatments performed in literature (Cuomo et al., 2009).

Treatment with mGluR ligands

After 7, 11 and 18 days of tumor establishment, animals were treated with mGluR ligands (10 nmol LY341495; 10 nmol LY379268; 100 nmol L-AP4; 100 nmol MSOP), or vehicle, directly into the cerebrospinal fluid through reverse puncture in cisterna cerebellomedullaris (intracisternal treatment – i.c.). Concetration of ligands were chosen according to intracerebroventricular treatments performed in literature (Thomsen and Dalby, 1998). For this, animals were individually anesthetized using a mixture of medical oxygen (and O_2 to 0.4 L/min) and isoflurane (5 % induction and 2–3 % maintenance dose). After initial

sedation, animals were fixed in a stereotaxic rodent structure only for head attachment. The animals' heads were gently tilted downwards at an angle that allows better exposure of the cavity in which the magna cistern is located. Infusion of 3 µL of the mGluR ligands cocktail (0.5 min/µL) was done in magna cistern using a gingival needle coupled to a Hamilton syringe. Immediately before infusion of treatments, a cerebrospinal puncture test was performed to verify if the needle hit the right spot.

Treatment with temozolomide

TMZ treatment was performed according to Zanotto-Filho et al., (2015). Between the 11^{th} and 15^{th} day after tumor implantation, rats were treated daily, totaling 5 treatments, with 10 mg/Kg/day (i.p.) of temozolomide or DMSO (vehicle). The drug was dissolved in DMSO at a final concentration of 10%.

[^{18}F]FDG synthesis

[^{18}F]FDG synthesis was performed in the automated FASTlab module (GE Healthcare) available in the Radiopharmaceutical Production Center of Instituto do Cérebro do Rio Grande do Sul (Brain Institute - BraIns) based on the methodology used by (Fowler and Ido, 2002).

[^{18}F]FDG MicroPET Scan

Rats were transported to the Preclinical Research Center (CPP) of the Brain Institute (BraIns) of Rio Grande do Sul 24 h before microPET scanning procedures. Rats were scanned in a longitudinal fashion four days before (baseline) gliobastoma injection, and at 3, 10, 17 and 24 days after, according to Baptista et al., (2015). Rats were briefly anesthetized using a mixture of isoflurane and medical oxygen (3–4 % induction and 2–3 % maintenance dose) and 1 mCi of [^{18}F]FDG was administered through the tail vein. Then, animals were returned to their home cages for a 40 min period of conscious [^{18}F]FDG uptake. Then, animals were scanned for 10 min (static aquicistion) with the TriumphTM microPET (LabPET-4, TriFoil Imaging,

Northridge, CA, USA). Throughout these procedures, animals were kept on a pad heated to 36 ºC. All data were reconstructed using a 3D maximum-likelihood expectation-maximization (3D-MLEM) algorithm with 20 iterations and no attenuation correction (Bahri et al., 2009; Kim and Zee, 2007). Each reconstructed microPET image was spatially normalized into an [^{18}F]FDG template using brain normalization in PMOD v3.5 and the Fusion Toolbox (PMOD Technologies, Zurich, Switzerland). An MRI template was used to coregister normalized images. [^{18}F]FDG standard uptake (SUV) value was calculated as (image radioactivity)/(dose injected/body weight).

RESULTS AND DISCUSSION

For *in vivo* evaluation of the potential of mGluR gene signature proposed by *in silico* experiments, GBM-implanted rats were treated intracisternally with mGluR ligands and intraperitoneally by standard chemotherapy, TMZ. C6 lineage was treated *in vitro* 24 h before implantation and was injected together with the treatment. This protocol was performed to mimic tumors with high mGluR3 activity and low mGluR6 activity (cells treated with the antagonist of group II, LY341495, and with the agonist of group III, L-AP4). Among the 10 animals analyzed (n = 2, for each treatment), two died before the last day of scanning (each of different experimental groups). Additionally, GBM cells backflowed and did not grow exactly in right striatum in some animals. Besides, some of tumors have settled outside the right cerebral hemisphere, between brain tissue and meninges, forming a very conspicuous mass visible at the time of brain dissection. For these reasons, unfortunately only one animal from each group was able to be analyzed.

In **Figure 2**, two scans of these five animals are shown. The first scan was performed four days before implantation (-4 d) and the last, 24 days post-implantation of GBM. Images from the last scan were merged into a rat magnetic resonance imaging (MRI) template for better comparison of [^{18}F]FDG uptake among brain structures. The overlaps of MRI template with the last scan are shown in **Figure 2** in a coronal, sagittal and transverse plane. In **Figure 2F**, the images of this MRI template are found in coronal, sagittal and transverse planes showing a cross pointing to a coordinate within the right striatum. All images of **Figure 2** were recorded from this coordinate. [^{18}F]FDG uptake profile from each animal were adjusted by standard uptake value (SUV) to remove variability introduced by differences in animal size and the amount of injected [^{18}F]FDG, making uptake values of each animal comparable, and the images of each animal were adjusted by specific SUV extensions (range), making them visually comparable to each other.

In some animals, [^{18}F]FDG uptake appears to show the tumor in right hemisphere of the last scan (**Figure 2 A and E**). However, confirmation of this result is necessary to use

histological analysis of the brains. In the last scan of the animal of **Figure 2D**, [^{18}F]FDG labeling appears to demonstrate tumor formation externally to cerebral hemispheres. However, in the scans shown in **Figures 2 B and C**, the intense [^{18}F]FDG labeling does not appear to mark a tumor, since radioactivity seems concentrated in the left hemisphere of these animals. Although we cannot clearly define the delimitation of GBM tumors using only [^{18}F]FDG uptake, we can conclude, by analyzing the pre-surgical scanning and the last scan, that implantation of GBM in the right striatum of these animals changed the pattern of cerebral [^{18}F]FDG uptake after 24 days of surgery.

In **Figure 3**, images of the five scans performed with these animals are included. All images were recorded from the same coordinate of the striatum. Through the visual analysis of these images, we can conclude that implantation of GBM changed the [^{18}F]FDG incorporation, mainly after 10 days of surgery. However, it is possible that this alteration is due to an inflammatory process. On 24th day after implantation, this alteration in [^{18}F]FDG uptake is less pronounced. This is evident when we observe, in particular, **Figures 3A and E**, which show that, after 24 days of implantation, the intensity of [^{18}F]FDG labeling decreased significantly compared to previous scans (10d and 17 d post-implantation), being almost possible a visual delimitation of the probable tumor. In **Figures 3 B and C**, it is not possible to determine whether this inflammatory process extends to the last day of the scan, and therefore it is not possible to make a visual delimitation of the tumor. Although it is not possible to correctly visualize the delimitation of the tumors in the scans, it should be pointed out that when we dissected the animals, the tumors were observed in the right striatum.

In an attempt to make an estimated quantification of the presence of GBM tumors, the SUV of the left striatum was subtracted from the right striatum value and the final value of the two scans was plotted on **Figure 4A**. At the first scan of the five animals the final SUV was close to zero, indicating that incorporation of [^{18}F]FDG in both striatum before tumor implantation was apparently very similar. In the last scans, the final SUV of four experimental groups (control; LY341495 + L-AP4 + LY379268 + MSOP; TMZ and TMZ + LY341495 + L-

AP4) presented positive SUV, hinting that in right striatum, where the tumor was inserted, there was a greater incorporation of [^{18}F]FDG in relation to left striatum, suggesting the possible presence of the tumor after 24 days of implantation. However, in the animal treated only with LY341595 + L-AP4, the final SUV was negative, suggesting that in the left striatum, in which the tumor was not implanted, there was a greater incorporation of [^{18}F]FDG in relation to the other. The SUV values are calculated taking into account the amount of [^{18}F]FDG that has been injected into the animal and its weight. As can be seen in **Figure 4B**, the animal treated with LY341495 + L-AP4 was the rat with the highest weight in relation to the others. Thus, the representation of [^{18}F]FDG uptake in these animals by SUV was not the most adequate to make a comparison between them, since the weight of one of them was very different from the others. An alternative would be standardizing [^{18}F]FDG uptake values in a different way to eliminate variability between animals. In addition, the weight of the animals varied greatly among the groups throughout the experiment **Figure 4 B and C**.

By analyzing these preliminary *in vivo* data from rats implanted with GBM and treated with mGluR ligands, we cannot conclude whether the treatments interfered or not in tumor formation. However, we can conclude that rat GBM-implantation changed the pattern of cerebral [^{18}F]FDG uptake until 24 days of surgery.

CONCLUSION

Our *in vivo* results are preliminary and inconclusive in relation to mGluR ligands treatment. Although GBM tumors cannot be well delimited only by [^{18}F]FDG uptake using this weekly treatment protocol, it is possible to conclude, by analyzing animals longitudinal scans, that rat GBM-implantation changed the pattern of cerebral [^{18}F]FDG uptake until 24 days after surgery. To complement *in vivo* studies, histological analysis of GBM tumors of each animal should be performed in the next experiments in order to correctly delimit the tumor volume and to correlate it with [^{18}F]FDG uptake values. We will probably have to change the weekly treatment protocol trying to avoid the increase in [^{18}F]FDG uptake caused by possible inflammation. Although our treatment schedule was not ideal for assessing tumor volume using the [^{18}F]FDG uptake imaging method, this method has a great potential for imaging rodent brain tumors (Assadian et al., 2008; Bolcaen et al., 2015; Wyss et al., 2007). It should be noted that experiments performed in this work were the first performed in *InsCer-PUCRS (Porto Alegre, Brazil)* using experimental model of brain tumors. We hope that future adequacy of our treatment protocol will be very promising to obtain GBM tumor volume.

REFERENCES

Arcella, A., G. Carpinelli, G. Battaglia, M. D'Onofrio, F. Santoro, R.T. Ngomba, V. Bruno, P. Casolini, F. Giangaspero, and F. Nicoletti. 2005. Pharmacological blockade of group II metabotropic glutamate receptors reduces the growth of glioma cells in vivo. *Neuro Oncol*. 7:236-245.

Assadian, S., A. Aliaga, R.F. Del Maestro, A.C. Evans, and B.J. Bedell. 2008. FDG-PET imaging for the evaluation of antiglioma agents in a rat model. *Neuro Oncol*. 10:292-299.

Bahri, M.A., A. Plenevaux, G. Warnock, A. Luxen, and A. Seret. 2009. NEMA NU4-2008 image quality performance report for the microPET focus 120 and for various transmission and reconstruction methods. *J Nucl Med*. 50:1730-1738.

Baptista, P.P., L. Saur, P.B. Bagatini, S. Greggio, G.T. Venturin, S.P. Vaz, K.o.R. Ferreira, J.S. Junqueira, D.R. Lara, J.C. DaCosta, C.M. Jeckel, R.G. Mestriner, and L.L. Xavier. 2015. Antidepressant Effects of Ketamine Are Not Related to ^{18}F-FDG Metabolism or Tyrosine Hydroxylase Immunoreactivity in the Ventral Tegmental Area of Wistar Rats. *Neurochem Res*. 40:1153-1164.

Bolcaen, J., B. Descamps, K. Deblaere, T. Boterberg, F. De Vos Pharm, J.P. Kalala, C. Van den Broecke, E. Decrock, L. Leybaert, C. Vanhove, and I. Goethals. 2015. (18)F-fluoromethylcholine (FCho), (18)F-fluoroethyltyrosine (FET), and (18)F-fluorodeoxyglucose (FDG) for the discrimination between high-grade glioma and radiation necrosis in rats: a PET study. *Nucl Med Biol*. 42:38-45.

Ciceroni, C., A. Arcella, P. Mosillo, G. Battaglia, E. Mastrantoni, M.A. Oliva, G. Carpinelli, F. Santoro, P. Sale, L. Ricci-Vitiani, R. De Maria, R. Pallini, F. Giangaspero, F. Nicoletti, and D. Melchiorri. 2008. Type-3 metabotropic glutamate receptors negatively modulate bone morphogenetic protein receptor signaling and support the tumourigenic potential of glioma-initiating cells. *Neuropharmacology*. 55:568-576.

Ciceroni, C., M. Bonelli, E. Mastrantoni, C. Niccolini, M. Laurenza, L.M. Larocca, R. Pallini, A. Traficante, P. Spinsanti, L. Ricci-Vitiani, A. Arcella, R. De Maria, F. Nicoletti, G. Battaglia, and D. Melchiorri. 2013. Type-3 metabotropic glutamate receptors regulate chemoresistance in glioma stem cells, and their levels are inversely related to survival in patients with malignant gliomas. *Cell Death Differ*. 20:396-407.

Cuomo, D., G. Martella, E. Barabino, P. Platania, D. Vita, G. Madeo, C. Selvam, C. Goudet, N. Oueslati, J.P. Pin, F. Acher, A. Pisani, C. Beurrier, C. Melon, L. Kerkerian-Le Goff, and P. Gubellini. 2009. Metabotropic glutamate receptor subtype 4 selectively modulates both glutamate and GABA transmission in the striatum: implications for Parkinson's disease treatment. *J Neurochem*. 109:1096-1105.

D'Onofrio, M., A. Arcella, V. Bruno, R.T. Ngomba, G. Battaglia, V. Lombari, G. Ragona, A. Calogero, and F. Nicoletti. 2003. Pharmacological blockade of mGlu2/3 metabotropic glutamate receptors reduces cell proliferation in cultured human glioma cells. *J Neurochem*. 84:1288-1295.

Figueiró, F., A. Bernardi, R.L. Frozza, T. Terroso, A. Zanotto-Filho, E.H. Jandrey, J.C. Moreira, C.G. Salbego, M.I. Edelweiss, A.R. Pohlmann, S.S. Guterres, and A.M. Battastini. 2013. Resveratrol-loaded lipid-core nanocapsules treatment reduces in vitro and in vivo glioma growth. *J Biomed Nanotechnol*. 9:516-526.

Fowler, J.S., and T. Ido. 2002. Initial and subsequent approach for the synthesis of 18FDG. *Semin Nucl Med*. 32:6-12.

Kim, P.E., and C.S. Zee. 2007. Imaging of the cerebrum. *Neurosurgery*. 61:123-146; discussion 146.

Thomsen, C., and N.O. Dalby. 1998. Roles of metabotropic glutamate receptor subtypes in modulation of pentylenetetrazole-induced seizure activity in mice. *Neuropharmacology*. 37:1465-1473.

Wyss, M.T., N. Spaeth, G. Biollaz, J. Pahnke, P. Alessi, E. Trachsel, V. Treyer, B. Weber, D. Neri, and A. Buck. 2007. Uptake of 18F-Fluorocholine, 18F-FET, and 18F-FDG in C6 gliomas and correlation with 131I-SIP(L19), a marker of angiogenesis. *J Nucl Med*. 48:608-614.

Zanotto-Filho, A., E. Braganhol, K. Klafke, F. Figueiró, S.R. Terra, F.J. Paludo, M. Morrone, I.J. Bristot, A.M. Battastini, C.M. Forcelini, A.J. Bishop, D.P. Gelain, and J.C. Moreira. 2015. Autophagy inhibition improves the efficacy of curcumin/temozolomide combination therapy in glioblastomas. *Cancer Lett*. 358:220-231.

Zhou, K., Y. Song, W. Zhou, C. Zhang, H. Shu, H. Yang, and B. Wang. 2014. mGlu3 receptor blockade inhibits proliferation and promotes astrocytic phenotype in glioma stem cells. *Cell Biol Int*. 38:426-434.

FIGURES

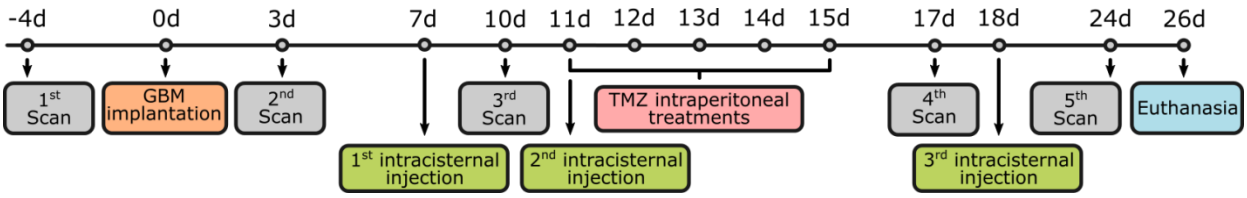

Figure 1 - Timeline depicting the experimental procedure of treatment and scanning of GBM-implanted rats.

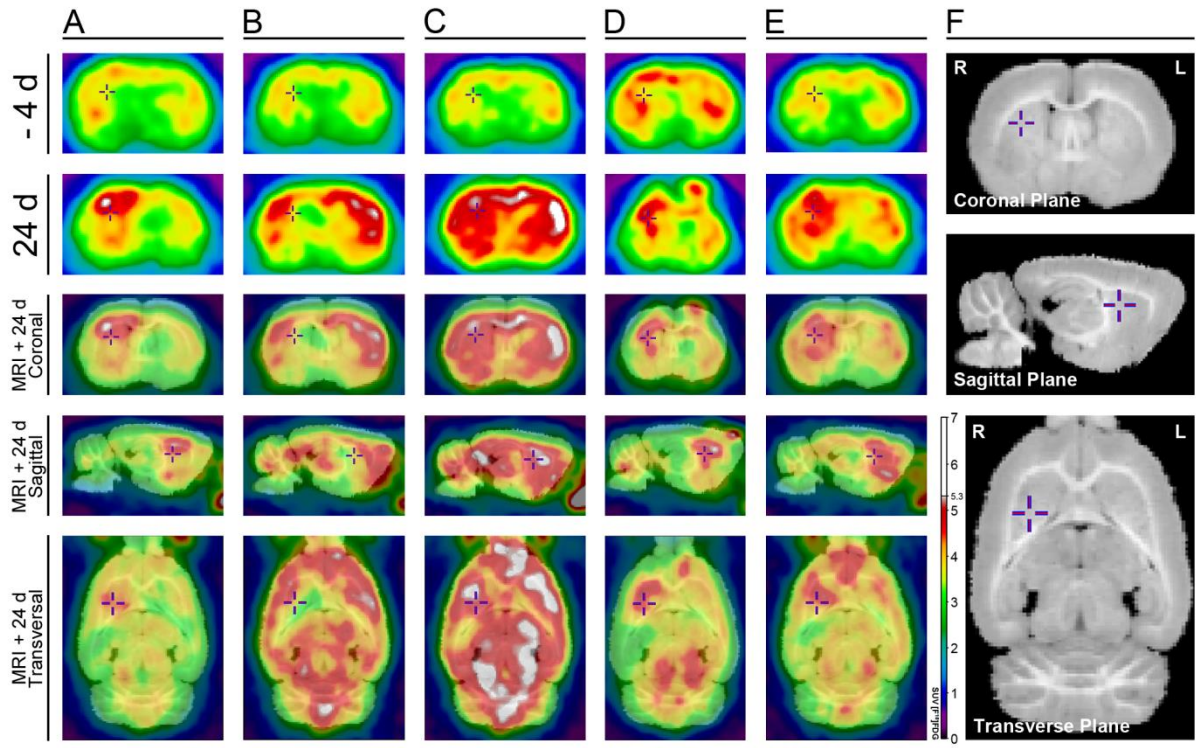

Figure 2 – Micro-PET of GBM-implanted rats trated intracisternally with mGluR ligands and intraperitoneally by TMZ. Representative [^{18}F]FDG uptake among brain structures of five experimental groups (n=1) – (A) Control group; (B) LY341495+L-AP4 group; (C) LY341495+L-AP4+LY379268+MSOP group; (D) TMZ group; (E) TMZ+LY341495+L-AP4 group. In the first pictures line is the scans performed four days before implantation (-4 d). In the second images line is the last scan (5th), performed 24 days after GBM implantation (24 d). Images from the last scan were merged into a rat magnetic resonance imaging (MRI) template. In the third line is the MRI/5thscan overlap in coronal plane; in the fourth, the MRI/5thscan overlap in sagittal plane; and in the sixth, the MRI/5thscan overlap in transverse plane. In (F) is the MRI template in coronal, sagittal and transverse planes with a cross pointing to a coordinate within the right striatum (R represents the right cerebral hemisphere and L, the left). All scans were recorded from this coordinate and [^{18}F]FDG uptake profile was expressed in standard uptake value (SUV). The scan images of each animal were adjusted by specific SUV extensions (range) for better visualization of [^{18}F]FDG incorporation, being possible to visually compare the scans from the same animal, but scans from one animal cannot be visually comparable to scans from other animals. These *in vivo* results are preliminary and inconclusive in relation to mGluR treatment. GBM tumors cannot be well delimited only by [^{18}F]FDG uptake using this weekly treatment protocol, however it is possible to conclude, by analyzing the first and the last scan, that rat GBM-implantation changed the pattern of cerebral [^{18}F]FDG uptake after 24 days of surgery.

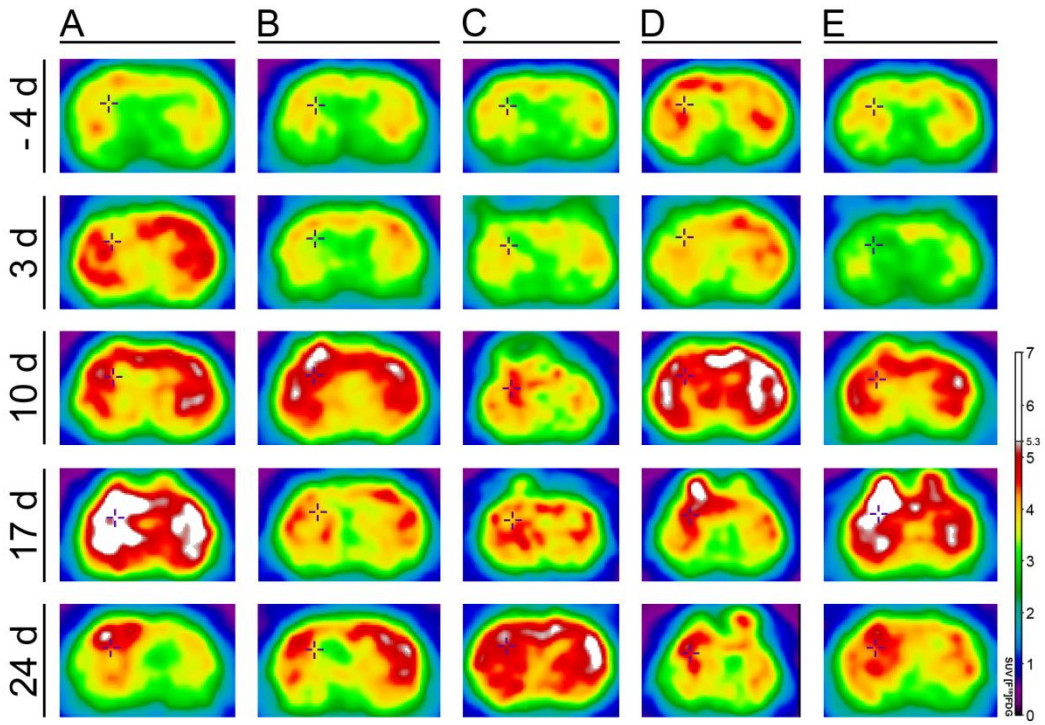

Figure 3 – Longitudinal Micro-PET scans of GBM-implanted rats treated intracisternally with mGluR ligands and intraperitoneally by TMZ. Representative [^{18}F]FDG uptake among brain structures of five experimental groups (n=1) – (A) Control group; (B) LY341495+L-AP4 group; (C) LY341495+L-AP4+LY379268+MSOP group; (D) TMZ group; (E) TMZ+LY341495+L-AP4 group. Four days before glioblastomas injection and also at 3, 10, 17 and 24 days after implantation surgery, the animals were scanned. Rats received 1 mCi of [^{18}F]FDG in tail vein and were left in their home cage for a 40 min period of conscious tracer uptake. After, rats was placed in a head-first prone position and scanned with the TriumphTM microPET (LabPET-4, TriFoil Imaging, Northridge, CA, USA) under inhalatory anesthesia and kept on a pad heated to 36 ºC. For radiotracer readings, 10 min list mode static acquisitions were acquired with the field of view (FOV; 3.75 cm) centered on rat's head. All data were reconstructed using a 3D maximum-likelihood expectation-maximization (3D-MLEM) algorithm with 20 iterations and no attenuation correction. Each reconstructed microPET image was spatially normalized into an [^{18}F]FDG template using brain normalization in PMOD v3.5 and the Fusion Toolbox (PMOD Technologies, Zurich, Switzerland). An MRI rat brain VOI template was used to overlay the normalized images, previously coregistered to the microPET image database. Lines represent the day of scans (four days before GBM implantation, -4 d, and the days after GBM implantation, 3, 10, 17 and 24 days. All images were recorded from the same coordinate of the striatum, [^{18}F]FDG uptake profile was expressed in standard uptake value (SUV) and images of each animal were adjusted by specific extensions of SUV (range). In this way, images from the same animal can be compared to each other, but cannot be compared to those from another animal. Visual analysis of these images indicates that GBM implantation caused a very marked change in [^{18}F]FDG incorporation, mainly after 10 days of surgery. At day 24 after implantation, alteration in [^{18}F]FDG uptake is less pronounced. These *in vivo* results are preliminary and inconclusive in relation to mGluR treatment. GBM tumors cannot be well delimited only by [^{18}F]FDG uptake using this weekly treatment protocol, however it is possible to conclude, by analyzing the longitudinal scans, that rat GBM-implantation changed the pattern of cerebral [^{18}F]FDG uptake.

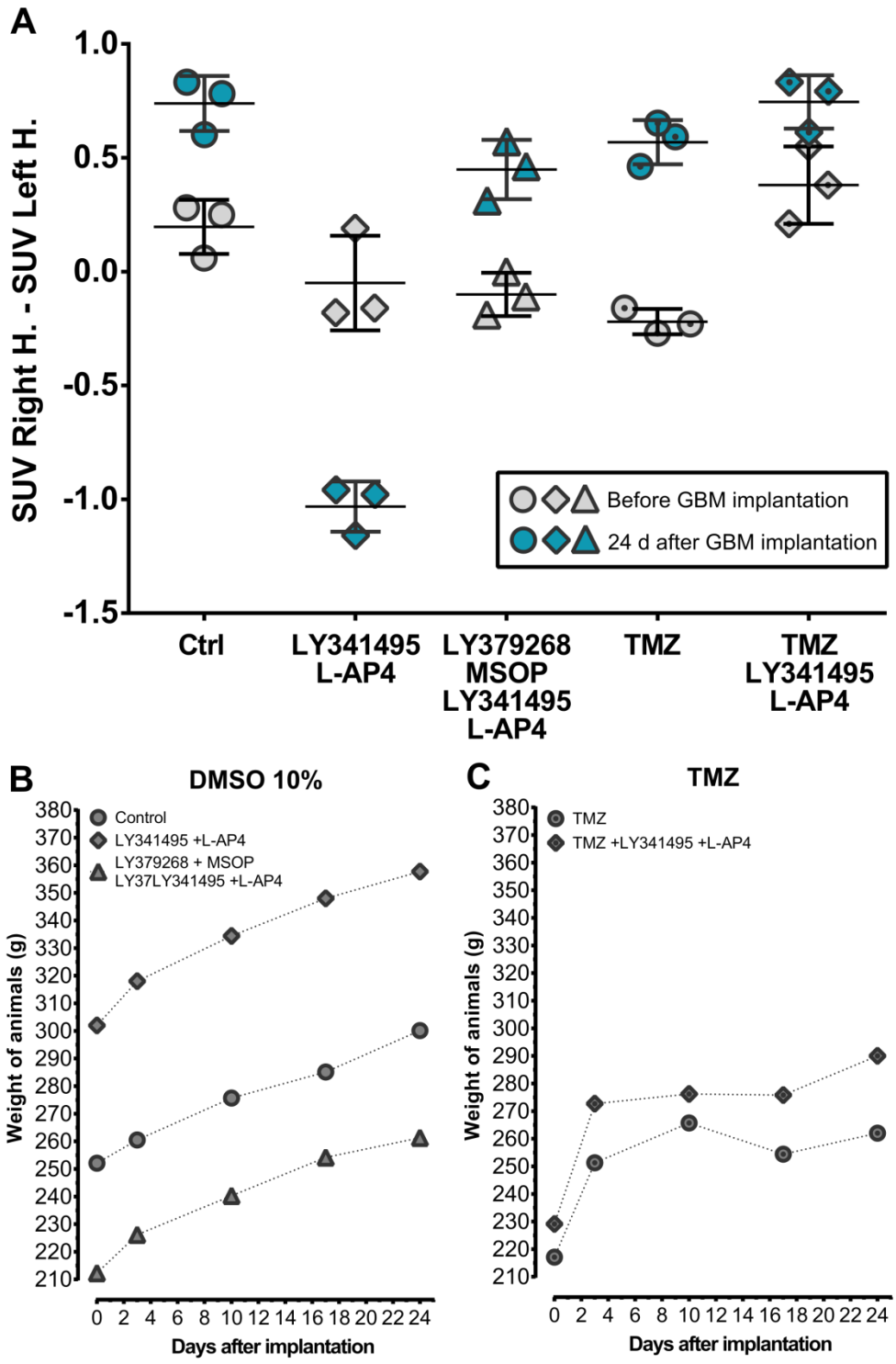

Figure 4 – Standard [^{18}F]FDG uptake values (SUV) of GBM-implanted rats treated intracisternally with mGluR ligands and intraperitoneally by TMZ and weight curve. (A) [^{18}F]FDG radioactivity was evaluated in three coordinates of the left and right striatal and expressed as standard uptake values (SUV). The values of the coordinates of the left striatum were subtracted from the values of the coordinates of the right striatum, in which the tumor would theoretically be present (n=1, for each of the five treatments). In gray is represented the final SUV from the first scan, before GBM implantation, and in blue is represented the final SUV from the last scan, 24 days after GBM implantation. (B) The weight of the animals varied greatly among the groups throughout the experiment.

PARTE II

DISCUSSÃO

O glioblastoma (GBM) é o mais comum dos tumores primários malignos que afetam o Sistema Nervoso Central e é considerado um dos cânceres mais letais (Cloughesy et al., 2014; Omuro and DeAngelis, 2013). O tratamento de intervenção inicial mais utilizado nos pacientes é a ressecção cirúrgica seguida da radioterapia e da quimioterapia, a qual geralmente é opcional. Embora essa estratégia terapêutica aumente a sobrevida, a maioria dos pacientes vai a óbito em até um ano após o diagnóstico (DeAngelis, 2001). Para piorar o quadro clínico, os GBM estão entre os tumores mais resistentes à radiação e à quimioterapia (Cloughesy et al., 2014; Masui et al., 2012). Com o intuito de melhorar a qualidade de vida dos pacientes e aumentar o tempo de sobrevida, muitos estudos buscam por novas estratégias terapêuticas, focando, principalmente em proteínas de membrana que possam regular especificamente a proliferação em GBM. Os receptores metabotrópicos de glutamato (mGluR) estão predominantemente envolvidos na manutenção da homeostasia celular do sistema nervoso central (SNC) (Niswender and Conn, 2010). Entretanto, muitos estudos têm sugerido outros papéis dos mGluR em tumores humanos, incluindo GBM (Teh and Chen, 2012; Willard and Koochekpour, 2013; Yu et al., 2016).

No **capítulo I** deste trabalho consta uma revisão, já publicada na revista *Oncotarget* (Pereira et al., 2017), relatando todos os trabalhos que demonstraram o envolvimento da sinalização intracelular mediada por mGluR sobre a progressão, agressividade e recorrência de gliomas malignos, principalmente de GBM, ressaltando o potencial terapêutico dos ligantes de mGluR. Resumidamente, o bloqueio farmacológico de mGluR1 e mGluR3 tem poder anti-proliferativo e anti-migratório, diminuindo a ativação das vias de sinalização da MAPK e da PI3K (Arcella et al., 2005; Ciceroni et al., 2008; D'Onofrio et al., 2003; Zhang et al., 2015). A inibição farmacológica de mGluR3 promoveu a diferenciação astroglial de células de GBM (Ciceroni et al., 2008; Zhou et al., 2014) e permitiu a ação citotóxica do quimioterápico padrão, temozolamida (TMZ) (Ciceroni et al., 2013). A toxicidade da TMZ dependente de mGluR3 foi mediada pela via de sinalização da PI3K e NF-κB, a qual desencadeou o aumento dos transcritos

de MGMT, uma proteína relacionada à resistência a quimioterápicos alquilantes (Ciceroni et al., 2013). Além disso, O bloqueio farmacológico contínuo de mGluR1 e 3 *in vivo* diminuiu o volume dos tumores em dois modelos xenográficos diferentes (Arcella et al., 2005; Ciceroni et al., 2008; Ciceroni et al., 2013; Zhang et al., 2015; Zhou et al., 2014). Somente um trabalho da literatura avaliou o poder preditivo da expressão de mGluR3 em biópsias de GBM humanos, mostrando que a alta expressão gênica desse receptor está relacionada a um pior prognóstico para o paciente (Ciceroni et al., 2013).

Devido a essa deficiência de estudos em biópsias de pacientes, nosso grupo de pesquisa decidiu avaliar o valor prognóstico da expressão gênica dos oito subtipos de receptores de mGluR em biópsias de GBM de duas coortes de pacientes obtidas de dois bancos de dados independentes depositados no *Gene Expression Omnibus database* (GSE16011 e GSE4412) com o intuito de propor uma assinatura gênica dos mGluR capaz de predizer o desfecho dos pacientes. Este estudo encontra-se no **Capítulo II** desta tese. Através da meta-análise dos dados de microarranjo de amostras de GBM dessas duas coortes, observou-se uma correlação entre a expressão gênica dos oito subtipos de mGluR (mGluR1-8) e a sobrevida média dos pacientes com GBM. Esta correlação foi verificada através de uma análise de cluster hierárquico com base na expressão gênica de cada mGluR. Baseado nos dados obtidos, cada coorte foi subdividida em 2 grupos: um grupo que se destacava pela alta expressão gênica de mGluR3 e baixa de mGluR 4 e 6; e um grupo que se destacava pela baixa expressão gênica de mGluR3 e alta de mGluR4 e 6. O grupo que apresentou maior expressão gênica de mGluR3 teve aproximadamente 1,5 vezes mais chance de ir a óbito em relação ao grupo outro grupo na coorte teste e 2,1 vezes mais chance, na coorte de validação.

No mesmo **capítulo II**, a avaliação do potencial da assinatura gênica de mGluR proposta *in silico* foi verificada *in vitro*. A ação farmacológica de ligantes do grupo II e III foi avaliada em duas linhagens de GBM (C6 e U-87 MG) após 72 h de tratamento em meio sem soro. O tratamento das linhagens com antagonistas de grupo II (EGLU ou LY341495) foi realizado com o intuito de mimetizar uma condição de baixa expressão de mGluR3. Já o tratamento com o

agonista de grupo III (L-AP4) foi realizado com a intenção de mimetizar uma condição de alta expressão de mGluR6, visto que as linhagens não apresentaram imunoconteúdo para mGluR4. Apenas a linhagem C6 foi sensível ao tratamento com os ligantes de mGluR. Quando tratada isoladamente com os antagonistas de grupo II ou com o agonista de grupo III, permaneceram no poço aproximadamente 80% das células da linhagem C6. O tratamento em conjunto com esses ligantes não teve efeito sinérgico. Estes resultados demonstraram o envolvimento de mGluR3 e mGluR6 na progressão de GBM *in vitro*, corroborando com a assinatura gênica proposta *in silico*, assim como indicam que a via de sinalização intracelular ativada é a mesma, visto que o bloqueio de mGluR3 e ativação de mGluR6 em conjunto não apresentou efeito aditivo. Entretanto, mais experimentos *in vitro* em condições proliferantes devem ser realizados para melhor comprovar a assinatura gênica dos mGluR. Apesar da expressão gênica de mGluR de grupo III já ter sido avaliada em culturas e amostras de GBM humanos (Stepulak et al., 2009), este foi o primeiro estudo que avaliou farmacologicamente o envolvimento dos mGluR de grupo III sobre a malignidade de gliomas.

No **Capítulo III** encontra-se uma descrição metodológica explicitando cada passo realizado para execução do protocolo de injeção intracisternal (na cisterna cerebelo-medular) adaptado em nosso laboratório para realização dos tratamentos *in vivo* com os ligantes de mGluR (**Anexo)**. Como um dos ligantes (L-AP4) presente no coquetel de tratamento com o qual tratamos nossos animais implantados com GBM não ultrapassa a barreira hemato-encefálica, o tratamento *in vivo* com esse ligante só seria possível através da sua liberação direta no SNC. Como, em geral, os tratamentos diretos no SNC necessitam de procedimentos cirúrgicos estereotáxicos para implantação de cânulas de tratamento, nós decidimos realizar um protocolo de tratamento direto no líquor que fosse menos agressivo para os animais, visto que havia a necessidade de realizar tratamentos seriados (semanais) e visto que esses tratamentos seriam realizados após um procedimento cirúrgico para implantação dos GBM. A injeção na cisterna cerebelo-medular dos animais (também conhecida como cisterna magna em humanos) foi uma adaptação do protocolo de punção de líquor em modelos roedores. A aplicação de azul de

metileno na cisterna cerebelo-medular através dessa técnica de injeção intracisternal tingiu exatamente a região entre o cerebelo e a medula banhada pelo líquor acumulado nesta cisterna, demonstrando a eficiência do nosso protocolo de injeção. Cabe salientar que os animais tratados semanalmente com esse tipo de injeção (**Anexo**) tiveram uma boa recuperação após esse procedimento, não apresentando sinais externos de inflamação no local da aplicação ou outros sinais de dano causados por esse tipo de injeção. Devido a esse caráter menos invasivo, esse tipo de tratamento direto no SNC pode ser adaptável para aplicações de qualquer tipo de fármaco em qualquer tipo de modelo animal roedor.

No **Anexo** do **Capítulo III**, experimentos *in vivo* utilizando ratos implantados com GBM e tratados intracisternalmente com um coquetel de ligantes de mGluR (LY341495 e L-AP4) foram realizados para avaliar o potencial da assinatura gênica de mGluR proposta pelas análises *in sílico*. As células da linhagem C6 foram tratadas 24 h com o coquetel de ligantes e implantadas juntamente com os tratamentos no estriado direito de ratos. Uma vez por semana (nos 7º, 11º e 18º dias pós-implantação) os ratos foram tratados com os ligantes, ou com o veículo, diretamente no líquor através de punção inversa na cisterna cerebelo-medular, totalizando 3 tratamentos. Do 11º ao 15º dia pós-implantação, eles receberam TMZ, ou veículo, intraperitonealmente. Os animais receberam injeção intracaudal de [^{18}F]FDG, um radiofármaco amplamente usado para diagnóstico de tumores cerebrais em humanos (Rohren et al., 2004), e o cérebro foi escaneado em aparelho de microPET do InsCer/PUCRS 4 dias antes da implantação e nos 3º, 10º, 17º e 24º dias pós-implantação do GBM. Os resultados obtidos com os experimentos *in vivo*, além de preliminares, são inconclusivos em relação aos tratamentos com o coquetel de ligantes de mGluR, pois, dentre os dez animais escaneados (n=2, para cada tratamento), dois deles (um de cada grupo) morreram antes do último escaneamento. Além disso, a incorporação de [^{18}F]FDG tanto na região tumoral quanto na região peritumoral foi muito elevada, indicando que mudanças no protocolo de escaneamento deverão ser realizadas. Devido a isso, neste trabalho foram apresentados dados completamente preliminares de um animal de cada grupo experimental. Devido ao número amostral pequeno, nenhuma comparação

estatística entre os grupos animais pôde ser realizada. Os escaneamentos longitudinais dos nossos animais mostraram que a implantação do GBM no estriado dos animais alterou os níveis de captação de [^{18}F]FDG até 24 dias pós-cirurgia, quando comparados com o escaneamento anterior à implantação das células tumorais. Em geral, aos 10 e 17 dias pós-implantação é possível observar uma alteração muito exacerbada na captação de [^{18}F]FDG, quando comparada com o escaneamento basal. É possível que essa alteração se deva a um provável processo inflamatório, o qual pode estar mascarando a captação desse rádio-fármaco pelas células tumorais. Se realmente esse processo está ocorrendo, ele pode ser devido ao nosso protocolo semanal de injeção intracisternal, ou pela própria implantação das células malignas. Devido a isso, provavelmente teremos que alterar o cronograma de injeções intracisternais nos próximos experimentos para evitar que as imagens obtidas pelo microPET sejam realizadas durante o provável período de máxima inflamação. A alteração no perfil de captação desse rádio-fármaco, em alguns animais pareceu delimitar bem o volume dos tumores, porém não podemos fazer essa afirmação, pois infelizmente não foram realizadas análises histológicas no cérebro desses animais para confirmar se a marcação com o [^{18}F]FDG demarca exatamente o local no qual os tumores estariam inseridos. Devido a isso, nos próximos experimentos *in vivo,* será obrigatória a análise histológica do cérebro dos animais tratados com os ligantes para podermos demarcar o volume do tumor histologicamente e relacionar esse volume à captação de [^{18}F]FDG nos escaneamentos longitudinais. Apesar de ainda não termos podido delimitar corretamente o volume tumoral, a técnica de análise de tumores cerebrais em roedores através da aquisição de imagens por microPET após a captação de [^{18}F]FDG é muito utilizada na literatura (Assadian et al., 2008; Bolcaen et al., 2015; Corroyer-Dulmont et al., 2016; Wyss et al., 2007) e com algumas adaptações no cronograma de tratamento intracisternal, nossos resultados serão promissores.

CONCLUSÃO

Este trabalho visou avaliar o papel dos mGluR como possíveis biomarcadores prognósticos e alvos terapêuticos em glioblastomas (GBM), com o intuito de propor uma assinatura gênica desses receptores com valor preditivo de desfecho e de tratamento complementar adjuvante. Através da meta-análise de duas coorte de amostras de GBM humanos foi possível a identificação de uma assinatura gênica dos mGluR, na qual biópsias com alta expressão gênica de mGluR3 e baixa de mGluR4 e mGluR6 predizem um pior prognóstico para os pacientes.

O potencial dessa assinatura sobre a agressividade dos GBM foi avaliado por experimentos *in vitro* utilizando o tratamento de linhagens de GBM com ligantes de mGluR. O bloqueio farmacológico de mGluR do grupo II e a ativação farmacológica de mGluR de grupo III diminuíram a porcentagem de células da linhagem C6 em 25-28 %. A combinação desses tratamentos não apresentou efeito aditivo. O potencial da assinatura gênica também foi avaliado *in vivo* utilizando ratos implantados ortotopicamente com células da linhagem C6 e tratados intracisternalmente com os ligantes de mGluR e intraperitonealmente com a quimioterapia padrão, TMZ. Os resultados obtidos nos experimentos *in vivo* ainda são muito preliminares em relação ao tratamento com os ligantes de mGluR, entretanto a técnica de tratamento intracisternal seriada seguida da aquisição de imagem de [^{18}F]FDG captado pelos tumores cerebrais por microPET é muito promissora. Além de possibilitar uma interação do nosso grupo de pesquisa com o Instituto de cérebro (InsCer/PUCRS), sendo o primeiro estudo de avaliação de tumores cerebrais de rato por microPET realizado neste centro de pesquisa, a realização dos experimentos *in vivo* é de fundamental importância para verificar o efeito dos ligantes de mGluR em tumores inseridos em um sistema mais complexo, melhor avaliando o potencial da assinatura gênica dos mGluR proposta *in silico*.

Em suma, este estudo demonstrou que os níveis de expressão gênica de mGluR3, 4 e 6 em biópsias de GBM humanos possui um grande potencial prognóstico. A diminuição do

número de células da linhagem C6 após o tratamento *in vitro* com ligantes de mGluR está de acordo com o comportamento de agressividade predito *in silico*. Embora mais experimentos *in vitro* e *in vivo* sejam necessários para melhor avaliação do potencial da assinatura gênica dos mGluR, os resultados obtidos indicam que a avaliação da expressão dos oito subtipos de mGluR em biópsias de GBM pode ser considerada em âmbito clínico para guiar futuras intervenções quimioterápicas.

PERSPECTIVAS

Para melhor avaliação *in vitro* do potencial da assinatura gênica de mGluR como biomarcador prognóstico para os pacientes, é necessária a realização de mais experimentos *in vitro* em linhagens de GBM tratadas com ligantes de mGluR em condições proliferantes. A melhor opção seria a adição de fatores de crescimento como, por exemplo, o *Epidermal growth fator* (EGF).

A análise do volume de tumores cerebrais em roedores tratados intracisternalmente através de imagens da captação de [^{18}F]FDG é muito promissora e necessita de ajustes no protocolo para eliminar/limitar fatores que possam aumentar a captação desse rádio-fármaco em outras partes cerebrais, como, por exemplo, processos inflamatórios, mascarando a captação específica na região tumoral.

Para complementar o capítulo III, pretende-se realizar imagens de microPET em ratos tratados intracisternalmente com rádio-fármacos para verificar a difusão de tratamentos através desta via de aplicação.

Para confirmar a assinatura gênica de mGluR em biópsias de GBM como fator prognóstico para os pacientes, é necessária a realização de um estudo prospectivo. Para isso, pretende-se formar um biorrepositório de biópsias de tumores cerebrais, incluindo GBM. A formação desse biorrepositório seguirá as Diretrizes da Portaria Nº 2.201. As craniotomias para retirada de tumores cerebrais serão realizadas em dois hospitais de Porto Alegre/RS: Hospital São José e Hospital Cristo Redentor. As biópsias serão preparadas para posterior uso em ensaios de expressão gênica e para verificação do imunoconteúdo proteico, principalmente de mGluR.

Pretende-se realizar uma nova meta-análise para avaliar o valor prognóstico da expressão gênica dos oito subtipos de receptores de mGluR em biópsias de gliomas de Grau III das mesmas duas coortes de pacientes obtidas de dois bancos de dados independentes depositados no *Gene Expression Omnibus database* (GSE16011 e GSE4412) com o intuito de propor uma assinatura gênica dos mGluR capaz de predizer o desfecho desses pacientes. A confirmação dessa assinatura gênica seria através da análise do imunoconteúdo proteico de mGluR e da expressão gênica desses receptores nas biópsias armazenadas no biorrepositório.

REFERÊNCIAS

Arcella, A., G. Carpinelli, G. Battaglia, M. D'Onofrio, F. Santoro, R.T. Ngomba, V. Bruno, P. Casolini, F. Giangaspero, and F. Nicoletti. 2005. Pharmacological blockade of group II metabotropic glutamate receptors reduces the growth of glioma cells in vivo. *Neuro Oncol*. 7:236-245.

Assadian, S., A. Aliaga, R.F. Del Maestro, A.C. Evans, and B.J. Bedell. 2008. FDG-PET imaging for the evaluation of antiglioma agents in a rat model. *Neuro Oncol*. 10:292-299.

Balcar, V.J., and Y. Li. 1992. Heterogeneity of high affinity uptake of L-glutamate and L-aspartate in the mammalian central nervous system. *Life Sci*. 51:1467-1478.

Behrens, P.F., H. Langemann, R. Strohschein, J. Draeger, and J. Hennig. 2000. Extracellular glutamate and other metabolites in and around RG2 rat glioma: an intracerebral microdialysis study. *J Neurooncol*. 47:11-22.

Bolcaen, J., B. Descamps, K. Deblaere, T. Boterberg, F. De Vos Pharm, J.P. Kalala, C. Van den Broecke, E. Decrock, L. Leybaert, C. Vanhove, and I. Goethals. 2015. (18)F-fluoromethylcholine (FCho), (18)F-fluoroethyltyrosine (FET), and (18)F-fluorodeoxyglucose (FDG) for the discrimination between high-grade glioma and radiation necrosis in rats: a PET study. *Nucl Med Biol*. 42:38-45.

Bondy, M.L., M.E. Scheurer, B. Malmer, J.S. Barnholtz-Sloan, F.G. Davis, D. Il'yasova, C. Kruchko, B.J. McCarthy, P. Rajaraman, J.A. Schwartzbaum, S. Sadetzki, B. Schlehofer, T. Tihan, J.L. Wiemels, M. Wrensch, P.A. Buffler, and B.T.E. Consortium. 2008. Brain tumor epidemiology: consensus from the Brain Tumor Epidemiology Consortium. *Cancer*. 113:1953-1968.

Bowman, C.L., L. Yohe, and J.W. Lohr. 1999. Enzymatic modulation of cell volume in C6 glioma cells. *Glia*. 27:22-31.

Bruno, V., G. Battaglia, A. Copani, M. D'Onofrio, P. Di Iorio, A. De Blasi, D. Melchiorri, P.J. Flor, and F. Nicoletti. 2001. Metabotropic glutamate receptor subtypes as targets for neuroprotective drugs. *J Cereb Blood Flow Metab*. 21:1013-1033.

Burger, P.C., E.R. Heinz, T. Shibata, and P. Kleihues. 1988. Topographic anatomy and CT correlations in the untreated glioblastoma multiforme. *J Neurosurg*. 68:698-704.

Ciceroni, C., A. Arcella, P. Mosillo, G. Battaglia, E. Mastrantoni, M.A. Oliva, G. Carpinelli, F. Santoro, P. Sale, L. Ricci-Vitiani, R. De Maria, R. Pallini, F. Giangaspero, F. Nicoletti, and D. Melchiorri. 2008. Type-3 metabotropic glutamate receptors negatively modulate bone morphogenetic protein receptor signaling and support the tumourigenic potential of glioma-initiating cells. *Neuropharmacology*. 55:568-576.

Ciceroni, C., M. Bonelli, E. Mastrantoni, C. Niccolini, M. Laurenza, L.M. Larocca, R. Pallini, A. Traficante, P. Spinsanti, L. Ricci-Vitiani, A. Arcella, R. De Maria, F. Nicoletti, G. Battaglia, and D. Melchiorri. 2013. Type-3 metabotropic glutamate receptors regulate chemoresistance in glioma stem cells, and their levels are inversely related to survival in patients with malignant gliomas. *Cell Death Differ*. 20:396-407.

Cloughesy, T.F., W.K. Cavenee, and P.S. Mischel. 2014. Glioblastoma: from molecular pathology to targeted treatment. *Annu Rev Pathol*. 9:1-25.

Collingridge, G.L., and R.A. Lester. 1989. Excitatory amino acid receptors in the vertebrate central nervous system. *Pharmacol Rev*. 41:143-210.

Corroyer-Dulmont, A., E.A. Pérès, A.N. Gérault, A. Savina, F. Bouquet, D. Divoux, J. Toutain, M. Ibazizène, E.T. MacKenzie, L. Barré, M. Bernaudin, E. Petit, and S. Valable. 2016. Multimodal imaging based on MRI and PET reveals [(18)F]FLT PET as a specific and early indicator of treatment efficacy in a preclinical model of recurrent glioblastoma. *Eur J Nucl Med Mol Imaging*. 43:682-694.

D'Onofrio, M., A. Arcella, V. Bruno, R.T. Ngomba, G. Battaglia, V. Lombari, G. Ragona, A. Calogero, and F. Nicoletti. 2003. Pharmacological blockade of mGlu2/3 metabotropic glutamate receptors reduces cell proliferation in cultured human glioma cells. *J Neurochem*. 84:1288-1295.

Dai, C., and E.C. Holland. 2001. Glioma models. *Biochim Biophys Acta*. 1551:M19-27.

Danbolt, N.C. 2001. Glutamate uptake. *Prog Neurobiol*. 65:1-105.

De Blasi, A., P.J. Conn, J. Pin, and F. Nicoletti. 2001. Molecular determinants of metabotropic glutamate receptor signaling. *Trends Pharmacol Sci*. 22:114-120.

de Groot, J., and H. Sontheimer. 2011. Glutamate and the biology of gliomas. *Glia*. 59:1181-1189.

DeAngelis, L.M. 2001. Brain tumors. *N Engl J Med*. 344:114-123.

Dohrmann, G.J., J.R. Farwell, and J.T. Flannery. 1976. Glioblastoma multiforme in children. *J Neurosurg*. 44:442-448.

Durand, G.M., Y. Kovalchuk, and A. Konnerth. 1996. Long-term potentiation and functional synapse induction in developing hippocampus. *Nature*. 381:71-75.

Ferlay, J., I. Soerjomataram, R. Dikshit, S. Eser, C. Mathers, M. Rebelo, D.M. Parkin, D. Forman, and F. Bray. 2015. Cancer incidence and mortality worldwide: sources, methods and major patterns in GLOBOCAN 2012. *Int J Cancer*. 136:E359-386.

Fonnum, F. 1984. Glutamate: a neurotransmitter in mammalian brain. *J Neurochem*. 42:1-11.

Fukuda, S., and T. Taga. 2006. [Roles of BMP in the development of the central nervous system]. *Clin Calcium*. 16:781-785.

Gerson, S.L. 2004. MGMT: its role in cancer aetiology and cancer therapeutics. *Nat Rev Cancer*. 4:296-307.

GLOBOCAN. 2012. Estimated Cancer Incidence, Mortality and Prevalence Worldwide in 2012. International Agency for Research in Cancer - World Health Organization (WHO), http://globocan.iarc.fr/Default.aspx, Last accessed 11 August 2016.

Gramatzki, D., S. Dehler, E.J. Rushing, K. Zaugg, S. Hofer, Y. Yonekawa, H. Bertalanffy, A. Valavanis, D. Korol, S. Rohrmann, M. Pless, J. Oberle, P. Roth, H. Ohgaki, and M. Weller. 2016. Glioblastoma in the Canton of Zurich, Switzerland revisited: 2005 to 2009. *Cancer*. 122:2206-2215.

Gu, J., Y. Liu, A.P. Kyritsis, and M.L. Bondy. 2009. Molecular epidemiology of primary brain tumors. *Neurotherapeutics*. 6:427-435.

Hamel, W., and M. Westphal. 2000. Growth factors in gliomas revisited. *Acta Neurochir (Wien)*. 142:113-137; discussion 137-118.

Hanse, E., G.M. Durand, O. Garaschuk, and A. Konnerth. 1997. Activity-dependent wiring of the developing hippocampal neuronal circuit. *Semin Cell Dev Biol*. 8:35-42.

Headley, P.M., and S. Grillner. 1990. Excitatory amino acids and synaptic transmission: the evidence for a physiological function. *Trends Pharmacol Sci*. 11:205-211.

Hegi, M.E., A.C. Diserens, T. Gorlia, M.F. Hamou, N. de Tribolet, M. Weller, J.M. Kros, J.A. Hainfellner, W. Mason, L. Mariani, J.E. Bromberg, P. Hau, R.O. Mirimanoff, J.G. Cairncross, R.C. Janzer, and R. Stupp. 2005. MGMT gene silencing and benefit from temozolomide in glioblastoma. *N Engl J Med*. 352:997-1003.

Hottinger, A.F., and Y. Khakoo. 2007. Update on the management of familial central nervous system tumor syndromes. *Curr Neurol Neurosci Rep*. 7:200-207.

INCA. 2015. Estimativa 2016: Incidência de câncer no Brasil. *In* INCA, 2015. Instituto Nacional de Câncer José Alencar Gomes da Silva - Coordenação de Prevenção e Vigilância, Rio de Janeiro. 122.

Ishiuchi, S., K. Tsuzuki, Y. Yoshida, N. Yamada, N. Hagimura, H. Okado, A. Miwa, H. Kurihara, Y. Nakazato, M. Tamura, T. Sasaki, and S. Ozawa. 2002. Blockage of Ca(2+)-permeable AMPA receptors suppresses migration and induces apoptosis in human glioblastoma cells. *Nat Med*. 8:971-978.

Ishiuchi, S., Y. Yoshida, K. Sugawara, M. Aihara, T. Ohtani, T. Watanabe, N. Saito, K. Tsuzuki, H. Okado, A. Miwa, Y. Nakazato, and S. Ozawa. 2007. Ca2+-permeable AMPA receptors regulate growth of human glioblastoma via Akt activation. *J Neurosci*. 27:7987-8001.

Izquierdo, I., L.R. Bevilaqua, J.I. Rossato, J.S. Bonini, J.H. Medina, and M. Cammarota. 2006. Different molecular cascades in different sites of the brain control memory consolidation. *Trends Neurosci*. 29:496-505.

Jungk, C., D. Chatziaslanidou, R. Ahmadi, D. Capper, J.L. Bermejo, J. Exner, A. von Deimling, C. Herold-Mende, and A. Unterberg. 2016. Chemotherapy with BCNU in recurrent glioma: Analysis of clinical outcome and side effects in chemotherapy-naïve patients. *BMC Cancer*. 16:81.

Khan, L., H. Soliman, A. Sahgal, J. Perry, W. Xu, and M.N. Tsao. 2016. External beam radiation dose escalation for high grade glioma. *Cochrane Database Syst Rev*:CD011475.

Kleihues, P., and W. Cavenne. 2000. Pathology and genetic tumors of the nervous system. IARC Press. 314 pp.

Kleihues, P., H. Ohgaki, and A. Aguzzi. 1995. Gliomas. *In* Neuroglia. H. Kettenmann and B. Ransom, editors. Oxford University Press. 1044 - 1060.

Komuro, H., and P. Rakic. 1993. Modulation of neuronal migration by NMDA receptors. *Science*. 260:95-97.

Krebs, H.A. 1935. Metabolism of amino-acids: The synthesis of glutamine from glutamic acid and ammonia, and the enzymic hydrolysis of glutamine in animal tissues. *Biochem J*. 29:1951-1969.

Kurihara, H., K. Hashimoto, M. Kano, C. Takayama, K. Sakimura, M. Mishina, Y. Inoue, and M. Watanabe. 1997. Impaired parallel fiber-->Purkinje cell synapse stabilization during cerebellar development of mutant mice lacking the glutamate receptor delta2 subunit. *J Neurosci*. 17:9613-9623.

Linos, E., T. Raine, A. Alonso, and D. Michaud. 2007. Atopy and risk of brain tumors: a meta-analysis. *J Natl Cancer Inst*. 99:1544-1550.

Logan, W.J., and S.H. Snyder. 1972. High affinity uptake systems for glycine, glutamic and aspaspartic acids in synaptosomes of rat central nervous tissues. *Brain Res*. 42:413-431.

Louis, D.N., H. Ohgaki, O.D. Wiestler, W.K. Cavenee, P.C. Burger, A. Jouvet, B.W. Scheithauer, and P. Kleihues. 2007. The 2007 WHO classification of tumours of the central nervous system. *Acta Neuropathol*. 114:97-109.

Louis, D.N., A. Perry, G. Reifenberger, A. von Deimling, D. Figarella-Branger, W.K. Cavenee, H. Ohgaki, O.D. Wiestler, P. Kleihues, and D.W. Ellison. 2016. The 2016 World Health Organization Classification of Tumors of the Central Nervous System: a summary. *Acta Neuropathol*. 131:803-820.

Marín, Y.E., and S. Chen. 2004. Involvement of metabotropic glutamate receptor 1, a G protein coupled receptor, in melanoma development. *J Mol Med (Berl)*. 82:735-749.

Masui, K., T.F. Cloughesy, and P.S. Mischel. 2012. Review: molecular pathology in adult high-grade gliomas: from molecular diagnostics to target therapies. *Neuropathol Appl Neurobiol*. 38:271-291.

McDonald, J.W., and M.V. Johnston. 1990. Physiological and pathophysiological roles of excitatory amino acids during central nervous system development. *Brain Res Brain Res Rev*. 15:41-70.

Nakanishi, S., Y. Nakajima, M. Masu, Y. Ueda, K. Nakahara, D. Watanabe, S. Yamaguchi, S. Kawabata, and M. Okada. 1998. Glutamate receptors: brain function and signal transduction. *Brain Res Brain Res Rev*. 26:230-235.

Nicoletti, F., A. Arcella, L. Iacovelli, G. Battaglia, F. Giangaspero, and D. Melchiorri. 2007. Metabotropic glutamate receptors: new targets for the control of tumor growth? *Trends Pharmacol Sci*. 28:206-213.

Nicoletti, F., V. Bruno, A. Copani, G. Casabona, and T. Knöpfel. 1996. Metabotropic glutamate receptors: a new target for the therapy of neurodegenerative disorders? *Trends Neurosci*. 19:267-271.

Niswender, C.M., and P.J. Conn. 2010. Metabotropic glutamate receptors: physiology, pharmacology, and disease. *Annu Rev Pharmacol Toxicol*. 50:295-322.

Noch, E., and K. Khalili. 2009. Molecular mechanisms of necrosis in glioblastoma: the role of glutamate excitotoxicity. *Cancer Biol Ther*. 8:1791-1797.

Ohgaki, H., and P. Kleihues. 2005. Epidemiology and etiology of gliomas. *Acta Neuropathol*. 109:93-108.

Omuro, A., and L.M. DeAngelis. 2013. Glioblastoma and other malignant gliomas: a clinical review. *JAMA*. 310:1842-1850.

Ostrom, Q.T., H. Gittleman, J. Fulop, M. Liu, R. Blanda, C. Kromer, Y. Wolinsky, C. Kruchko, and J.S. Barnholtz-Sloan. 2015. CBTRUS Statistical Report: Primary Brain and Central Nervous System Tumors Diagnosed in the United States in 2008-2012. *Neuro Oncol*. 17 Suppl 4:iv1-iv62.

Ozawa, S., H. Kamiya, and K. Tsuzuki. 1998. Glutamate receptors in the mammalian central nervous system. *Prog Neurobiol*. 54:581-618.

Pereira, M.S., F. Klamt, C.C. Thomé, P.V. Worm, and D.L. de Oliveira. 2017. Metabotropic glutamate receptors as a new therapeutic target for malignant gliomas. *Oncotarget*.

Piccirillo, S.G., and A.L. Vescovi. 2006. Bone morphogenetic proteins regulate tumorigenicity in human glioblastoma stem cells. *Ernst Schering Found Symp Proc*:59-81.

Pilkington, G.J. 1994. Tumour cell migration in the central nervous system. *Brain Pathol*. 4:157-166.

Rabacchi, S., Y. Bailly, N. Delhaye-Bouchaud, and J. Mariani. 1992. Involvement of the N-methyl D-aspartate (NMDA) receptor in synapse elimination during cerebellar development. *Science*. 256:1823-1825.

Rohren, E.M., T.G. Turkington, and R.E. Coleman. 2004. Clinical applications of PET in oncology. *Radiology*. 231:305-332.

Rothstein, J.D., M. Dykes-Hoberg, C.A. Pardo, L.A. Bristol, L. Jin, R.W. Kuncl, Y. Kanai, M.A. Hediger, Y. Wang, J.P. Schielke, and D.F. Welty. 1996. Knockout of glutamate transporters reveals a major role for astroglial transport in excitotoxicity and clearance of glutamate. *Neuron*. 16:675-686.

Rzeski, W., L. Turski, and C. Ikonomidou. 2001. Glutamate antagonists limit tumor growth. *Proc Natl Acad Sci U S A*. 98:6372-6377.

Sant, M., P. Minicozzi, S. Lagorio, T. Børge Johannesen, R. Marcos-Gragera, S. Francisci, and E.W. Group. 2012. Survival of European patients with central nervous system tumors. *Int J Cancer*. 131:173-185.

Schaeffer, H.J., and M.J. Weber. 1999. Mitogen-activated protein kinases: specific messages from ubiquitous messengers. *Mol Cell Biol*. 19:2435-2444.

Schoepp, D.D., D.E. Jane, and J.A. Monn. 1999. Pharmacological agents acting at subtypes of metabotropic glutamate receptors. *Neuropharmacology*. 38:1431-1476.

Segovia, G., A. Porras, A. Del Arco, and F. Mora. 2001. Glutamatergic neurotransmission in aging: a critical perspective. *Mech Ageing Dev*. 122:1-29.

Sonoda, Y., T. Ozawa, K.D. Aldape, D.F. Deen, M.S. Berger, and R.O. Pieper. 2001. Akt pathway activation converts anaplastic astrocytoma to glioblastoma multiforme in a human astrocyte model of glioma. *Cancer Res*. 61:6674-6678.

Sontheimer, H. 2008. A role for glutamate in growth and invasion of primary brain tumors. *J Neurochem*. 105:287-295.

Stepulak, A., H. Luksch, C. Gebhardt, O. Uckermann, J. Marzahn, M. Sifringer, W. Rzeski, C. Staufner, K.S. Brocke, L. Turski, and C. Ikonomidou. 2009. Expression of glutamate receptor subunits in human cancers. *Histochem Cell Biol*. 132:435-445.

Takano, T., J.H. Lin, G. Arcuino, Q. Gao, J. Yang, and M. Nedergaard. 2001. Glutamate release promotes growth of malignant gliomas. *Nat Med*. 7:1010-1015.

Tanabe, Y., M. Masu, T. Ishii, R. Shigemoto, and S. Nakanishi. 1992. A family of metabotropic glutamate receptors. *Neuron*. 8:169-179.

Teh, J., and S. Chen. 2012. mGlu Receptors and Cancerous Growth. *Wiley Interdiscip Rev Membr Transp Signal*. 1:211-220.

Theeler, B.J., W.K. Yung, G.N. Fuller, and J.F. De Groot. 2012. Moving toward molecular classification of diffuse gliomas in adults. *Neurology*. 79:1917-1926.

Tsao, M.N., M.P. Mehta, T.J. Whelan, D.E. Morris, J.A. Hayman, J.C. Flickinger, M. Mills, C.L. Rogers, and L. Souhami. 2005. The American Society for Therapeutic Radiology and Oncology (ASTRO) evidence-based review of the role of radiosurgery for malignant glioma. *Int J Radiat Oncol Biol Phys*. 63:47-55.

Vajkoczy, P., R. Goldbrunner, M. Farhadi, G. Vince, L. Schilling, J.C. Tonn, P. Schmiedek, and M.D. Menger. 1999. Glioma cell migration is associated with glioma-induced angiogenesis in vivo. *Int J Dev Neurosci*. 17:557-563.

Verhaak, R.G., K.A. Hoadley, E. Purdom, V. Wang, Y. Qi, M.D. Wilkerson, C.R. Miller, L. Ding, T. Golub, J.P. Mesirov, G. Alexe, M. Lawrence, M. O'Kelly, P. Tamayo, B.A. Weir, S. Gabriel, W. Winckler, S. Gupta, L. Jakkula, H.S. Feiler, J.G. Hodgson, C.D. James, J.N. Sarkaria, C. Brennan, A. Kahn, P.T. Spellman, R.K. Wilson, T.P. Speed, J.W. Gray, M. Meyerson, G. Getz, C.M. Perou, D.N. Hayes, and C.G.A.R. Network. 2010. Integrated genomic analysis identifies clinically relevant subtypes of glioblastoma characterized by abnormalities in PDGFRA, IDH1, EGFR, and NF1. *Cancer Cell*. 17:98-110.

Wesseling, P., D.J. Ruiter, and P.C. Burger. 1997. Angiogenesis in brain tumors; pathobiological and clinical aspects. *J Neurooncol*. 32:253-265.

Westphal, M., D.C. Hilt, E. Bortey, P. Delavault, R. Olivares, P.C. Warnke, I.R. Whittle, J. Jääskeläinen, and Z. Ram. 2003. A phase 3 trial of local chemotherapy with biodegradable carmustine (BCNU) wafers (Gliadel wafers) in patients with primary malignant glioma. *Neuro Oncol*. 5:79-88.

Willard, S.S., and S. Koochekpour. 2013. Glutamate signaling in benign and malignant disorders: current status, future perspectives, and therapeutic implications. *Int J Biol Sci*. 9:728-742.

Wyss, M.T., N. Spaeth, G. Biollaz, J. Pahnke, P. Alessi, E. Trachsel, V. Treyer, B. Weber, D. Neri, and A. Buck. 2007. Uptake of 18F-Fluorocholine, 18F-FET, and 18F-FDG in C6 gliomas and correlation with 131I-SIP(L19), a marker of angiogenesis. *J Nucl Med*. 48:608-614.

Ye, Z.C., and H. Sontheimer. 1999. Glioma cells release excitotoxic concentrations of glutamate. *Cancer Res*. 59:4383-4391.

Yelskaya, Z., V. Carrillo, E. Dubisz, H. Gulzar, D. Morgan, and S.S. Mahajan. 2013. Synergistic inhibition of survival, proliferation, and migration of U87 cells with a combination of LY341495 and Iressa. *PLoS One*. 8:e64588.

Yoshida, Y., K. Tsuzuki, S. Ishiuchi, and S. Ozawa. 2006. Serum-dependence of AMPA receptor-mediated proliferation in glioma cells. *Pathol Int*. 56:262-271.

Yu, L.J., B.A. Wall, J. Wangari-Talbot, and S. Chen. 2016. Metabotropic glutamate receptors in cancer. *Neuropharmacology*.

Zhang, C., X.R. Yuan, H.Y. Li, Z.J. Zhao, Y.W. Liao, X.Y. Wang, J. Su, S.S. Sang, and Q. Liu. 2015. Anti-cancer effect of metabotropic glutamate receptor 1 inhibition in human glioma U87 cells: involvement of PI3K/Akt/mTOR pathway. *Cell Physiol Biochem*. 35:419-432.

Zhou, K., Y. Song, W. Zhou, C. Zhang, H. Shu, H. Yang, and B. Wang. 2014. mGlu3 receptor blockade inhibits proliferation and promotes astrocytic phenotype in glioma stem cells. *Cell Biol Int*. 38:426-434.